Development of New Catalytic Processes for Organic Chemistry

Ph.D. Thesis (October 2016)

Calum W. Muir

Development of New Catalytic Processes for Organic Chemistry

by

Calum W. Muir

A thesis submitted to the Department of Pure and Applied Chemistry, University of Strathclyde, in part fulfilment of the regulations for the degree of Doctor of Philosophy in Chemistry.

I certify that the thesis has been written by me. Any help I have received in my research work and the preparation of the thesis itself has been acknowledged. In addition, I certify that all information sources and literature used are indicated in the thesis.

This thesis is the result of the author's original research. It has been composed by the author and has not been previously submitted for examination which has led to the award of a degree.

Signed:

Date:

Acknowledgements

Contents

List of Schemes

List of Figures

List of Tables

Publications

One-Pot Homologation of Boronic Acids: A Platform for Diversity-Oriented Synthesis.[1]

Abstracts

Chapter 1 - Brønsted Acid-catalysed Enantioselective Conjugate Addition to Vinyl *N*-Heterocycles

This chapter details work towards the development of a new catalytic and enantioselective carbon-carbon and carbon-heteroatom bond forming method to enable access to desirable heterocyclic motifs containing functionalised stereocentres. Chiral Brønsted acid-catalysed conjugate addition to vinyl *N*-heterocycles was predicted to facilitate enantiocontrolled access to heterocycles containing a chiral benzylic and/or homobenzylic functionality (Scheme 1).
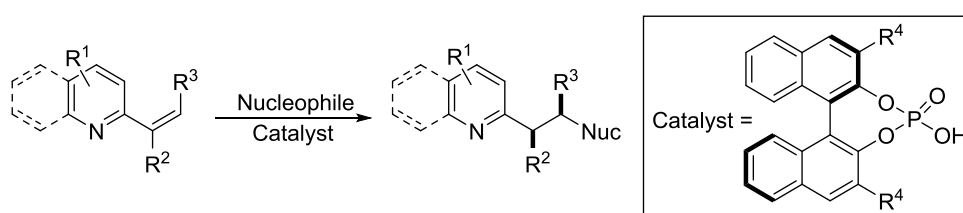
Scheme 1. Brønsted acid-catalysed conjugate addition to substituted vinyl *N*-heterocycles.

From initial investigations, it became apparent that the most competent nucleophile was aniline which was selected as the nucleophile for optimisation studies. Vinyl pyridine systems displayed poor reactivity towards the conjugate addition, whereas a vinyl quinoline compound was found to be significantly more reactive and was chosen as a more competent Michael acceptor (Scheme 2).
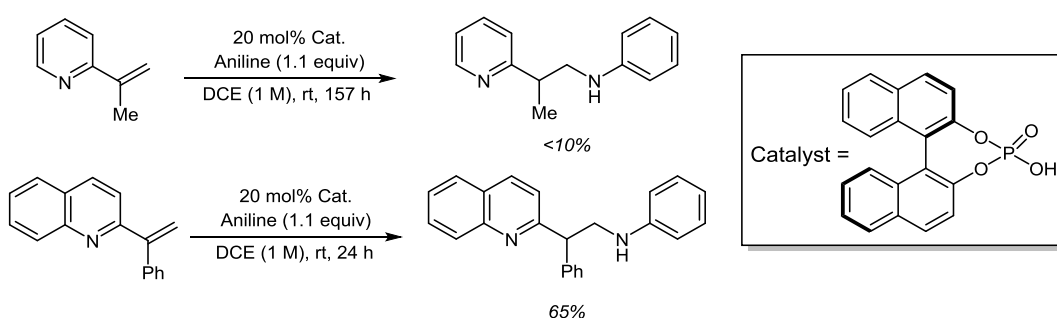
Scheme 2. Reactivity of vinyl quinoline system compared to vinyl pyridine system.

Optimisation of the process showed high selectivity could be achieved at the expense of conversion (33% conversion, 80% ee) and, conversely, high conversion could be achieved at the expense of selectivity (72% conversion, 64% ee). The rate of proton transfer in

asymmetric protonations is an important factor in their success and controlling this will be key to developing the current methodology towards high selectivity at an appropriate degree of reactivity. Efforts to reconcile these have, so far, proved unsuccessful and work towards doing so will be undertaken within the group in the future.

Chapter 2 - One-pot Formal Homologation of Boronic Acids: A Platform for Diversity-oriented Synthesis

This chapter details methodology in which chemoselective formal homologation of boronic acids has been developed. Chemoselective Suzuki-Miyaura cross-coupling between a boronic acid and a haloaryl MIDA boronate (BMIDA) followed by controlled BMIDA hydrolysis reveals the formally homologated boronic acid product (Scheme 3). The chemoselectivity in this process arises from the selective cross-coupling of the haloarene with one boron species preferentially over the other.
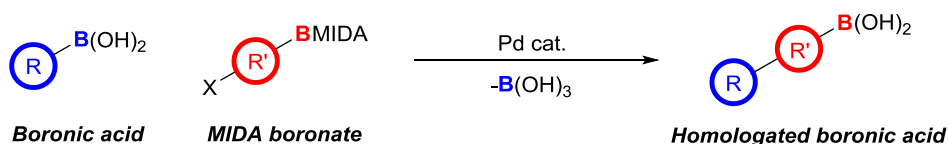
Scheme 3. Chemoselective formal homologation of boronic acids.

The process was immediately validated and efficiently optimised through the careful control of the reaction media (Scheme 4).
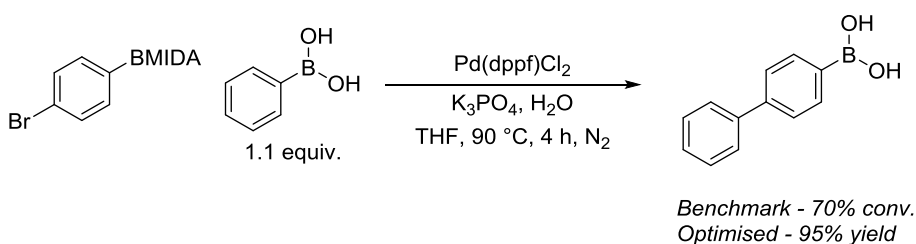
Scheme 4. Validation and optimisation of homologation reaction.

Once optimised, the process was applied to a wide range of substrates which were successfully delivered in good to excellent yields (46-95%), a significant proportion of which are novel boronic acids (Scheme 5).
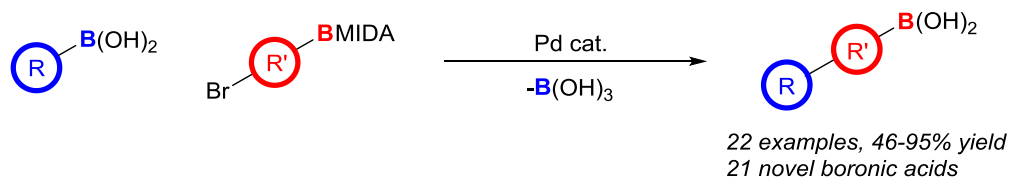
Scheme 5. Scope of the developed boronic acid homologation reaction.

With the reaction scope firmly established, the next step would be to utilise the proven ability of the reaction to tolerate a range of substrates to synthesise a boronic acid which could act as a valuable precursor to a biologically relevant molecule. This boronic acid would then act as the platform for diversification in a display of the value of the methodology towards drug discovery programmes. Application of this procedure was successfully achieved in the synthesis of a range of bromodomain binding inhibitors (Scheme 6).
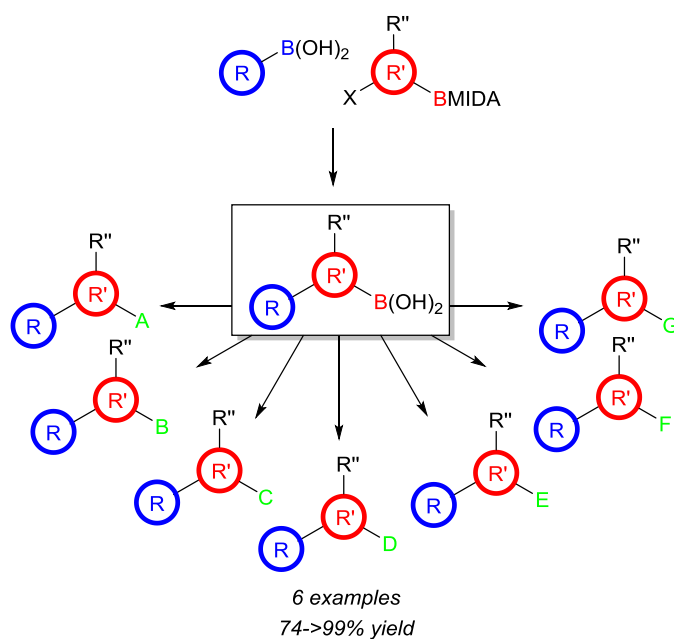
Scheme 6. Application of the methodology towards diversity oriented synthesis.

Abbreviations

ABC - anion binding catalysis

ACDC - asymmetric counterion-directed catalysis/catalyst(s)

BINOL - 1,1'-bi(2-naphthol)

Br. s - broad singlet

Cat. - catalyst

CADC - chiral anion-directed catalysis

CBC - cation binding catalysis

CCDC - chiral cation-directed catalysis

CPA - chiral protonating agent

CyHex - cyclohexane

d - doublet

dd - doublet of doublets

ddd - doublet of doublets of doublets

dt - doublet of triplets

D - Debyes

DCE - 1,2-dichloroethane

DCM - dichloromethane

DEAD - diethyl azodicarboxylate

DEM - diethyl malonate

DMF – *N*,*N*-dimethylformamide

DPP - diphenyl phosphate

dr - diastereomeric ratio

DTBM SegPhos - (*R*)-(−)-5,5'-Bis[di(3,5-di-tert-butyl-4-methoxyphenyl)phosphino]-4,4'-bi-1,3-benzodioxole, [(4*R*)-(4,4'-bi-1,3-benzodioxole)-5,5'-diyl]bis[bis(3,5-di-tert-butyl-4-methoxyphenyl)phosphine]

E_a - activation energy

ee - enantiomeric excess

er - enantiomeric ratio

equiv. - equivalents

h - hours

HPLC - high-performance liquid chromatography

HRMS - high-resolution mass spectrometry

IPA - isopropyl alcohol

L - length

μw - microwave

M - multiplet

M - molar

min - minutes

Nuc - nucleophile

PTC - phase transfer catalysis

P - pentet

PTSA - *p*-toluenesulfonic acid

rt - room temperature

s – singlet

SegPhos - (*R*)-(+)-5,5'-Bis(diphenylphosphino)-4,4'-bi-1,3-benzodioxole, [4(*R*)-(4,4'-bi-1,3-benzodioxole)-5,5'-diyl]bis[diphenylphosphine]

t_R - retention time

t - triplet

td - triplet of doublets

TFA - trifluoroacetic acid

TFE – trifluoroethanol

THF - tetrahydrofuran

TLC - thin layer chromatography

TRIP - 2,4,6-(*i*-Pr)C_6H_2

WalPhos - (R)-1-{(RP)-2-[2-[Bis(4-methoxy-3,5-dimethylphenyl)phosphino]phenyl]ferrocenyl}ethylbis[3,5-bis(trifluoromethyl)phenyl]phosphine

Xphos - 2-Dicyclohexylphosphino-2',4',6'-triisopropylbiphenyl

Chapter 1 - Brønsted Acid-catalysed Enantioselective Conjugate Addition to Vinyl *N*-Heterocycles

1. Introduction

1.1. Asymmetric Protonation

1.1.1. Principles of Asymmetric Protonation

Asymmetric protonation is a well-known methodology for direct access to compounds with high levels of enantioenrichment.[2,3,4] One method for the generation of a tertiary carbon stereocentre is to protonate a carbanion intermediate. However, asymmetric transfer of a proton holds significant challenges, i.e., manipulating a very small atom and controlling asymmetry while doing so. Due to this, the conditions generated for efficient asymmetric protonation of a substrate or substrate class may be very specific to that particular substrate or substrate class and may perform poorly when applied to others. This makes the development of a general method for asymmetric protonation extremely challenging, yet, equally as desirable since tertiary carbon stereocentres are very common in biologically valuable compounds.[5] Therefore, the development of synthetically useful asymmetric protonation methods to form such stereocentres is of high value.

The concept of asymmetric protonation is a relatively simple one: a prochiral molecule is protonated selectively on one enantiotopic face, for example, on an enolate derivative (Figure 1). The protonating agent must be chiral in order to achieve the desired enantiofacial discrimination when associating the proton source with the prochiral molecule, **1**, during protonation.
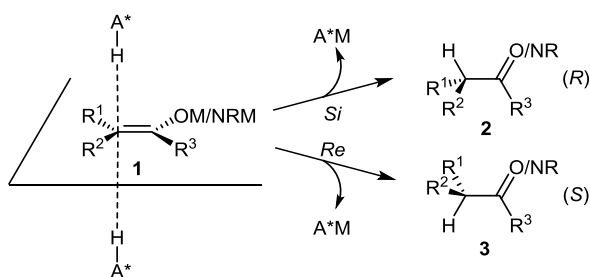
Figure 1. Selective facial protonation of a generic prochiral *N/O*-based enolate.

While Figure 1 shows a generic model demonstrating the principle of asymmetric protonation by a chiral proton source based on metallated enolates or enamines, **1**, there

are, however, additional modes of induction for asymmetric protonation. The chiral protonating agent (CPA) can be a chiral proton source where the enolate has no chirality (Figure 2 (a)), a chiral metal enolate where the chirality resides on the metal (Figure 2 (b)), or a hybrid system in which the chiral proton source serves as a ligand to the metal which is bound to the prochiral enolate (Figure 2 (c)).
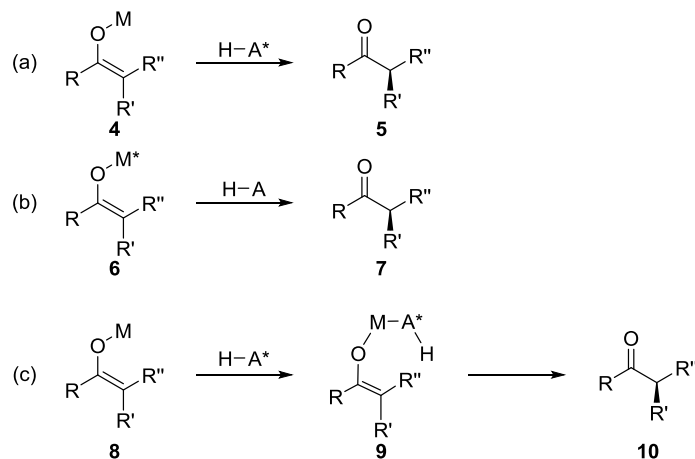
Figure 2. Modes of induction in asymmetric protonation of metal enolates.

1.1.2. Important Factors for Achieving Asymmetric Protonation

Given the inherent difficulties (discussed in section 1.1.1.) associated with asymmetric protonation in a general sense, there are a number of important parameters which should be considered when attempting these reactions.

1.1.2.1. Rate of Proton Transfer

One of the most important factors in determining the outcome of an asymmetric protonation is the speed with which a proton transfers from one (hetero)atom to another in solution. This is one of the fastest processes in chemistry[6] and controlling this is, of course, significantly challenging. One method of doing so is to reduce the temperature of the reaction such that all molecules in solution are rotating and moving more slowly, making it possible to slow down the rate of proton transfer.[7,8,9,10] The rate of transfer of the proton is not the only challenge associated with asymmetric protonation - its ability to readily transfer from one heteroatom to another rapidly in solution can cause significant difficulty when attempting to selectively protonate prochiral intermediates.

1.1.2.2. Structure of the CPA

Structurally, a CPA is most effective in achieving high levels of enantioselectivity if it contains both a site acting as a hydrogen-bond acceptor and a site acting as a hydrogen-bond donor, ideally in close proximity, and in a *syn*-relationship (Figure 3).[2]
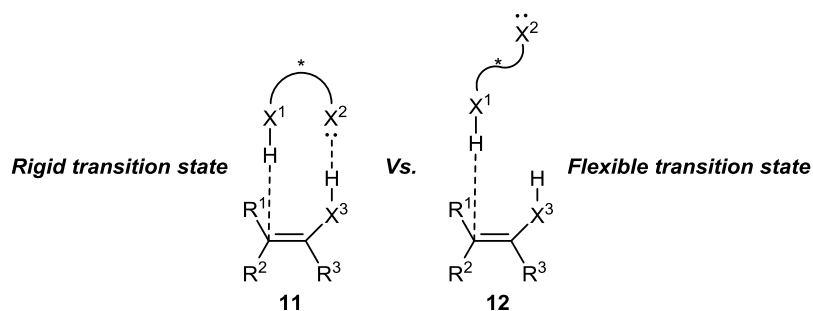
Figure 3. Structural benefit of a CPA having both proton donating and accepting group in a *syn*-like relationship.

It can be seen from Figure 3 that the enantioselectivity of the protonation can be significantly influenced by the structural properties of the CPA in that the formation of a more rigid intermolecular H-bonding network between the CPA and the intermediate, **11**, is highly favourable in terms of generating robust asymmetric induction.[2] Such an H-bonding network is favourable in that it establishes a strong interaction between the CPA and one particular enantiotopic face of the prochiral molecule, depending on the substitution on the prochiral intermediate, which leads to selective facial protonation. If the rigid H-bonding network is not achieved or is weak or flexible (if the X groups of the CPA are in an *anti*-relationship or are not in close proximity), then the H-bonding interaction between X^2 on the CPA and X^3-H on the prochiral intermediate would be too flexible, **12**, to generate sufficient asymmetric induction. Consequently, this would have a detrimental effect on the facial selectivity of the protonation.

1.1.2.3. pK_a of the CPA

Another factor of the CPA which is important in achieving high enantioselectivity is its acidity. This is important because it must be acidic enough to protonate all of, or the vast majority of, the substrate so that on workup of the reaction the remaining un-protonated substrate is in a low enough quantity, or ideally is non-existent, so that the resulting racemic product

afforded by quenching with an achiral proton source would not affect the overall ee. Vedejs conducted pK_a studies to probe the importance of ΔpK_a between the CPA and the prochiral substrate in asymmetric protonation reactions.[11] These studies show that ΔpK_a (ΔpK_a = pK_a substrate - pK_a CPA) of different catalysts lead to 91%, 97%, and 99% protonation by the CPA. One of the findings that it is important to take into account is that as the ΔpK_a is lowered, proton transfer is slower, and enantioselectivity is consequently higher. So, it can be deduced that it is important to find a balance between enantioselectivity (requiring low ΔpK_a) and extent of protonation (requiring high ΔpK_a) and that is found to be in the region of $2 \leq \Delta pK_a \leq 4$.

In 2008, Yamamoto reported the first metal-free Brønsted acid catalysed asymmetric protonation reactions of silyl enol ethers using a chiral Brønsted acid catalyst in the presence of a less acidic, achiral Brønsted acid (Table 1).[12]

Entry	Catalyst	pK_a	Time (h)	Yield[a] (%), er[b]
1	15	4.2[13] (DMSO)	96	NR, ND
2	16	-	96	NR, ND
3	17	3.34[14] (DMSO)	4.5	>99, 77:23 (*S*)
4	18-1	-	3.5	>99, 89:11 (*S*)
5	19	-	3.5	>99, 86:14 (*S*)

[a]NR = No reaction, [b]ND = Not determined.
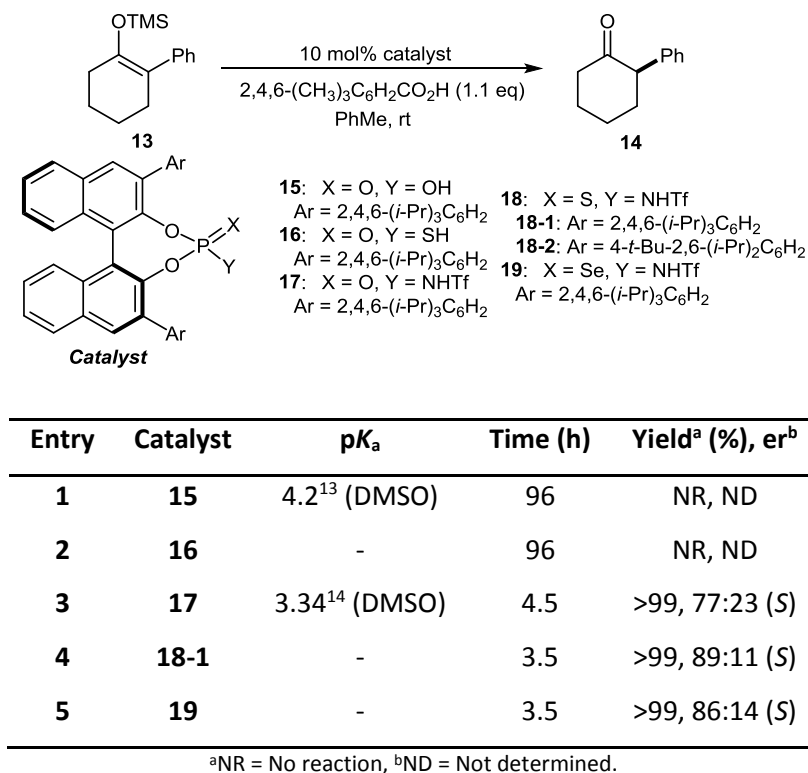
Table 1. Yamamoto's enantioselective protonations using chiral Brønsted acid catalysts.

This work, as well as showing that enantioselective protonation of prochiral enolate derivatives under chiral Brønsted acid catalysis is possible, further illustrates the importance of ΔpK_a between the CPA and the enolate in terms of the extent of protonation (in some cases

0% protonation and in others >99% protonation) and the enantioselectivity (ranging from 54% ee to 78% ee). The desired product was delivered quantitatively in entries 3, 4 and 5 in reaction times under five hours which indicates that, although proton transfer is rapid, it can be controlled to a significant extent under controlled reaction conditions. In entries 1 and 2, there was no reaction, possibly due to the inadequate acidity of the acids used and the introduction of an NHTf group significantly improved the acidity to a level where the rapid reaction times discussed above could be achieved.

1.1.2.4. (*E*)/(*Z*) Configuration of the Prochiral Molecule

(*E*)- and (*Z*)-Prochiral molecules have different enantiofacial selectivities since the two diastereomeric transition states for the protonation of the (*E*)-isomer are different from those for the (*Z*)-isomer. This is represented in Figure 4.
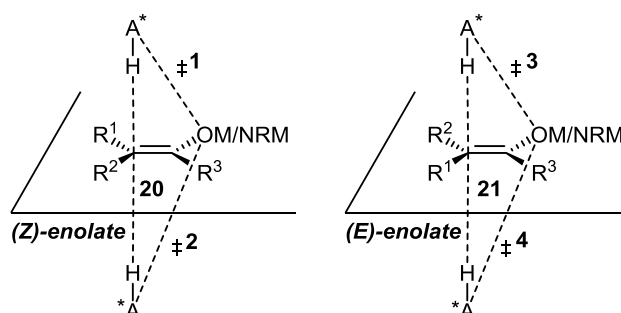
Figure 4. The four different diastereomeric transition states for protonation of (*E*)- and (*Z*)-enolates.

If one was to carry out an asymmetric protonation on a prochiral enolate (or equivalent), using either the (*E*)- or (*Z*)-isomer exclusively, there would be competition between two different transition states, making a selective protonation possible under the correct conditions. However, when using a mixture of the (*E*)- and (*Z*)-isomers (as may very likely be the case when forming and protonating the prochiral intermediate *in situ*), there would be four possible transition states, making the selective protonation much more challenging.

Although protonation through ‡1 on the (*Z*)-isomer, **20**, and ‡4 on the (*E*)-isomer, **21**, would lead to the same stereochemistry in the final product (as is the case with ‡2 and ‡3), this relies on both their energies being lower than both ‡2 and ‡3 in order to achieve a selective protonation. This presents a significant challenge to overcome in asymmetric protonation

since, in order to increase the chance of a selective protonation, one would have to pre-form and isolate exclusively the (*E*)- or (*Z*)-intermediate before exposing it to the reaction conditions.

1.1.3. Methods in Asymmetric Protonation

1.1.3.1. Enzymatic Methods of Asymmetric Protonation

Nature has developed several efficient methods for the asymmetric protonation of useful molecules. One such report by Ohta[15] demonstrates how the arylmalonate decarboxylase (AMDase) enzyme catalyses the decarboxylative asymmetric protonation of α-aryl-α-methyl-malonates in high enantiopurity (Scheme 7).
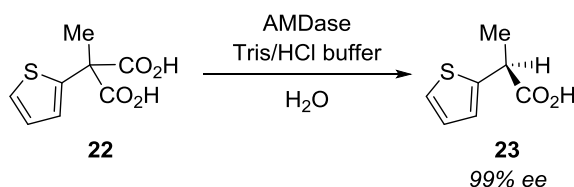
Scheme 7. Enzymatic decarboxylative asymmetric protonation.

Many more enzymatic methods of asymmetric protonation have been reported, but a more detailed analysis of these is outwith the scope of this discussion.

1.1.3.2. Non-enzymatic Methods of Asymmetric Protonation

Taking inspiration from the way that enzymatic systems achieve asymmetric protonation through the synergistic use of chiral proton donors and prochiral proton acceptors, many efficient non-enzymatic methods of asymmetric protonation have been developed, encompassing a wide range of substrates and CPAs. Figure 5 details a selection of these transformations.
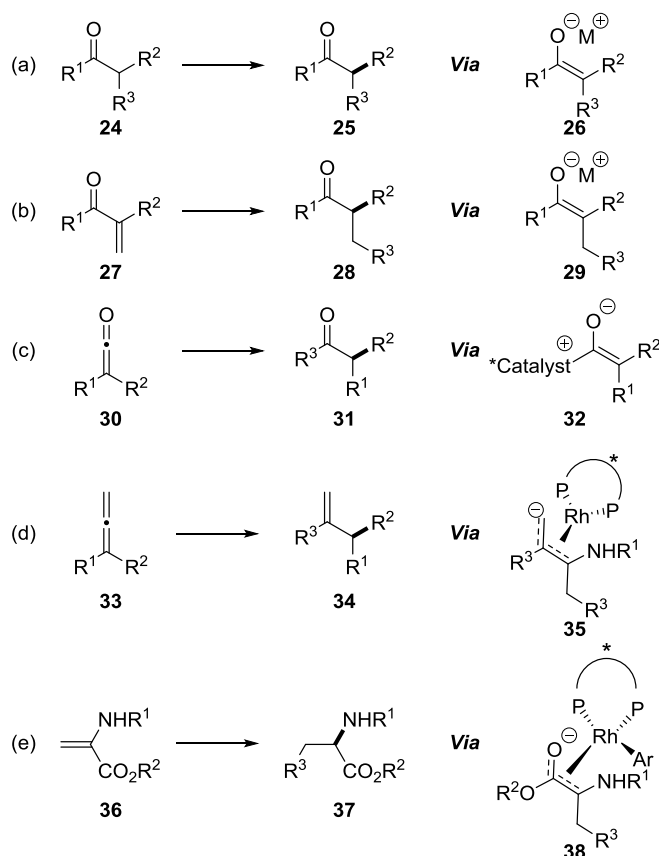
Figure 5. Asymmetric protonation in non-enzymatic systems.

As can be seen from Figure 5, many useful functional groups such as carbonyl compounds (a), α,β-unsaturated carbonyl compounds (b)/(e),[16] ketenes (c)[17] and allenes (d)[18] can undergo asymmetric protonation to afford their functionalised, enantiopure derivatives. It is important to notice that, in each of these examples, the functionalised products are always formed by asymmetric protonation of their respective prochiral enolate derivatives. This is the case with the vast majority of enantioselective protonations carried out in the laboratory and the methodology has been developed to utilise this reaction pathway to such an extent that most asymmetric protonations are carried out on pre-formed silyl enol ethers.

In terms of CPAs, there are many chiral proton sources which can be employed in asymmetric protonation reactions and these vary widely in structure, acidity, functionality and solubility in order to cover a wide range of asymmetric protonations. A selection of CPAs is shown in Figure 6.

7
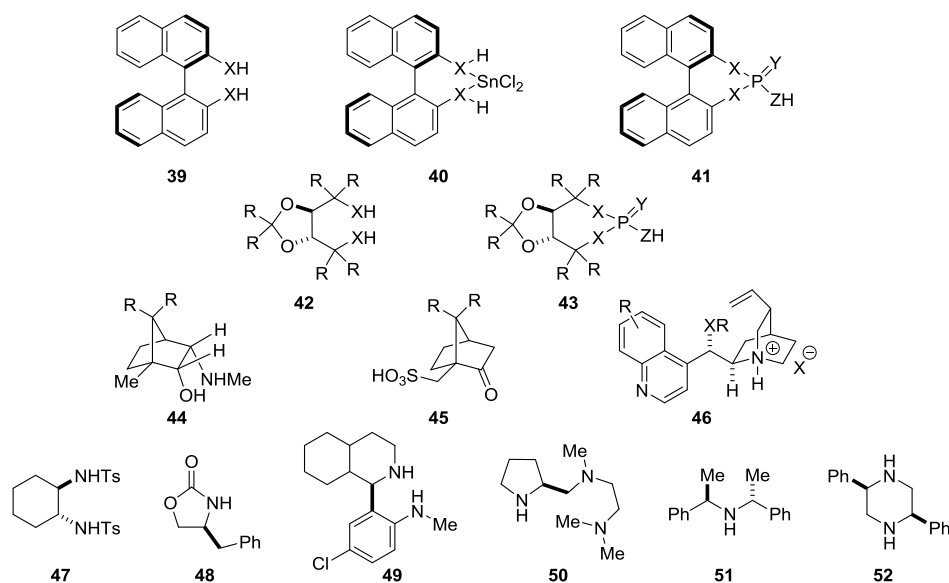
Figure 6. Commonly employed CPAs in asymmetric protonation reactions.

Studying Figure 6, it is immediately apparent that there is a wide range of CPAs available which can perform asymmetric protonations. The large scope of CPAs is such that choosing a protonating agent can be based on various catalyst parameters such as acidity, chiral pocket size/shape, solubility, chelation/H-bonding capacity and the functional group tolerance of the reaction being performed. The suitability of such parameters can be evaluated based on the nature of the prochiral substrate and the reaction conditions, and makes possible the logical selection of a CPA for a particular asymmetric protonation reaction. The exploration of CPAs has been, and will continue to be, the most significant factor in furthering progress in catalytic, asymmetric protonation. A disadvantage of having such a large and varied selection of CPAs is that choosing a CPA for a particular transformation may not necessarily be intuitive since, generally, CPAs which are effective for particular transformations have been discovered through screening a range of CPAs and selecting the most effective. However, the most commonly employed CPAs are chiral BINOL-based phosphoric acids (**41**), and are used in a wide range of asymmetric organic transformations.[19]

1.1.4. Generation of the Prochiral Intermediate

By surveying the asymmetric protonation literature (summarised in the sections above), it is clear that the vast majority of asymmetric protonations adjacent to a carbonyl group are carried out on the pre-formed, isolated enolate. This has a number of advantages in that (i)

the asymmetric protonation reaction would be 'clean' meaning that there are no by-products associated with the formation of the enolate in the reaction mixture, (ii) the enolate (*E*)/(*Z*)-ratio can be controlled, and (iii) by exposing only one isolated isomer to the reaction conditions, the formation of undesired product enantiomer can be minimised (see section 1.1.2.4.).

While the desired outcome is indeed achieved when pre-forming and isolating the prochiral intermediate, in that the asymmetric protonation can be performed efficiently, the generation and isolation of the intermediate may not be straight forward, desirable or even possible for many compounds. *In situ* generation and tandem asymmetric protonation of prochiral intermediates has been explored and this works well, giving high yields and ee's, and also functions as a method to circumvent the isolation of the prochiral intermediate.[16]

One particular example of this is Deng's asymmetric ketone alkylation (Scheme 8).[20]
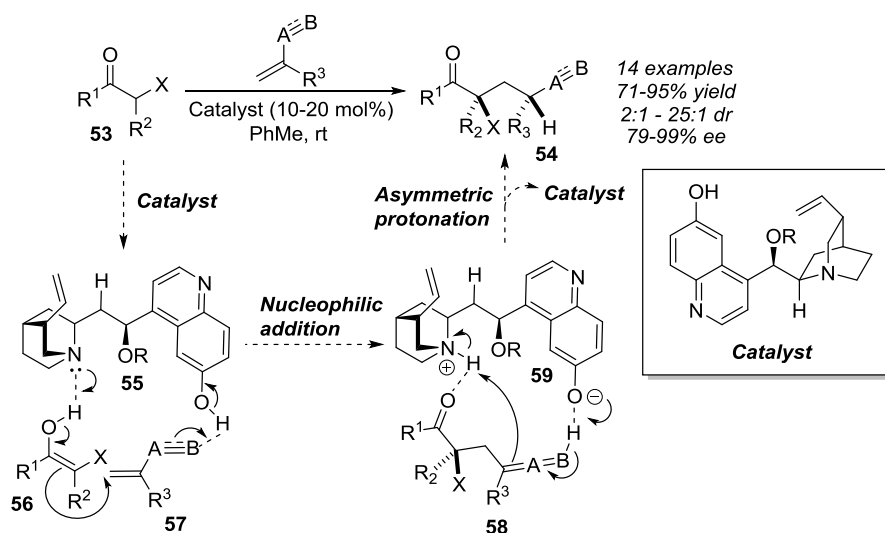
Scheme 8. Deng's cinchona alkaloid-catalysed, *in situ* generation and asymmetric protonation of a prochiral ethenimine.

In Deng's system, the functionalised ketone is first tautomerised to its prochiral enol form, **56**, by association with the chiral cinchona alkaloid catalyst. Prochiral enol **56** then attacks the electrophile, **57**, which is also associated with the chiral catalyst, **55**, generating a second prochiral intermediate, ethenimine **58** (A = C, B = N). Association of **58** with the chiral catalyst salt forms a diastereomeric complex which can then undergo asymmetric protonation to form the final product in high yield, dr and ee.

9

This is a particularly significant example as it shows that, by using the correct conditions, tandem *in situ* generation/conjugate addition/asymmetric protonation of prochiral intermediates can be carried out efficiently using a single hydrogen-bonding catalyst. This report holds promise for other similar methods to be developed.

1.2. Nucleophilic Conjugate Addition

Standard 1,2-nucleophilic additions involve the addition of a nucleophile to an electrophile such as a double or triple π-bond, very often aided by the polarisation of the π-bond with an electron-withdrawing heteroatom, i.e., functional groups such as carbonyl compounds, **60**, imines, **61**, and nitriles, **62**, which carry a partial positive charge on the carbon atom adjacent to the heteroatom (Scheme 9).
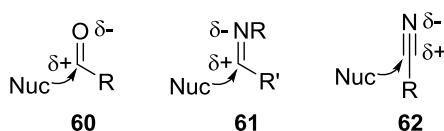
Scheme 9. General 1,2-nucleophilic addition to polarised π-bonds.

Most alkene compounds do not show 1,2-reactivity due to a lack of polarity across the π-bond, unless the alkene is activated with polar substituents such as electronegative heteroatoms.[21] In the case of α,β-unsaturated carbonyl compounds, cyclohexenone for example, it can be understood from the resonance structures that the β-position is the electrophilic site which is susceptible to nucleophilic attack. This type of nucleophilic addition is termed a nucleophilic conjugate addition (1,4-nucleophilic addition). An illustration of this is shown in Scheme 10.
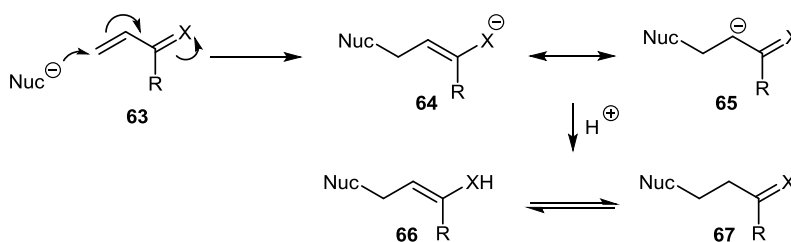
Scheme 10. Generic nucleophilic conjugate (1,4-) addition reaction mechanism.

In a generic conjugate addition (Scheme 10), the mechanism proceeds as follows: the nucleophile attacks the electrophilic position of the α,β-unsaturated system, **63**, generating

an enolate intermediate, **64** and **65**. This enolate is subsequently quenched by protonation on the α-carbon to afford the saturated product which can tautomerise between its enol form, **66**, and keto form, **67**. If the enolate is prochiral, that is to say that if there is a substituent (not a hydrogen atom) on the α-position of the carbonyl group, protonation of the enolate would lead to an α-stereocentre being generated. Herein lies the possibility for asymmetric induction in the conjugate addition reaction if a CPA was to be used for the protonation event.

There are many variations of the conjugate addition reaction in that the nucleophile need not be carbon-based. As such, heteroatomic nucleophiles such as alcohols,[22] amines,[23] thiols,[24] and phosphines[25] can be used successfully in conjugate addition reactions. In addition, many different reaction conditions and catalysts (metal-based and metal-free) have been successfully used in conjugate addition chemistry, which have allowed the conjugate addition reaction to advance as one of the most important bond forming methods in organic synthesis.[21]

1.2.1. Copper-catalysed Conjugate Addition Reactions

The use of copper catalysis is firmly established in asymmetric conjugate addition reactions.[26,27] Copper complexes are used to facilitate 1,4-additions of hard nucleophiles, such as organometallic reagents, to α,β-unsaturated carbonyl compounds - a reaction pathway which is best suited to soft nucleophiles (Scheme 11).
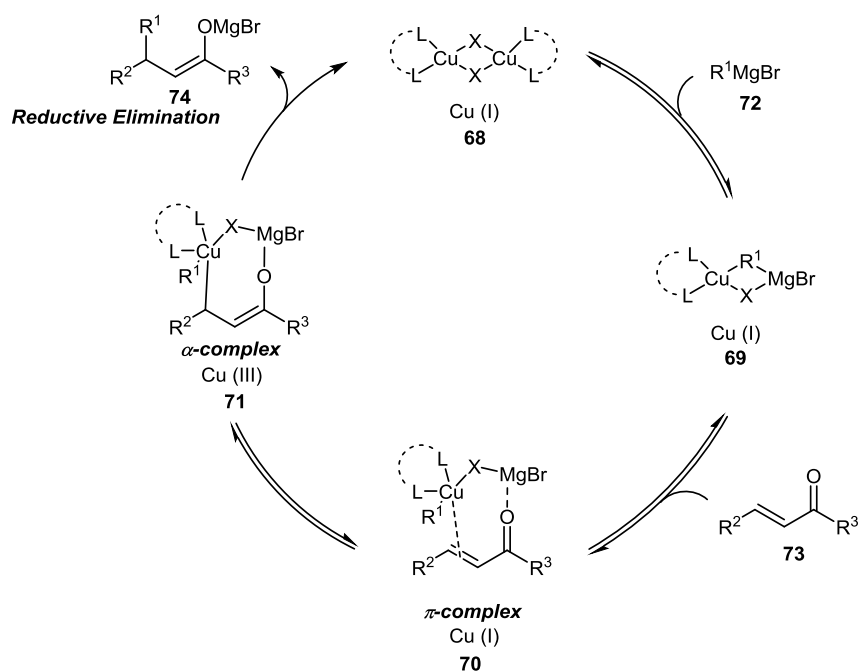
Scheme 11. Copper-catalysed 1,4-addition of a Grignard reagent to an α,β-unsaturated compound.

The seminal work in the field of copper-catalysed conjugate addition chemistry was published by the groups of Lippard[28] and Desimoni[29] in which conjugate additions to α,β-unsaturated carbonyl compounds were carried out asymmetrically in high yields. The field has since expanded as one of the most effective strategies for carrying out conjugate addition reactions to α,β-unsaturated substrates such as esters, ketones, aldehydes, nitriles, and nitro compounds.[26,27]

1.2.2. Conjugate Addition Reactions to Vinyl *N*-Heterocycles

Conjugate additions have been successfully applied to vinyl heterocycles under acidic[30,31] and basic[32] conditions, and under transition metal catalysis.[33,34] The field is well precedented, incorporating carbon-, nitrogen-, oxygen-, and sulphur-based nucleophiles.[35] The mechanism for such reactions proceeds as shown in Scheme 12, using the acid-catalysed mechanism as an example.
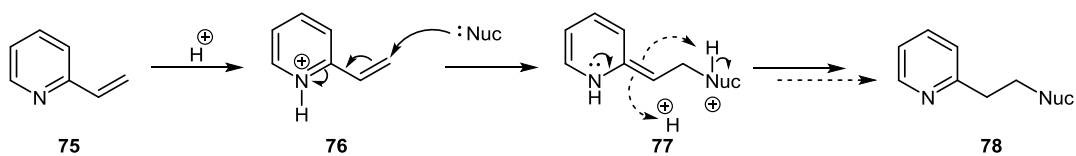
Scheme 12. Acid-mediated conjugate addition to a prototypical protonated vinyl *N*-heterocycle.

Upon protonation of the heterocyclic nitrogen, the vinyl heterocycle, **75**, is activated *via* the pyridinium intermediate, **76**, to conjugate addition. The nucleophile then attacks the Michael acceptor, generating an enamine intermediate, **77**. Rearomatisation of intermediate **77** *via* the nitrogen lone pair to reform the pyridine core and subsequent pick up of a proton in the benzylic position generates the conjugate addition product, **78**.

1.2.2.1. General Conjugate Additions to Vinyl *N*-Heterocycles

The seminal work in the field was published in 1955 when Reich and Levine used protonated pyridine as a Michael acceptor in the conjugate addition reaction between an aniline nucleophile and 2-vinyl pyridine, **75**, to generate 2-ethylamino pyridines, **80**, under stoichiometric acidic conditions (Scheme 13).[30]
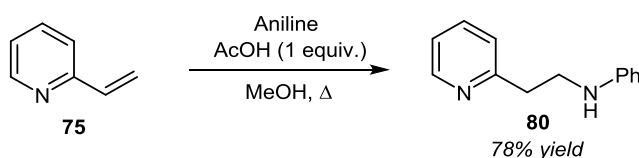
Scheme 13. Conjugate addition of amines to vinyl pyridine under acidic conditions.

This discovery shows the basis for the acid-mediated activation of the Michael acceptor *via* the pyridinium, subsequent addition of the nucleophile to generate the enamine intermediate, and rearomatisation with protonation to generate the secondary amine product in 78% yield.

Following this, in 2000, Yoshida reported the conjugate addition reaction between vinyl pyridine, **75**, and a range of thiol nucleophiles (Scheme 14).[36]
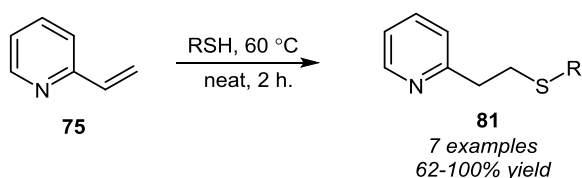
Scheme 14. Conjugate addition of thiol nucleophiles to vinyl pyridine.

It is important to note that this reaction does not require an acid to facilitate the conjugate addition. This can be explained by a comparison of the pK_a of thiophenol (*ca.* 6)[37] and the pK_aH of pyridine (*ca.* 5.25).[38] Upon heating, the pyridine lone pair can deprotonate the thiophenol, generating an electrophilic vinyl pyridinium species and a nucleophilic thiophenolate. The conjugate addition reaction then proceeds *via* nucleophilic attack of the nucleophile to the vinyl functionality of the pyridinium, generating 2-ethylthio pyridines, **81**.

In 2009, Schaaf carried out similar acid-mediated conjugate addition reactions of sodium methanesulfinate to vinyl pyridines (Scheme 15).[31]
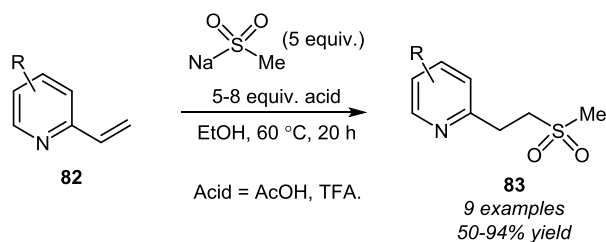
Scheme 15. Conjugate addition to vinyl pyridine under super-stoichiometric acidic conditions.

The synthesis was also applied to pyrimidines and various other nitrogen-containing vinyl heterocycles.

It can be seen from the examples discussed above that there is a lack of a synthetic strategy to carry out conjugate additions to vinyl pyridines without using harsh reaction conditions, such as large equivalents of acid and/or refluxing. It is apparent that there is also no synthesis of these substrates which operates catalytically or asymmetrically. However, conjugate additions to other compounds containing a heterocyclic motif under more mild conditions have been documented:

14

In 2010, Kerr carried out a series of conjugate addition reactions to a vinyl oxadiazole, **84**, using various carbon-, nitrogen-, and sulphur-based nucleophiles under acidic, basic, and neutral reaction conditions (Table 2).[32]

Table 2. Results of Kerr's conjugate addition to vinyl oxadiazoles under acidic, basic, and neutral conditions.
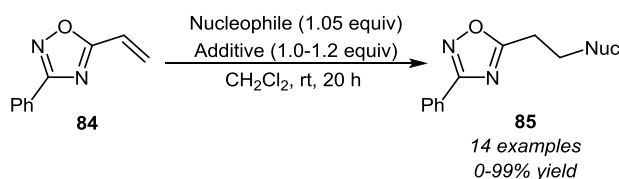
Nucleophile	Yield (Additive)	Yield (Additive)	Uncatalysed Yield
n-BuNH$_2$	-	-	98%
Et$_2$NH	-	-	99%
PhNH$_2$	54% (BF$_3$.OEt)	-	14%
	35% (AcOH)		
n-BuSH	88% (HCl)	8% (K$_2$CO$_3$)	No Reaction
PhSH	40% (HCl)	85% (K$_2$CO$_3$)	94%
ROH	63% (HCl)	78% (NaH)	-
Diethyl Malonate	-	51% (NaH)	-
n-Bu$_2$CuLi	-	-	40%

Table 2. Results of Kerr's conjugate addition to vinyl oxadiazoles under acidic, basic, and neutral conditions.

This work shows, again, the ability of vinyl *N*-heterocycles to act as conjugate acceptors for various nucleophiles and suggests that there is scope for such transformations to be carried out asymmetrically in the cases where an additive is used to facilitate the conjugate addition under mild reaction conditions.

1.2.2.2. Asymmetric Transition Metal-catalysed Conjugate Additions to Vinyl *N*-Heterocycles

Asymmetric conjugate additions to vinyl *N*-heterocycles have been reported using metal catalysis[33] and PTC.[39] In 2009, during work on copper-catalysed asymmetric conjugate reductions of β,β'-disubstituted 2-alkenylheteroarenes, Lam found that nitrogen-containing aromatic heterocycles, **86**, can provide effective activation of an adjacent alkene for highly enantioselective catalytic conjugate addition reactions (Scheme 16).[33]
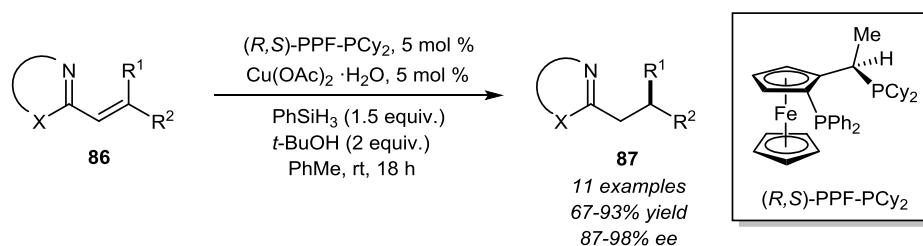
Scheme 16. Lam's copper-catalysed enantioselective conjugate addition to vinyl *N*-heterocycles.

It can be seen from Lam's work that the transformation described can be achieved asymmetrically using the catalyst and ligand combination detailed in Scheme 16. This shows promise for conjugate addition reactions to be carried out asymmetrically on vinyl *N*-heterocycles. It can also be seen that there is room for improvement upon the synthetic strategy used to achieve such a transformation, such as using an organocatalyst.

Lam also discovered in 2010 that Rh-catalysed additions of arylboronic acids to 1,2-disubstituted vinyl *N*-heterocycles, **88**, can be carried out asymmetrically and in high yields (Scheme 17).[34]
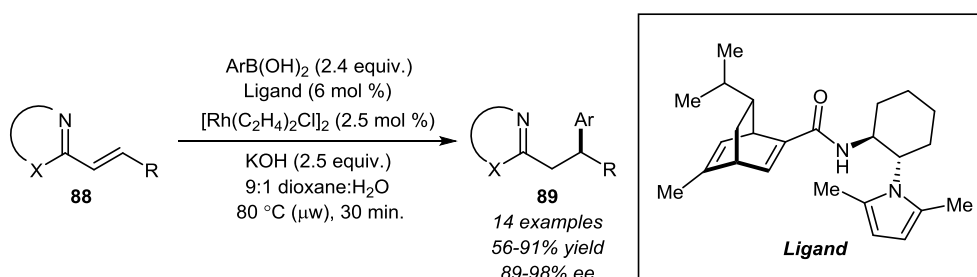
Scheme 17. Lam's Rh-catalysed asymmetric conjugate addition to vinyl *N*-heterocycles.

This work further exemplifies the capacity of vinyl *N*-heterocycles to act as Michael acceptors in asymmetric conjugate addition reactions under transition metal catalysis using a chiral ligand to control the stereoselectivity.

Further to this work, Lam also reported the use of a new ligand to improve the overall enantioselectivity and scope of the above Rh-catalysed conjugate addition reaction.[40] The ligand previously employed was a first generation chiral pool-derived ligand with stereocentres additional to the chiral diene functionality, and the group questioned whether this secondary chiral environment on the ligand was necessary. The catalyst which was

eventually developed was a second generation derivative of the chiral diene with an achiral group on the amide functionality, rather than a chiral cyclohexane, which improved overall enantioselectivity and reaction scope (Scheme 18).
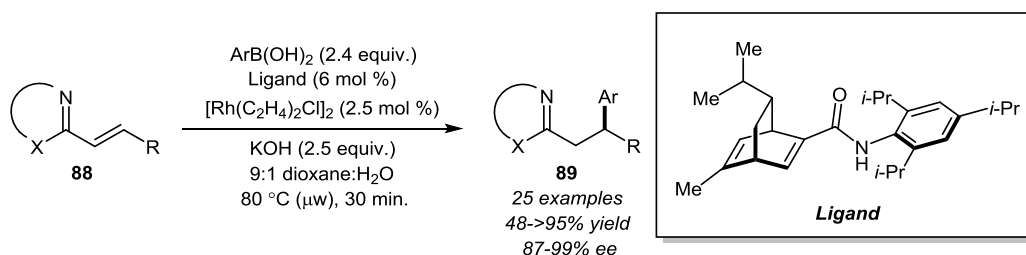
Scheme 18. Ligand optimisation in Lam's asymmetric conjugate addition.

1.2.2.3. Asymmetric Organocatalysed Conjugate Additions to Vinyl *N*-Heterocycles

Although transition metal-catalysed conjugate additions to vinyl heterocycles are broadly successful, generation of an organocatalysed process would be a valuable addition to the field. This would negate the need for any transition metals which have their associated problems such as being toxic[41–43] and difficult to completely remove from reaction mixtures. As such, in 2009, Bernardi published the first asymmetric conjugate addition involving 5-styrylisoxazoles, **90**, and nitroalkanes under mildly basic conditions using PTC (Scheme 19).[39]
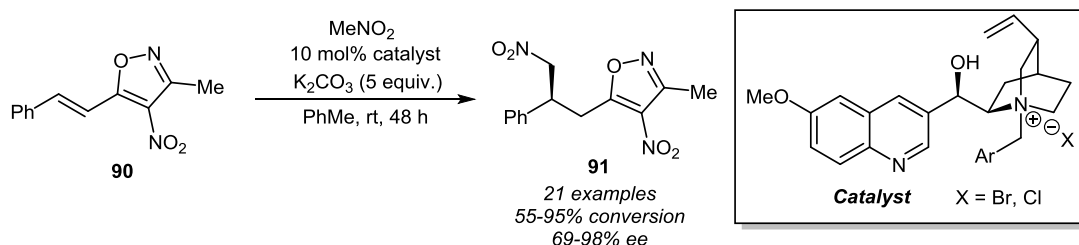
Scheme 19. Bernardi's conjugate addition to 5-styrylisoxazoles under basic conditions.

This process uses soft nucleophiles, i.e., nitroalkanes, to attack the electrophilic substrate using a chiral PTC to do so in an asymmetric fashion with mostly high conversion and generally good levels of enantioselectivity. A particularly attractive aspect of this example is the mild reaction temperature since, generally speaking, acid-and base-catalysed conjugate additions to vinyl heterocycles tend to require higher temperatures than is optimal for asymmetric induction.[35] In terms of the mechanism by which the conjugate addition proceeds, the heterocyclic heteroatoms are uninvolved, since the strongly conjugate-accepting nitro functionality on the heterocycle facilitates the resonance of electrons during

the conjugate addition event (Scheme 20). However, this report shows promise that such transformations on a vinyl heterocycle can be carried out asymmetrically using an organocatalyst.
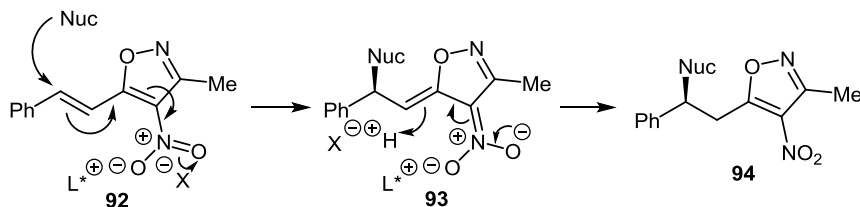
Scheme 20. Mechanism of Bernardi's conjugate addition of nitroalkanes to 5-styrylisoxazoles.

In 2015, Terada reported a process in which a range of pyrazoles and indazoles were asymmetrically conjugately added to a range of 1,2-disubstituted vinyl benzimidazoles, generating the chiral products in generally excellent yields and selectivities (Scheme 21).[44] The process is catalysed by a chiral anthracenyl BINOL-based phosphoric acid.
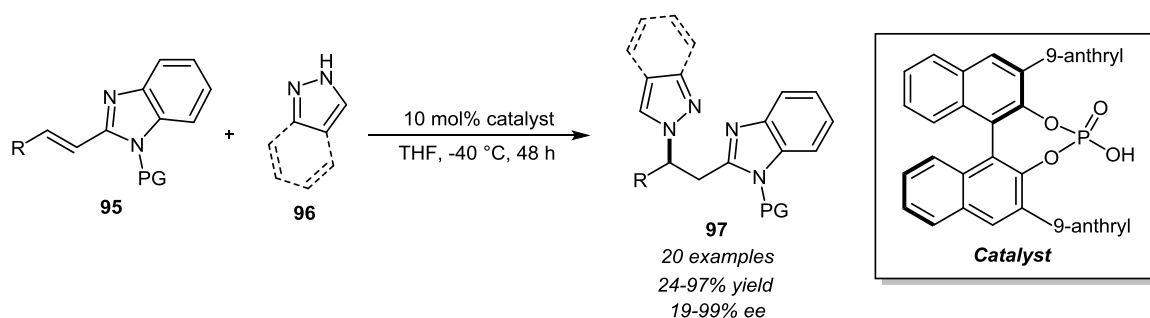
Scheme 21. Chiral phosphoric acid-catalysed conjugate addition to vinyl heterocycles.

This work shows that chiral BINOL-based phosphoric acids can indeed be used to successfully facilitate asymmetric conjugate addition reactions to vinyl *N*-heterocycles. This chemistry utilised the control of nucleophile approach to provide the asymmetry in the reaction, followed by symmetric protonation upon rearomatisation to give access to the desired functionalised heterocycles.

2. Proposed Work

The examples discussed above consist of asymmetric conjugate addition to vinyl *N*-heterocycles in which the stereo-defining event is the attack of the nucleophile to β-carbon of the α,β-unsaturated system, followed by symmetric protonation on the α-carbon, generating a homobenzylic stereocentre (Scheme 22 (a)). Another avenue for access to functionalised, chiral heterocycles is through the symmetric conjugate addition of the nucleophile to the β-position of the α,β-unsaturated system, followed by asymmetric protonation in the α-position, generating a benzylic stereocentre (Scheme 22 (b)). A combination of both these mechanisms would lead to heterocycles furnished with vicinal stereocentres in the benzylic and homobenzylic positions (Scheme 22 (c)).
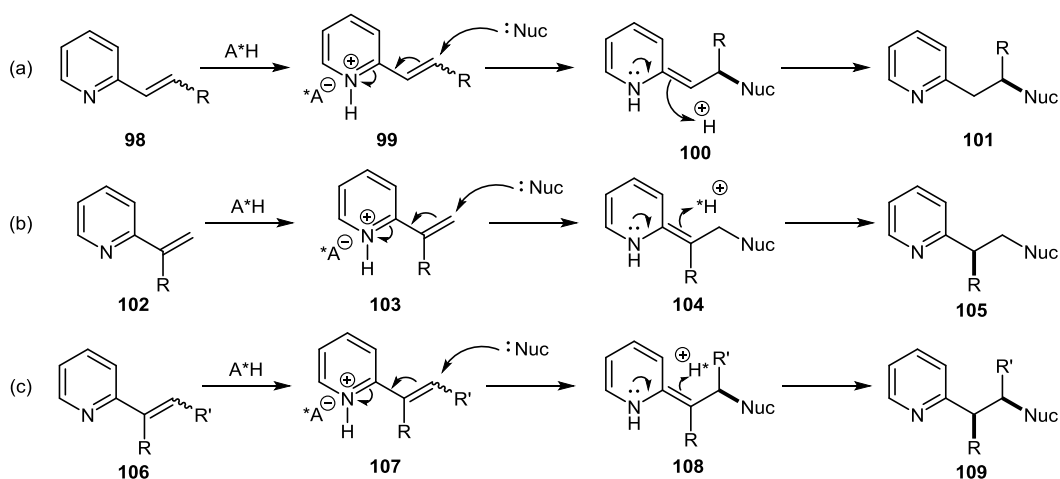
Scheme 22. Formation of benzylic (b), homobenzylic (a), and vicinal stereocentres (c) *via* asymmetric conjugate addition and protonation.

As such, the main aims of this work were to:

i) Validate the concept of Brønsted acid-catalysed conjugate addition to vinyl heterocycles.

ii) Gain access to a selection of 1,1-disubstituted olefins with diverse functionality to act as conjugate acceptors.

iii) Identify nucleophiles competent in the conjugate addition reactions.

iv) Optimise reaction conditions for efficient, enantioselective synthesis of heterocycles with benzylic stereocentres.

2.1. Synthesis of Vinyl *N*-Heterocyclic Starting Materials

Two principle routes were considered viable in gaining access to the requisite vinyl heterocycles, **112**. Initially, performing a Wittig reaction (Scheme 23 (b)) on the ketone using MePPh$_3$Br was proposed to be the best route. In addition, it was proposed that Grignard addition (Scheme 23 (a)) to the 2-carboxyl *N*-heterocycles, **110**, followed by subsequent acid-mediated dehydration would also be a viable method.
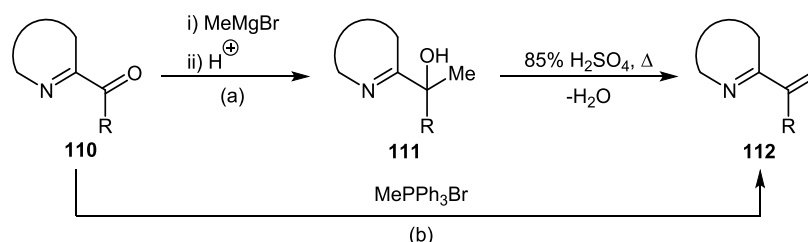
Scheme 23. Synthesis of vinyl *N*-heterocycles.

2.2. Validation of the Nucleophilic Conjugate Addition Reaction

The initial validation of the Brønsted acid-mediated conjugate addition to vinyl *N*-heterocycles was to be investigated by means of a combined nucleophile and acid screen using 2-(prop-1-en-2-yl)pyridine, **113** (Scheme 24).
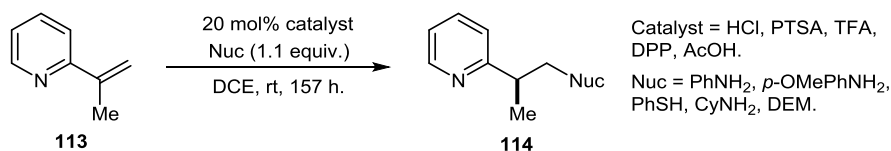
Scheme 24. Initial investigation of conjugate addition reaction.

If successful in validating the concept, one specific nucleophile and acid would be selected for optimisation of the process.

2.3. Scope of Conjugate Addition Reaction

Once an optimised synthetic strategy had been developed, a range of vinyl *N*-heterocycles and nucleophiles would be reacted to afford a selection of heterocyclic products with chiral benzylic/homobenzylic functionalities, preferably in high yields and ee's (Scheme 25).
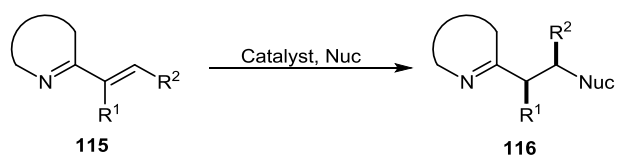
Scheme 25. Representative reaction scope.

3. Results and Discussion

3.1. Synthesis of Starting Materials

The first task at hand in the process of developing the new catalytic asymmetric conjugate addition process was to gain access to the required vinyl *N*-heterocyclic starting materials. The first heterocycle to be to be trialled was the 1,1-disubstituted 2-(prop-1-en-2-yl)pyridine, **113**, which was synthesised in high yield *via* the Wittig reaction between 2-acetylpyridine, **117**, and MePPh₃Br (Scheme 26).
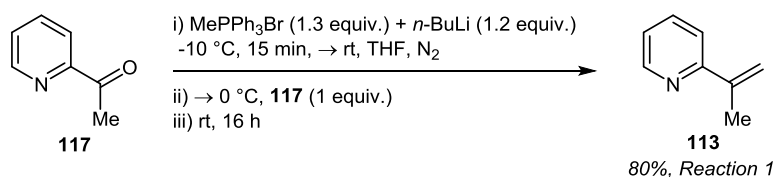
Scheme 26. Preparation of 2-(prop-1-en-2-yl)pyridine, **113**.

The second vinyl *N*-heterocycle to be trialled in the synthesis was the 1,1-disubstituted 2-(1-phenylvinyl)pyridine, **119**. The initial synthesis of this was to be by means of a Wittig reaction between 2-benzoyl pyridine, **118**, and MePPh₃Br (Scheme 27).
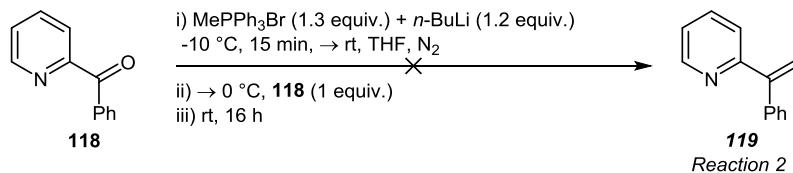
Scheme 27. Initial attempt to synthesise 2-(1-phenylvinyl)pyridine, **119**.

However, the reaction did not afford the desired product. Instead, an uncharacterisable mixture was obtained on three separate attempts of the Wittig reaction. An alternative route to synthesise compound **119** was then devised which gave the product in high yield. This involved a Grignard addition of MeMgBr to 2-benzoyl pyridine, **118**, to form tertiary alcohol **120**, then subsequent acid-mediated dehydration to afford **119** (Scheme 28).
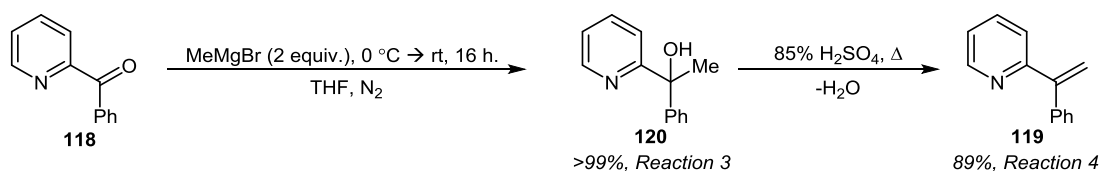
Scheme 28. Preparation of 2-(1-phenylvinyl)pyridine, **119**.

The vinyl quinolines (which were eventually used due to the poor reactivity of the vinyl pyridine system) could have been prepared *via* a Wittig reaction between the 2-carbonyl quinolones and MePPh₃Br. However, based on the previous failure of the Wittig reaction to produce 2-(1-phenylvinyl)pyridine, **119**, (Scheme 27) and the contrary success of the alternative route of Grignard addition and subsequent dehydration (Scheme 28), the 1,1-disubstituted vinyl quinolines were prepared from quinoline-2-carboxaldehyde, **121**, *via* the route of the alcohol formation and dehydration illustrated in Scheme 29.
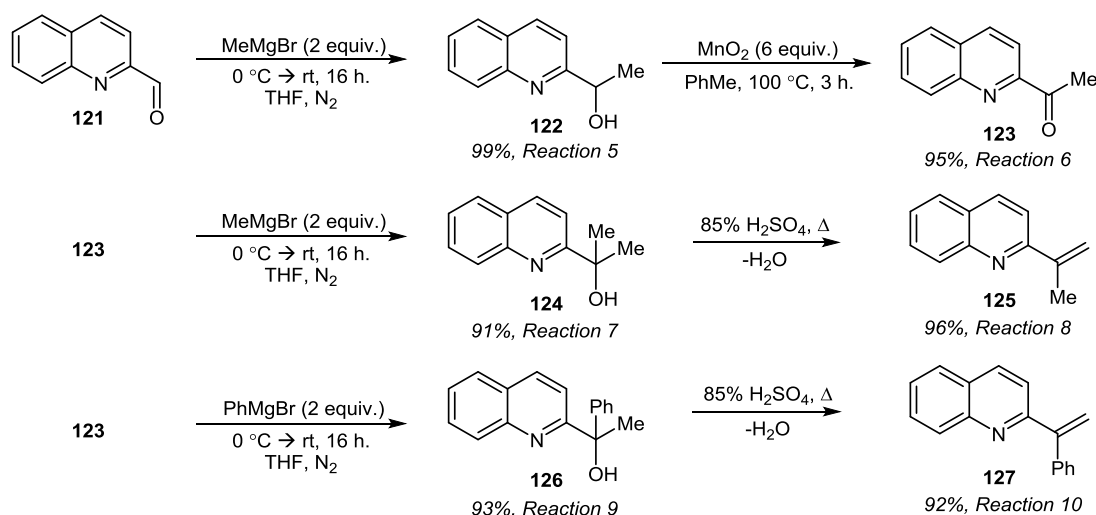
Scheme 29. Preparation of vinyl quinolines **125** and **127**.

Firstly, to gain access to **125** and **127**, quinoline-2-carboxaldehyde, **121**, was subjected to the Grignard addition of MeMgBr to afford **122** in 99% yield. **122** was then oxidised to the corresponding ketone to produce common intermediate **123** in 95% yield. **123** was then seperately subjected to the Grignard additions of MeMgBr and PhMgBr to afford the corresponding alcohols, **124** and **126**, in 91% and 93% yield, respectively. **124** and **126** were then dehydrated by refluxing in 85% aqueous H_2SO_4 to produce the corresponding vinyl quinoline derivatives, **125** and **127**, in 96% and 92% yield, respectively.

3.2. Initial Studies of Conjugate Addition Reactions to Vinyl *N*-Heterocycles

3.2.1. Proposed Reaction Mechanism

In terms of mechanism, the reaction, based on a prototypical substrate, was proposed to proceed *via* the process detailed in Scheme 30.
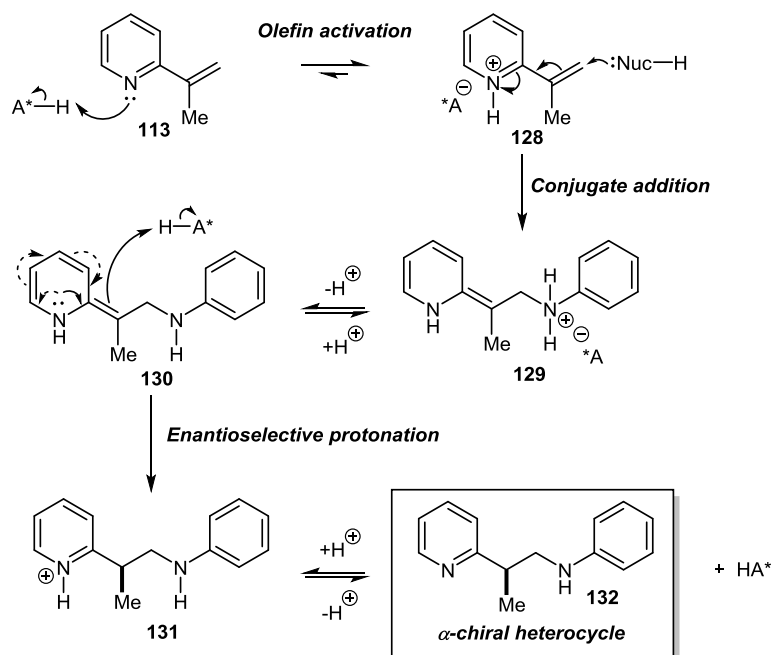
Scheme 30. Mechanism of the conjugate addition reaction based on a prototypical substrate.

The first step in the mechanism is to activate the vinyl *N*-heterocycle, **113**, to nucleophilic attack. This is achieved *via* protonation of **113** by the chiral phosphoric acid to afford an activated pyridinium (or equivalent), **128**. Protonation of the heterocyclic nitrogen causes a release of electron density from the heterocycle to the newly formed nitrogen-hydrogen sigma bond, significantly lowering the LUMO of the electrophile, making it more susceptible to nucleophilic attack.[45] This activated species can then act as the Michael acceptor. The nucleophile then attacks Michael acceptor **128** *via* 1,4-addition to generate a prochiral enamine intermediate, **129**. The nitrogen lone pair on **130** can then re-aromatise the pyridine, subsequently picking up a proton from the chiral proton source. This is the key stereodefining event in the process. The subsequently generated pyridinium form of the product, **131**, can then be neutralised, producing the desired product, **132**.

3.2.2. Asymmetric Protonation in the Conjugate Addition Reaction

The proposed protonation of enamine species, **130** (Scheme 30), is the key stereodefining event in the reaction. The field of asymmetric protonation is one which has been pioneered by groups such as Fehr[46] and has since evolved as a highly effective method of generating enantioenriched compounds from either their racemate or from their prochiral precursors.[2] The principles and applications of asymmetric protonation have been discussed in Section 1. In the context of this project, the asymmetric protonation is a result of rearomatisation of the heterocycle-derived enamine intermediate **133** (Figure 7). However, the principles of enantioselective protonation remain the same in any case.
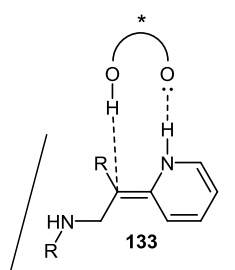
Figure 7. Prochiral enamine intermediate hydrogen bonding to a chiral catalyst.

3.2.3. Conjugate Addition to 1,1-Disubstituted Vinyl Pyridines

The various Brønsted acid catalysts used in the reactions herein are structurally represented in Figure 8 for convenience of reference.

134. R = H
135. R = NHTf
136. R = t-Bu
137. R = 4-(F$_3$C)C$_6$H$_4$
138. R = 3,5-(F$_3$C)C$_6$H$_4$
139. R = 3,5-(MeO)C$_6$H$_4$
140. R = 2-naphthyl
141. R = Mes
142. R = 4-(Mes)C$_6$H$_4$
143. R = 3,5-(Mes)C$_6$H$_4$
144. R = 4-(Cl)C$_6$H$_4$
145. R = 4-(Ph)C$_6$H$_4$
146. R = 2,4,6-(i-Pr)C$_6$H$_2$

147. R = I
148. R = 4-(Cl)C$_6$H$_4$
149. R = 4-(Ph)C$_6$H$_4$
150. R = 4-(i-Pr)C$_6$H$_4$
151. R = 3,5-(Cl)C$_6$H$_3$
152. R = Ph
153. R = 1-Naphthyl
154. R = Mes
155. R = 2,4,6-(i-Pr)C$_6$H$_2$
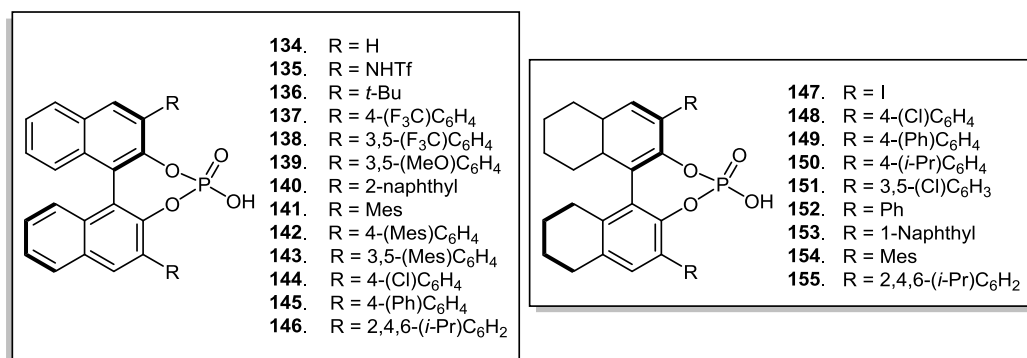
Figure 8. Brønsted acid catalysts used in the conjugate addition reactions explored in this chapter.

With 2-(prop-1-en-2-yl)pyridine **113** in hand, the next step in the process was to validate the concept of the Brønsted acid-mediated conjugate addition reaction. This heterocycle was reacted with a range of nucleophiles and acid catalysts to develop an initial understanding of the reactivity of the system (Table 3).
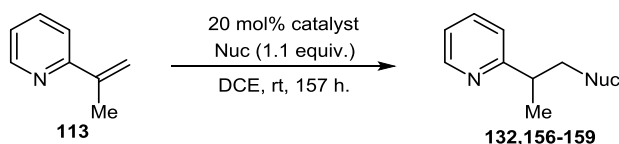
Nucleophile	Product Number	Catalyst (% Conversion, *Reaction no.*)[a]					
		HCl	PTSA	TFA	DPP	AcOH	No cat.
PhNH$_2$	132	24%, *11*	22%, *12*	28%, *13*	44%, *14*	5%, *15*	NR, *16*
p-OMePhNH$_2$	156	50%, *17*	51%, *18*	22%, *19*	39%, *20*	8%, *21*	NR, *22*
PhSH	157	78%, *23*	81%, *24*	77%, *25*	71%, *26*	74%, *27*	55%, *28*
CyNH$_2$	158	NR, *29*	NR, *30*	NR, *31*	NR, *32*	NR, *33*	NR, *34*
DEM	159	NR, *35*	NR, *36*	6%, *37*	NR, *38*	NR, *39*	NR, *40*

[a] NR = no reaction. Reactions analysed by NMR.

Table 3. Results of initial trial reactions.

The initial trial reactions were carried out using nucleophiles including an aromatic primary amine (PhNH$_2$), an electron-rich aromatic primary amine (*p*-MeOPhNH$_2$), an aliphatic primary amine (CyNH$_2$), an aromatic thiol-based nucleophile (PhSH), and a carbon-based nucleophile (DEM). The different acid catalysts were selected to create a pK_a range[38] from -8 to 5 (HCl = *ca.* -8, PTSA = *ca.* -2, TFA = *ca.* -0.25, DPP = *ca.* 2, AcOH = *ca.* 4.8) to develop a relationship between the acid catalyst pK_a and reactivity. Control reactions were carried out for each nucleophile to determine which nucleophiles, if any, had an uncatalysed background reaction.

Aniline displayed good reactivity in the system with HCl, PTSA, TFA, and DPP. However, poor reaction was achieved with AcOH. This could be due to the fact that the pK_a of AcOH (*ca.* 4.8) and the pK_aH of pyridine (*ca.* 5.2) are very close, which could cause the equilibrium to disfavour pyridinium formation, thus, the electrophile may not be sufficiently activated to the conjugate addition reaction. The control reaction for aniline afforded no product which

showed promise that there was no background reaction involved and that the process is indeed acid-catalysed. These preliminary studies gave the indication that aniline could be a good nucleophile in the proposed conjugate addition reaction.

p-Anisidine displayed generally similar reactivity to aniline in the reactions with HCl, PTSA, TFA, and DPP. Again, only the AcOH reaction afforded poor conversion to product, possibly due to the small pK_a difference between the carboxylic acid and pyridinium. The reactivity with *p*-anisidine was slightly increased in the reactions with HCl and PTSA since it is a stronger nucleophile than aniline, due to the electron-donating methoxy group *para* to the amine functionality. However, the reactions with TFA and DPP showed slightly less reactivity than the corresponding aniline reactions. As with aniline, the control reaction for *p*-anisidine afforded no product. These preliminary studies gave the indication that *p*-anisidine could be a suitable nucleophile in the conjugate addition reaction.

Thiophenol displayed very significant reactivity with each acid. Importantly, thiophenol demonstrated a strong background reaction in the control. This indicated that the thiophenol reaction may have been self-catalysed (Scheme 31).
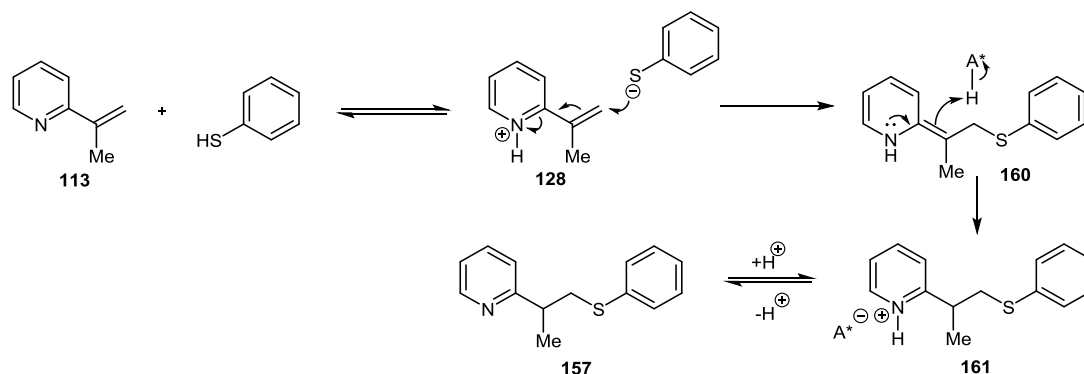
Scheme 31. Self-catalysed thiophenol conjugate addition.

When the pK_aH of pyridine (*ca.* 5.3) is compared with the pK_a of thiophenol (*ca.* 6), it is reasonable to envisage protonation of the pyridine by the acidic proton of the thiophenol. This would generate the pyridinium cation, **128**, which could be attacked by the thiophenolate anion to afford the conjugate addition product, **157**. Since this background reaction is self-catalysed and does not need the assistance of an acid catalyst, there would be no ion pairing with the chiral acid catalyst, eliminating the possibility of an enantioselective process. This gave the indication that if aryl thiol-based nucleophiles are to

be used in the enantioselective conjugate addition reaction, the background reaction would have to be thermally controlled. While no conjugate additions with alkyl thiols have been trialled thus far, the pK_a of such compounds (*ca.* 10) suggests that these nucleophiles may react desirably in the conjugate addition with no background reaction.

Cyclohexylamine displayed no reactivity. It could be reasoned that since cyclohexylamine is more nucleophilic than aniline or *p*-anisidine, it should therefore have displayed better reactivity. However, this was not reflected in the reactivity seen in the trialled conjugate addition reactions. This was likely due to cyclohexylamine acting as more of a Brønsted base than a nucleophile in the reaction, leading to an equilibrium in favour of generating the cyclohexyl aminium, **162**, (pK_a = *ca.* 10), rather than the required conjugate acceptor pyridinium, **128**, (pK_a = *ca.* 5.3) (Scheme 32).
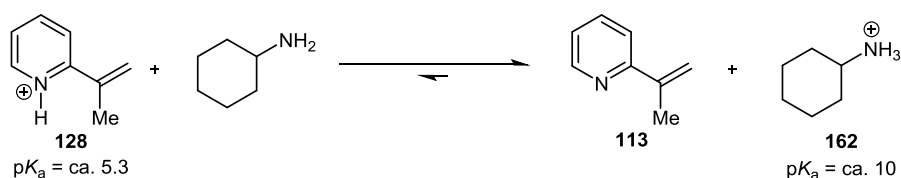
Scheme 32. Equilibrium in favour of aminium over pyridinium.

This would diminish the chance of the electrophile being activated *via* the pyridinium, **128**, rendering the conjugate addition reaction inactive. However, since the pK_aH of aniline (*ca.* 4.6) is less than the pK_aH of pyridine (*ca.* 5.2), the equilibrium in that case would be more balanced, allowing the formation of **128** and subsequent conjugate addition, which would explain why, even though aniline is less nucleophilic than cyclohexylamine, aniline outperformed cyclohexylamine as a nucleophile in the conjugate addition reaction (Scheme 33).
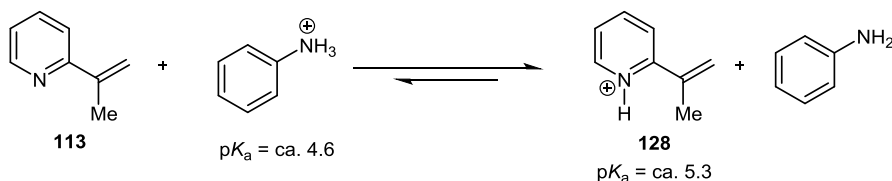
Scheme 33. Equilibrium in favour of pyridinium over anilinium.

The only acid to facilitate a reaction with diethyl malonate was TFA, which led to very poor conversion. This indicated that if carbon-based nucleophiles are to be used in the conjugate

addition reaction then acid catalysis may not be an effective method and perhaps chiral base catalysis would be more effective in order to activate the carbogenic nucleophile to attack the Michael acceptor.

Overall, based on the reactivities observed in the trial reactions, aniline and anisidine appeared to be the nucleophiles best suited for further exploration. To this effect, aniline was selected as the nucleophile of choice for optimisation.

3.2.3.1. Nucleophile Screen at Raised Temperature

Having carried out an initial study of nucleophiles and acid catalysts at room temperature and achieving no reactivity in some cases (Table 3), the next step was to carry out the reactions at raised temperature to determine which nucleophiles would be applicable to the conjugate addition reaction upon thermal promotion (Table 4).
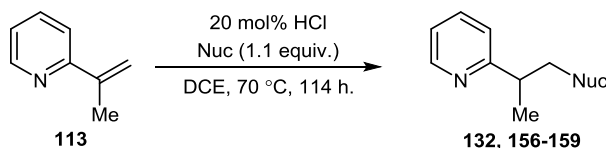
Nucleophile	Product Compound Number	% Conversion, *Reaction no.*
PhNH$_2$	132	49%, *41*
p-OMePhNH$_2$	156	76%, *42*
PhSH	157	90%, *43*
CyNH$_2$	158	11%, *44*
DEM	159	7%, *45*

Reactions analysed by NMR.

Table 4. Nucleophile screen under thermal promotion.

Based on the results in Table 4 it can be seen that, by raising the temperature of the reaction, the previously unreactive nucleophiles such as CyNH$_2$ and diethyl malonate showed some susceptibility towards the conjugate addition reaction. However, both nucleophiles showed limited reactivity at best (Tables 3 and 4), even under thermal promotion, which gave a further indication that the Brønsted acid-catalysed route may not be best suited to relatively strongly basic nucleophiles (CyNH$_2$) or carbon-based nucleophiles (diethyl malonate).

3.2.3.2. Cinchona Alkaloid-catalysed Malonate Addition

Due to the poor reactivity observed in the Brønsted acid-catalysed conjugate addition reaction with diethyl malonate, both at room temperature (Table 3) and at raised temperature (Table 4), a base-catalysed process directed by a chiral counter-cation was envisaged and trialled with a chiral cinchona alkaloid catalyst, (+)-cinchonine, that would generate an ion pair between the malonate anion and the (+)-cinchonine cation. If this ion pairing could be sustained throughout the conjugate addition process, generation of the desired product, **159**, in an asymmetric fashion could be achieved (Scheme 34).
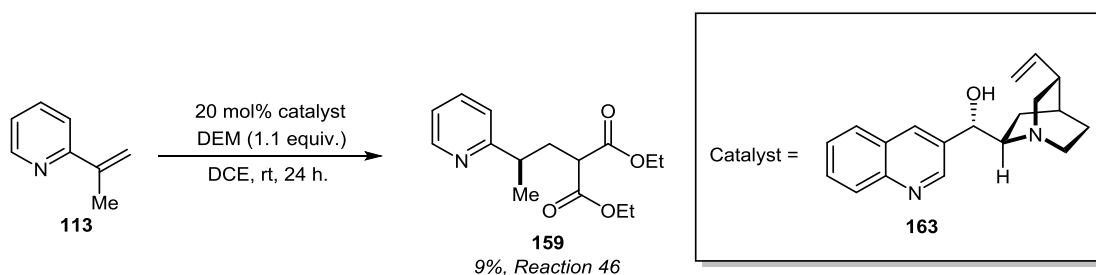
Scheme 34. Cinchona alkaloid-catalysed conjugate addition of DEM.

NMR analysis of this reaction showed 9% conversion at room temperature after 24 hours, which was an improvement over the outcome of heating DEM with the olefin in acid for 114 hours (Table 4, **Reaction 45**), which only gave a trace of product. This suggested that if carbon-based nucleophiles are to be used in the conjugate addition reaction, chiral base-mediated nucleophile activation could be preferred over a Brønsted acid-catalysed process.

3.2.3.3. Variation of the Olefin Substituent – Conjugate Addition to 1,1-Disubstituted Vinyl Pyridine Bearing an Aromatic Group

To achieve a further understanding of the reactivity of the system, it was necessary to undertake studies into the reactivities of the vinyl N-heterocyclic Michael acceptors. To determine the relative reactivities of an olefinic Michael acceptor bearing an alkyl substituent (2-(prop-1-en-2-yl)pyridine), **113**, and one bearing an aromatic substituent (2-(1-phenylvinyl)pyridine), **119**, when exposed to both an electron-rich nucleophile and an electron-deficient nucleophile, a set of reactions were carried out subjecting each electrophile to the conjugate addition reaction with both *p*-anisidine and *p*-nitroaniline (Table 5).
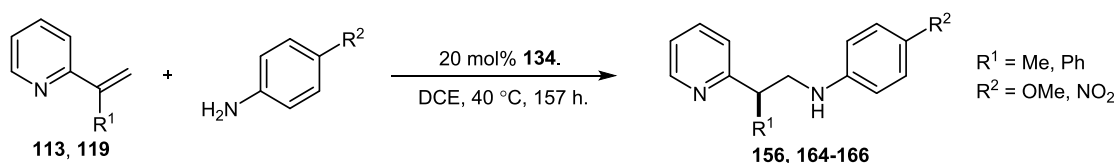
R¹ (Compound Number)	R², % Conversion, (Compound Number), *Reaction no.*	
	OMe	NO₂
Me (113)	48%, (156), *47*	27%, (164), *48*
Ph (119)	87%, (165), *49*	46%, (166), *50*

^a Reactions analysed by NMR.

[a] Reactions analysed by NMR.

Table 5. Preliminary studies into the effects of olefin substitution and nucleophile strength on the conjugate addition reaction.

As expected, the results of these experiments were consistent with *p*-anisidine being more nucleophilic and *p*-nitroaniline being less nucleophilic, as a stronger reaction is displayed with *p*-anisidine than *p*-nitroaniline with both Michael acceptors. The Michael acceptor bearing the aromatic ring substituent proved to be more susceptible to the conjugate addition reaction than the acceptor bearing a methyl group. This could be rationalised in that the connectivity between the aromatic rings on an aromatic 1,1-disubstituted vinyl *N*-heterocycle, **119**, is that of a cross-conjugated system where conjugation between both aromatic rings cannot be achieved through the connecting terminal olefin. Therefore, conversion to a fully conjugated system, **168**, by means of nucleophilic attack of the terminal olefin and resonance of electrons through the connecting benzylic carbon to form a fully conjugated system would be energetically favourable (Scheme 35).
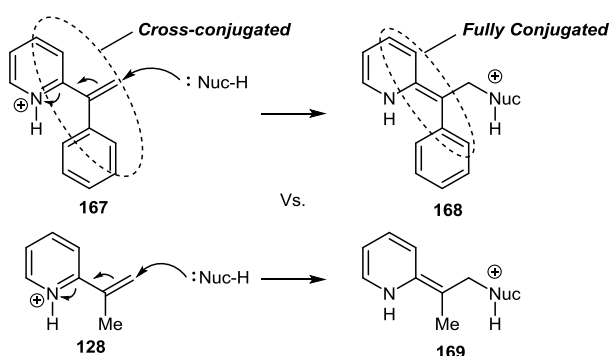
This suggests generally that vinyl *N*-heterocyclic Michael acceptors bearing an aromatic substituent may be more susceptible to the conjugate addition reaction than the corresponding alkyl substituted Michael acceptor. Indeed, this was the reactivity profile observed upon analysis of the reactions (Table 5).

3.4. Concentration and Temperature Studies

The first parameters to be evaluated were concentration and temperature. To achieve this, parallel reactions were run at a range of concentrations at room temperature (Scheme 36) using **134** (Figure 8). Time points of each reaction were analysed by HPLC. The results of the concentration study at room temperature are shown in Figure 9.

Conc.	Time (*Reaction no.*)
0.2 M	24 h (*51*), 48 h (*52*), 72 (*53*), 96 (*54*), 157 (*55*)
0.5 M	24 h (*56*), 48 h (*57*), 72 (*58*), 96 (*59*), 157 (*60*)
1 M	24 h (*61*), 48 h (*62*), 72 (*63*), 96 (*64*), 157 (*65*)
2 M	24 h (*66*), 48 h (*67*), 72 (*68*), 96 (*69*), 157 (*70*)
5 M	24 h (*71*), 48 h (*72*), 72 (*73*), 96 (*74*), 157 (*75*)
10 M	24 h (*76*), 48 h (*77*), 72 (*78*), 96 (*79*), 157 (*80*)
Neat	24 h (*81*), 48 h (*82*), 72 (*83*), 96 (*84*), 157 (*85*)
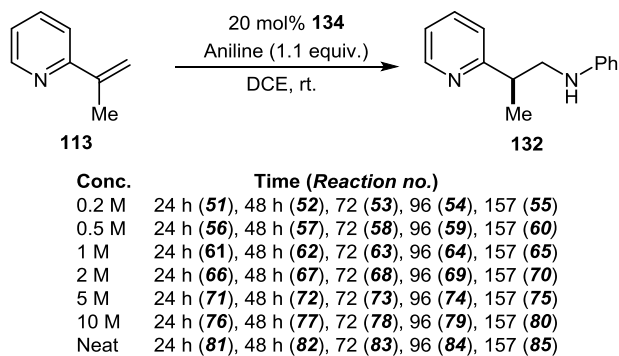
Scheme 36. Concentration study of conjugate addition reaction of aniline to **113** at room temperature.
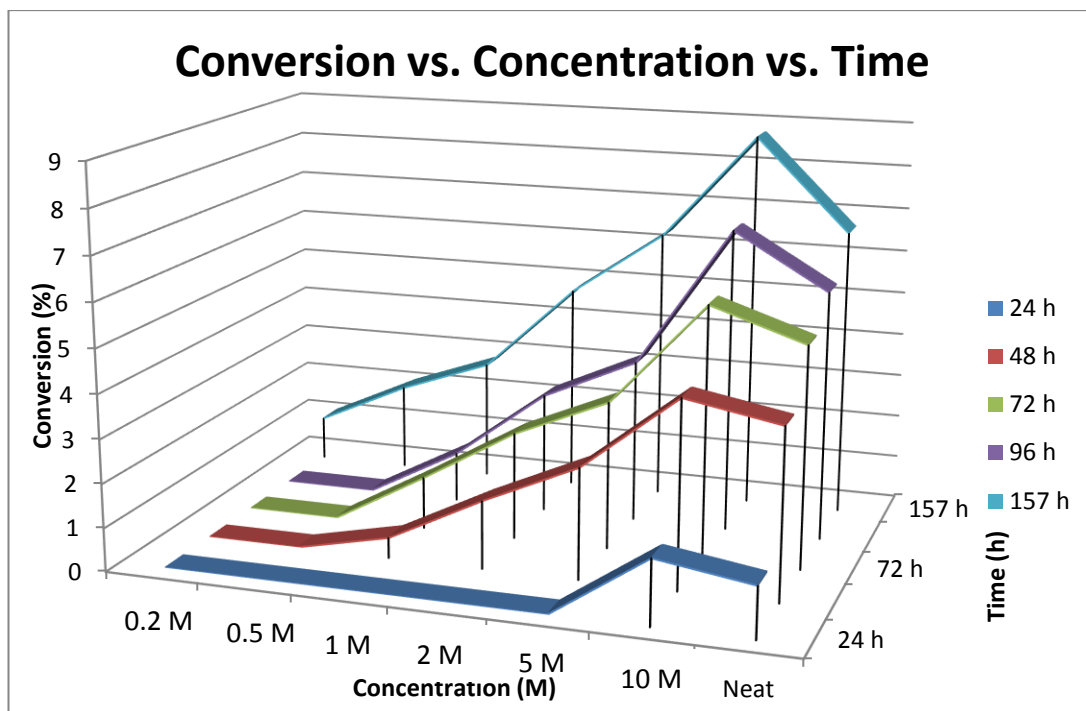
Figure 9. Conversion vs.concentration vs. time at room temperature.

Although conversion was below 10% in this study, making interpretation of the results difficult, the results loosely suggested that as the concentration increased, the conversion increased to a level where the optimum appeared to be 10 M.

However, the conversion at room temperature was below 10% after 157 hours, which indicated that the reaction may need thermal promotion to increase the conversion to a synthetically useful level. To this effect, the same reactions were repeated at 40 °C (Scheme 37), the results of which are shown in Figure 10.

Conc.	Time (*Reaction no.*)			
0.2 M	30 h (**86**),	54 h (**87**),	78 (**88**),	157 (**89**)
0.5 M	30 h (**90**),	54 h (**91**),	78 (**92**),	157 (**93**)
1 M	30 h (**94**),	54 h (**95**),	78 (**96**),	157 (**97**)
2 M	30 h (**98**),	54 h (**99**),	78 (**100**),	157 (**101**)
5 M	30 h (**102**),	54 h (**103**),	78 (**104**),	157 (**105**)
10 M	30 h (**106**),	54 h (**107**),	78 (**108**),	157 (**109**)
Neat	30 h (**110**),	54 h (**111**),	78 (**112**),	157 (**113**)
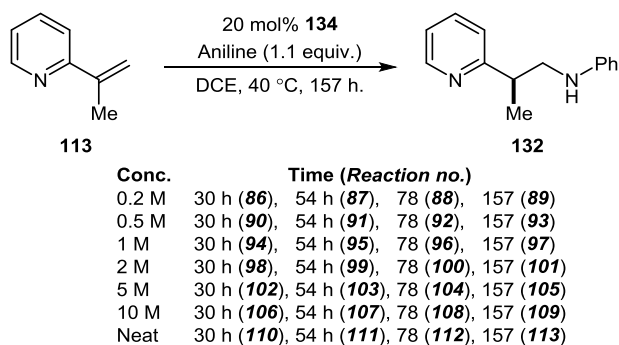
Scheme 37. Concentration study of conjugate addition reaction of aniline to **113** at 40 °C.
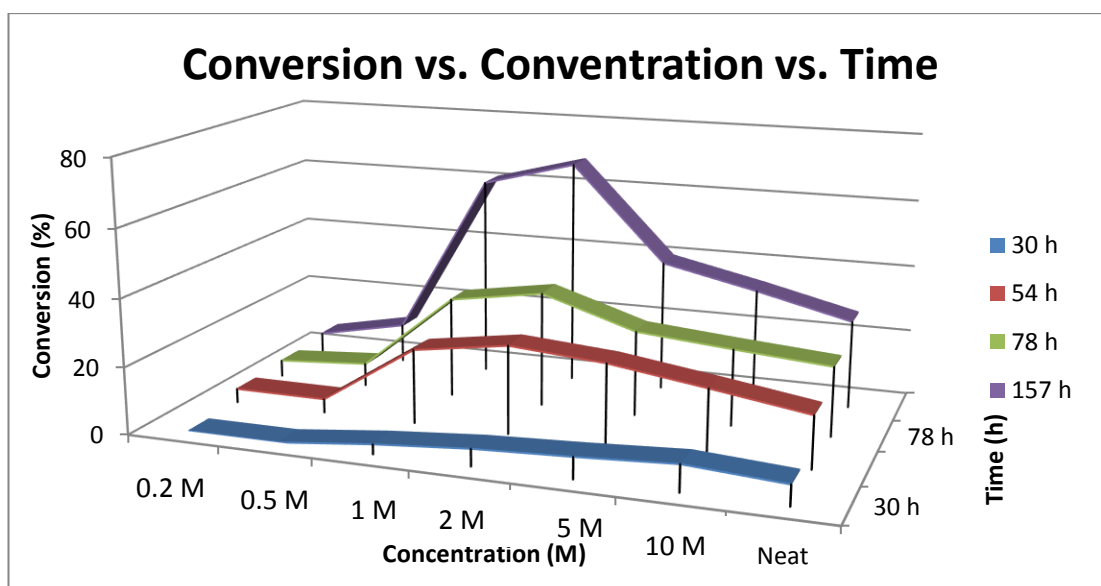
Figure 10. Conversion vs. concentration vs. time at 40 °C.

From Figure 10 it was clear that as the temperature of the reaction was increased, conversion also increased. The result of carrying out the reactions at 40 °C instead of room temperature was a 7.5 fold increase from 9% to 68%. However, it is noteworthy that the optimum concentration for conversion at 40 °C is not 10 M as with the room temperature reactions, but 2 M. Approaching 2 M, the conversion increased rapidly and decreased thereafter. The general trend was the conversion increased as the concentration increased until, after the optimum concentration, the conversion decreased. However, the optimum concentration for each temperature was different. The reason for such a difference in optimum concentrations at different temperatures was unclear at this stage. However, a possible rationale for this could be that as the reaction mixture was heated, the reagents (particularly the catalysts which, for the most part, were partially soluble in these reaction mixtures at lower temperatures) became more soluble and, thus, were more able to react. This would give a more accurate representation of how the reaction proceeded (with particular regard to optimum concentration) when all reagents were fully in solution.

3.5. Solvent Screening

The next parameter investigated was the choice of reaction solvent. This was achieved *via* a simple solvent screen by performing the reaction using solvents with a range of polarities from 0 D to 4 D (Scheme38). The three different types of solvent used for screening were:

polar protic solvents (MeOH, EtOH, IPA), polar aprotic solvents (DMF, acetone, MeCN, DMSO, DCM, DCE, Et₂O, THF), and apolar aprotic solvents (hexane, PhMe). The results of the solvent screen at room temperature are shown in Figure 11.
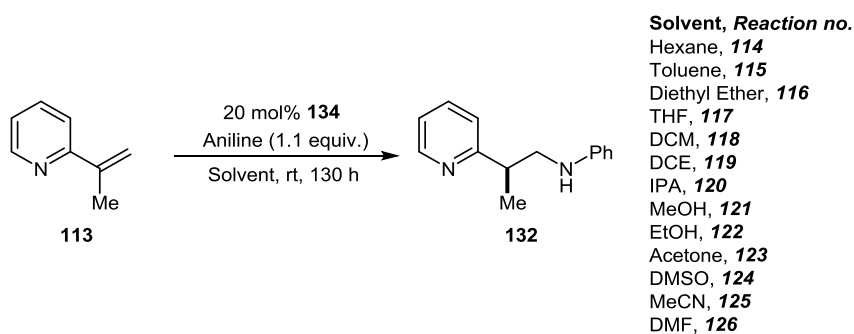
Scheme 38. Solvent screen for the conjugate addition reaction of aniline to **113**.
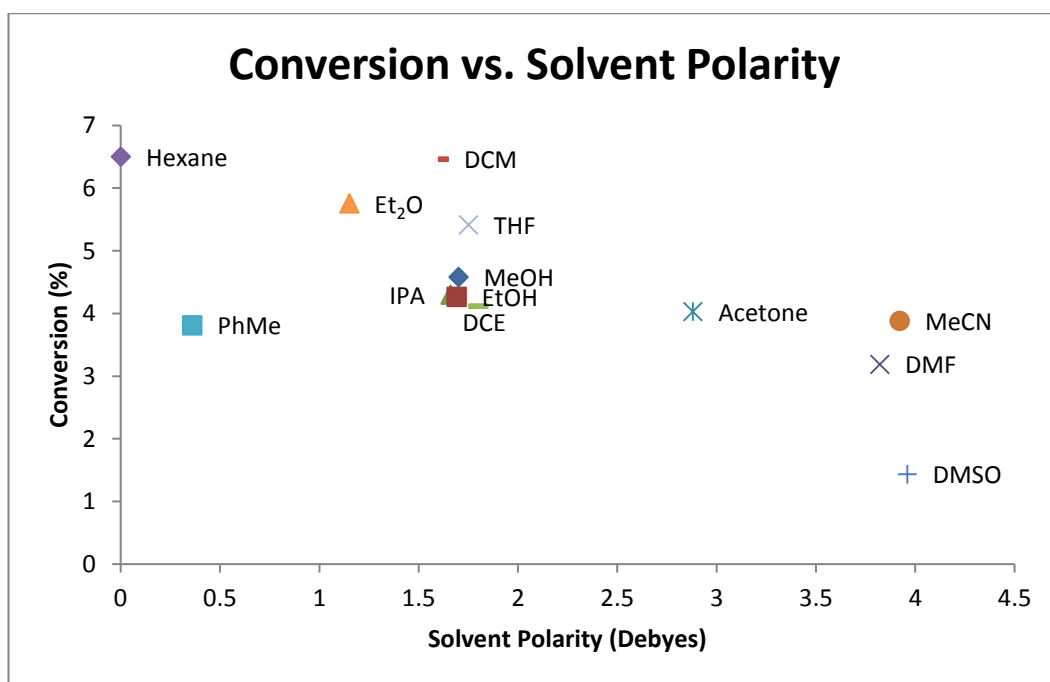
Figure 11. Conversion vs. solvent polarity.

From the results of the solvent screen in Figure 11 it can be seen that, again, conversion was below 10%. Therefore, interpretation of the results became difficult.

3.6. Study of the Optimum pK_a of the Acid Catalyst

Based on the results of the initial nucleophile/acid screen (Table 3) it was apparent that, for each nucleophile, the choice of acid catalyst had an effect on the extent of the reaction. Therefore, a further investigation of this was carried out in the form of an acid screen (Scheme 39). A number of acids were chosen based on their pK_a values[38] to create a wide spectrum of catalyst acidity. The acid catalysts chosen were PTSA (pK_a = *ca.* 0.9), HCl (pK_a = *ca.* 2), **135** (Figure 8, pK_a = *ca.* 3.34), **134** (Figure 8, pK_a = *ca.* 3.37) TFA (pK_a = *ca.* 3.4), and AcOH (pK_a = *ca.* 12.6). The results of this pK_a study are shown in Figure 12. The pK_a values are reported in DMSO as this was the only solvent in which experimentally calculated pK_a values for each of the acids used had been reported.[38, 47, 48] However, any trends observed based on acid pK_a in DMSO may not be a true reflection of trends in other reaction solvents as pK_a's are known to differ to varying extents in different solvents.

Acid	Acidity	Time (*Reaction no.*)
PTSA	0.9	24 h (*127*), 48 h (*128*), 72 (*129*), 96 (*130*)
HCl	2	24 h (*131*), 48 h (*132*), 72 (*133*), 96 (*134*)
135	3.34	24 h (*135*), 48 h (*136*), 72 (*137*), 96 (*138*)
134	3.37	24 h (*139*), 48 h (*140*), 72 (*141*), 96 (*142*)
TFA	3.4	24 h (*143*), 48 h (*144*), 72 (*145*), 96 (*146*)
AcOH	12.6	24 h (*147*), 48 h (*148*), 72 (*149*), 96 (*150*)
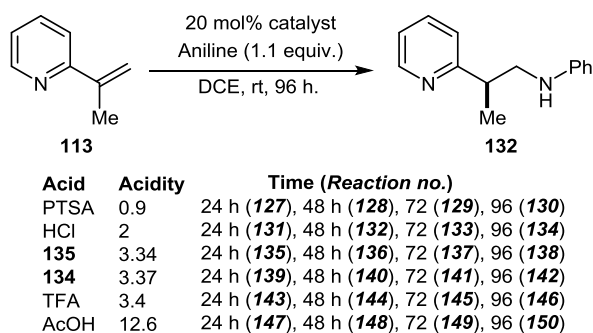
Scheme 39. Acid screen for the conjugate addition of aniline to **113**.
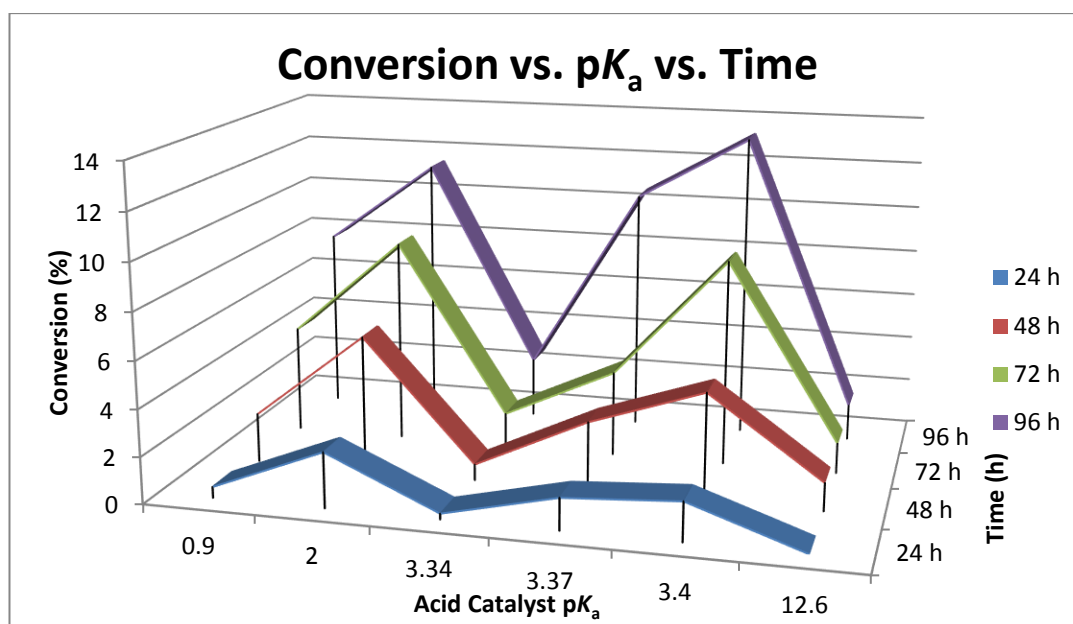
Figure 12. Conversion vs. pK_a vs. time.

An unexpected reactivity profile was observed upon analysis of the data generated from the acid screen (Figure 12). As the pK_a was increased from 0.9 (PTSA) to 2 (HCl), the conversion increased. However, upon further increase to 3.34 (**135**), the conversion dropped sharply. The conversion then increased in the reaction with **134** (pK_a = 3.37) and increased further upon using the catalyst with *p*K_a to 3.4 (TFA). **134**, **135** and TFA, all having essentially the same pK_a value, showed marked differences in their reactivities, suggesting that pK_a alone cannot be the determining factor in an acids ability to facilitate this reaction. As such, factors such as solubility of the acid catalyst may play an important role. In the reaction with AcOH (pK_a = 12.6), the conversion then dropped significantly. It was expected that the conversion would increase with decreasing pK_a in that by increasing the pK_a of the acid catalyst, the pyridine/pyridinium equilibrium would disfavour pyridinium (Scheme 40).
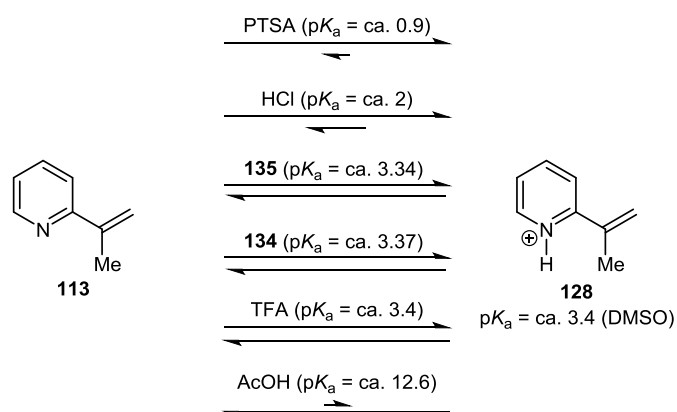
Scheme 40. Illustrative relative pyridine/pyridinium equilibria for PTSA, HCl, **135**, **134**, TFA, and AcOH.

However, this was not the trend observed upon analysis of the results. This gave an indication that the pK_a of the catalyst alone was not the determining factor in the extent of the reaction. As such, the solubility or size of the catalyst appeared to also have a large influence on the reaction outcome. At this point, the cause of this unexpected reactivity was unknown and requires further investigation.

3.7. Probing the Enantioselectivity *via* a Catalyst Screen.

In order to determine whether any asymmetric induction could be achieved in the conjugate addition reaction, a catalyst screen was carried out (Scheme 41). Ten catalysts were trialled in the conjugate addition reaction, initially at room temperature (Figure 13). The catalysts used in this study are structurally illustrated in Figure 8.

Catalyst	Reaction no.
134	151
136	152
137	153
138	154
139	155
140	156
141	157
142	158
143	159
148	160
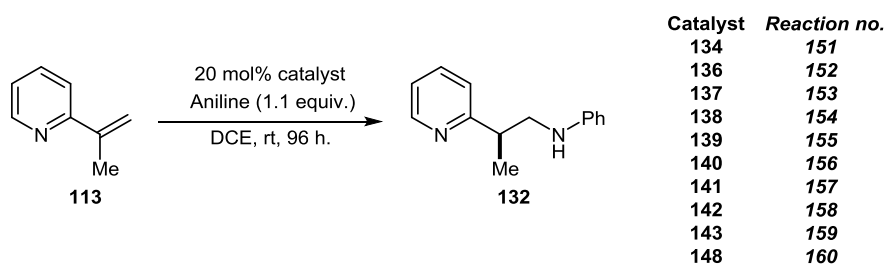
Scheme 41. Catalyst screening in the conjugate addition reaction.
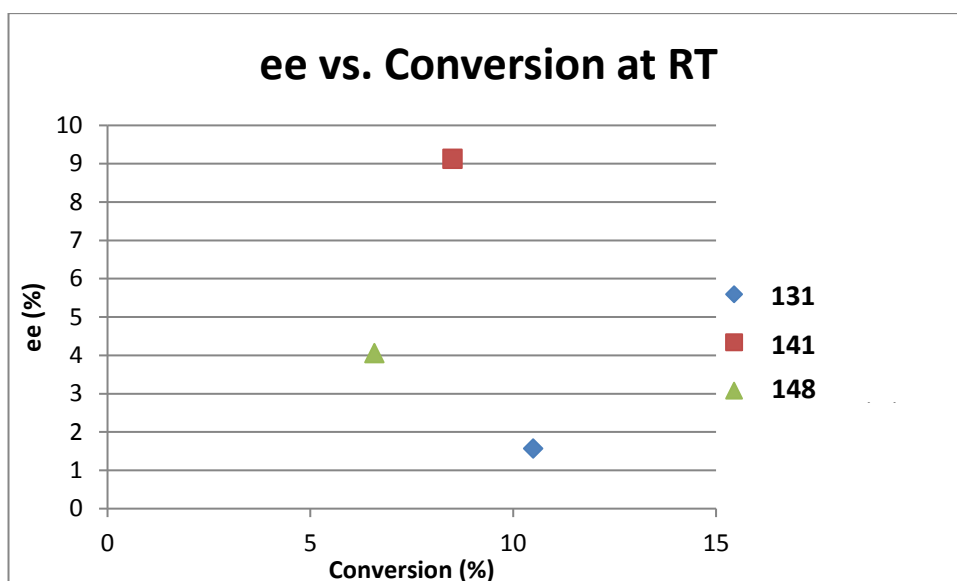
Figure 13. ee vs. conversion for **134**, **141**, and **148** at rt.

As can be seen from Figure 13, after 96 hours at room temperature, only three catalysts led to the formation of any product, which were catalysts **134**, **141,** and **148**. In terms of conversion, it was difficult to interpret results at such low conversion but it seems that the least sterically hindered catalyst may have led to the highest conversion (R = H = 10.5% conversion) and the catalysts with the larger bulk in the 3/3' positions (**136**-**140**, **142**, **143**) gave no conversion to product

Since seven of the reactions trialled in Scheme 41 failed to generate any product, these were re-run at 40 °C for the same period of time to determine the conversion and ee using these catalysts under thermal promotion (Scheme 42 and Figure 14). The catalysts used in this study are structurally illustrated in Figure 8.

Catalyst	Reaction no.
136	161
137	162
138	163
139	164
140	165
142	166
143	167
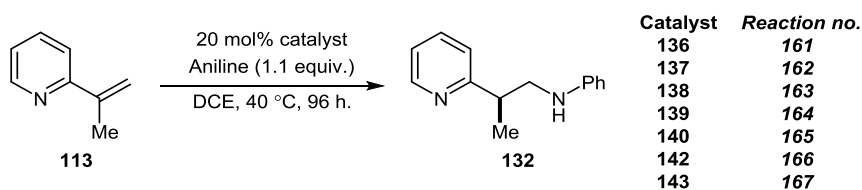
Scheme 42. Catalyst screen at elevated temperature.
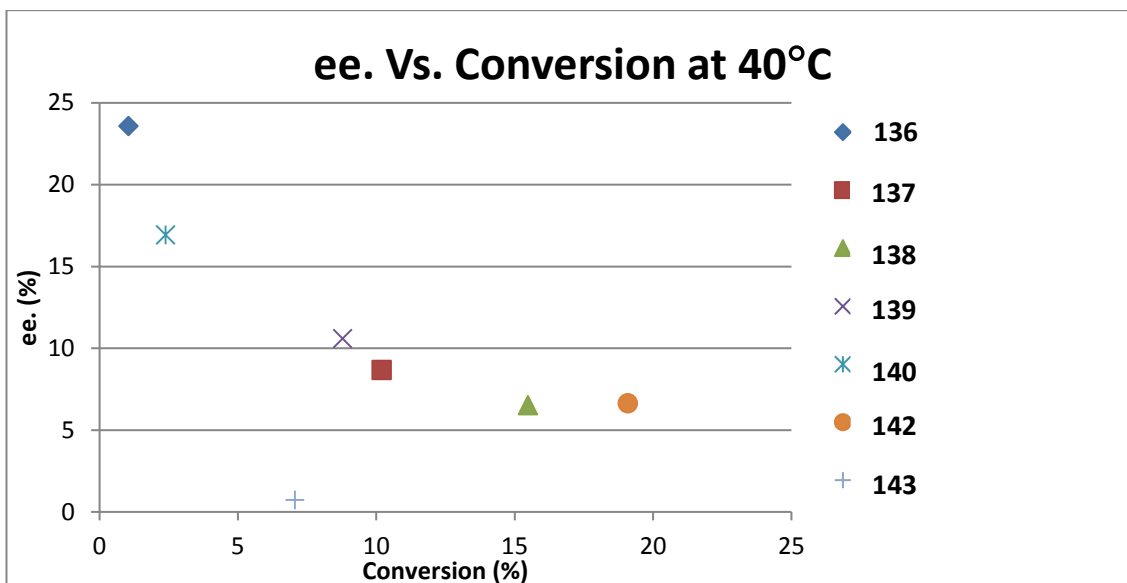
Figure 14. ee vs. conversion for **136**-**140**, **142**, **143** at 40 °C.

The results observed in Figure 14 suggested that as the steric bulk of the substituents in the 3/3' positions of the catalyst increased, the conversion decreased as the substrate has more difficulty in binding the catalyst. However, as this steric bulk increased, the enantioselectivity also increased since the catalyst's pocket would be further restricted which would favour association of one enantiotopic face of the prochiral enamine intermediate. This suggests that in order to achieve high levels of enantioselectivity while at the same time achieving high conversion, the steric bulk of the catalyst substituents, thus, the dimensions of the pocket, must be appropriately tuned.

3.8. Conjugate Addition to 1,1-Disubstituted Vinyl Quinolines

Based on the lack of reactivity observed in the vinyl pyridine studies, and with the lack of interpretable results obtained in the studies with them, the next logical step was to develop a system which was more reactive. Examination of the proposed reaction mechanism led to the proposal that vinyl quinolines would prove to be a more suitable system (Figure 15). Backed up by the increase in reactivity observed upon variation of the olefinic substituent (Table 5), the next step was to examine how the conjugate addition reaction responded to variation of the heterocycle core from a pyridine, **170**, to a quinoline, **172**. The rationale behind this was that, in the conjugate addition reaction, to generate the enamine intermediate, **171**, the energy required to perturb the aromaticity in pyridine would be

greater than energy required to perturb the aromaticity in quinoline. The reason for this energy difference is that the enamine derivative of quinoline, **173**, retains aromaticity in the adjacent ring whereas pyridine will have lost all aromaticity (Figure 15).
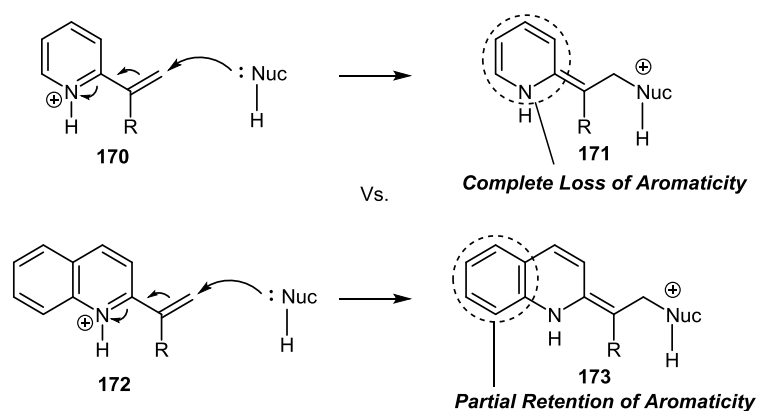
Figure 15. Aromaticity retention in vinyl quinoline system.

The expected effect of this energy difference is that nucleophilic attack and subsequent enamine intermediate generation should occur more readily for quinoline-based Michael acceptors than their pyridine-based counterparts, leading to greater reactivity and higher levels of conversion. If this could be reflected in the conjugate addition reaction, quinoline-based nucleophiles could prove to be suitable substrates in the scope of the reaction.

Another factor which allows for higher reactivity is the conversion of a cross-conjugated system to a fully conjugated system upon conjugate addition, shown in Figure 16. This was validated with the vinyl pyridine series (Table 5).
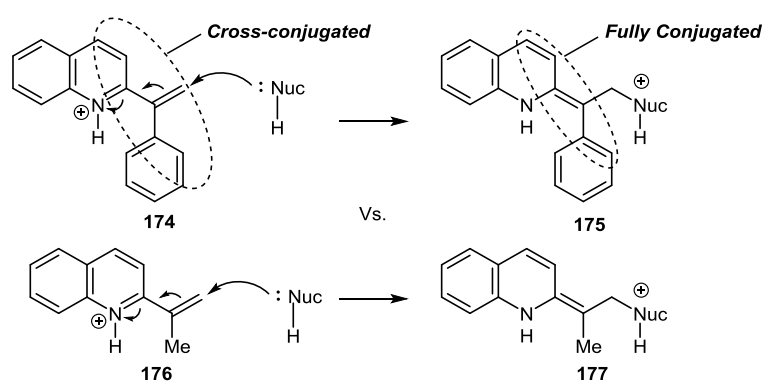
Figure 16. Conversion of a cross conjugated system to a fully conjugated system in the quinoline system.

As can be seen from Figure 16, when the substituent on the vinyl heterocycle is an aromatic ring, the system generated upon conjugate addition would be that of a fully and highly conjugated system. This would generate the potential for a more reactive system than the corresponding alkyl group system where there would be less capability for conjugation.

3.8.1. Initial Studies with Vinyl Quinolines

Based on the rationales discussed above, it was predicted that vinyl quinolines bearing an aromatic substituent would be more reactive than the previously tested vinyl pyridine system. This prediction was verified in an initial reaction between 2-(1-phenylvinyl)quinoline, **127**, and aniline (Scheme 43).
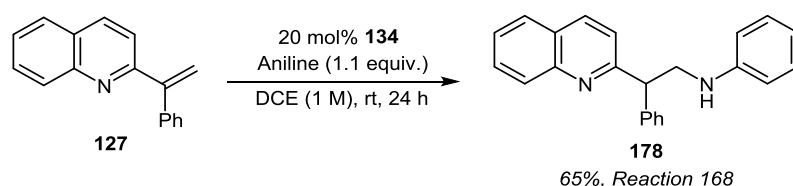
Scheme 43. Conjugate addition of aniline to **127**.

This initial result was promising in that after only 24 hours, an approximately 40 fold increase in reactivity was observed over the vinyl pyridine reaction, isolating the product in 65% yield (the conversion observed in the vinyl pyridine system was negligable (approximately 2%) under the same reaction conditions).

Based on the promising result obtained in the vinyl quinoline system, this was taken on as the preferred substrate for optimisation studies. Since compound **127** was not commercial it was synthesised according to the procedure detailed in Scheme 29.

3.8.2. Optimisation Studies with 2-(1-Phenylvinyl)quinoline

3.8.2.1. BINOL-based Phosphoric Acid Screen

With vinyl quinoline **127** in hand, the first task was to prepare and screen a larger range of chiral BINOL-based phosphoric acid catalysts than that which had already been used to determine which would be the most appropriate catalyst(s) for optimisation of the reaction conditions. The general synthesis of the generated catalysts is detailed in Scheme 44.
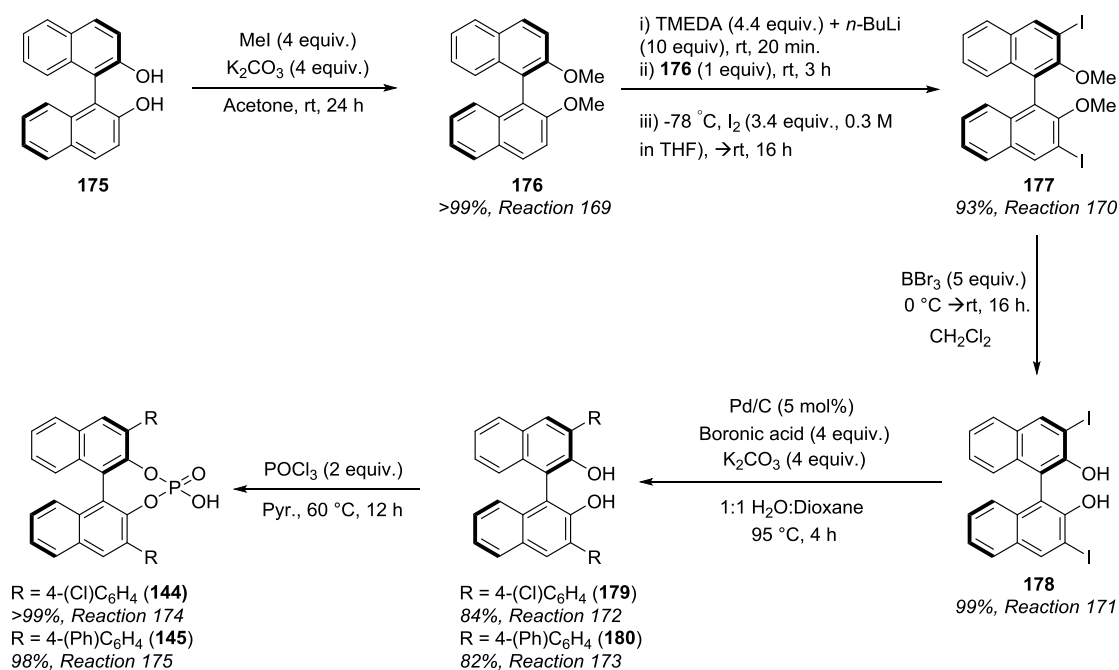
Scheme 44. General synthesis of BINOL-based phosphoric acid catalysts.

Firstly, (*R*)-BINOL, **175**, was converted to its methyl protected derivative, **176**, using iodomethane. Compound **176** was then regioselectively iodinated to generate **177**. Compound **177** was then deprotected using boron tribromide to form cross-coupling binaphthol precursor **178**. Once access to **178** was gained, this was split into different batches to perform different Suzuki cross-coupling reactions using Pd/C to generate 3,3'-difunctonalised BINOL catalyst precursors, **179** and **180**. These precursors were then converted to their respective chiral phosphoric acids, **144** and **145**, in high yields using phosphoryl chloride. A range of BINOL-based phosphoric acids, **134** and **136-145** (Figure 8) (It is appropriate to note at this point that catalysts **135-143** (Figure 8) were obtained from a project collaborator), were screened in the conjugate addition reaction at temperatures of 0 °C, room temperature and 60 °C in both THF and PhMe. The full results of this screen are shown in Table 6 along with the corresponding catalyst structures.

	0 °C				RT				60 °C			
Cat.	**THF**		**PhMe**		**THF**		**PhMe**		**THF**		**PhMe**	
	Conv.	**ee^a**	**Conv.**	**ee^a**	**Conv.**	**ee^a**	**Conv.**	**ee^a**	**Conv.**	**ee^a**	**Conv.**	**ee^a**
134	78	11, **176**^{b}	65	12, **177**^{b}	87	10, **178**^{b}	90	13, **179**^{b}	87	5, **180**^{b}	88	6, **181**^{b}
136	12	0, **182**^{b}	74	31, **183**^{b}	45	1, **184**^{b}	37	5, **185**^{b}	94	4, **186**^{b}	75	0, **187**^{b}
137	74	30, **188**^{b}	12	1, **189**^{b}	90	36, **190**^{b}	90	10, **191**^{b}	81	7, **192**^{b}	74	2, **193**^{b}
138	36	19, **194**^{b}	66	-5, **195**^{b}	63	23, **196**^{b}	96	30, **197**^{b}	86	20, **198**^{b}	89	23, **199**^{b}
139	57	-2, **200**^{b}	76	10, **201**^{b}	72	-1, **202**^{b}	92	-3, **203**^{b}	75	-2, **204**^{b}	80	-2, **205**^{b}
140	10	24, **206**^{b}	21	7, **207**^{b}	16	22, **208**^{b}	32	11, **209**^{b}	31	10, **210**^{b}	48	5, **211**^{b}
141	96	44, **212**^{b}	7	0, **213**^{b}	92	43, **214**^{b}	100	13, **215**^{b}	86	22, **216**^{b}	95	9, **217**^{b}
142	73	21, **218**^{b}	8	20, **219**^{b}	81	5, **220**^{b}	91	22, **221**^{b}	97	8, **222**^{b}	88	13, **223**^{b}
143	42	1, **224**^{b}	90	19, **225**^{b}	66	3, **226**^{b}	85	7, **227**^{b}	75	5, **228**^{b}	78	7, **229**^{b}
144	46	34, **230**^{b}	75	33, **231**^{b}	57	29, **232**^{b}	71	27, **233**^{b}	55	17, **234**^{b}	51	16, **235**^{b}
145	58	32, **236**^{b}	58	27, **237**^{b}	61	26, **238**^{b}	53	17, **239**^{b}	50	15, **240**^{b}	53	9, **241**^{b}

134
78% conv.
11% ee
THF

136
74% conv.
31% ee
PhMe

140
10% conv.
24% ee
THF

141
96% conv.
44% ee
THF

144
75% conv.
33% ee
PhMe

137
74% conv.
30% ee
THF

145
58% conv.
32% ee
THF

142
73% conv.
21% ee
THF

139
76% conv.
10% ee
PhMe

138
36% conv.
19% ee
THF

143
90% conv.
19% ee
PhMe
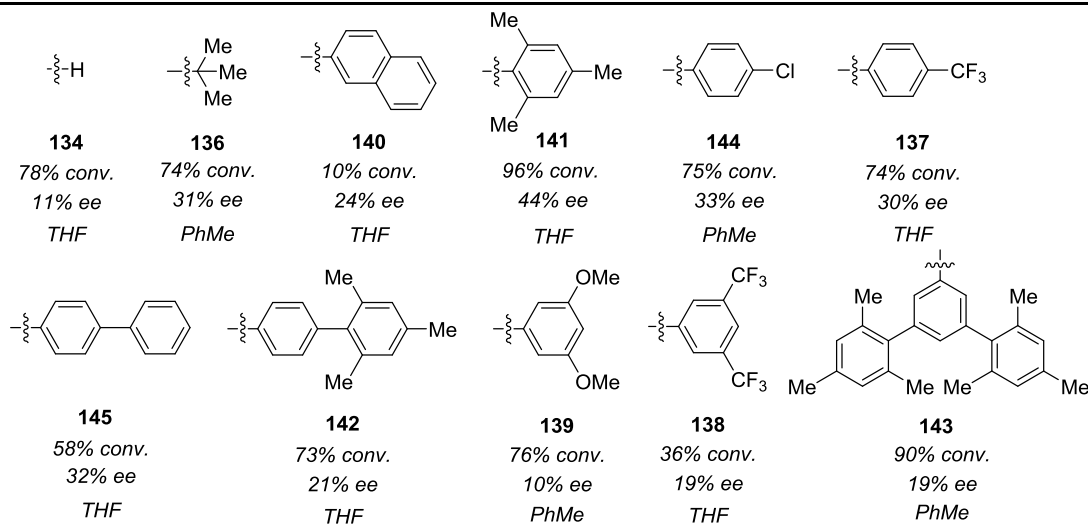
Table 6. Results obtained using BINOL-based phosphoric acid catalysts. ^{a} Conversion and ee determined by HPLC. ^{b} Reaction no.

The results shown in Table 6 suggested that although the conjugate addition to vinyl quinolines is suitably reactive, the selectivity of the process still needed to be improved as the ee's were moderate. Differences in conversion between catalysts may reasonably be attributed to the differing solubilities of the catalysts in the chosen solvents, i.e., reactions which resulted in high conversion existed as homogeneous mixtures in which the catalyst and all other reagents were completely in solution. The choice of reaction solvent also had an effect on enantiomeric excess, which was to be expected. However, what was not entirely expected was that the selectivity varied not only from catalyst to catalyst but also from solvent to solvent as the catalyst changed, in that neither solely THF nor PhMe was consistently the better solvent for selectivity.

3.8.2.2. Octahydro (H$_8$) BINOL Catalyst Screen

Based on the limited success of the several BINOL-based phosphoric acid catalysts tested in the reaction, further catalyst screening was carried out. **148** was found to perform noticeably well in terms of selectivity in the reaction (Scheme 45).
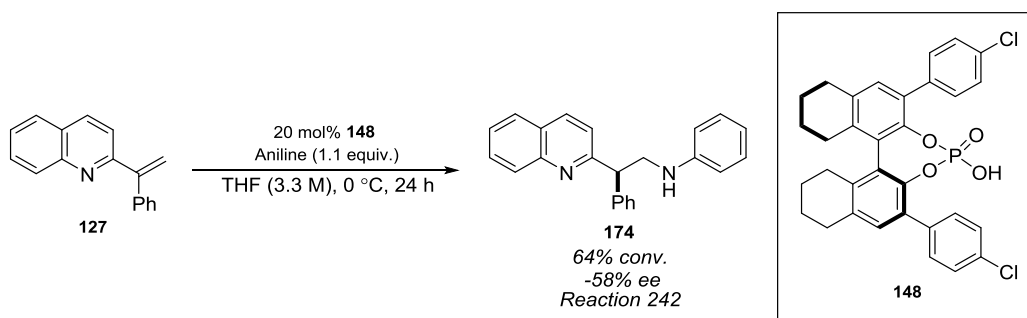
Scheme 45. Trial reaction with catalyst **148**.

It was observed that changing from BINOL catalyst **144** (R = 4-(Cl)C$_6$H$_4$, Table 6) to the corresponding H$_8$BINOL **148** (R = 4-(Cl)C$_6$H$_4$), the ee improved from 34% ee to -58% ee ((*S*)-enantiomer). This significant increase in selectivity was thought to have been due to a combination of several factors:

i)   The hybridisation of the left hand side of the naphthol rings ring had increased in p character from sp^2 to sp^3, slightly increasing the bulk of the rings and forcing the dihedral angle of the catalyst to become slightly larger (from 54.5° to 57.9°

(calculated computationally[49])), having a positive effect on the selectivity of the reaction.

ii)   The hybridisation change not only has an effect on the sterics of the catalyst, but also on its electronics. As discussed in Figure 19, the inductively electron donating effect of the saturated part of the ring slightly increases the pK_a of the catalyst from 3.06 to 4.51,[14] increasing the strength of its conjugate base anion, consequently increasing the strength of its interaction with the prochiral enamine cation.

iii)   The solubility of the catalyst, particularly its conjugate base, may be better as ring saturation increases, having a positive effect on the selectivity of the catalyst.

Based on this promising result and the potential rationales discussed, a range of chiral H$_8$BINOL-based phosphoric acid catalysts were then prepared (Scheme 46).
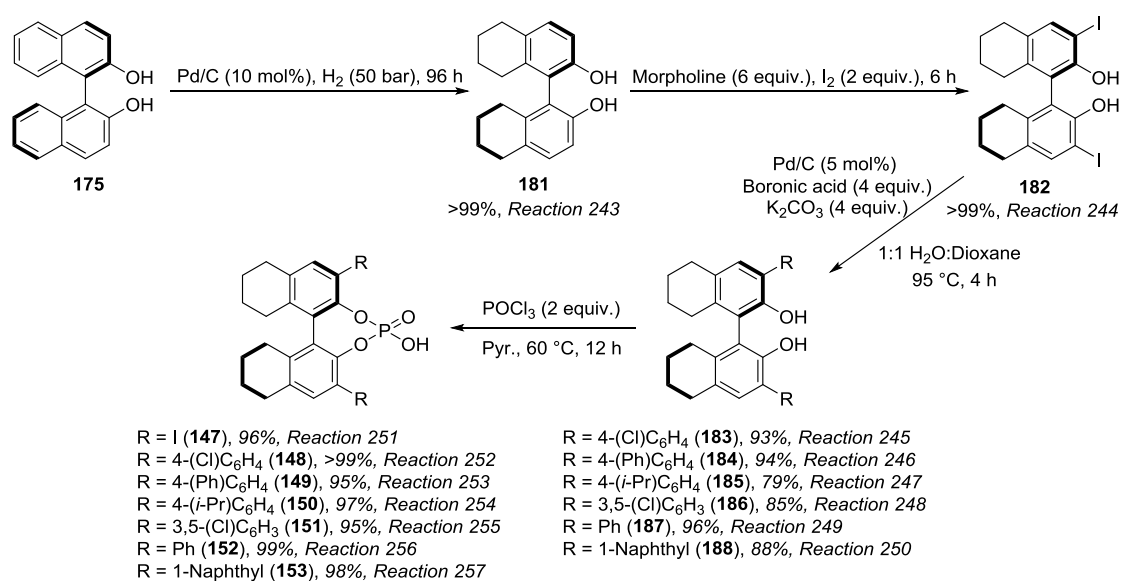
Scheme 46. General synthesis of H$_8$BINOL catalysts.

Firstly, (*R*)-BINOL, **175**, was partially hydrogenated to H$_8$BINOL, **181,** using Pd/C and H$_2$. **181,** was then regioselectively iodinated to generate the cross-coupling precursor H$_8$I$_2$BINOL, **182**. **182** was then used in several Suzuki reactions to generate the desired functionalised H$_8$BINOL catalyst precursors, **183-188**. These precursors, along with **182**, were then converted to their respective chiral phosphoric acids **147-153**. A range of H$_8$BINOL-based phosphoric acids were

screened in the conjugate addition reaction at temperatures of 0 °C, room temperature and 60 °C in both THF and PhMe (Table 7).

Cat.	0 °C				RT				60 °C			
	THF		PhMe		THF		PhMe		THF		PhMe	
	Conv.	ee^a	Conv.	ee^a	Conv.	ee^a	Conv.	ee^a	Conv.	ee^a	Conv.	ee^a
14	62	15, **258**^{b}	53	28, **259**^{b}	69	17, **260**^{b}	84	28, **261**^{b}	51	15, **262**^{b}	48	13, **263**^{b}
15^c	64	-58, **264**^{b}	40	-58, **265**^{b}	74	-52, **266**^{b}	77	-48, **267**^{b}	93	-30, **268**^{b}	40	-6, **269**^{b}
16	86	48, **270**^{b}	47	45, **271**^{b}	51	43, **272**^{b}	86	37, **273**^{b}	87	22, **274**^{b}	49	3, **275**^{b}
17	56	37, **276**^{b}	39	40, **277**^{b}	59	31, **278**^{b}	52	33, **279**^{b}	76	24, **280**^{b}	68	29, **281**^{b}
18	65	17, **282**^{b}	44	11, **283**^{b}	72	12, **284**^{b}	56	8, **285**^{b}	87	9, **286**^{b}	75	4, **287**^{b}
19	74	33, **288**^{b}	59	39, **289**^{b}	73	25, **290**^{b}	77	32, **291**^{b}	56	9, **292**^{b}	45	17, **293**^{b}
20	61	36, **294**^{b}	48	33, **295**^{b}	48	31, **296**^{b}	90	21, **297**^{b}	51	14, **298**^{b}	82	9, **299**^{b}

Table 7. Results obtained using H_8BINOL-based phosphoric acid catalysts. ^{a} Conversion and ee determined by HPLC. ^{b} Reaction no. ^{c} (S)-enantiomer.

The results shown in Table 7 again show that although the conjugate addition was suitably reactive, the selectivity still needed work in order to improve. Consistent with the results obtained with the BINOL-based catalysts (Table 6), the selectivity varied from solvent to solvent but remained at moderate levels throughout. Also consistent with the results obtained from the BINOL-based catalysts, the selectivity varied not only from catalyst to catalyst but also from solvent to solvent as the catalyst changed.

Although the selectivity did improve significantly as a result of increasing the ring saturation of the catalyst (Figure 17), work was still required to reach an acceptable level of selectivity.
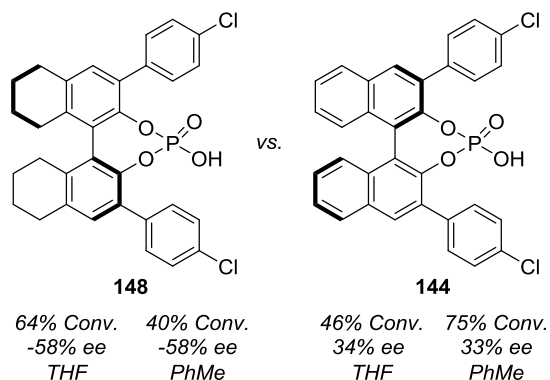
Figure 17. 4-(Cl)H$_8$BINOL catalyst (**148**) vs. 4-(Cl)BINOL catalyst (**144**).

3.8.3. TRIP Catalyst Synthesis and Results

Before moving on from the catalyst screen to optimise other parameters such as concentration and temperature etc., several more catalysts were synthesised and trialled to ensure that the catalyst screen had been satisfactorily exhausted. These included **146**, **154** and **155**.

For the synthesis of the H$_8$BINOL **154** and **155** (Scheme 47), H$_8$I$_2$BINOL, **181**, was CH$_3$ protected prior to the Kumada cross-coupling step due to the relatively acidic nature of the naphthol functionalities. For the cross-couplings, the Grignard reagents had to be synthesised from their corresponding bromides by reaction with elemental magnesium. The prepared Grignard solutions were then titrated to confirm molarity and used in the Kumada reaction with **189** using Ni(PCy$_3$)$_2$Cl$_2$ as the catalyst. Ni(PPh$_3$)$_2$Cl$_2$ was initially used as the catalyst but this led to no conversion to product. The resulting cross-coupled products, **190** and **191** were then deprotected using boron tribromide to form catalyst precursors which were then converted to their corresponding acid catalysts **154** and **155**.

The synthesis of BINOL catalyst **146** was prepared from the previously protected cross-coupling precursor **177**, following the same route as the H$_8$BINOL catalysts, **154** and **155**, described above and Illustrated in Scheme 47.
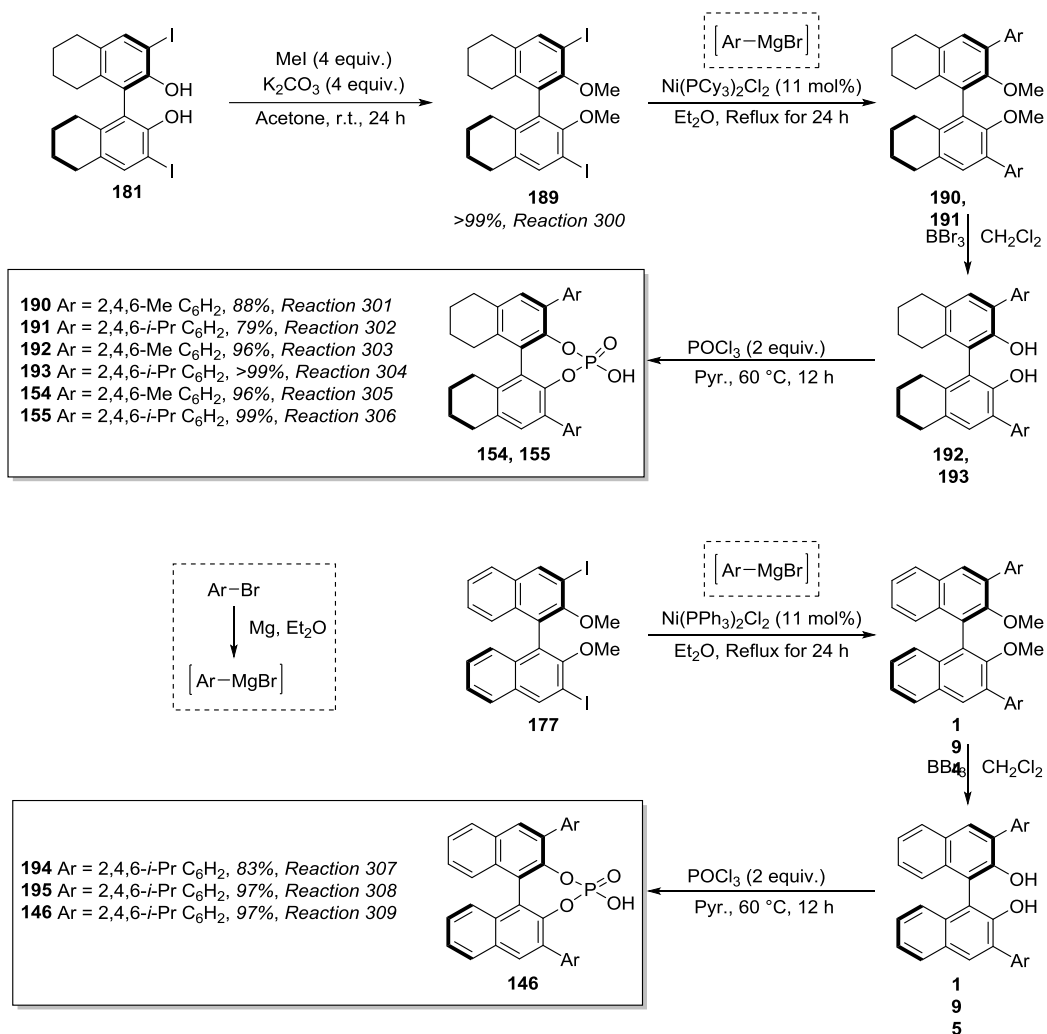
Scheme 47. General syntheses of catalysts involving Kumada cross-couplings.

146, **154**, **155** and (*R*)-VAPOL hydrogen phosphate (**196**) were then tested in the conjugate addition reaction, the results of which are shown in Table 8.

	0 °C				RT				60 °C			
	THF		PhMe		THF		PhMe		THF		PhMe	
Cat.	Conv.	ee[a]	Conv.	ee[a]	Conv.	ee[a]	Conv.	ee[a]	Conv.	ee[a]	Conv.	ee[a]
154	65	33, **310**[b]	89	20, **311**[b]	71	18, **312**[b]	83	8, **313**[b]	56	10, **314**[b]	54	0, **315**[b]
155	7	22, **316**[b]	23	15, **317**[b]	35	13, **318**[b]	21	3, **319**[b]	60	-5, **320**[b]	50	7, **321**[b]
146	37	64, **322**[b]	49	4, **323**[b]	98	6, **324**[b]	77	3, **325**[b]	82	5, **326**[b]	60	1, **327**[b]
196	58	42, **328**[b]	50	39, **329**[b]	58	39, **330**[b]	54	34, **331**[b]	88	23, **332**[b]	40	10, **333**[b]
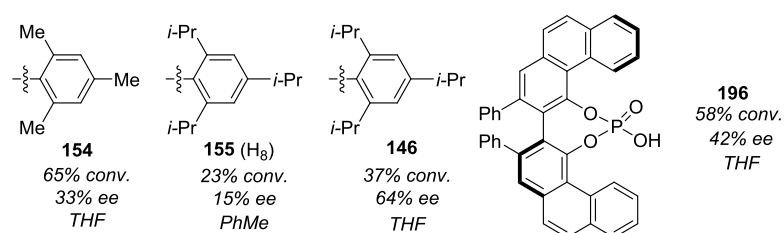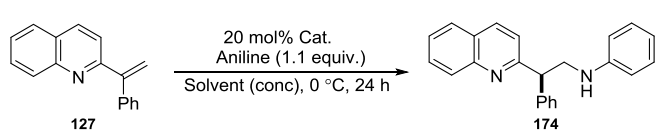
Table 8. Results obtained using catalysts **146**, **154**, **155** and **196**. [a] Conversion and ee determined by HPLC. [b] Reaction no.
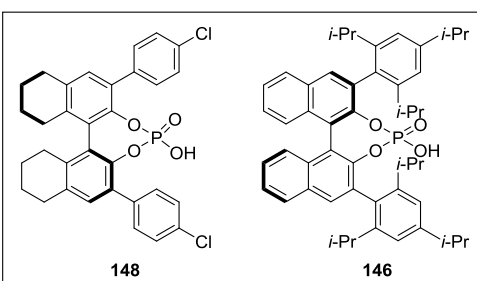
146 bearing the 2,4,6-^{i}Pr-C$_6$H$_2$ (TRIP) groups in combination with the BINOL structure proved to be the most effective combination with respect to selectivity. The conversion, however, was not at a desirable level but it was hoped that, with further optimisation based around this catalyst, these values would improve. It was interesting to note that when this same TRIP group was combined with the H$_8$BINOL catalyst backbone, the negative effects on both conversion and selectivity were significant.

The next step in the optimisation stage was to take the catalysts which had performed best so far and subject these to further optimisation based on varying the reaction concentration and the choice of solvent.

3.8.4. Concentration and Solvent Optimisation

The catalysts which were taken forward for further optimisation were **148** (4-Cl H$_8$BINOL) and **146** (TRIP BINOL) as they had performed best. A simple concentration study revealed that there was an optimum concentration for selectivity in the reaction. The results of the concentration studies with these catalysts are shown in Table 9.

Conc. (M)	THF				PhMe			
	146		**148**		**146**		**148**	
	Conv.	ee[a]	Conv.	ee[a]	Conv.	ee[a]	Conv.	ee[a]
0.01	0	0, *334*[b]	1	-67, *335*[b]	0	0, *336*[b]	1	-37, *337*[b]
0.1	0	0, *338*[b]	3	-86, *339*[b]	56	54, *340*[b]	34	-66, *341*[b]
0.25	19	74, *342*[b]	8	-56, *343*[b]	95	53, *344*[b]	37	-69, *345*[b]
0.5	26	81, *346*[b]	19	-62, *347*[b]	67	51, *348*[b]	26	-67, *349*[b]
1	33	80, *350*[b]	32	-63, *351*[b]	70	40, *352*[b]	72	-64, *353*[b]
2	45	74, *354*[b]	39	-61, *355*[b]	67	34, *356*[b]	70	-60, *357*[b]
3.3	37	64, *358*[b]	64	-58, *359*[b]	57	30, *360*[b]	40	-58, *361*[b]
5	54	64, *362*[b]	57	-52, *363*[b]	69	32, *364*[b]	65	-49, *365*[b]
10	76	54, *366*[b]	91	-46, *367*[b]	80	29, *368*[b]	95	-45, *369*[b]

Table 9. Concentration study with **146** and **148** in THF and PhMe. [a] Conversion and ee determined by HPLC. [b] Reaction no.

The results of the concentration screening shown above have been represented graphically (Figures 18-21).
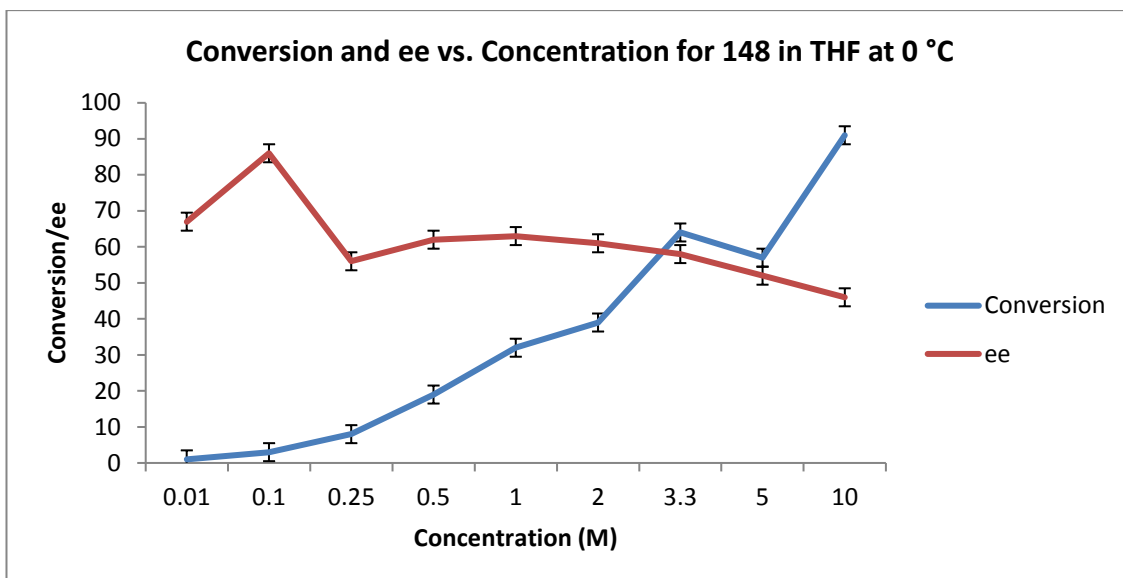
Figure 18. Conversion and ee vs. concentration for **148** in THF at 0 °C (ee's shown as positive values for ease of comparison).

It can be seen from Figure 18 that as concentration increased, conversion generally increased. This general trend can be rationalised in that as the solvent volume decreases, the reacting molecules are forced closer together, increasing the rate of reaction. The selectivity profile formed a smooth curve with respect to conversion (discounting the first two values for ee at 1% and 3% conversion which are not at appropriate levels to examine ee), peaking at 1 M (-63% ee at 32% conversion).
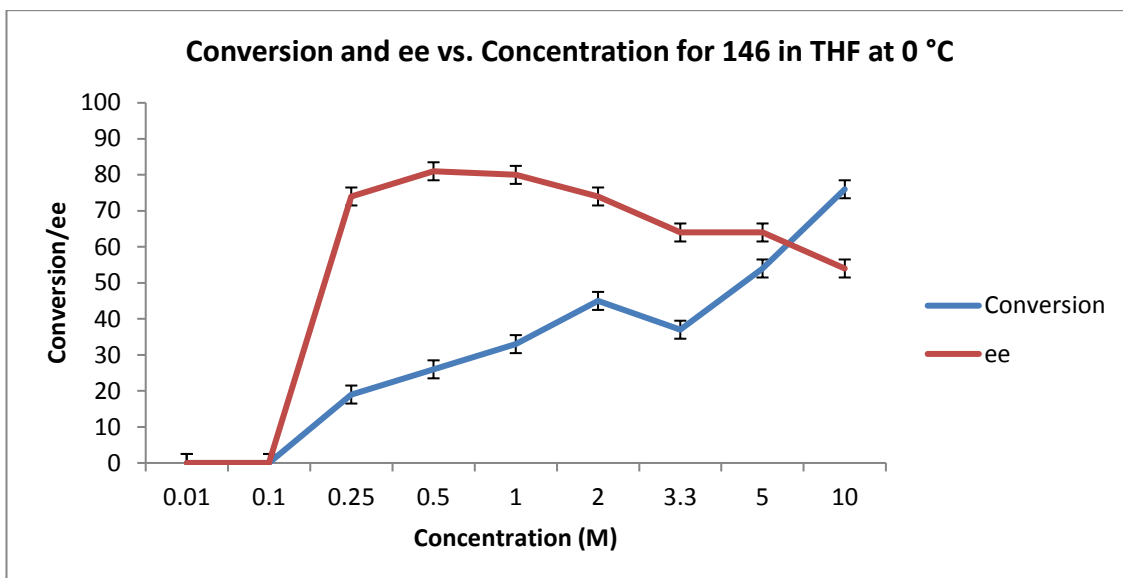
Figure 19. Conversion and ee vs. concentration for **146** in THF at 0 °C.

In Figure 19, switching from the 4-Cl H$_8$BINOL catalyst, **148**, to the TRIP BINOL catalyst, **146**, in THF, it can be seen that the reaction profile followed similar trends for conversion and ee. As seen with **148**, the conversion generally increased with increasing concentration. The ee also followed a similar trend in that the data forms a curve, peaking at 0.5 M (26% conversion at 81% ee). Moving to 1 M, the conversion increased to 33% and the ee stayed consistent which suggested that the optimum concentration for selectivity in this reaction may be around 0.75 M.
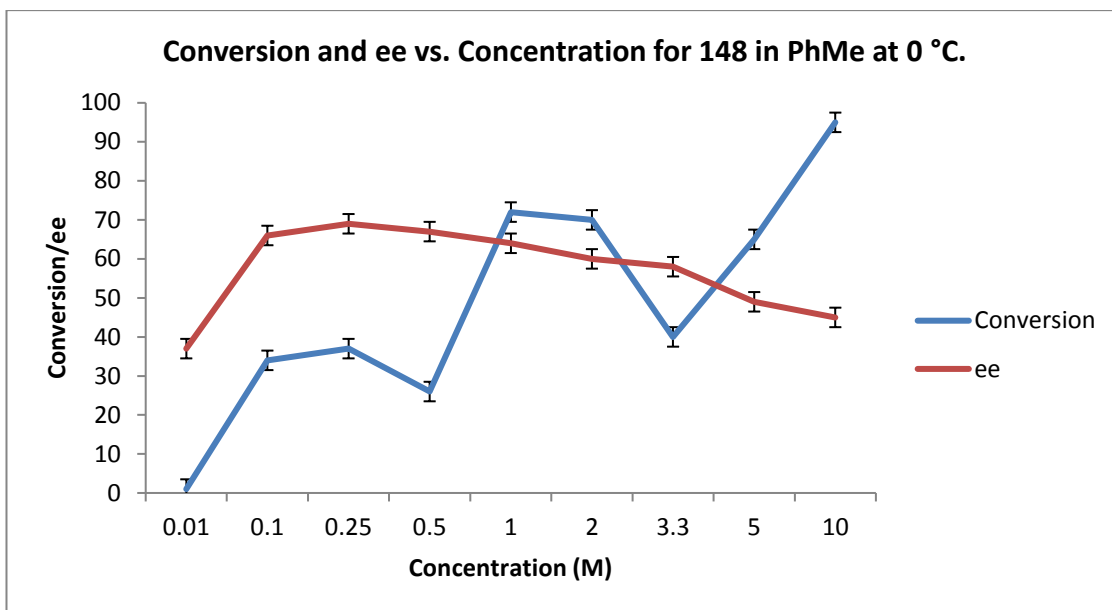
Figure 20. Conversion and ee vs. concentration for **148** in PhMe at 0 °C (ee's shown as positive values for ease of comparison).

Figure 20 shows that in changing from THF to PhMe for **148**, the trend for reactivity became more of a staggered, nonlinear profile with maxima at 0.25 M, 1 M and 10 M. However, the ee followed a more expected trend, peaking at 0.25 M (-69% ee at 37% conversion).
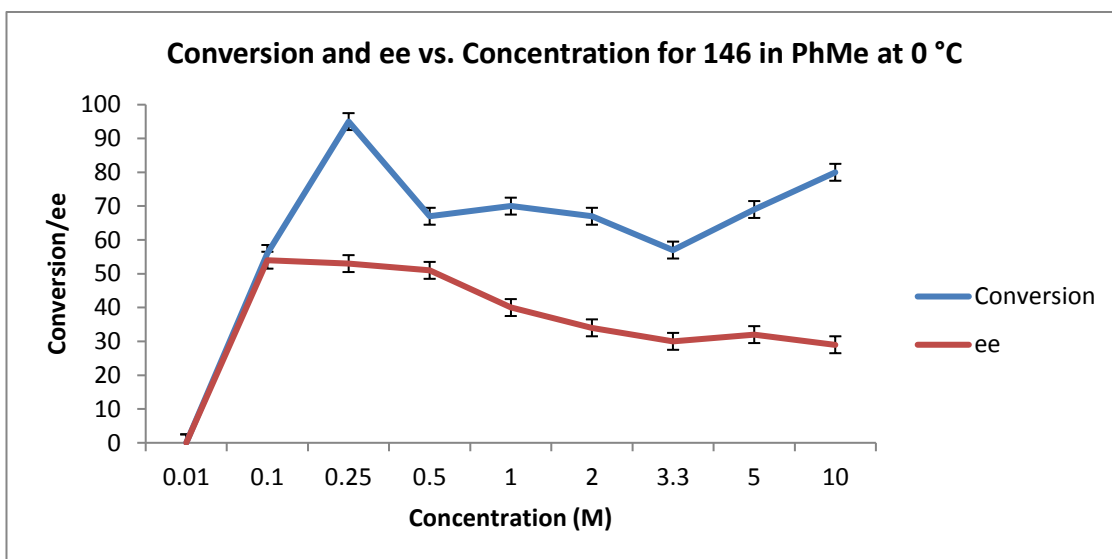
Figure 21. Conversion and ee vs. concentration for **146** in PhMe at 0 °C.

Figure 21 shows that, again, there was a staggered, nonlinear profile with maxima at 0.25 M, 1 M and 10 M (the same three conversion maxima as **148** in PhMe) on changing from THF to

PhMe for **146**. However, contrary to the conversion trend of **148** in PhMe, it appears that for **146** in PhMe, conversion was highest at lower concentrations. The ee, again as with **148** in PhMe, followed a more expected trend, peaking at 0.1 M (56% conversion, 54% ee) with 0.25 M giving 95% conversion and 53% ee.

From the results discussed above, it was proposed that a larger range of solvents be screened in order to arrive at a more optimisable system, which would involve further concentration studies and possibly solvent mixtures. To this effect, a range of solvents were selected based on varying polarity: MeOH, IPA, H_2O, TFE, ethylene glycol, acetone, DMF, 1,4-dioxane, EtOAc, $MeNO_2$, hexane, $CHCl_3$ DCM, DCE, Et_2O, CyHex, PhCl, and xylenes. **148** and **146** were tested in each solvent at 0 °C (Table 10).

20 mol% **Cat.**
Aniline (1.1 equiv.)
Solvent (conc), 0 °C, 24 h

127 → 174

148   146
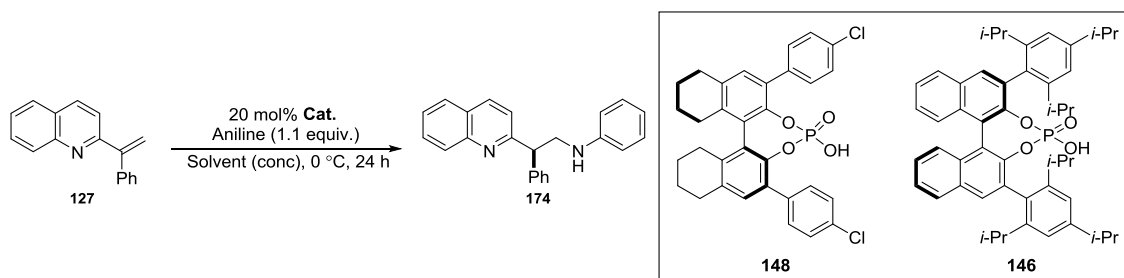
Solvent Class	Solvent	146		148	
		Conv.	ee[a]	Conv.	ee[a]
Polar Protic	MeOH	NA	6, **370**[b]	NA	-4, **391**[b]
	IPA	NA	13, **371**[b]	NA	-28, **392**[b]
	H$_2$O	NA	29, **372**[b]	NA	-31, **393**[b]
	TFE	NA	4, **373**[b]	NA	-3, **394**[b]
	Ethylene glycol	NA	3, **374**[b]	NA	-6, **395**[b]
Polar Aprotic	THF	37	64, **375**[b]	64	-58, **396**[b]
	Acetone	NA	12, **376**[b]	NA	-27, **397**[b]
	DMF	56	14, **377**[b]	9	-6, **398**[b]
	MeCN	NA	6, **378**[b]	NA	-20, **399**[b]
	1,4-Dioxane	33	28, **379**[b]	23	-58, **400**[b]
	EtOAc	NA	33, **380**[b]	NA	-56, **401**[b]
	MeNO$_2$	NA	3, **381**[b]	NA	-23, **402**[b]
Non-Polar	Hexane	NA	26, **382**[b]	NA	-46, **403**[b]
	CHCl$_3$	85	23, **383**[b]	100	-46, **404**[b]
	DCM	91	14, **384**[b]	31	-56, **405**[b]
	DCE	73	11, **385**[b]	24	-56, **406**[b]
	Et$_2$O	NA	28, **386**[b]	NA	-49, **407**[b]
	CyHex	NA	36, **387**[b]	11	-6, **408**[b]
Aromatic	PhMe	57	30, **388**[b]	40	-58, **409**[b]
	PhCl	100	22, **389**[b]	89	-46, **410**[b]
	Xylenes	83	31, **390**[b]	68	-16, **411**[b]

Table 10 Solvent screen with **146** and **148** at 0 °C. NA = Internal standard not soluble. [a]

Conversion and ee determined by HPLC. [b] Reaction no.

Table 10 shows that for **146**, THF was the stand-out solvent for this reaction with no other solvent coming close in terms of selectivity. There were other solvents which increased the reactivity, however, such as the chlorinated solvents and xylenes, which were to be probed when assessing solvent mixtures. **148**, however, showed generally good ee's throughout the non-polar solvents, reaching >50% with THF, 1,4-dioxane, EtOAc, DCM, DCE, and PhMe. Chlorobenzene proved to be the best solvent for reactivity with this catalyst, with THF and xylenes also achieving good reactivity. Again, these data further showed the need to try mixed solvent systems at different concentrations and temperatures to achieve high levels of both conversion and enantioselectivity. Solvents which proved to be highly active would be trialled at lower temperatures.

From the results obtained in the solvent screen, it became apparent that greater conversion could possibly be achieved by using a selection of solvents from the solvent screen and studying the concentration effects as with THF and PhMe. This is represented in Table 11.
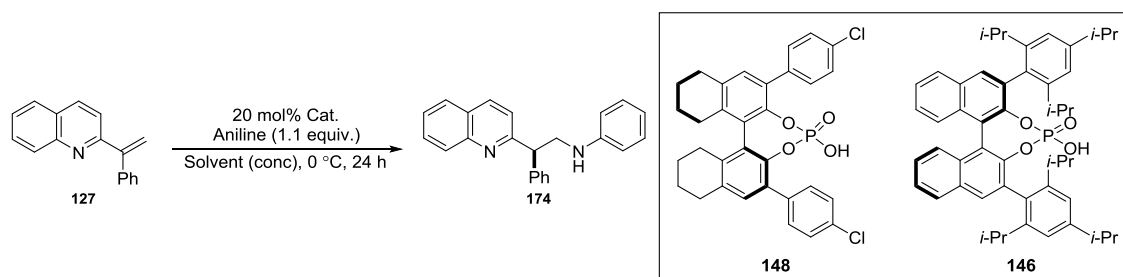
Solvent/Conc.	146		148	
	Conv.	ee[a]	Conv.	ee[a]
CHCl₃				
0.5 M	*19*	*22*, **412[b]**	*18*	*-33*, **424[b]**
1 M	*30*	*21*, **413[b]**	*30*	*-36*, **425[b]**
2 M	*54*	*21*, **414[b]**	*59*	*-39*, **426[b]**
DCM				
0.5 M	*21*	*15*, **415[b]**	*23*	*-35*, **427[b]**
1 M	*31*	*10*, **416[b]**	*48*	*-38*, **428[b]**
2 M	*64*	*9*, **417[b]**	*82*	*-40*, **429[b]**
DCE				
0.5 M	*15*	*11*, **418[b]**	*23*	*-28*, **430[b]**
1 M	*28*	*9*, **419[b]**	*53*	*-32*, **431[b]**
2 M	*70*	*10*, **420[b]**	*71*	*-34*, **432[b]**
PhCl				
0.5 M	*38*	*30*, **421[b]**	*40*	*-55*, **433[b]**
1 M	*43*	*19*, **422[b]**	*41*	*-41*, **434[b]**
2 M	*60*	*24*, **423[b]**	*58*	*-52*, **435[b]**

Table 11. Solvent and concentration screen using **146** and **148**. [a] Conversion and ee determined by HPLC. [b] Reaction no.

By examining the different solvents, it was found that at increased concentrations, the conversion increased significantly without compromising selectivity to any significant extent (an effect which was not achieved in THF or PhMe). An important visual observation of the reaction mixtures was that the catalysts were fully soluble in the above solvents, whereas in THF and PhMe there was often precipitate when dissolving the catalysts. This increased

solubility could be the reason for the increased conversion in these reactions. It was then proposed that by mixing THF with the selected solvents in a 1:1 ratio, a synergistic solvent effect could possibly be achieved where the THF could facilitate a selective reaction and the combined solvent could help to solubilize the catalyst and boost the conversion. This was put
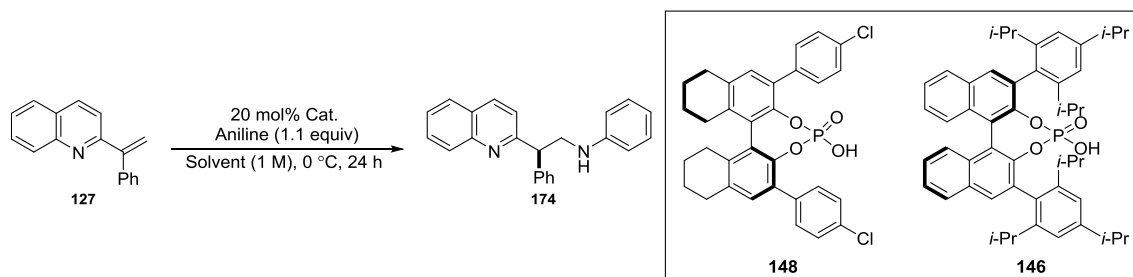
into practice in a mixed solvent screen (Table 12).

Solvent	146		148	
	Conv.	ee[a]	Conv.	ee[a]
1:1 THF:CHCl$_3$	37	49, **436**[b]	36	-58, **441**[b]
1:1 THF:CH$_2$Cl$_2$	34	48, **437**[b]	38	-58, **442**[b]
1:1 THF:DCE	33	46, **438**[b]	31	-48, **443**[b]
1:1 THF:PhCl	40	50, **439**[b]	38	-54, **444**[b]
1:1 THF:PhMe	53	64, **440**[b]	38	-68, **445**[b]

Table 12. Mixed solvent screen. [a] Conversion and ee determined by HPLC. [b] Reaction no.

Carrying out a mixed solvent screen with the selected solvents failed to enhance the conversion and, at the same time, was generally detrimental to selectivity. By analysing the data from each of the solvent screens, it was immediately apparent that the choice of reaction solvent had a large effect on the reaction outcome.

At this point, the methodology had been developed to a stage where all reasonable efforts to develop the process to a high standard had been undertaken but had ultimately failed to deliver a system in which both high reactivity and high selectivity could be achieved under the same reaction conditions. However, both high reactivity and high selectivity could be achieved independently by applying simple changes to the reaction systems which represents promising headway into this challenging process.

4. Conclusions

The methodology under development was at a stage where the concept of chiral Brønsted acid-catalysed asymmetric conjugate addition to vinyl *N*-heterocycles had been validated and respectable levels of reactivity and selectivity have been achieved in the system. However, the significant difficulty of performing a complete conjugate addition reaction while at the same time maintaining high selectivity in the asymmetric protonation event has become problematic.

Efforts to generate a reaction which is simultaneously highly reactive and selective have so far given limited success. The best results obtained at this stage are illustrated below, which show the level to which the methodology has been developed at this stage.
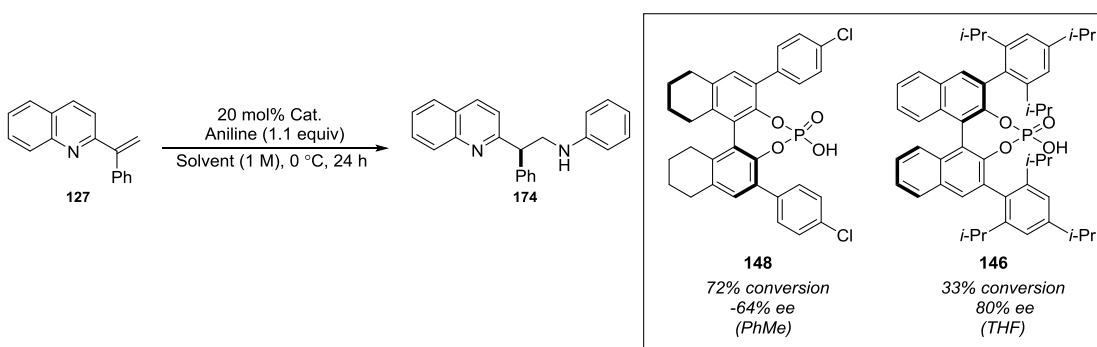
Scheme 48. Summary of best results.

A possible rationale for the observed limits in reactivity and selectivity could be that the reaction may be inhibited by protonation of the nucleophile, resulting in the conjugate acid of the nucleophile becoming the protonating species which, due to the pK_aH difference between the nucleophile and the heterocycle, may result in the reaction proceeding very slowly with an eventual plateau. Under conditions where reaction inhibition in this way may not be an issue, the reaction would be allowed to proceed to a high level of conversion in an acceptable timeframe. However, in doing so, the reaction then would be susceptible to becoming less selective.

In attempts to overcome this, a wide range of catalysts, solvents, solvent combinations, concentrations and temperatures have been explored and although respectable optimisation has been achieved, the generation of a fully optimised system has not.

5. Future Work

For the methodology to be developed to a higher level, it would be necessary to explore:

i) A range of nucleophiles with varying nucleophilicities and basicities in order to understand which class of nucleophile may inhibit the reaction and which class of nucleophile is nucleophilic enough to react fully but not basic enough to inhibit the reaction. Such nucleophiles may include substituted anilines, secondary anilines, *N/O*-protected hydroxylamines, thiols, phosphines, and carbogenic nucleophiles (Scheme 49).
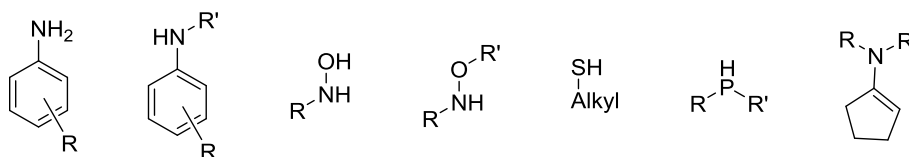
Scheme 49. Nucleophiles to trial in the conjugate addition reaction.

ii) Water effects. The reaction may benefit from being performed under anhydrous conditions. Since water is such a competent molecule in bridging the transferral of protons in solution through intermolecular hydrogen bonding networks, it may be necessary to study the effects of water on the system (Scheme 50).
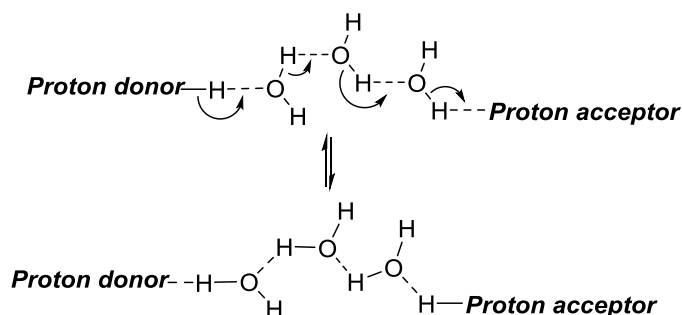
Scheme 50. Water-bridged proton transfer from a proton donor to a proton acceptor.

If water in the reaction mixture is bridging proton transfer in the asymmetric protonation step, this could have a significant detrimental effect on the overall enantioselectivity.

iii) The Michael acceptor. Studying a wider range of vinyl heterocycles may also be of benefit to the reaction since different heterocycles and different olefinic substituents will affect the susceptibility of the Michael acceptor towards the conjugate addition reaction (Scheme 51).
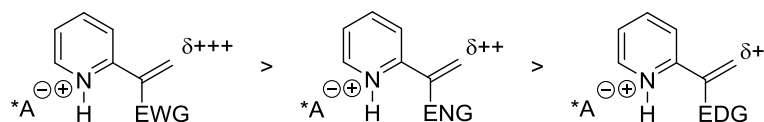
Scheme 51. Relative reactivities of heterocycles bearing different olefinic substituents. ENG = electron-neutral group.

iv) The (*E*)-/(*Z*)-geometry of the *in situ* generated prochiral enamine intermediate. Since the *in situ* generation of the prochiral intermediate may not be particularly selective for one isomer over the other, and it has been shown in section 1.1.2.4. that each isomer can give rise to different enantiomers of product during protonation, tethering the olefin may improve the selectivity of the reaction (Scheme 52).
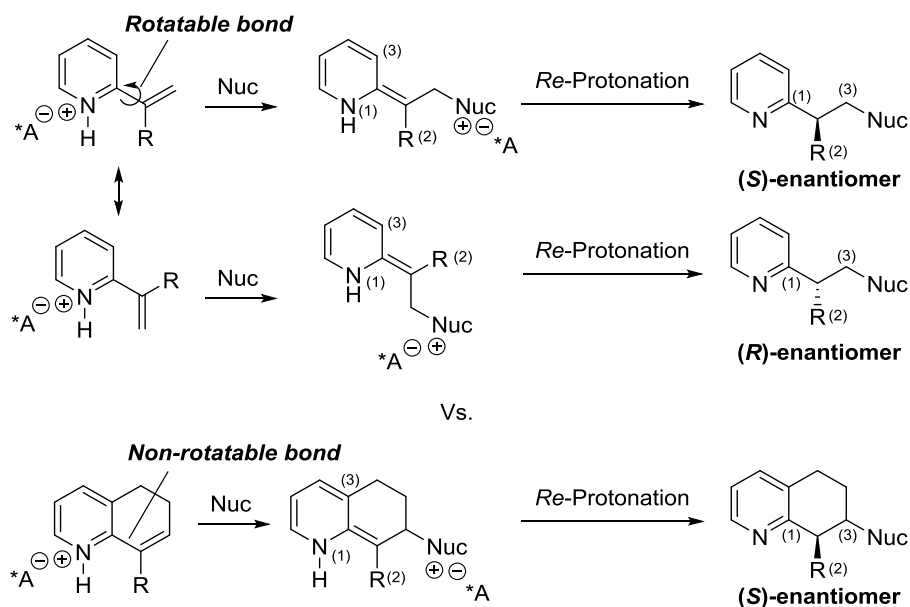
Scheme 52. Product enantiomers arising from the (*E*)-/(*Z*)-mix of the prochiral intermediate.

6. Experimental

6.1 Reagents

All reagents and solvents were obtained from commercial suppliers and were used without further purification unless otherwise stated. Purification was carried out according to standard laboratory methods.[50]

6.1.1. Purification of Solvents

i) All solvents used for dry reactions (tetrahydrofuran, diethyl ether, dichloromethane) were obtained from a PureSolv SPS-400-5 solvent purification system. These solvents were transferred to and stored in a septum-sealed, oven-dried flask over previously activated 4 Å molecular sieves and purged with and stored under nitrogen.

ii) Dichloromethane, ethyl acetate, toluene, and petroleum ether 40-60° for purification purposes were used as obtained from commercial suppliers without further purification.

6.1.2 Purification of Starting Materials

Aniline was purified by heating to reflux over calcium chloride, distilled under reduced pressure, then purged with and stored under nitrogen over 4 Å molecular sieves.

6.1.3 Organometallic Reagents

n-Butyllithium (1.6 M in hexanes) was used as obtained from commercial suppliers.

6.1.4 Experimental Details

i) Moisture-sensitive reactions were carried out using oven-dried glassware purged with N_2 before use.

ii) Purging refers to a vacuum/nitrogen-refilling procedure.

iii) Reactions carried out at 0 °C and -20 °C were done so using a ThermoHaake EK90 reaction cooling system.

iv) Room temperature was generally *ca.* 18 °C.

v) Reactions carried out at elevated temperatures were done so using a temperature-regulated hotplate/stirrer.

6.1.5 Purification of Products

i) Thin layer chromatography was carried out using Merck silica plates coated with fluorescent indicator UV254. These were analysed under 254 nm UV light or developed using potassium permanganate solution.

ii) Normal phase flash chromatography was carried out using ZEOprep 60 HYD 40-63 μm silica gel.

6.1.6 Analysis of Products

i) Fourier Transformed Infra-Red (FTIR) spectra were obtained on a Shimadzu IRAffinity-1 machine.

ii) ^1H and ^{13}C NMR spectra were obtained on a Bruker AV 400 at 400 MHz and 125 MHz, respectively. Chemical shifts are reported in ppm and coupling constants are reported in Hz with $CDCl_3$ referenced at 7.27 ppm (^1H) and 77.36 ppm (^{13}C).

iii) High-resolution mass spectra were obtained through analysis at the EPSRC UK National Mass Spectrometry Facility at Swansea University.

iv) HPLC data was obtained on an Agilent 1260 series HPLC using a DAICEL CHIRALPAK® IA column, 4.6 mm x 250 mm, particle size = 5 μm. Samples for HPLC analysis were prepared through the addition of 0.5 mL of non-standardised reaction solvent to the completed reaction mixture containing the standardised reaction solvent along with a few drops of sat. $NaHCO_3$. The resulting biphasic solution was then stirred before the removal of the organic phase. The organic phase was diluted to 1 mL with non-standardised reaction solvent, filtered and analysed by HPLC against established conversion factors.

> i) For **132**, conversion and enantiomeric excess analysis was performed using an isocratic method, eluting with 2.5% IPA/hexane over 22 minutes at a flow rate of 0.5 mL/min. t_R enantiomer 1 = 14.1 min., t_R enantiomer 2 = 19.3 min.

> ii) For **174**, conversion analysis was performed using a gradient method, eluting with 20 - 50% IPA/hexane over 17 minutes at a flow rate of 0.5 mL/min. Enantiomeric

excess analysis was performed using an isocratic method, eluting with 50% IPA/hexane over 13 minutes at a flow rate of 0.5 mL/min. t_R enantiomer 1 = 10.4 min., t_R enantiomer 2 = 11.3 min.

v) Specific rotation values were obtained using a Perkinelmer polarimeter 341 (wavelength = 589 nm (sodium D line), temperature = 20 °C). Values are quoted in units of deg mL g^{-1} dm^{-1}.

7. General Experimental Procedures and Reaction Data

General Experimental Procedure A: Grignard addition to carbonyl compounds.

For example, for 1-phenyl-1-(pyridin-2-yl)ethanol, **120**.

An oven-dried flask equipped with a stirrer bar and fitted with a septum was purged with N_2. To the flask was added phenyl(pyridin-2-yl)methanone (1 equiv, 20 mmol, 3.66 g) and dry THF (120 mL). The flask was then cooled to 0 °C. MeMgBr ((2 equiv, 40 mmol, 13.33 mL (3 M Et_2O solution)) was then added dropwise to the reaction mixture. The reaction was then allowed to warm to room temperature for 18 hours. The reaction was then quenched with 25 mL HCl (36% in H_2O) and basified with sat. aq. K_2CO_3. EtOAc (20 mL) was added and the phases separated. The aqueous layer was then re-extracted with EtOAc (3 x 5 mL). The combined organic phases were dried using Na_2SO_4, passed through a hydrophobic frit, and concentrated under reduced pressure to afford **120** as a white amorphous solid (3.96 g, >99%).

Reaction no.	Qty. Carbonyl	Qty. Grignard	Product, Mass, Yield
3	3.66 g	13.33 mL	**120**, 3.96 g, >99 %
5	1.57 g	6.66 mL	**122**, 1.71 g, 99 %
7	1.37 g	5.33 mL	**124**, 1.36 g, 91 %
9	1.37 g	5.33 mL	**126**, 1.85 g, 93 %

General Experimental Procedure B: Wittig reaction of carbonyl compounds.

For example, for 2-(prop-1-en-yl)pyridine, **113**.

Reaction 1. An oven-dried flask equipped with a stirrer bar and fitted with a septum was purged with N_2. To the flask was added MePPh$_3$Br (1.3 equiv, 65.0 mmol, 23.24 g) and 200 mL dry THF. The flask was then cooled to -10 °C and *n*-BuLi (1.2 equiv, 60 mmol, 37.44 mL (1.6 M hexane solution)) was added in a dropwise manner. The reaction proceeded for 30 min until being allowed to warm to room temperature for 15 minutes. The reaction was then cooled to 0 °C and 2-acetyl pyridine (1 equiv, 50 mmol, 6.57 g, 6.08 mL) was added in a dropwise manner. The reaction was allowed to proceed for 30 min at 0 °C before being allowed to warm to room temperature for 12 hours. The reaction was then quenched with

water (10 mL) and EtOAc (1 mL) was added and the phases separated. The aqueous layer was then re-extracted with EtOAc (3 x 10 mL). The combined organic phases were dried using Na$_2$SO$_4$, passed through a hydrophobic frit, and concentrated under reduced pressure to afford a residue that was purified by flash column chromatography (1:9 EtOAc/petroleum ether 40 °C - 60 °C) to afford **113** as a colourless liquid (4.73 g, 80%).

General Experimental Procedure C: Conjugate addition of nucleophiles to vinyl *N*-heterocycles.

For example, for *N*-(2-(pyridin-2-yl)propyl)aniline, **132**.

To a test tube was added a stirrer bar, 2-(prop-1-en-yl)pyridine (**113**, 1 equiv, 1 mmol, 116.2 mg) and 0.5 mL DCE. (*R/S*)-(-)-1,1'-Binaphthyl-2,2'-diyl hydrogenphosphate (0.2 equiv, 0.2 mmol, 69.7 mg) was then added to the reaction mixture. Aniline (1.1 equiv, 1.1 mmol, 100.5 µL) was then added dropwise and the reaction was allowed to proceed for the allocated time. The reaction was quenched with sat. aq. K$_2$CO$_3$ (15 mL), EtOAc (15 mL) was added and the layers separated. The aqueous layer was then re-extracted with EtOAc (3 x 5 mL), and the combined organic phases were dried using Na$_2$SO$_4$, passed through a hydrophobic frit, and concentrated under reduced pressure to afford a residue that was purified by flash column chromatography (1:4 EtOAc/petroleum ether 40 °C - 60 °C) to afford **132** as a yellow amorphous solid (42.5 mg, 20%).

Reaction no.	Qty. Vinyl Het.	Qty. Cat.	Qty. Nucleophile	Product, Mass, Yield
14	116.2 mg	69.6 mg	0.101 mL	**132**, 42.5 mg, 20 %
168	231.3 mg	69.7 mg	0.101 ml	**174**, 210.9 mg, 65 %

General Experimental Procedure D: Oxidation of alcohols.

For example, for 1-(quinolin-2-yl)ethanone, **123**.

Reaction 6. To a flask was added a stirrer bar, 1-(quinolin-2-yl)ethanol (**122**, 1 equiv, 9 mmol, 1.56 g) and 90 mL dry PhMe. MnO$_2$ (6 equiv, 54 mmol, 4.69 g) was then added in five portions to the reaction mixture. The reaction was then allowed to proceed for 3 hours. The resulting mixture was then filtered through a pad of Celite, washing through with EtOAc (50 mL). The combined organic phases were dried using Na$_2$SO$_4$, passed through a hydrophobic frit, and

concentrated under reduced pressure to afford to afford **123** as a brown/orange amorphous solid (1.46 g, 95%).

General Experimental Procedure E: dehydration of benzylic vinyl alcohols.

For example, for 2-(prop-1-en-2-yl)quinoline, **125**.

To a flask was added 2-(quinolin-2-yl)propan-2-ol (**124**, 1 equiv, 7 mmol, 1.31 g). 7 mL H_2SO_4 (85% H_2O solution) was then added and the reaction was heated at 100 °C for 3 hours before quenching with 4 M aq. NaOH (15 mL) at 0 °C. EtOAc (20 mL) was added and the phases separated. The aqueous layer was then re-extracted with EtOAc (3 x 5 mL). The combined organic phases were dried using Na_2SO_4, passed through a hydrophobic frit, and concentrated under reduced pressure to afford **125** as a yellow amorphous solid (1.13 g, 96%).

Reaction no.	Qty. Alcohol	Qty. 85% aq. H_2SO_4	Product, Mass, Yield
4	370.0 mg	2 mL	**119**, 322.3 mg, 89 %
8	1.31 g	7 mL	**125**, 1.13 g, 96 %
10	1.74 g	7 mL	**127**, 1.49 g, 92 %

General Experimental Procedure F: *O*-dimethylation of BINOL.

For example, for (*R*)-3,3'-diiodo-2,2'-dimethoxy-5,5',6,6',7,7',8,8'-octahydro-1,1'-binaphthalene, **189**.

A flask was charged with acetone (20 mL) and to this was added (*R*)-3,3'-diiodo-5,5',6,6',7,7',8,8'-octahydro-[1,1'-binaphthalene]-2,2'-diol (**181**, 1 equiv, 10 mmol, 5.46 g), iodomethane (4 equiv, 40 mmol, 1.31 g, 0.57 mL), and potassium carbonate (4 equiv, 40 mmol, 1.27 g). The flask was then sealed with a septum and the reaction was allowed to proceed at room temperature for 16 hours. Upon completion, H_2O (20 mL) was added and the mixture was stirred for a further 3 h. The suspension was then passed through a filter and washed with H_2O (3 x 5 mL). The resulting precipitate was then dissolved in 10 mL dichloromethane, dried using Na_2SO_4, passed through a hydrophobic frit and concentrated under reduced pressure to afford **189** as a white amorphous solid (5.72 g, >99%).

Reaction no.	Qty. BINOL	Qty. MeI	Qty. K_2CO_3	Product, Mass, Yield
169	2.86 g	0.57 mL	1.27 g	**176**, 3.12 g, >99 %
189	5.46 g	0.57 mL	1.27 g	**189**, 5.72 g, >99 %

General Experimental Procedure G: Iodination of methoxy binaphthalenes.

For example, for (*R*)-3,3'-diiodo-2,2'-dimethoxy-1,1'-binaphthalene, **177.**

Reaction 170. An oven dry flask was fitted with a septum and a stirrer bar, purged with N_2 and charged with diethyl ether (50 mL) and TMEDA (4.4 equiv, 6.29 mmol, 0.94 mL). ^{n}BuLi (2.5 M in hexanes, 10 equiv, 14.30 mmol, 5.72 mL) was then added. The reaction mixture was stirred at room temperature for 20 minutes. (*R*)-2,2'-Dimethoxy-1,1'-binaphthalene (**176**, 1 equiv, 1.43 mmol, 450.0 mg) was then added in one portion in solid form and the reaction was allowed to proceed for a further 3 hours at room temperature. The reaction was cooled to -78 °C and I_2 (3.4 equiv, 4.86 mmol, 1.23 g) was then added as a solution in THF (20 mL) in a drop wise manner. The reaction was then allowed to warm room temperature and to stir overnight. Upon completion, 20 mL of a half saturated solution of $Na_2S_2O_3$ (prepared by making a saturated solution and diluting this by a factor of two) was added and the reaction was allowed to quench by stirring for 1 hour. The layers were then allowed to separate and the organic layer was subsequently washed with H_2O (2 x 10 mL) and brine (2 x 10 mL). The organic layer was then dried using Na_2SO_4, passed through a hydrophobic frit, and concentrated under reduced pressure to give a crude residue which was purified by flash column chromatography (30% PhMe in petroleum ether 40 °C - 60 °C) to afford **177** as a white amorphous solid (527.1 mg, 93%).

General Experimental Procedure H: Deprotection of methyl protected binaphthols.

For example, for (*R*)-3,3'-bis(2,4,6-triisopropylphenyl)-[1,1'-binaphthalene]-2,2'-diol, **195**.

A flask was fitted with a stirrer bar and charged with (*R*)-2,2'-dimethoxy-3,3'-bis(2,4,6-triisopropylphenyl)-1,1'-binaphthalene (**194**, 1 equiv, 1 mmol, 719.1 mg) and CH_2Cl_2 (10 mL). The flask was then purged with N_2 and cooled to 0 °C. BBr_3 (5 equiv, 5 mmol, 5.0 mL (1 M CH_2Cl_2 solution)) was added. Upon completion (approximately 5 hours), the reaction was quenched with 10 mL water in a drop wise manner at 0 °C, stirring at room temperature for

1 hour. CH_2Cl_2 (10 mL) was then added and the organic layer separated. The organic layer was then washed with H_2O (2 x 5 mL) and brine (2 x 5 mL). The organic layer was then dried using Na_2SO_4, passed through a hydrophobic frit and concentrated under reduced pressure to afford **195** as a white amorphous solid (670.3 mg, 97%).

Reaction no.	Qty. OMe BINOL	Qty. BBr_3	Product, Mass, Yield
171	1.13 g	10.0 mL	**178**, 1.06 g, 99 %
308	719.1 mg	5.0 mL	**195**, 670.3 mg, 97 %

General Experimental Procedure I: Suzuki-Miyaura cross-coupling of iodo binaphthalenes.

For example, for (*R*)-3,3'-di([1,1'-biphenyl]-4-yl)-[1,1'-binaphthalene]-2,2'-diol, **180**.

A flask was fitted with a stirrer bar and charged with a mix of 0.80 mL 1,4-dioxane and H_2O (0.20 mL). To this mixture was added Pd/C (0.05 equiv, 0.0095 mmol, 10 mg of 10% wt powder), K_2CO_3 (4 equiv, 0.76 mmol, 105.0 mg), 4-biphenyl boronic acid (4 equiv, 0.76 mmol, 150.5 mg), and 3,3'-diiodo-[1,1'-binaphthalene]-2,2'-diol (**178**, 1 equiv, 0.19 mmol, 100.0 mg). The reaction was heated to 100 °C overnight. Upon completion, 5 mL CH_2Cl_2 was then added and the layers separated. The organic layer was then washed with H_2O (2 x 2 mL) and brine (1 x 2 mL). The combined organic layers were then dried using Na_2SO_4 and concentrated under reduced pressure to give a crude residue which was purified using flash column chromatography (5% diethyl ether in petroleum ether 40 °C - 60 °C) to afford **180** as a white amorphous solid (92.1 mg, 82 %).

Reaction no.	Qty. Pd/C	Qty. K_2CO_3	Qty. Boronic Aicd	Qty. BINOL	Product, Mass, Yield
172	28.0 mg	309.5 mg	350.3 mg	300.0 mg	**179**, 238.7 mg, 84 %
173	10.0 mg	105.0 mg	150.5 mg	100.0 mg	**180**, 92.1 mg, 82 %
245	25.0 mg	276.4 mg	312.7 mg	273.1 mg	**183**, 239.7 mg, 93 %
246	25.0 mg	276.4 mg	396.1 mg	273.1 mg	**184**, 281.4 mg, 94 %
247	25.0 mg	276.4 mg	328.0 mg	273.1 mg	**185**, 209.6 mg, 79 %
248	25.0 mg	276.4 mg	381.6 mg	273.1 mg	**186**, 248.4 mg, 85 %

249	25.0 mg	276.4 mg	243.9 mg	273.1 mg	**187**, 214.4 mg, 96 %
250	25.0 mg	276.4 mg	344.0 mg	273.1 mg	**188**, 240.6 mg, 88 %

General Experimental Procedure J: Phosphorylation of binaphthalenes.

For example, for (2r)-4-hydroxy-2,6-bis(2,4,6-triisopropylphenyl)dinaphtho[2,1-d:1',2'-f][1,3,2]dioxaphosphepine 4-oxide, **146**.

A flask was fitted with a stirrer bar and charged with (*R*)-3,3'-bis(2,4,6-triisopropylphenyl)-[1,1'-binaphthalene]-2,2'-diol (**195**, 1 equiv, 0.20 mmol, 140.0 mg). Pyridine (0.4 mL) was added before the drop wise addition of $POCl_3$ (2 equiv, 0.40 mmol, 37 μL). The reaction was heated to 60 °C overnight. Upon completion, the reaction was quenched with 5M HCl (1 mL) at 0°C, stirring at 60 °C for 1 hour. CH_2Cl_2 (5 mL) was then added and the organic layer separated. The organic layer was then washed with H_2O (2 x 5 mL) and brine (2 x 5 mL). The organic layer was then dried using Na_2SO_4, passed through a hydrophobic frit and concentrated under reduced pressure to afford **146** as a white solid (146.0 mg, 97 %).

Reaction no.	Qty. BINOL	Qty. $POCl_3$	Product, Mass, Yield
174	200.0 mg	0.072 mL	**144**, 220.9 mg, >99 %
175	80.0 mg	0.024 mL	**145**, 83.2 mg, 98 %
251	163.9 mg	0.055 mL	**147**, 175.1 mg, 96 %
252	154.6 mg	0.055 mL	**148**, 172.7 mg, >99 %
253	179.6 mg	0.055 mL	**149**, 188.3 mg, 95 %
254	159.2 mg	0.055 mL	**150**, 172.5 mg, 97 %
255	175.3 mg	0.055 mL	**151**, 184.2 mg, 95 %
256	134.0 mg	0.055 mL	**152**, 151.0 mg, 99 %
257	164.0 mg	0.055 mL	**153**, 178.9 mg, 98 %
306	699.1 mg	0.184 mL	**155**, 753.4 mg, 99 %
309	140.0 mg	0.037 mL	**146**, 146.0 mg, 97 %

General Experimental Procedure K: Hydrogenation of BINOL.

For example, for (*R*)-5,5',6,6',7,7',8,8'-octahydro-[1,1'-binaphthalene]-2,2'-diol, **181**.

Reaction 243. (*R*)-BINOL (**175**, 1 equiv, 6.98 mmol, 2.00 g) and palladium on activated carbon (0.1 equiv, 0.69 mmol, 742 mg of 10% wt. powder) was added to EtOH (70 mL). The reaction was allowed to proceed for 96 h at room temperature under 50 bars of hydrogen. Upon completion, the reaction mixture was passed through a pad of celite, dried using Na_2SO_4, and concentrated under reduced pressure to afford **181** as a white solid (2.05 g, >99%).

General Experimental Procedure L: Regioselective iodination of H_8BINOL.

For example, for (*R*)-3,3'-diiodo-5,5',6,6',7,7',8,8'-octahydro-[1,1'-binaphthalene]-2,2'-diol, **182**.

Reaction 244. A flask was fitted with a stirrer bar and charged with CH_2Cl_2 (10 mL), (*R*)-5,5',6,6',7,7',8,8'-Octahydro-[1,1'-binaphthalene]-2,2'-diol (**181**, 1 equiv, 1 mmol, 294.4 mg), morpholine (6 equiv, 6 mmol, 522.7 mg, 0.525 mL), and I_2 (2 equiv, 2 mmol, 507.6 mg). The reaction was allowed to proceed at room temperature for 16 hours. Upon completion, the reaction was acidified with 1M HCl (10 mL). The layers were separated and a half saturated solution of $Na_2S_2O_3$ (10 mL) (prepared by making a saturated solution and diluting this by a factor of two) was added to the organic layer and allowed to stir for 1 hour. The organic layer was then dried using Na_2SO_4 and concentrated under reduced pressure to afford **182** as a white solid (545.1 mg, >99%).

General Experimental Procedure M: Kumada cross-coupling of iodinated binaphthalenes.

For example, for (*R*)-2,2'-dimethoxy-3,3'-bis(2,4,6-triisopropylphenyl)-1,1'-binaphthalene, **194**.

Reaction 307. An oven dry flask was fitted with a stirrer bar and charged with magnesium filings (1.77 equiv, 19.05 mmol, 463 mg). The flask was then purged with N_2 and 20% (approx. 3.1 mL) of a 0.7 M solution of 1-bromo-2,4,6-triisopropyl benzene (1 equiv, 10.75 mmol, 2.925 mL) in dry Et_2O (12.7 mL) was added in a drop wise manner. To the reaction was then added 1,2-dibromoethane (0.00015 mol%, 0.00032 mmol, 2.5 µL) as an activator. After addition of the 1,2-dibromoethane, the reaction was heated to reflux and the remaining 1-bromo-2,4,6-triisopropyl benzene solution was added over 1 hour. The reaction was then allowed to proceed at reflux for 16 hours. At this point, the concentration of the formed Grignard solution was determined to be 0.64 M (94% conversion to the Grignard reagent) by titration of with (*E*)-2-((2-phenylhydrazono)methyl)phenol. Once the molarity of the Grignard

solution had been determined, for the Kumada cross-coupling, 15 mL (3 equiv with respect to **177**, 9.6 mmol, 15 mL) of this solution was then added in a drop wise manner to a N_2 purged flask containing a solution of (R)-3,3'-diiodo-2,2'-dimethoxy-1,1'-binaphthalene (**177**, 1 equiv, 3.2 mmol, 1.77 g) and Ni(PPh$_3$)$_2$Cl$_2$ (11 mol%, 0.35 mmol, 229 mg) in dry Et$_2$O (37.6 mL). The reaction was then heated to reflux for 16 hours. Upon completion, the reaction mixture was cooled to 0 °C and acidified with 1M HCl. EtOAc (5 mL) was then added and the layers separated. The organic layer was passed through a short pad of silica, dried using Na$_2$SO$_4$ and concentrated under reduced pressure to afford a crude residue which was purified by flash column chromatography (2% Et$_2$O in petroleum ether 40 °C - 60 °C) to afford **194** as a white solid (1.90 g, 83%).

General Experimental Procedure N: Asymmetric conjugate addition of aniline to vinyl *N*-heterocycles.

For example, for *N*-(2-phenyl-2-(quinolin-2-yl)ethyl)aniline, **174**.

A test tube was fitted with a stirrer bar and charged with 2-(1-phenylvinyl)quinoline (1 equiv, 0.05 mmol, 11.6 mg), Catalyst (**146**, 0.2 equiv, 0.01 mmol 6.1 mg) and THF (50 μL of a THF solution containing the reaction standard (9-bromoanthracene, 0.075 equiv, 0.00375 mmol, 0.075 M solution of 9-bromoanthracene in THF)). Aniline (1.1 equiv, 0.055 mmol, 5.0 μL). The reaction was allowed to proceed for 24 hours at the designated temperature before being analysed by HPLC to obtain values for conversion to *N*-(2-phenyl-2-(quinolin-2-yl)ethyl)aniline (based on 9-bromoanthracene as an internal standard) and enantiomeric excess.

Reaction no.	Qty. Vinyl Het.	Qty. Cat.	Qty. Nuc.	Conv., ee
176	11.6 mg	3.5 mg	5.0 μL	78 %, 11 %
177	11.6 mg	3.5 mg	5.0 μL	65 %, 12 %
178	11.6 mg	3.5 mg	5.0 μL	87 %, 10 %
179	11.6 mg	3.5 mg	5.0 μL	90 %, 13 %
180	11.6 mg	3.5 mg	5.0 μL	87 %, 5 %
181	11.6 mg	3.5 mg	5.0 μL	88 %, 6 %
182	11.6 mg	4.6 mg	5.0 μL	12 %, 0 %
183	11.6 mg	4.6 mg	5.0 μL	74 %, 31 %

184	11.6 mg	4.6 mg	5.0 µL	45 %, 1 %
185	11.6 mg	4.6 mg	5.0 µL	37 %, 5 %
186	11.6 mg	4.6 mg	5.0 µL	94 %, 4 %
187	11.6 mg	4.6 mg	5.0 µL	75 %, 0 %
188	11.6 mg	6.4 mg	5.0 µL	74 %, 30 %
189	11.6 mg	6.4 mg	5.0 µL	12 %, 1 %
190	11.6 mg	6.4 mg	5.0 µL	90 %, 36 %
191	11.6 mg	6.4 mg	5.0 µL	90 %, 10 %
192	11.6 mg	6.4 mg	5.0 µL	81 %, 7 %
193	11.6 mg	6.4 mg	5.0 µL	74 %, 2 %
194	11.6 mg	7.7 mg	5.0 µL	36 %, 19 %
195	11.6 mg	7.7 mg	5.0 µL	66 %, -5 %
196	11.6 mg	7.7 mg	5.0 µL	63 %, 23 %
197	11.6 mg	7.7 mg	5.0 µL	96 %, 30 %
198	11.6 mg	7.7 mg	5.0 µL	86 %, 20 %
199	11.6 mg	7.7 mg	5.0 µL	89 %, 23 %
200	11.6 mg	6.2 mg	5.0 µL	57 %, -2 %
201	11.6 mg	6.2 mg	5.0 µL	76 %, 10 %
202	11.6 mg	6.2 mg	5.0 µL	72 %, -1 %
203	11.6 mg	6.2 mg	5.0 µL	92 %, -3 %
204	11.6 mg	6.2 mg	5.0 µL	75 %, -2 %
205	11.6 mg	6.2 mg	5.0 µL	80 %, -2 %
206	11.6 mg	6.0 mg	5.0 µL	10 %, 24 %
207	11.6 mg	6.0 mg	5.0 µL	21 %, 7 %
208	11.6 mg	6.0 mg	5.0 µL	16 %, 22 %
209	11.6 mg	6.0 mg	5.0 µL	32 %, 11 %
210	11.6 mg	6.0 mg	5.0 µL	31 %, 10 %
211	11.6 mg	6.0 mg	5.0 µL	48 %, 5 %
212	11.6 mg	5.8 mg	5.0 µL	96 %, 44 %
213	11.6 mg	5.8 mg	5.0 µL	7 %, 0 %
214	11.6 mg	5.8 mg	5.0 µL	92 %, 43 %
215	11.6 mg	5.8 mg	5.0 µL	100 %, 13 %

216	11.6 mg	5.8 mg	5.0 µL	86 %, 22 %
217	11.6 mg	5.8 mg	5.0 µL	95 %, 9 %
218	11.6 mg	7.4 mg	5.0 µL	73 %, 21 %
219	11.6 mg	7.4 mg	5.0 µL	8 %, 20 %
220	11.6 mg	7.4 mg	5.0 µL	81 %, 5 %
221	11.6 mg	7.4 mg	5.0 µL	91 %, 22 %
222	11.6 mg	7.4 mg	5.0 µL	97 %, 8 %
223	11.6 mg	7.4 mg	5.0 µL	88 %, 13 %
224	11.6 mg	9.7 mg	5.0 µL	42 %, 1 %
225	11.6 mg	9.7 mg	5.0 µL	90 %, 19 %
226	11.6 mg	9.7 mg	5.0 µL	66 %, 3 %
227	11.6 mg	9.7 mg	5.0 µL	85 %, 7 %
228	11.6 mg	9.7 mg	5.0 µL	75 %, 5 %
229	11.6 mg	9.7 mg	5.0 µL	78 %, 7 %
230	11.6 mg	5.7 mg	5.0 µL	46 %, 34 %
231	11.6 mg	5.7 mg	5.0 µL	75 %, 33 %
232	11.6 mg	5.7 mg	5.0 µL	57 %, 29 %
233	11.6 mg	5.7 mg	5.0 µL	71 %, 27 %
234	11.6 mg	5.7 mg	5.0 µL	55 %, 17 %
235	11.6 mg	5.7 mg	5.0 µL	51 %, 16 %
236	11.6 mg	6.5 mg	5.0 µL	58 %, 32 %
237	11.6 mg	6.5 mg	5.0 µL	58 %, 27 %
238	11.6 mg	6.5 mg	5.0 µL	61 %, 26 %
239	11.6 mg	6.5 mg	5.0 µL	53 %, 17 %
240	11.6 mg	6.5 mg	5.0 µL	50 %, 15 %
241	11.6 mg	6.5 mg	5.0 µL	53 %, 9 %
258	11.6 mg	3.6 mg	5.0 µL	62 %, 15 %
259	11.6 mg	3.6 mg	5.0 µL	53 %, 28 %
260	11.6 mg	3.6 mg	5.0 µL	69 %, 17 %
261	11.6 mg	3.6 mg	5.0 µL	84 %, 28 %
262	11.6 mg	3.6 mg	5.0 µL	51 %, 15 %
263	11.6 mg	3.6 mg	5.0 µL	48 %, 13 %

264	11.6 mg	5.8 mg	5.0 μL	64 %, -58 %
265	11.6 mg	5.8 mg	5.0 μL	40 %, -58 %
266	11.6 mg	5.8 mg	5.0 μL	74 %, -52 %
267	11.6 mg	5.8 mg	5.0 μL	77 %, -48 %
268	11.6 mg	5.8 mg	5.0 μL	93 %, -30 %
269	11.6 mg	5.8 mg	5.0 μL	40 %, -6 %
270	11.6 mg	6.6 mg	5.0 μL	86 %, 48 %
271	11.6 mg	6.6 mg	5.0 μL	47 %, 45 %
272	11.6 mg	6.6 mg	5.0 μL	51 %, 43 %
273	11.6 mg	6.6 mg	5.0 μL	86 %, 37 %
274	11.6 mg	6.6 mg	5.0 μL	87 %, 22 %
275	11.6 mg	6.6 mg	5.0 μL	49 %, 3 %
276	11.6 mg	5.9 mg	5.0 μL	56 %, 37 %
277	11.6 mg	5.9 mg	5.0 μL	39 %, 40 %
278	11.6 mg	5.9 mg	5.0 μL	59 %, 31 %
279	11.6 mg	5.9 mg	5.0 μL	52 %, 33 %
280	11.6 mg	5.9 mg	5.0 μL	76 %, 24 %
281	11.6 mg	5.9 mg	5.0 μL	68 %, 29 %
282	11.6 mg	6.5 mg	5.0 μL	65 %, 17 %
283	11.6 mg	6.5 mg	5.0 μL	44 %, 11 %
284	11.6 mg	6.5 mg	5.0 μL	72 %, 12 %
285	11.6 mg	6.5 mg	5.0 μL	56 %, 8 %
286	11.6 mg	6.5 mg	5.0 μL	87 %, 9 %
287	11.6 mg	6.5 mg	5.0 μL	75 %, 4 %
288	11.6 mg	5.1 mg	5.0 μL	74 %, 33 %
289	11.6 mg	5.1 mg	5.0 μL	59 %, 39 %
290	11.6 mg	5.1 mg	5.0 μL	73 %, 25 %
291	11.6 mg	5.1 mg	5.0 μL	77 %, 32 %
292	11.6 mg	5.1 mg	5.0 μL	56 %, 9 %
293	11.6 mg	5.1 mg	5.0 μL	45 %, 17 %
294	11.6 mg	6.1 mg	5.0 μL	61 %, 36 %
295	11.6 mg	6.1 mg	5.0 μL	48 %, 33 %

296	11.6 mg	6.1 mg	5.0 µL	48 %, 31 %
297	11.6 mg	6.1 mg	5.0 µL	90 %, 21 %
298	11.6 mg	6.1 mg	5.0 µL	51 %, 14 %
299	11.6 mg	6.1 mg	5.0 µL	82 %, 9 %
310	11.6 mg	5.8 mg	5.0 µL	65 %, 33 %
311	11.6 mg	5.8 mg	5.0 µL	89 %, 20 %
312	11.6 mg	5.8 mg	5.0 µL	71 %, 18 %
313	11.6 mg	5.8 mg	5.0 µL	83 %, 8 %
314	11.6 mg	5.8 mg	5.0 µL	56 %, 10 %
315	11.6 mg	5.8 mg	5.0 µL	54 %, 0 %
316	11.6 mg	5.9 mg	5.0 µL	7 %, 22%
317	11.6 mg	5.9 mg	5.0 µL	23 %, 15 %
318	11.6 mg	5.9 mg	5.0 µL	35 %, 13 %
319	11.6 mg	5.9 mg	5.0 µL	21 %, 3 %
320	11.6 mg	5.9 mg	5.0 µL	60 %, -5 %
321	11.6 mg	5.9 mg	5.0 µL	50 %, 7 %
322	11.6 mg	6.1 mg	5.0 µL	37 %, 64 %
323	11.6 mg	6.1 mg	5.0 µL	49 %, 4 %
324	11.6 mg	6.1 mg	5.0 µL	98 %, 6 %
325	11.6 mg	6.1 mg	5.0 µL	77 %, 3 %
326	11.6 mg	6.1 mg	5.0 µL	82 %, 5 %
327	11.6 mg	6.1 mg	5.0 µL	60 %, 1 %
328	11.6 mg	6.0 mg	5.0 µL	58 %, 42 %
329	11.6 mg	6.0 mg	5.0 µL	50 %, 39 %
330	11.6 mg	6.0 mg	5.0 µL	58 %, 39 %
331	11.6 mg	6.0 mg	5.0 µL	54 %, 34 %
332	11.6 mg	6.0 mg	5.0 µL	88 %, 23 %
333	11.6 mg	6.0 mg	5.0 µL	40 %, 10 %
334	11.6 mg	6.1 mg	5.0 µL	0 %, 0 %
335	11.6 mg	5.8 mg	5.0 µL	1 %, -67 %
336	11.6 mg	6.1 mg	5.0 µL	0 %, 0 %
337	11.6 mg	5.8 mg	5.0 µL	1 %, -37 %

338	11.6 mg	6.1 mg	5.0 μL	0 %, 0 %
339	11.6 mg	5.8 mg	5.0 μL	3 %, -86 %
340	11.6 mg	6.1 mg	5.0 μL	5 %, 54 %
341	11.6 mg	5.8 mg	5.0 μL	34 %, -66 %
342	11.6 mg	6.1 mg	5.0 μL	19 %, 74 %
343	11.6 mg	5.8 mg	5.0 μL	8 %, -56 %
344	11.6 mg	6.1 mg	5.0 μL	95 %, 53 %
345	11.6 mg	5.8 mg	5.0 μL	37 %, -69 %
346	11.6 mg	6.1 mg	5.0 μL	26 %, 81 %
347	11.6 mg	5.8 mg	5.0 μL	19 %, -62 %
348	11.6 mg	6.1 mg	5.0 μL	67 %, 51 %
349	11.6 mg	5.8 mg	5.0 μL	26 %, -67 %
350	11.6 mg	6.1 mg	5.0 μL	33 %, 80 %
351	11.6 mg	5.8 mg	5.0 μL	32 %, -63 %
352	11.6 mg	6.1 mg	5.0 μL	70 %, 40 %
353	11.6 mg	5.8 mg	5.0 μL	72 %, -64 %
354	11.6 mg	6.1 mg	5.0 μL	45 %, 74 %
355	11.6 mg	5.8 mg	5.0 μL	39 %, -61 %
356	11.6 mg	6.1 mg	5.0 μL	67 %, 34 %
357	11.6 mg	5.8 mg	5.0 μL	70 %, -60 %
358	11.6 mg	6.1 mg	5.0 μL	37 %, 64 %
359	11.6 mg	5.8 mg	5.0 μL	64 %, -58 %
360	11.6 mg	6.1 mg	5.0 μL	57 %, 30 %
361	11.6 mg	5.8 mg	5.0 μL	40 %, -58 %
362	11.6 mg	6.1 mg	5.0 μL	54 %, 64 %
363	11.6 mg	5.8 mg	5.0 μL	57 %, -52 %
364	11.6 mg	6.1 mg	5.0 μL	69 %, 32 %
365	11.6 mg	5.8 mg	5.0 μL	65 %, -49 %
366	11.6 mg	6.1 mg	5.0 μL	76 %, 54 %
367	11.6 mg	5.8 mg	5.0 μL	91 %, -46 %
368	11.6 mg	6.1 mg	5.0 μL	80 %, 29 %
369	11.6 mg	5.8 mg	5.0 μL	95 %, -45 %

370	11.6 mg	6.1 mg	5.0 μL	NA %, 6 %
371	11.6 mg	6.1 mg	5.0 μL	NA %, 13 %
372	11.6 mg	6.1 mg	5.0 μL	NA %, 29 %
373	11.6 mg	6.1 mg	5.0 μL	NA %, 4 %
374	11.6 mg	6.1 mg	5.0 μL	NA %, 3 %
375	11.6 mg	6.1 mg	5.0 μL	37 %, 64%
376	11.6 mg	6.1 mg	5.0 μL	NA %, 12 %
377	11.6 mg	6.1 mg	5.0 μL	56 %, 14 %
378	11.6 mg	6.1 mg	5.0 μL	NA %, 6 %
379	11.6 mg	6.1 mg	5.0 μL	33 %, 28%
380	11.6 mg	6.1 mg	5.0 μL	NA %, 33 %
381	11.6 mg	6.1 mg	5.0 μL	NA %, 3 %
382	11.6 mg	6.1 mg	5.0 μL	NA %, 26 %
383	11.6 mg	6.1 mg	5.0 μL	85 %, 23 %
384	11.6 mg	6.1 mg	5.0 μL	91 %, 14 %
385	11.6 mg	6.1 mg	5.0 μL	73 %, 11 %
386	11.6 mg	6.1 mg	5.0 μL	NA %, 28 %
387	11.6 mg	6.1 mg	5.0 μL	NA %, 36 %
388	11.6 mg	6.1 mg	5.0 μL	57 %, 30%
389	11.6 mg	6.1 mg	5.0 μL	100 %, 22 %
390	11.6 mg	6.1 mg	5.0 μL	83 %, 31%
391	11.6 mg	5.8 mg	5.0 μL	NA %, -4 %
392	11.6 mg	5.8 mg	5.0 μL	NA %, -28 %
393	11.6 mg	5.8 mg	5.0 μL	NA %, -31 %
394	11.6 mg	5.8 mg	5.0 μL	NA %, -3 %
395	11.6 mg	5.8 mg	5.0 μL	NA %, -6 %
396	11.6 mg	5.8 mg	5.0 μL	64 %, -58 %
397	11.6 mg	5.8 mg	5.0 μL	NA %, -27 %
398	11.6 mg	5.8 mg	5.0 μL	9 %, -6%
399	11.6 mg	5.8 mg	5.0 μL	NA %, -20 %
400	11.6 mg	5.8 mg	5.0 μL	23 %, -58 %
401	11.6 mg	5.8 mg	5.0 μL	NA %, -56 %

402	11.6 mg	5.8 mg	5.0 µL	NA %, -23 %
403	11.6 mg	5.8 mg	5.0 µL	NA %, -46 %
404	11.6 mg	5.8 mg	5.0 µL	100 %, -46 %
405	11.6 mg	5.8 mg	5.0 µL	31 %, -56 %
406	11.6 mg	5.8 mg	5.0 µL	24 %, -56 %
407	11.6 mg	5.8 mg	5.0 µL	NA %, -49 %
408	11.6 mg	5.8 mg	5.0 µL	11 %, -6 %
409	11.6 mg	5.8 mg	5.0 µL	40 %, -58 %
410	11.6 mg	5.8 mg	5.0 µL	89 %, -46 %
411	11.6 mg	5.8 mg	5.0 µL	68 %, -16 %
412	11.6 mg	6.1 mg	5.0 µL	19 %, 22 %
413	11.6 mg	6.1 mg	5.0 µL	30 %, 21 %
414	11.6 mg	6.1 mg	5.0 µL	54 %, 21 %
415	11.6 mg	6.1 mg	5.0 µL	21 %, 15 %
416	11.6 mg	6.1 mg	5.0 µL	31 %, 10 %
417	11.6 mg	6.1 mg	5.0 µL	64 %, 9 %
418	11.6 mg	6.1 mg	5.0 µL	15 %, 11 %
419	11.6 mg	6.1 mg	5.0 µL	28 %, 9 %
420	11.6 mg	6.1 mg	5.0 µL	70 %, 10 %
421	11.6 mg	6.1 mg	5.0 µL	38 %, 30 %
422	11.6 mg	6.1 mg	5.0 µL	43 %, 19 %
423	11.6 mg	6.1 mg	5.0 µL	60 %, 24 %
424	11.6 mg	5.8 mg	5.0 µL	18 %, -33 %
425	11.6 mg	5.8 mg	5.0 µL	30 %, -36 %
426	11.6 mg	5.8 mg	5.0 µL	59 %, -39 %
427	11.6 mg	5.8 mg	5.0 µL	23 %, -35 %
428	11.6 mg	5.8 mg	5.0 µL	48 %, -38 %
429	11.6 mg	5.8 mg	5.0 µL	82 %, -40 %
430	11.6 mg	5.8 mg	5.0 µL	23 %, -28 %
431	11.6 mg	5.8 mg	5.0 µL	53 %, -32 %
432	11.6 mg	5.8 mg	5.0 µL	71 %, -34 %
433	11.6 mg	5.8 mg	5.0 µL	40 %, -55 %

434	11.6 mg	5.8 mg	5.0 µL	41 %, -41 %
435	11.6 mg	5.8 mg	5.0 µL	58 %, -52 %
436	11.6 mg	6.1 mg	5.0 µL	37 %, 49 %
437	11.6 mg	6.1 mg	5.0 µL	34 %, 48 %
438	11.6 mg	6.1 mg	5.0 µL	33 %, 46 %
439	11.6 mg	6.1 mg	5.0 µL	40 %, 50 %
440	11.6 mg	6.1 mg	5.0 µL	53 %, 64 %
441	11.6 mg	5.8 mg	5.0 µL	36 %, -58 %
442	11.6 mg	5.8 mg	5.0 µL	38 %, -58 %
443	11.6 mg	5.8 mg	5.0 µL	31 %, -48 %
444	11.6 mg	5.8 mg	5.0 µL	38 %, -54 %
445	11.6 mg	5.8 mg	5.0 µL	38 %, -68 %

8. Compound Characterisation Data

2-(Prop-1-en-2-yl)pyridine, **113**.[51]
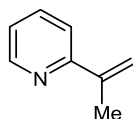
Prepared according to General Experimental Procedure B using 1-(pyridin-2-yl)ethanone (1 equiv, 50 mmol, 6.57 g, 6.08 mL) and methyltriphenylphosphonium bromide (1.3 equiv, 65.0 mmol, 23.24 g), and *n*-butyllithium (1.2 equiv, 60 mmol, 37.44 mL (1.6 M hexane solution)) to afford **113** as a colourless liquid (4.73 g, 80%).

υ_{max} (neat): 3082, 2974, 1584, 1564, 1466, 1431 cm^{-1}.

^{1}H NMR (400 MHz, CDCl$_3$): δ 8.60 (ddd, 1H, *J* = 4.8, 1.8, 0.9 Hz), 7.65 (td, 1H, *J* = 7.8, 1.8 Hz), 7.49 (dt, 1H, *J* = 8.0, 1.0 Hz), 7.17 (ddd, 1H, *J* = 7.5, 4.8, 1.1 Hz), 5.86 (dd, 1H, *J* = 1.6, 0.8 Hz), 5.31 (app. p, 1H, *J* = 1.5 Hz), 2.23 (s, 3H).

^{13}C NMR (400 MHz, CDCl$_3$): δ 158.4, 149.0, 143.4, 136.4, 122.2, 119.9, 115.7, 20.6.

HRMS: exact mass calculated for [M+H]$^{+}$ (C$_8$H$_{10}$N) requires *m/z* 120.0808, found [M+H]$^{+}$ *m/z* 120.0809.

2-(1-Phenylvinyl)pyridine, **119**.[51]
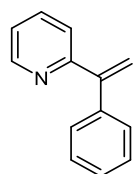
Prepared according to General Experimental Procedure E using 1-phenyl-1-(pyridin-2-yl)ethanol (**120**, 1 equiv, 2 mmol, 370.0 mg) and H$_2$SO$_4$ (2 mL (85% H$_2$O solution)) to afford **119** as an orange oil (322.3 mg, 89%).

υ_{max} (neat): 3049, 1580, 1503, 1486, 1427 cm^{-1}.

^{1}H NMR (400 MHz, CDCl$_3$): δ 8.56 (ddd, 1H, J = 4.8, 1.7, 0.8 Hz), 7.55 (td, 1H, J = 7.7, 1.9 Hz), 7.28-7.24 (m, 5H), 7.19-7.17 (m, 1H), 7.13 (ddd, 1H, J = 7.5, 4.8, 1.1 Hz), 5.92 (d, 1H, J = 1.4 Hz), 5.53 (d, 1H, J = 1.4 Hz).

^{13}C NMR (400 MHz, CDCl$_3$): δ 158.6, 149.5, 149.3, 140.5, 136.3, 128.5, 128.4, 127.9, 122.9, 122.5, 117.8.

HRMS: exact mass calculated for [M+H]$^+$ (C$_{13}$H$_{12}$N) requires m/z 182.0964, found [M+H]$^+$ m/z 182.0959.

1-Phenyl-1-(pyridin-2-yl)ethanol, **120**.[52]
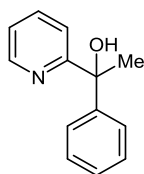
Prepared according to General Experimental Procedure A using phenyl(pyridin-2-yl)methanone (1 equiv, 20 mmol, 3.66 g) and methylmagnesium bromide (2 equiv, 40 mmol, 13.33 mL (3 M Et$_2$O solution)) to afford **120** as a white amorphous solid (3.96 g, >99%).

Melting point: 189 - 191 °C. Lit melting point: 189 °C.[53]

υ$_{max}$ (solid): 3319, 2978, 2930, 1589, 1388 cm^{-1}.

^{1}H NMR (400 MHz, CDCl$_3$): δ 8.54 (d, 1H, J = 4.8 Hz), 7.66 (td, 1H, J = 7.8, 1.7 Hz), 7.51-7.48 (m, 2H), 7.34-7.29 (m, 3H), 7.23 (tt, 1H, J = 7.8, 1.7 Hz), 7.19 (ddd, 1H, 7.3, 4.9, 0.7 Hz), 5.82 (brs, 1H), 1.95 (s, 3H).

^{13}C NMR (400 MHz, CDCl$_3$): δ 165.1, 147.7, 147.5, 137.3, 128.5, 127.3, 126.2, 122.4, 120.7, 75.4, 29.6.

1-(Quinolin-2-yl)ethanol, **122**.[54]
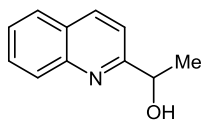
Prepared according to General Experimental Procedure A using quinoline-2-carboxaldehyde (**121**, 1 equiv, 10 mmol, 1.57 g) and methylmagnesium bromide (2 equiv, 20 mmol, 6.66 mL (3 M Et$_2$O solution)) to afford **122** as a white amorphous solid (1.71 g, 99%).

Melting point: 77-79 °C. Lit melting point: 81-82 °C.[55]

υ_{max} (solid): 3246, 2966, 2914, 1597, 1503, 1427 cm^{-1}.

^{1}H NMR (400 MHz, CDCl$_3$): δ 8.16 (d, 1H, J = 8.5 Hz), 8.09 (d, 1H, J = 8.3 Hz), 7.83 (dd, 1H, J = 8.1, 1.1 Hz), 7.73 (ddd, 1H, J = 8.5, 7.0, 1.5 Hz), 7.55 (ddd, 1H, J = 8.1, 7.0, 1.2 Hz), 7.37 (d, 1H, J = 8.5 Hz), 5.05 (q, 1H, J = 6.6 Hz. 1 x OH signal underneath (1H)), 1.59 (d, 3H, J = 6.6 Hz).

^{13}C NMR (400 MHz, CDCl$_3$): δ 163.3, 146.7, 137.4, 130.2, 129.1, 127.9, 127.8, 126.7, 118.3, 69.1, 24.4.

HRMS: exact mass calculated for [M+H]$^+$ (C$_{11}$H$_{12}$NO) requires m/z 174.0913, found [M+H]$^+$ m/z 174.0909.

1-(Quinolin-2-yl)ethanone, **123**.[56]
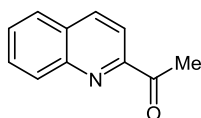
Prepared according to General Experimental Procedure D using **122** (1 equiv, 9 mmol, 1.56 g) and MnO$_2$ (6 equiv, 54 mmol, 4.69 g) to afford **123** as a brown/orange amorphous solid (1.46 g, 95%).

Melting point: 49 - 51 °C. Lit melting point: 48 - 50.5 °C.[56]

υ_{max} (solid): 2922, 2851, 1694, 1600, 1503, 1435 cm^{-1}.

^{1}H NMR (400 MHz, CDCl$_3$): δ 8.28 (d, 1H, J = 8.1 Hz), 8.22 (d, 1H, J = 8.2 Hz), 8.14 (d, 1H, J = 8.1 Hz), 7.88 (d, 1H, J = 8.2 Hz), 7.80 (ddd, 1H, J = 8.1, 6.9, 1.4 Hz), 7.66 (ddd, 1H, J = 8.1, 6.9, 1.1 Hz), 2.88 (s, 3H).

^{13}C NMR (400 MHz, CDCl$_3$): δ 201.0, 153.6, 147.6, 137.2, 130.9, 130.3, 129.9, 128.9, 128.0, 118.3, 25.9.

HRMS: exact mass calculated for [M+H]$^+$ (C$_{11}$H$_{10}$NO) requires m/z 172.0757, found [M+H]$^+$ m/z 172.0753.

2-(Quinolin-2-yl)propan-2-ol, **124**.
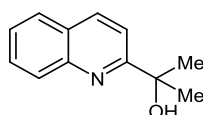
Prepared according to General Experimental Procedure A using **123** (1 equiv, 8 mmol, 1.37 g) and methylmagnesium bromide (2 equiv, 16 mmol, 5.33 mL (3 M Et$_2$O solution)) to afford **124** as an orange amorphous solid (1.36 g, 91%).

Melting point: 66 - 68 °C.

υ_{max} (solid): 3393, 2972, 2928, 1694, 1599, 1454 cm^{-1}.

^{1}H NMR (400 MHz, CDCl$_3$): δ 8.07 (d, 1H, J = 8.5 Hz), 8.02 (d, 1H, J = 8.4 Hz), 7.73 (d, 1H, J = 8.1 Hz), 7.63 (t, 1H, J = 7.6 Hz), 7.45 (t, 1H, J = 7.5 Hz), 7.39 (d, 1H, J = 8.6 Hz), 5.91 (brs, 1H), 1.60 (s, 6H).

^{13}C NMR (400 MHz, CDCl$_3$): δ 166.8, 145.9, 137.4, 129.8, 128.8, 127.5, 127.1, 126.4, 117.1, 71.9, 30.6.

HRMS: exact mass calculated for [M+H]$^+$ (C$_{12}$H$_{14}$NO) requires m/z 188.1070, found [M+H]$^+$ m/z 188.1066.

2-(Prop-1-en-2-yl)quinoline, **125**.[57]
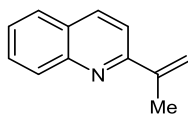
Prepared according to General Experimental Procedure E using **124** (1 equiv, 7 mmol, 1.31 g) and H_2SO_4 (7 mL, 85% H_2O solution)) to afford **125** as a yellow amorphous solid (1.13 g, 96%).

Melting point: 49 - 51 °C.

υ_{max} (solid): 3057, 2951, 2920, 1695, 1597, 1555, 102, 1425 cm^{-1}.

^{1}H NMR (400 MHz, CDCl$_3$): δ 8.11 (dd, 2H, J = 8.5, 1.9 Hz), 7.79 (dd, 1H, J = 8.1, 1.2 Hz), 7.72-7.68 (m, 2H), 7.50 (ddd, 1H, J = 8.1, 6.9, 1.1 Hz), 5.94 (s, 1H), 5.50 (app. p, 1H, J = 1.4 Hz), 2.38 (dd, 3H, J = 1.4, 0.9 Hz).

^{13}C NMR (400 MHz, CDCl$_3$): δ 158.8, 148.0, 144.8, 136.3, 130.0, 129.7, 127.6, 127.5, 126.5, 118.6, 117.3, 20.9.

HRMS: exact mass calculated for [M+H]$^+$ (C$_{12}$H$_{12}$N) requires m/z 170.0964, found [M+H]$^+$ m/z 170.0960.

1-Phenyl-1-(quinolin-2-yl)ethanol, **126**.[58]
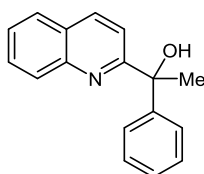
Prepared according to General Experimental Procedure A using **123** (1 equiv, 8 mmol, 1.37 g) and phenylmagnesium bromide (2 equiv, 16 mmol, 5.33 mL (3 M Et$_2$O solution)) to afford **126** as a white amorphous solid (1.85 g, 93%).

Melting point: 100 - 102 °C. Lit melting point: 101 - 101.5 °C.[59]

υ_{max} (solid): 3337, 2961, 2924, 1595, 1503, 1447, 1385 cm^{-1}.

^{1}H NMR (400 MHz, CDCl$_3$): δ 8.17 (d, 1H, J = 8.4 Hz), 8.10 (d, 1H, J = 8.6 Hz), 7.81 (dd, 1H, J = 8.4, 1.4 Hz), 7.77 (ddd, 1H, J = 8.4, 7.0, 1.4 Hz), 7.59-7.54 (m, 3H), 7.37-7.31 (m, 3H), 7.27-7.25 (m, 1H), 6.72 (brs, 1H), 2.04 (s, 3H).

^{13}C NMR (400 MHz, CDCl$_3$): δ 164.8, 146.6, 138.1, 130.6, 129.1, 128.9, 127.8, 128.7, 127.6, 127.5, 127.2, 126.6, 118.9, 75.5, 29.0.

HRMS: exact mass calculated for [M+H]$^+$ (C$_{17}$H$_{16}$NO) requires m/z 250.1226, found [M+H]$^+$ m/z 250.1224.

2-(1-Phenylvinyl)quinoline, **127**.[57]
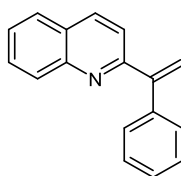
Prepared according to General experimental Procedure E using **126** (1 equiv, 7 mmol, 1.74 g) and H$_2$SO$_4$ (7 mL, 85% H$_2$O solution)) to afford **127** as an orange amorphous solid (1.49 g, 92%).

Melting point: 110 - 112 °C. Lit melting point: 111- 113 °C.[57]

υ$_{max}$ (solid): 3049, 2918, 1591, 1553, 1491, 1443 cm^{-1}.

^{1}H NMR (400 MHz, CDCl$_3$): δ 8.17 (d, J = 8.4 Hz, 1H), 8.10 (d, 1H, J = 8.6 Hz), 7.82 (dd, 1H, J = 8.1, 1.2 Hz), 7.73 (ddd, 1H, J = 8.4, 6.9, 1.5 Hz), 7.55 (ddd, 1H, J = 8.1, 6.9, 1.2 Hz), 7.45 - 7.34 (m, 6H), 6.13 (d, 1H, J = 1.4 Hz), 5.79 (d, 1H, J = 1.4 Hz).

^{13}C NMR (400 MHz, CDCl$_3$): δ 159.2, 149.9, 148.3, 140.5, 136.4, 130.2, 129.9, 128.7, 128.7, 128.3, 127.7, 126.8, 121.5, 119.1. 1 carbon signal not observed/coincident.

HRMS: exact mass calculated for [M+H]$^+$ (C$_{17}$H$_{14}$N) requires m/z 232.1112, found [M+H]$^+$ m/z 232.1116.

N-(2-(Pyridin-2-yl)propyl)aniline, **132**.
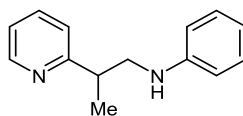
Prepared according to General Experimental Procedure C using **113** (1 equiv, 1 mmol, 116.2 mg), 4-hydroxydinaphtho[2,1-d:1',2'-f][1,3,2]dioxaphosphepine-4-oxide (0.2 equiv, 0.2 mmol, 69.7 mg), and aniline (1.1 equiv, 1.1 mmol, 100.5 μL) to afford **132** as a yellow amorphous solid (42.5 mg, 20%).

Melting point: 183 - 185 °C.

υ_{max} (solid): 3271, 2926, 2828, 1591, 1497, 1433 cm^{-1}.

^{1}H NMR (400 MHz, CDCl$_3$): δ 8.60 (ddd, 1H, *J* = 4.8, 1.7, 0.9 Hz), 7.62 (td, 1H, *J* = 7.7, 1.9 Hz), 7.21-7.12 (m, 4H), 6.68 (tt, 1H, *J* = 7.4, 1.1 Hz), 6.63-6.58 (m, 2H), 3.48 (dd, 1H, *J* = 12.4, 8.2 Hz), 3.40 (dd, 1H, *J* = 12.9, 5.5 Hz), 3.32-3.20 (m, 1H), 1.40 (d, 3H, *J* = 7.0 Hz). 1 deuterium-exchangeable NH signal missing.

^{13}C NMR (400 MHz, CDCl$_3$): δ 164.3, 149.6, 148.6, 137.0, 129.5, 122.6, 121.9, 117.5, 113.2, 50.1, 41.3, 18.8.

HRMS: exact mass calculated for [M+H]$^+$ (C$_{14}$H$_{17}$N$_2$) requires *m/z* 213.1386, found [M+H]$^+$ *m/z* 213.1381.

HPLC assay: t_R enantiomer 1 = 14.1 min., t_R enantiomer 2 = 19.3 min.

(*R*)-2,6-Bis(4-chlorophenyl)-4-hydroxydinaphtho[2,1-d:1',2'-f][1,3,2]dioxaphosphepine 4-oxide, **144**.
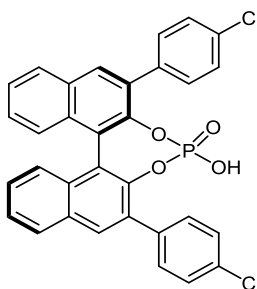
Prepared according to General Experimental Procedure J using **179** (1 equiv, 0.39 mmol, 200.0 mg) and POCl$_3$ (2 equiv, 0.78 mmol, 72.1 μL) to afford **144** as a white amorphous solid (220.9 mg, >99%).

Melting point: 251 - 253 °C.

υ$_{max}$ (solid): 3055, 2934, 1396, 1304, 1213 cm^{-1}.

[α]$_D^{20}$ +187.5 (c = 1.00, CHCl$_3$).

^{1}H NMR (400 MHz, CDCl$_3$): δ 8.11 (s, 1H), 8.07 (s, 1H), 8.03 (dd, 2H *J* = 8.1, 5.8 Hz), 7.69-7.66 (m, 2H), 7.64-7.61 (m, 2H), 7.60-7.56 (m, 2H), 7.50-7.46 (m, 4H), 7.41-7.36 (m, 4H). 1 deuterium-exchangeable OH peak missing.

HRMS: exact mass calculated for [M-H]$^-$ (C$_{32}$H$_{18}$Cl$_2$O$_4$P) requires *m/z* 568.0359 (Cl^{35}), found [M-H]$^-$ *m/z* 568.0350 (Cl^{35}), 569.0297 (Cl^{37}).

(*R*)-2,6-Di([1,1'-biphenyl]-4-yl)-4-hydroxydinaphtho[2,1-d:1',2'-f][1,3,2]dioxaphosphepine 4-oxide, **145**.[60]
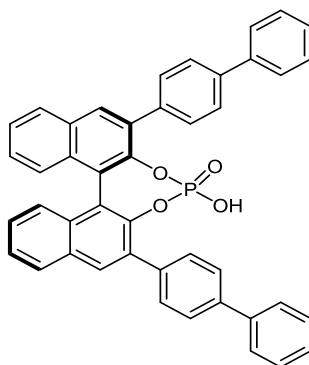
Prepared according to General Experimental Procedure J using **179** (1 equiv, 0.13 mmol, 80.0 mg) and POCl$_3$ (2 equiv, 0.26 mmol, 24.0 μL) to afford **145** as a white amorphous solid (83.2 mg, 98%).

Melting point: 267 - 269 °C.

υ$_{max}$ (solid): 3028, 1487, 1416, 1180, 1150, 1018, 843 cm^{-1}.

[α]$_D^{20}$ -348.2 (c = 1.00, CHCl$_3$).

^{1}H NMR (400 MHz, CDCl$_3$): δ 8.19 (s, 1H), 8.15 (s, 1H), 8.05 (dd, 2H, J = 8.2, 4.2 Hz), 7.86-7.84 (m, 2H), 7.80-7.68 (m, 10H), 7.60-7.57 (m, 2H), 7.53-7.44 (m, 5H), 7.41-7.35 (m, 5H). 1 deuterium-exchangeable OH signal missing.

HRMS: exact mass calculated for [M-H]$^-$ (C$_{44}$H$_{28}$O$_4$P) requires m/z 651.1731, found [M-H]$^-$ m/z 651.1715.

(R)-(2r)-4-Hydroxy-2,6-bis(2,4,6-triisopropylphenyl)dinaphtho[2,1-d:1',2'-f][1,3,2]dioxaphosphepine 4-oxide, **146**.[61]
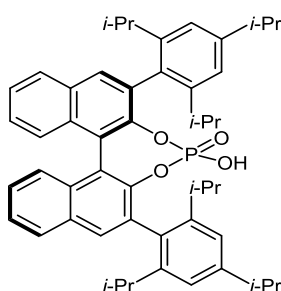
Prepared according to General Experimental Procedure J using **195** (1 equiv, 0.20 mmol, 140.0 mg) and POCl$_3$ (2 equiv, 0.40 mmol, 37 µL) to afford **146** as a white amorphous solid (146.0 mg, 97%).

Melting point: 311 - 313 °C.

υ$_{max}$ (solid): 2959, 2868, 1462, 1362, 1173, 1150, 1018 cm^{-1}.

[α]$_D^{20}$ -101.5 (c = 1.00, CHCl$_3$).

^{1}H NMR (400 MHz, CDCl$_3$): δ 7.93 (s, 1H), 7.90 (s, 1H), 7.86 (s, 2H), 7.54-7.50 (m, 2H), 7.34 (m, 4H), 7.02-7.01 (m, 4H), 2.89 (app. p, 2H, J = 7.9 Hz), 2.68-2.59 (m, 4H), 1.26 (d, 12H, J = 6.8 Hz), 1.11 (d, 6H, J = 6.8 Hz), 1.08 (d, 6H, J = 6.8 Hz), 0.94 (d, 6H, J = 6.8 Hz), 0.90 (d, 6H, J = 6.5 Hz). 1 deuterium-exchangeable OH signal missing.

^{13}C NMR (400 MHz, CDCl$_3$): δ 148.9, 148.4, 147.9, 133.0, 132.7, 132.5, 132.4, 131.6, 131.4, 128.5, 127.7, 126.6, 126.1, 122.3, 121.4, 120.7, 34.6, 31.3, 31.0, 26.8, 25.4, 24.4, 24.3, 23.6, 23.1.

HRMS: exact mass calculated for [M-H]$^-$ (C$_{50}$H$_{56}$O$_4$P) requires *m/z* 751.3922, found [M-H]$^-$ *m/z* 751.3916.

(*R*)-4-Hydroxy-2,6-diiodo-8,9,10,11,12,13,14,15-octahydrodinaphtho[2,1-d:1',2'-f][1,3,2]dioxaphosphepine 4-oxide, **147**.
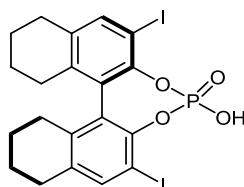
Prepared according to General Experimental Procedure J using **182** (1 equiv, 0.3 mmol, 163.9 mg) and POCl$_3$ (2 equiv, 0.6 mmol, 55.4 μL) to afford **147** as a white amorphous solid (175.1 mg, 96%).

Melting point: 286 - 288 °C.

υ_{max} (solid): 3707, 3665, 2938, 2864, 1314, 1055, 1007 cm^{-1}.

[α]$_D^{20}$ -96.5 (c = 1.00, CHCl$_3$).

^{1}H NMR (400 MHz, CDCl$_3$): δ 7.66 (d, 2H, *J* = 4.0 Hz), 2.81 (t, 4H, *J* = 4.0 Hz), 2.61-2.50 (m, 2H), 2.26-2.16 (m, 2H), 1.84-1.73 (m, 8H). 1 deuterium-exchangeable OH signal missing.

^{13}C NMR (400 MHz, CDCl$_3$): δ 145.7, 140.7, 139.0, 138.9, 137.3, 127.3, 29.1, 28.0, 22.6, 22.5.

HRMS: exact mass calculated for [M-H]$^-$ (C$_{20}$H$_{18}$I$_2$O$_4$P) requires *m/z* 606.9038 (I^{127}), found [M-H]$^-$ *m/z* 606.9020 (I^{127}), 607.9053 (I^{128}).

(*S*)-(11b*S*)-2,6-Bis(4-chlorophenyl)-4-hydroxy-8,9,10,11,12,13,14,15-octahydrodinaphtho[2,1-d:1',2'-f][1,3,2]dioxaphosphepine 4-oxide, **148**.[62]
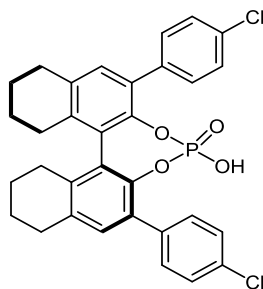
Prepared according to General Experimental Procedure J using **183** (1 equiv, 0.3 mmol, 154.6 mg) and POCl$_3$ (2 equiv, 0.6 mmol, 55.4 μL) to afford **148** as a white amorphous solid (172.7 mg, >99%).

Melting point: 250 - 252 °C. Lit melting point: 252 - 254 °C (*(R)*-enantiomer).[62]

υ_{max} (solid): 2934, 1495, 1431, 1016, 953 cm^{-1}.

[α]$_D^{20}$ +147.3 (c = 0.21, CHCl$_3$). Lit [α]$_D^{25}$ -137.0 (c = 0.21, CHCl$_3$) (*(R)*-enantiomer).[62]

^{1}H NMR (400 MHz, CDCl$_3$): 7.41-7.38 (m, 4H), 7.27-7.23 (m, 4H), 7.11 (s, 2H), 2.88-2.83 (m, 4H), 2.73-2.65 (m, 2H), 2.36 (dt, 2H, *J* = 10.7, 5.7 Hz), 1.87-1.80 (m, 6H), 1.69-1.60 (m, 2H). 1 deuterium-exchangeable OH signal missing.

^{13}C NMR (400 MHz, CDCl$_3$): δ 142.9, 138.3, 136.0, 135.6, 133.6, 131.4, 131.0, 130.8, 129.6, 127.2, 29.5, 28.2, 22.9, 22.8.

HRMS: exact mass calculated for [M-H]$^-$ (C$_{32}$H$_{26}$Cl$_2$O$_4$P) requires *m/z* 575.0951 (Cl^{35}), found [M-H]$^-$ *m/z* 575.0947 (Cl^{35}), 577.0916 (Cl^{37}).

(*R*)-2,6-Di([1,1'-biphenyl]-4-yl)-4-hydroxy-8,9,10,11,12,13,14,15-octahydrodinaphtho[2,1-d:1',2'-f][1,3,2]dioxaphosphepine 4-oxide, **149**.
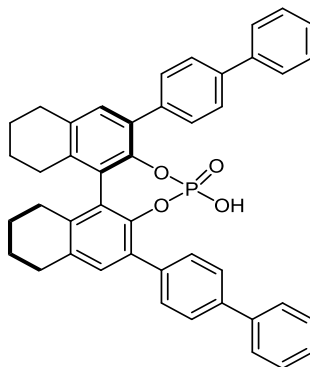
Prepared according to General Experimental Procedure J using **184** (1 equiv, 0.3 mmol, 179.6 mg) and POCl$_3$ (2 equiv, 0.6 mmol, 55.4 µL) to afford **149** as a white amorphous solid (188.3 mg, 95%).

Melting point: 267 - 269 °C.

υ_{max} (solid): 2930, 2361, 1016, 1007, 955, 837 cm^{-1}.

$[\alpha]_D^{20}$ -237.1 (c = 1.00, CHCl$_3$).

^{1}H NMR (400 MHz, CDCl$_3$): 7.50 (m, 4H), 7.39 (dd, 8H, *J* = 16.6, 7.1 Hz), 7.31-7.23 (m, 6H), 7.17 (s, 2H), 2.92-2.82 (m, 4H), 2.74-2.66 (m, 2H), 2.35 (dt, 2H, *J* = 10.4, 5.4 Hz), 1.87-1.78 (m, 6H), 1.66-1.59 (m, 2H). 1 deuterium-exchangeable OH signal missing.

^{13}C NMR (400 MHz, CDCl$_3$): δ 148.6, 141.3, 140.3, 137.2, 137.1, 132.1, 132.1, 130.7, 130.0, 129.1, 127.6, 127.5, 126.0, 120.4, 29.6, 27.6, 23.4, 23.3.

HRMS: exact mass calculated for [M-H]$^-$ (C$_{44}$H$_{36}$O$_4$P) requires *m/z* 659.2357, found [M-H]$^-$ *m/z* 659.2354.

(*R*)-4-Hydroxy-2,6-bis(4-isopropylphenyl)-8,9,10,11,12,13,14,15-octahydrodinaphtho[2,1-d:1',2'-f][1,3,2]dioxaphosphepine 4-oxide, **150**.
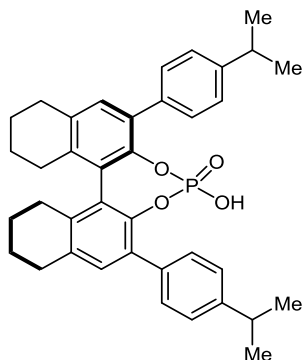
Prepared according to General Experimental Procedure J using **185** (1 equiv, 0.3 mmol, 159.2 mg) and POCl$_3$ (2 equiv, 0.6 mmol, 55.4 µL) to afford **150** as a white amorphous solid (172.5 mg, 97%).

Melting point: 261 - 263 °C.

υ_{max} (solid): 2934, 2249, 1508, 1303, 1213 cm^{-1}.

[α]$_D^{20}$ -166.6 (c = 1.00, CHCl$_3$).

^{1}H NMR (400 MHz, CDCl$_3$): 7.39 (d, 4H, *J* = 6.8 Hz), 7.11 (s, 2H), 7.08 (d, 4H, *J* = 7.5 Hz), 2.88-2.66 (m, 8H), 2.33 (dt, 2H, *J* = 9.0, 5.6 Hz), 1.85-1.78 (m, 6H), 1.64-1.59 (m, 2H), 1.12 (dd, 12H, *J* = 6.5, 5.3 Hz). 1 deuterium-exchangeable OH signal missing.

^{13}C NMR (400 MHz, CDCl$_3$): δ 147.8, 143.7, 137.3, 135.2, 134.9, 131.9, 131.4, 129.7, 127.6, 126.5, 34.0, 29.6, 28.2, 24.2, 24.1, 23.1, 23.0.

HRMS: exact mass calculated for [M-H]$^-$ (C$_{38}$H$_{40}$O$_4$P) requires *m/z* 591.2670, found [M-H]$^-$ *m/z* 591.2656.

(*R*)-2,6-bis(3,5-Dichlorophenyl)-4-hydroxy-8,9,10,11,12,13,14,15-octahydrodinaphtho[2,1-d:1',2'-f][1,3,2]dioxaphosphepine 4-oxide, **151**.
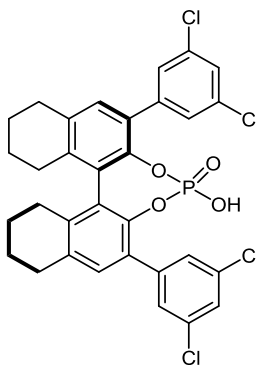
Prepared according to General Experimental Procedure J using **186** (1 equiv, 0.3 mmol, 175.3 mg) and POCl$_3$ (2 equiv, 0.6 mmol, 55.4 µL) to afford **151** as a white amorphous solid (184.2 mg, 95%).

Melting point: 287 - 289 °C.

υ_{max} (solid): 3514, 2955, 2924, 2361, 1456, 1233 cm^{-1}.

[α]$_D^{20}$ -113.4 (c = 1.00, CHCl$_3$).

^{1}H NMR (400 MHz, CDCl$_3$): 7.50 (d, 2H, *J* = 1.9 Hz), 7.43 (d, 2H, *J* = 1.8 Hz), 7.38-7.36 (m, 2H), 7.22 (s, 1H), 7.19 (s, 1H), 2.94-2.87 (m, 4H), 2.74-2.66 (m, 2H), 2.38 (tt, 2H, *J* = 16.0, 4.0 Hz), 1.90-1.84 (m, 6H), 1.70-1.66 (m, 2H). 1 deuterium-exchangeable OH signal missing.

^{13}C NMR (400 MHz, CDCl$_3$): δ 142.9, 142.9, 140.1, 138.9, 136.1, 134.8, 131.3, 130.1, 128.3, 127.6, 127.5, 29.5, 28.2, 22.9, 22.8.

HRMS: exact mass calculated for [M-H]$^-$ (C$_{32}$H$_{24}$Cl$_4$O$_4$P) requires *m/z* 645.0147 (Cl^{35}), found [M-H]$^-$ *m/z* 645.0141 (Cl^{35}), 647.0106 (Cl^{37}).

(*R*)-4-Hydroxy-2,6-diphenyl-8,9,10,11,12,13,14,15-octahydrodinaphtho[2,1-d:1',2'-f][1,3,2]dioxaphosphepine 4-oxide, **152**.[63]
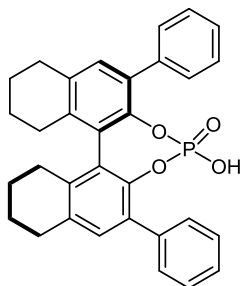
Prepared according to General Experimental Procedure J using **187** (1 equiv, 0.3 mmol, 134.0 mg) and POCl$_3$ (2 equiv, 0.6 mmol, 55.4 µL) to afford **152** as a white amorphous solid (151.0 mg, 99%).

Melting point: 288 - 290 °C. Lit melting point: 286 - 288 °C.[63]

υ_{max} (solid): 2930, 2857, 1414, 1310, 943 cm^{-1}.

[α]$_D^{20}$ -248.3 (c = 0.40, CHCl$_3$). Lit [α]$_D^{28}$ -241.5 (c = 0.40, CHCl$_3$).[63]

^{1}H NMR (400 MHz, CDCl$_3$): 7.62-7.60 (m, 2H), 7.55-7.53 (m, 2H), 7.42 (m, 4H), 7.38-7.33 (m, 2H), 7.26 (s, 1H), 7.22 (s, 1H), 2.91-2.87 (m, 4H), 2.76-2.68 (m, 2H), 2.46-2.31 (m, 2H), 1.91-1.81 (m, 6H), 1.72-1.65 (m, 2H). 1 deuterium-exchangeable OH signal missing.

HRMS: exact mass calculated for [M-H]$^-$ (C$_{32}$H$_{28}$O$_4$P) requires *m/z* 507.1731, found [M-H]$^-$ *m/z* 507.1720.

(*R*)-4-Hydroxy-2,6-di(naphthalen-1-yl)-8,9,10,11,12,13,14,15-octahydrodinaphtho[2,1-d:1',2'-f][1,3,2]dioxaphosphepine 4-oxide, **153**.[64]
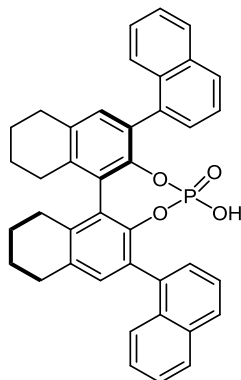
Prepared according to General Experimental Procedure J using **188** (1 equiv, 0.3 mmol, 164.0 mg) and $POCl_3$ (2 equiv, 0.6 mmol, 55.4 µL) to afford **153** as a white amorphous solid (178.9 mg, 98%).

Melting point: 301 - 303 °C.

υ_{max} (solid): 2924, 1491, 1298, 1196, 1151 cm^{-1}.

$[\alpha]_D^{20}$ -211.1 (c = 0.25, CHCl$_3$). Lit $[\alpha]_D^{25}$ -216.12 (c = 0.245, CHCl$_3$).[64]

^{1}H NMR (400 MHz, CDCl$_3$): δ 7.95-7.84 (m, 5H), 7.70-7.65 (m, 1H), 7.60-7.39 (m, 9H), 7.33-7.31 (m, 0.5H), 7.25-7.20 (m, 1.5H), 2.95-2.83 (m, 7H), 2.62-2.51 (m, 2H), 2.00-1.78 (m, 9H). 1 deuterium-exchangeable OH signal missing.

HRMS: exact mass calculated for [M-H]$^-$ (C$_{40}$H$_{32}$O$_4$P) requires *m/z* 607.2044, found [M-H]$^-$ *m/z* 607.2029.

(R)-(3r)-2,2'-Dimethoxy-3,3'-bis(2,4,6-triisopropylphenyl)-5,5',6,6',7,7',8,8'-octahydro-1,1'-binaphthalene, **155**.[65]
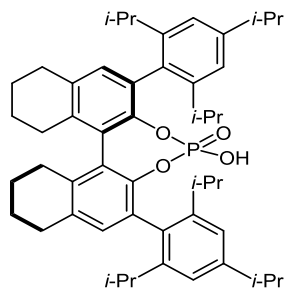
Prepared according to General Experimental Procedure J using **192** (1 equiv, 1 mmol, 699.1 mg) and POCl$_3$ (2 equiv, 2 mmol, 184.47μL) to afford **154** as a white amorphous solid (753.4 mg, 99%).

Melting point: 307 - 309 °C.

υ_{max} (solid): 2959, 2928, 2866, 1460, 1362, 1545, 1211 cm^{-1}.

$[\alpha]_D^{20}$ -62.3 (c = 1.00, CHCl$_3$). Lit $[\alpha]_D^{20}$ -65.9 (c = 1.00, CHCl$_3$).[65]

^{1}H NMR (400 MHz, CDCl$_3$): δ 7.10 (d, 2H, J = 8.0 Hz), 7.05 (s, 1H), 7.02 (s, 1H), 7.00 (d, 2H, J = 8.0 Hz), 2.95-2,80 (m, 8H), 2.78-2.70 (m, 2H), 2.64 (app. p, 2H, J = 8.0 Hz), 2.56 (app. p, 2H, J = 8.0 Hz), 2.28 (dt, 2H, J = 10.8, 5.6 Hz), 1.96-1.82 (m, 6H), 1.80-1.72 (m, 2H), 1.32-1.14 (m, 30H). 0.99 (d, 3H, J = 8.0 Hz), 0.89 (d, 3H, J = 8.0 Hz). 1 deuterium-exchangeable OH signal missing.

HRMS: exact mass calculated for [M-H]$^-$ (C$_{50}$H$_{64}$O$_4$P) requires m/z 759.4548, found [M-H]$^-$ m/z 759.4527.

N-(2-Phenyl-2-(quinolin-2-yl)ethyl)aniline, **174**.
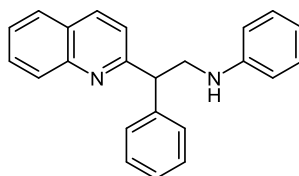
Prepared according to General Experimental Procedure C using **127** (1 equiv, 1 mmol, 231.3 mg), 4-hydroxydinaphtho[2,1-d:1',2'-f][1,3,2]dioxaphosphepine-4-oxide (0.2 equiv, 0.2

mmol, 69.7 mg), and aniline (1.1 equiv, 1.1 mmol, 100.5 μL) to afford **174** as a yellow amorphous solid (210.9 mg, 65%).

Melting point: 195 - 198 °C.

υ_{max} (solid): 3375, 3055, 3025, 1601, 1504, 1428, 1318, 1184, 750 cm^{-1}.

^{1}H NMR (400 MHz, CDCl$_3$): δ 8.18 (d, 1H, J = 8.3 Hz), 8.01 (d, 1H, J = 8.4 Hz), 7.76 (m, 2H), 7.54 (ddd, 1H, J = 8.1, 7.0, 1.2 Hz), 7.34-7.33 (m, 4H), 7.20-7.15 (m, 3H), 6.71 (m, 1H), 6.66 (dt, 2H, J = 3.2, 1.7 Hz), 4.61 (dd, 1H, J = 8.7, 5.8 Hz),4.44 (br.s, 1H), 4.26 (dd, 1H, 13.1, 8.7 Hz), 3.82 (dd, 1H, J = 13.1, 5.8 Hz).

^{13}C NMR (400 MHz, CDCl$_3$): δ 162.2, 148.4, 147.9, 142.0, 136.7, 129.7, 129.6, 129.1, 128.8, 127.9, 127.4, 127.3, 126.5, 122.7, 117.7, 113.6, 52.8, 48.2. 1 carbon signal not observed/coincident.

HRMS: exact mass calculated for [M+H]$^{+}$ (C$_{23}$H$_{21}$N$_2$) requires m/z 325.1699, found [M+H]$^{+}$ m/z 325.1698.

HPLC assay: t_R enantiomer 1 = 10.4 min., t_R enantiomer 2 = 11.3 min.

(*R*)-2,2'-Dimethoxy-1,1'-binaphthalene, **176**.[66]
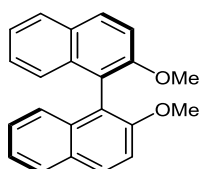
Prepared according to General Experimental Procedure F using (*R*)[1,1'-binaphthalene]-2,2'-diol (**175**, 1 equiv, 10 mmol, 2.86 g), iodomethane (4 equiv, 40 mmol, 1.31 g, 0.57 mL), and K$_2$CO$_3$ (4 equiv, 40 mmol, 1.27 g) to afford **176** as a white amorphous solid (3.12 g, >99%).

Melting point: 224 - 226 °C. Lit melting point: 228 - 232 °C.[61]

υ_{max} (solid): 3063, 2957, 2837, 1618, 1589, 1504, 1248, 1090, 1063 cm^{-1}.

[α]$_D^{20}$ +71.1 (c = 1.00, THF). Lit [α]$_D^{23}$ +75.8 (c = 1.00, THF)[67]

^{1}H NMR (400 MHz, CDCl$_3$): δ 7.99 (d, 2H, J = 8.0 Hz), 7.88 (d, 2H, J = 8.1 Hz), 7.47 (d, 2H, J = 8.0 Hz), 7.33 (t, 2H, J = 7.4 Hz), 7.22 (t, 2H, J = 7.6 Hz), 7.12 (d, 2H, J = 7.5.Hz), 3.78 (s, 6H).

^{13}C NMR (400 MHz, CDCl$_3$): δ 155.3, 134.4, 129.8, 129.6, 128.3, 126.7, 125.6, 123.9, 120.0, 114.6, 57.3.

HRMS: exact mass calculated for [M+H]$^+$ (C$_{22}$H$_{19}$O$_2$) requires m/z 315.1380, found [M+H]$^+$ m/z 315.1383.

(*R*)-3,3'-Diiodo-2,2'-dimethoxy-1,1'-binaphthalene, **177**.[68]
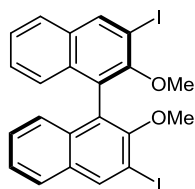
Prepared according to General Experimental Procedure G using **176** (1 equiv, 1.43 mmol, 450.0 mg), TMEDA (4.4 equiv, 6.29 mmol, 0.94 mL), *n*-butyllithium (10 equiv, 14.30 mmol, 5.72 mL (2.5 M hexanes solution)), and iodine (3.4 equiv, 4.86 mmol, 1.23 g) to afford **177** as a white amorphous solid (527.1 mg, 93%).

Melting point: 233 - 235 °C.

υ$_{max}$ (solid): 2928, 2858, 1452, 1231, 1038 cm^{-1}.

[α]$_D^{20}$ +99.2 (c = 1.00, CHCl$_3$).

^{1}H NMR (400 MHz, CDCl$_3$): δ 8.54 (s, 2H), 7.80 (d, 2H, J = 8.2 Hz), 7.42 (ddd, 2H, J = 8.2, 6.8, 1.2 Hz), 7.30-7.26 (m, 2H), 7.08 (d, 2H, J = 8.5 Hz), 3.43 (s, 6H).

^{13}C NMR (400 MHz, CDCl$_3$): δ 154.9, 140.3, 134.3, 134.2, 132.5, 127.4, 127.3, 126.1, 126.0, 92.7, 61.5.

HRMS: exact mass calculated for [M+H]$^+$ (C$_{22}$H$_{17}$I$_2$O$_2$) requires m/z 566.9312 (I^{127}), found [M+H]$^+$ m/z 565.9229 (I^{126}), 566.9306 (I^{127}), 567.9339 (I^{128}).

(R)-3,3'-Diiodo-[1,1'-binaphthalene]-2,2'-diol, **178**.[69]
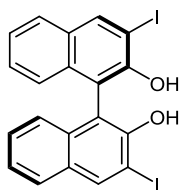
Prepared according to General Experimental Procedure H using **177** (1 equiv, 2 mmol, 1.13 g) and BBr$_3$ (5 equiv, 10 mmol, 10.0 mL (1 M DCM solution)) to afford **178** as a white amorphous solid (1.06 g, 99%).

Melting point: 308 - 310 °C. Lit melting point: 312 - 314 °C.[69]

υ_{max} (solid): 2934, 2826, 1558, 1385, 1229, 1136, 1084 cm^{-1}.

$[\alpha]_D^{20}$ +104.1 (c = 1.00, THF). Lit $[\alpha]_D^{20}$ +102.7 (c = 1.00, THF).[69]

^{1}H NMR (400 MHz, CDCl$_3$): δ 8.53 (s, 2H), 7.80 (d, 2H, J = 8.0 Hz), 7.40-7.37 (m, 2H), 7.34-7.31 (m, 2H), 7.08 (d, 2H, J = 8.5 Hz), 5.44 (s, 2H).

^{13}C NMR (400 MHz, CDCl$_3$): δ 150.5, 140.7, 133.6, 131.0, 128.3, 127.6, 125.1, 124.8, 112.9, 86.9.

HRMS: exact mass calculated for [M+H]$^+$ (C$_{20}$H$_{11}$I$_2$O$_2$) requires m/z 536.8854 (I^{127}), found [M+H]$^+$ m/z 536.8848 (I^{127}), 537.8879 (I^{128}).

(R)-3,3'-Bis(4-chlorophenyl)-[1,1'-binaphthalene]-2,2'-diol, **179**.[70]
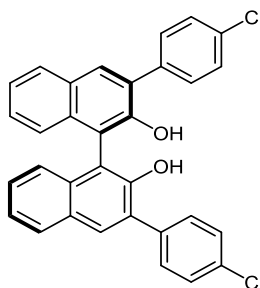
Prepared according to General Experimental Procedure I using **178** (1 equiv, 0.56 mmol, 300.0 mg), Pd/C (0.05 equiv, 0.028 mmol, 28.0 mg of 10% wt powder), K$_2$CO$_3$ (4 equiv, 2.24

mmol, 309.5 mg), and 4-chlorobenzeneboronic acid (4 equiv, 2.24 mmol, 350.3 mg) to afford **179** as a white amorphous solid (238.7 mg, 84%).

Melting point: 299 - 301 °C.

υ_{max} (solid): 1482, 3061, 1493, 1250, 1169, 1015 cm^{-1}.

$[\alpha]_D^{20}$ +66.1 (c = 1.00, CHCl$_3$).

^{1}H NMR (400 MHz, CDCl$_3$): δ 8.02 (s, 2H), 7.94 (d, 2H, J = 7.9 Hz), 7.71-7.67 (m, 4H), 7.48-7.45 (m, 4H), 7.42 (ddd, 2H, J = 8.1, 6.9, 1.2 Hz), 7.35 (ddd, 2H, J = 8.2, 6.8, 1.3 Hz), 7.21 (d, 2H, J = 8.4 Hz), 5.31, (s, 2H).

^{13}C NMR (400 MHz, CDCl$_3$): δ 150.5, 136.3, 136.2, 134.2, 133.3, 131.9, 131.3, 129.9, 129.8, 128.9, 128.9, 128.1, 125.0, 124.5.

HRMS: exact mass calculated for [M+NH$_4$]$^+$ (C$_{32}$H$_{24}$Cl$_2$O$_2$N) requires m/z 524.1179 (Cl^{35}), found [M+NH$_4$]$^+$ m/z 524.1175 (Cl^{35}), 526.1144 (Cl^{37}). Exact mass calculated for [M+H]$^+$ (C$_{32}$H$_{21}$Cl$_2$O$_2$) requires m/z 507.0913 (Cl^{35}), [M+H]$^+$ found 507.0911 (Cl^{35}), 509.0880 (Cl^{37}).

(R)-3,3'-Di([1,1'-biphenyl]-4-yl)-[1,1'-binaphthalene]-2,2'-diol, **180**.[71]
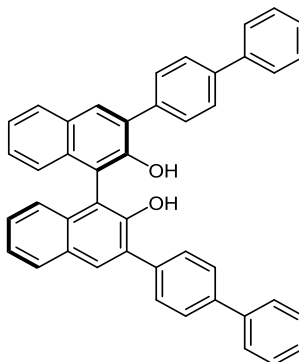
Prepared according to General Experimental Procedure I using **178** (1 equiv, 0.19 mmol, 100.0 mg), Pd/C (0.05 equiv, 0.0095 mmol, 10 mg of 10% wt powder), K$_2$CO$_3$ (4 equiv, 0.76 mmol, 105.0 mg), and 4-biphenyl boronic acid (4 equiv, 0.76 mmol, 150.5 mg) to afford **180** as a white amorphous solid (92.1 mg, 82 %).

Melting point: 315 - 317 °C.

υ_{max} (solid): 3516, 3026, 1485, 1360, 1234 cm^{-1}.

$[\alpha]_D^{20}$ -51.2 (c = 1.36, CHCl$_3$). Lit $[\alpha]_D^{23}$ -59.9 (c = 1.36, CHCl$_3$).[71]

^{1}H NMR (400 MHz, CDCl$_3$): δ 8.10 (s, 2H), 7.96 (d, 2H, J = 8.1 Hz), 7.86-7.83 (m, 4H), 7.75-7.72 (m, 4H), 7.68 (m, 4H), 7.48 (m, 4H), 7.44-7.33 (m, 6H), 7.28-7.26 (m, 2H, overlapping chloroform peak), 5.43 (s, 2H).

^{13}C NMR (400 MHz, CDCl$_3$): δ 150.6, 141.1, 141.0, 136.8, 133.3, 131.8, 130.6, 130.4, 129.9, 129.2, 128.9, 127.8, 127.8, 127.6, 127.5, 124.8, 124.6, 112.2.

HRMS: exact mass calculated for [M+H]$^+$ (C$_{44}$H$_{31}$O$_2$) requires m/z 591.2319, found [M+H]$^+$ m/z 591.2314.

(R)-5,5',6,6',7,7',8,8'-Octahydro-[1,1'-binaphthalene]-2,2'-diol, **181**.[72]
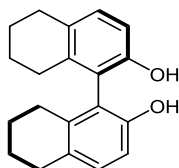
Prepared according to General Experimental Procedure K using (R)[1,1'-binaphthalene]-2,2'-diol (**175**, 1 equiv, 6.98 mmol, 2.00 g) and Pd/C (0.1 equiv, 0.69 mmol, 742 mg of 10% wt powder) to afford **181** as a white amorphous solid (2.05 g, >99%).

Melting point: 166 - 168 °C. Lit melting point: 161 °C.[72]

υ_{max} (solid): 3474, 3385, 2927, 1472, 1196, 812 cm^{-1}.

$[\alpha]_D^{20}$ +56.2 (c = 1.00, CHCl$_3$). Lit $[\alpha]_D^{27}$ +48.6 (c = 1.00, CHCl$_3$).[67]

^{1}H NMR (400 MHz, CDCl$_3$): δ 7.08 (d, 2H, J = 8.3 Hz), 6.84 (d, 2H, J = 8.3 Hz), 4.55 (br.s s, 2H), 2.76 (t, 4H, J = 6.2 Hz), 2.31 (dt, 2H, J = 17.1, 6.3 Hz), 2.18 (dt, 2H, J = 17.5, 6.3 Hz), 1.78-1.65 (m, 8H).

^{13}C NMR (400 MHz, CDCl$_3$): δ 151.7, 137.5, 131.4, 130.5, 119.2, 113.3, 29.6, 27.5, 23.4, 23.3.

HRMS (C$_{20}$H$_{23}$O$_2$) [M+H$^+$] requires 295.1693, found [M+H$^+$] 295.1696.

HRMS: exact mass calculated for [M+H]$^+$ (C$_{20}$H$_{23}$O$_2$) requires *m/z* 295.1693, found [M+H]$^+$ *m/z* 295.1696.

(*R*)-3,3'-Diiodo-5,5',6,6',7,7',8,8'-octahydro-[1,1'-binaphthalene]-2,2'-diol, **182**.[73]
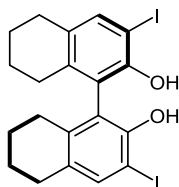
Prepared according to General Experimental Procedure L using **181** (1 equiv, 1 mmol, 294.4 mg), morpholine (6 equiv, 6 mmol, 522.7 mg, 0.525 mL), and iodine (2 equiv, 2 mmol, 507.6 mg) to afford **182** as a white amorphous solid (545.1 mg, >99%).

Melting point: 211 - 213 °C. Lit melting point: 214 °C.[73]

υ$_{max}$ (solid): 3449, 2934, 2857, 1458, 1337, 1177, 1151 cm^{-1}.

[α]$_D^{20}$ -23.1 (c = 1.00, CHCl$_3$). Lit [α]$_D^{20}$ -24.0 (c = 1.00, CHCl$_3$).[73]

^{1}H NMR (400 MHz, CDCl$_3$): δ 7.52 (s, 2H), 4.97 (s, 2H), 2.74 (t, 4H, *J* = 5.9 Hz), 2.28 (dt, 2H, *J* = 17.5, 6.0 Hz), 2.11 (dt, 2H, *J* = 12.4, 6.0 Hz), 1.76-1.63 (m, 8H).

^{13}C NMR (400 MHz, CDCl$_3$): δ 150.1, 139.7, 138.1, 132.8, 121.0, 81.4, 29.2, 27.3, 23.1, 23.0.

HRMS: exact mass calculated for [M+H]$^+$ (C$_{20}$H$_{21}$I$_2$O$_2$) requires *m/z* 546.9625 (I^{127}), found [M+H]$^+$ *m/z* 545.9543 (I^{126}), 546.9621(I^{127}), 547.9653 (I^{128}).

(*R*)-3,3'-Bis(4-chlorophenyl)-5,5',6,6',7,7',8,8'-octahydro-[1,1'-binaphthalene]-2,2'-diol, **183**.
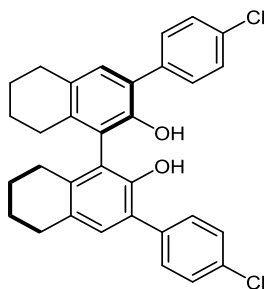
Prepared according to General Experimental Procedure I using **182** (1 equiv, 0.5 mmol, 273.1 mg), Pd/C (0.05 equiv, 0.025 mmol, 25.0 mg of 10% wt powder), K_2CO_3 (4 equiv, 2 mmol, 276.4 mg), and 4-chlorobenzeneboronic acid (4 equiv, 2 mmol, 312.7 mg) to afford **183** as a white amorphous solid (239.7 mg, 93%).

Melting point: 197 - 199 °C.

υ_{max} (solid): 3499, 2928, 1454, 1231, 1088, 804 cm^{-1}.

$[\alpha]_D^{20}$ -115.7 (c = 1.00, CHCl$_3$).

^{1}H NMR (400 MHz, CDCl$_3$): δ 7.57-7.54 (m, 4H), 7.41-7.38 (m, 4H), 7.14 (s, 2H), 4.86 (s, 2H), 2.81 (t, 4H, *J* = 6.1 Hz), 2.38 (dt, 2H, *J* = 17.4, 6.2 Hz), 2.25 (dt, 2H *J* = 17.3, 6.3 Hz), 1.81-1.69 (m, 8H).

^{13}C NMR (400 MHz, CDCl$_3$): δ 148.4, 137.3, 136.6, 133.3, 132.1, 130.9, 130.9, 128.8, 125.3, 120.1, 29.6, 27.5, 23.3, 23.3.

HRMS: exact mass calculated for [M+H]$^+$ (C$_{32}$H$_{29}$Cl$_2$O$_2$) requires *m/z* 516.1573 (Cl^{35}), found [M+H]$^+$ *m/z* 516.1565 (Cl^{35}), 517.1505 (Cl^{37}).

(*R*)-3,3'-Di([1,1'-biphenyl]-4-yl)-5,5',6,6',7,7',8,8'-octahydro-[1,1'-binaphthalene]-2,2'-diol, **184**.[74]
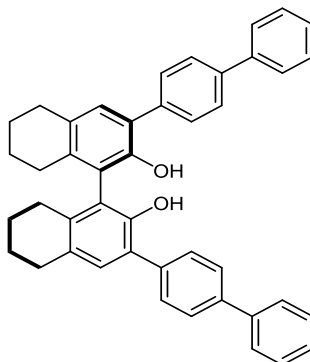
Prepared according to General Experimental Procedure I using **182** (1 equiv, 0.5 mmol, 273.1 mg), Pd/C (0.05 equiv, 0.025 mmol, 25.0 mg of 10% wt powder), K_2CO_3 (4 equiv, 2 mmol, 276.4 mg), and 4-biphenylboronic acid (4 equiv, 2 mmol, 396.1 mg) to afford **184** as a white amorphous solid (281.4 mg, 94%).

Melting point: 209 - 211 °C.

υ_{max} (solid): 3512, 2928, 2855, 1450, 1231, 1450, 1132 cm^{-1}.

$[\alpha]_D^{20}$ -201.2 (c = 1.00, CHCl$_3$). Lit $[\alpha]_D^{21}$ -205.1 (c = 1.00, CHCl$_3$).[74]

^{1}H NMR (400 MHz, CDCl$_3$): δ 7.22-7.64 (m, 12H), 7.48-7.44 (m, 4H), 7.38-7.34 (m, 2H), 7.23 (s, 2H), 4.27 (s, 2H), 2.84 (t, 4H, *J* = 6.0 Hz), 2.45 (dt, 2H, *J* = 17.0, 6.2 Hz), 2.29 (dt, 2H, *J* = 12.1, 6.3 Hz), 1.84-1.72 (m, 8H).

^{13}C NMR (400 MHz, CDCl$_3$): δ 148.6, 141.3, 140.3, 137.2, 137.1, 132.1, 130.7, 130.0, 129.1, 127.6, 127.5, 126.0, 120.4, 29.6, 27.6, 23.4. 2 carbon signals not observed/coincident.

HRMS: exact mass calculated for [M+H]$^+$ (C$_{44}$H$_{39}$O$_2$) requires *m/z* 599.2945, found [M+H]$^+$ *m/z* 599.2938.

(*R*)-3,3'-Bis(4-isopropylphenyl)-5,5',6,6',7,7',8,8'-octahydro-[1,1'-binaphthalene]-2,2'-diol, **185**.
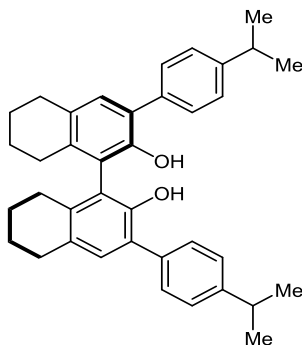
Prepared according to General Experimental Procedure I using **182** (1 equiv, 0.5 mmol, 273.1 mg), Pd/C (0.05 equiv, 0.025 mmol, 25.0 mg of 10% wt powder), K_2CO_3 (4 equiv, 2 mmol, 276.4 mg), and 4-cumenylboronic acid (4 equiv, 2 mmol, 328.0 mg) to afford **185** as a white amorphous solid (209.6 mg, 79%).

Melting point: 188 - 190 °C.

υ_{max} (solid): 3514, 2924, 2855, 2361, 1456, 1233, 1130 cm^{-1}.

$[\alpha]_D^{20}$ -117.6 (c = 1.00, CHCl$_3$).

^{1}H NMR (400 MHz, CDCl$_3$): δ 7.53 (d, 4H, *J* = 8.1 Hz), 7.30 (d, 4H, *J* = 8.1 Hz), 7.15 (s, 2H), 4.92 (s, 2H), 2.95 (app. p, 2H, *J* = 8.0 Hz), 2.81 (t, 4H, *J* = 6.0 Hz), 2.41 (dt, 2H, *J* = 12.3, 5.9 Hz), 2.25 (dt, 2H, *J* = 11.9, 6.2 Hz), 1.81-1.70 (m, 8H), 1.30 (d, 12H, *J* = 4.0 Hz).

^{13}C NMR (400 MHz, CDCl$_3$): δ 148.5, 148.0, 136.6, 135.6, 131.9, 130.4, 129.4, 126.9, 126.3, 120.5, 34.2, 29.6, 27.5, 24.3, 23.4. 1 carbon signal not observed/coincident.

HRMS: exact mass calculated for [M+H]$^+$ (C$_{38}$H$_{43}$O$_2$) requires *m/z* 531.3258, found [M+H]$^+$ *m/z* 531.3247.

(*R*)-3,3'-Bis(3,5-dichlorophenyl)-5,5',6,6',7,7',8,8'-octahydro-[1,1'-binaphthalene]-2,2'-diol, **186**.
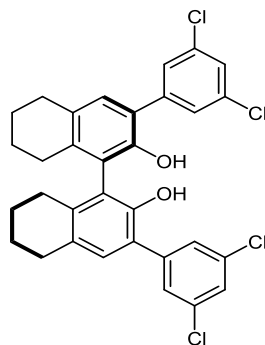
Prepared according to General Experimental Procedure I using **182** (1 equiv, 0.5 mmol, 273.1 mg), Pd/C (0.05 equiv, 0.025 mmol, 25.0 mg of 10% wt powder), K_2CO_3 (4 equiv, 2 mmol, 276.4 mg), and 3,5-dichlorobenzene-1-boronic acid (4 equiv, 2 mmol, 381.6 mg) to afford **186** as a white amorphous solid (248.4 mg, 85%).

Melting point: 235 - 237 °C.

υ_{max} (solid): 3510, 2928, 1584, 1557, 1234, 1177, 799 cm^{-1}.

$[\alpha]_D^{20}$ -89.8 (c = 1.00, CHCl$_3$).

^{1}H NMR (400 MHz, CDCl$_3$): 7.53 (d, 4H, *J* = 1.9 Hz), 7.32 (t, 2H, *J* = 1.9 Hz), 7.16 (s, 2H), 4.87 (s, 2H), 2.82 (t, 4H, *J* = 6.1 Hz), 2.38 (dt, 2H, *J* = 17.4, 6.2 Hz), 2.25 (dt, 2H, *J* = 17.4, 6.2 Hz), 1.83-1.71 (m, 8H).

^{13}C NMR (400 MHz, CDCl$_3$): δ 148.5, 141.1, 138.2, 135.0, 132.2, 131.3, 128.0, 127.3, 124.0, 119.9, 29.5, 27.6, 23.2. 1 carbon signal not observed/coincident.

HRMS: exact mass calculated for [M+H]$^+$ (C$_{32}$H$_{25}$Cl$_4$O$_2$) requires *m/z* 583.0585 (Cl^{35}), found [M+H]$^+$ *m/z* 583.0576 (Cl^{35}), 585.0546 (Cl^{37}).

(*R*)-3,3'-Diphenyl-5,5',6,6',7,7',8,8'-octahydro-[1,1'-binaphthalene]-2,2'-diol, **187**.[75]
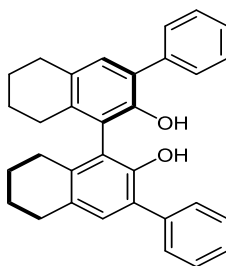
Prepared according to General Experimental Procedure I using **182** (1 equiv, 0.5 mmol, 273.1 mg), Pd/C (0.05 equiv, 0.025 mmol, 25.0 mg of 10% wt powder), K_2CO_3 (4 equiv, 2 mmol, 276.4 mg), and phenylboronic acid (4 equiv, 2 mmol, 243.9 mg) to afford **187** as a white amorphous solid (214.4 mg, 96%).

Melting point: 188 - 190 °C. Lit melting point: 185 °C.[76]

υ_{max} (solid): 3499, 2928, 1454, 1231, 1088 cm^{-1}.

$[\alpha]_D^{20}$ -31.7 (c = 1.07, $CHCl_3$). Lit $[\alpha]_D^{21}$ -29.3 (c = 1.07, $CHCl_3$).[75]

^{1}H NMR (400 MHz, $CDCl_3$): 7.62-7.60 (m, 4H), 7.46-7.42 (m, 4H), 7.33 (tt, 2H, *J* =8.0, 4.2 Hz), 7.16 (s, 2H), 4.84 (s, 2H), 2.82 (t, 4H, *J* = 6.1 Hz), 2.43 (dt, 2H, *J* = 17.2, 6.2 Hz), 2.27 (dt, 2H, *J* = 17.3, 6.3 Hz), 1.82-1.70 (m, 8H).

^{13}C NMR (400 MHz, $CDCl_3$): δ 148.5, 138.3, 136.9, 132.1, 130.6, 129.6, 128.7, 127.4, 126.4, 120.5, 29.6, 27.5, 23.4, 23.4

HRMS: exact mass calculated for [M+H]$^+$ ($C_{32}H_{31}O_2$) requires *m/z* 447.2319, found [M+H]$^+$ *m/z* 447.2313.

(*R*)-5',5'',6',6'',7',7'',8',8''-Octahydro-[1,2':4',1'':3'',1'''-quaternaphthalene]-2'',3'-diol, **188**.[73]
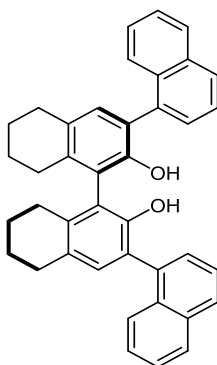
Prepared according to General Experimental Procedure I using **182** (1 equiv, 0.5 mmol, 273.1 mg), Pd/C (0.05 equiv, 0.025 mmol, 25.0 mg of 10% wt powder), K_2CO_3 (4 equiv, 2 mmol, 276.4 mg), and 1-naphthylboronic acid (4 equiv, 2 mmol, 344.0 mg) to afford **188** as a white amorphous solid (240.6 mg, 88%).

Melting point: 151 - 153 °C. Lit melting point: 149 °C.[73]

υ_{max} (solid): 3522, 2924, 1449, 1233, 802 cm^{-1}.

$[\alpha]_D^{20}$ -47.4 (c = 1.00, CHCl$_3$). Lit $[\alpha]_D^{25}$ -31.0 (c = 1.00, CHCl$_3$).[73]

^{1}H NMR (400 MHz, CDCl$_3$): 7.94-7.87 (m, 4H), 7.79-7.73 (m, 1.5H), 7.66 (d, 0.5H, *J* = 8.0 Hz), 7.59-7.34 (m, 8H), 7.11-7.10 (m, 2H), 4.74 (dd, 2H, J = 24.8, 12.1 Hz), 2.82-2.79 (m, 4H), 2.60-2.36 (m, 4H), 1.85-1.80 (m, 8H).

HRMS: exact mass calculated for [M+H]$^+$ (C$_{40}$H$_{35}$O$_2$) requires *m/z* 547.2632, found [M+H]$^+$ *m/z* 547.2619.

(*R*)-3,3'-Diiodo-2,2'-dimethoxy-5,5',6,6',7,7',8,8'-octahydro-1,1'-binaphthalene, **189**.
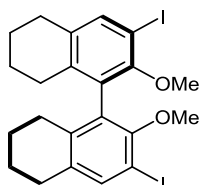
Prepared according to General Experimental Procedure F using **181** (1 equiv, 10 mmol, 5.46 g), iodomethane (4 equiv, 40 mmol, 1.31 g, 0.57 mL), and K_2CO_3 (4 equiv, 40 mmol, 1.27 g) to afford **189** as a white amorphous solid (5.72 g, >99%).

Melting point: 218 - 220 °C.

υ_{max} (solid): 2928, 1454, 1267, 1242, 1034, 995 cm^{-1}.

$[\alpha]_D^{20}$ -93.9 (c = 1.00, CHCl$_3$).

^{1}H NMR (400 MHz, CDCl$_3$): 7.57 (s, 2H), 3.51 (s, 6H), 2.76 (t, 4H, J = 6.3 Hz), 2.23 (dt, 2H, J = 17.2, 6.2 Hz), 2.10 (dt, 2H, J = 17.2, 6.4 Hz), 1.76-1.62 (m, 8H).

^{13}C NMR (400 MHz, CDCl$_3$): δ 154.7, 139.6, 137.7, 136.0, 131.8, 88.6, 60.8, 29.4, 27.8, 23.1, 23.0.

HRMS: exact mass calculated for [M+H]$^+$ ($C_{22}H_{25}I_2O_2$) requires m/z 574.9938 (I^{127}), found [M+H]$^+$ m/z 573.9862 (I^{126}), 574.9940 (I^{127}), 575.9968 (I^{128}).

(*R*)-(3r)-2,2'-Dimethoxy-3,3'-bis(2,4,6-triisopropylphenyl)-5,5',6,6',7,7',8,8'-octahydro-1,1'-binaphthalene, **190**.[65]
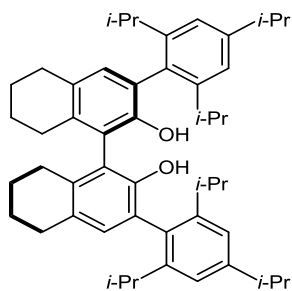
Prepared according to General Experimental Procedure H using **189** (1 equiv, 4 mmol, 2.91 g) and BBr$_3$ (5 equiv, 20 mmol, 20.0 mL (1 M DCM solution)) to afford **190** as a white amorphous solid (2.78 g, >99%).

Melting point: 287 - 289 °C.

υ_{max} (solid): 3528, 2957, 2928, 2866, 1605, 1460, 1230 cm^{-1}.

$[\alpha]_D^{20}$ -13.8 (c = 0.60, CHCl$_3$). Lit $[\alpha]_D^{20}$ -10.9 (c = 0.60, CHCl$_3$).[65]

^{1}H NMR (400 MHz, CDCl$_3$): 7.08 (dd, 4H, J = 9.8, 1.7 Hz), 6.84 (s, 2H), 4.41 (s, 2H), 2.94 (app. p, 2H, J = 8.0 Hz), 2.82-2.76 (m, 6H), 2.66 (app. p, 2H, J = 8.0 Hz), 2.46-2.32 (m, 4H), 1.84-1.72 (m, 8H), 1.30 (d, 12H, J = 6.9 Hz), 1.17 (d, 6H, J = 6.9 Hz), 1.12 (d, 6H, J = 6.9 Hz), 1.07 (d, 6H, J = 6.9 Hz), 1.01 (d, 6H, J = 6.9 Hz).

^{13}C NMR (400 MHz, CDCl$_3$): δ 148.9, 148.8, 148.1, 147.9, 136.2, 131.6, 131.6, 129.5, 124.5, 121.3, 121.2, 120.8, 67.4, 34.6, 31.0, 30.9, 29.6, 27.3, 24.5, 24.4, 24.4, 24.4, 24.1, 23.5, 23.5.

HRMS: exact mass calculated for [M+H]$^+$ (C$_{50}$H$_{67}$O$_2$) requires m/z 699.5136, found [M+H]$^+$ m/z 699.5134.

(R)-(3r)-2,2'-Dimethoxy-3,3'-bis(2,4,6-triisopropylphenyl)-1,1'-binaphthalene, **194**.[77]
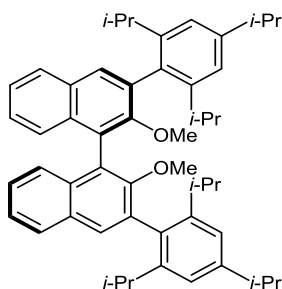
Prepared according to General Experimental Procedure M using **177** (1 equiv, 3.2 mmol, 1.77 g), 1-bromo-2,4,6-triisopropyl benzene (3.36 equiv, 10.75 mmol, 2.925 mL), magnesium filings (5.95 equiv, 19.05 mmol, 463 mg), and 1,2-dibromoethane (0.0001 mol%, 0.00032 mmol, 2.5 μL) to afford **194** as a white amorphous solid (1.90 g, 83%).

Melting point: 286 - 288 °C.

υ_{max} (solid): 2957, 2866, 1454, 1402, 1244, 1040, 1018 cm^{-1}

$[\alpha]_D^{20}$ -71.1 (c = 1.00, CHCl$_3$).

^{1}H NMR (400 MHz, CDCl$_3$): δ 7.86 (s, 1H), 7.84 (s, 1H), 7.74 (s, 2H), 7.43-7.39 (m, 2H), 7.35-7.29 (m, 4H), 7.10 (dd, 4H, J = 6.9, 1.6 Hz), 3.09 (s, 6H), 2.97 (app. p, 2H, J = 8.0 Hz), 2.86 (app.

p, 4H, J = 8.0 Hz), 2.80 (app. p, 2H, J = 8.0 Hz), 1.33 (d, 12H, J = 6.9 Hz), 1.20 (d, 6H, J = 6.8 Hz), 1.17 (d, 6H, J = 6.9 Hz), 1.13 (d, 6H, J = 6.9 Hz), 1.08 (d, 6H, J = 6.8 Hz).

^{13}C NMR (400 MHz, CDCl$_3$): δ 155.4, 148.4, 147.4, 147.1, 134.5, 134.2, 133.6, 131.2, 130.6, 128.2, 126.2, 126.1, 125.0, 124.9, 121.0, 60.1, 34.6, 31.3, 31.2, 25.8, 25.6, 24.5, 24.4, 23.7, 23.7.

HRMS: exact mass calculated for [M+ NH$_4$]$^+$ (C$_{52}$H$_{66}$O$_2$N) requires m/z 719.4750, found [M+ NH$_4$]$^+$ m/z 720.4861.

(*R*)-(3r)-3,3'-Bis(2,4,6-triisopropylphenyl)-[1,1'-binaphthalene]-2,2'-diol, **195**.[78]
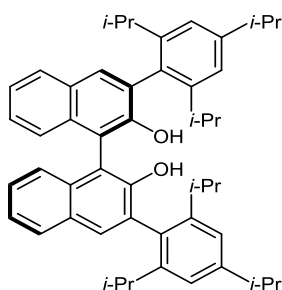
Prepared according to General Experimental Procedure H using **194** (1 equiv, 1 mmol, 719.1 mg) and BBr$_3$ (5 equiv, 5 mmol, 5.0 mL (1 M DCM solution)) to afford **195** as a white amorphous solid (670.3 mg, 97%).

Melting point: 303 - 305 °C.

υ$_{max}$ (solid): 3522, 2959, 1456, 1362, 1136, 1117 cm^{-1}.

[α]$_D^{20}$ -89.6 (c = 1.00, CHCl$_3$).

^{1}H NMR (400 MHz, CDCl$_3$): δ 7.88 (s, 1H), 7.86 (s, 1H), 7.77 (s, 2H), 7.40-7.36 (m, 2H, J = 8.1), 7.34-7.31 (m, 4H), 7.14 (dd, 4H, J = 8.0 Hz, 1.6 Hz), 4.93 (s, 2H), 2.97 (app. p, 2H, J = 8.0 Hz), 2.86 (app. p, 2H, J = 8.1 Hz), 2.70 (app. p, 2H, J = 7.9 Hz), 1.32 (d, 12H, J = 6.9 Hz), 1.22 (d, 6H, J = 6.8 Hz), 1.12 (d, 6H, J = 8.1 Hz), 1.10 (d, 6H, J = 4 Hz), 1.04 (d, 6H, J = 6.9 Hz).

^{13}C NMR (400 MHz, CDCl$_3$): δ 160.0, 149.5, 148.2, 148.1, 133.8, 131.0, 130.7, 129.5, 129.4, 128.6, 127.0, 124.9, 124.1, 121.6, 121.5, 113.5, 34.7, 31.2, 31.2, 24.7, 24.6, 24.4, 24.3, 24.3, 24.1. 1 carbon signal not observed/coincident.

HRMS: exact mass calculated for [M-H]$^-$ (C$_{50}$H$_{57}$O$_2$) requires m/z 689.4634, found [M-H]$^-$ m/z 689.4347.

Chapter 2 - One-pot formal homologation of boronic acids: A platform for diversity-oriented synthesis

1. Introduction

1.1. The Suzuki-Miyaura Reaction

Since the 1979 discovery of the Suzuki-Miyaura reaction,[79] it has grown to become one of the most generally used reactions for catalytic C–C bond formation.[80,81] The main factors which make this reaction so attractive are; i) the high functional group tolerance, ii) the generally mild reaction conditions, and iii) the broad availability of organoboron coupling partners.

The Suzuki-Miyaura reaction involves the coupling of an organoboron compound with an organic (pseudo)halide, catalysed by a transition metal, specifically Pd (Scheme 1).[79]
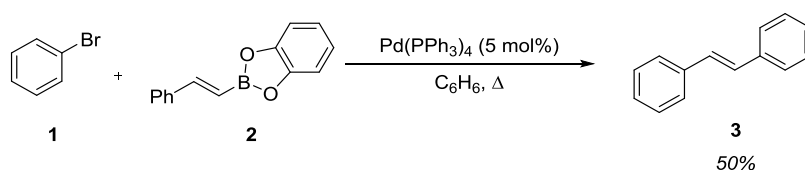
Scheme 1. Initial 1979 report of the Suzuki-Miyaura reaction coupling an aryl bromide with a styrenyl catechol borane.

The discovery of this fundamental reaction led to the Nobel Prize being awarded to Suzuki in 2010 for his contribution to cross-coupling chemistry. Heck and Negishi also won the Nobel Prize in the same year for their work in the cross-coupling field.[82]

1.1.1. Mechanistic Aspects of the Suzuki-Miyaura Reaction

Mechanistically, a typical palladium-catalysed cross-coupling reaction follows the oxidative addition, transmetallation, and reductive elimination cycle shown in Scheme 2.
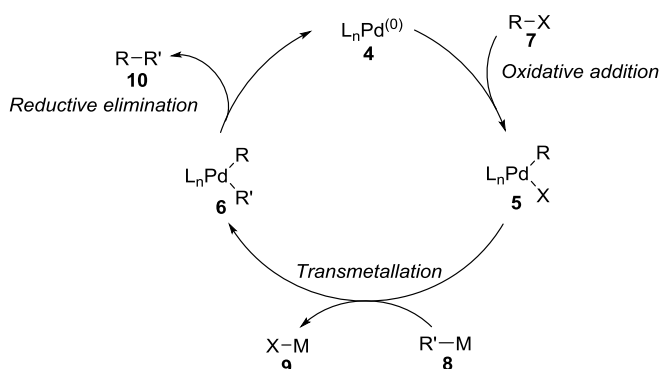
Scheme 2. Generic transition metal-catalysed cross-coupling cycle.

The first step of the catalytic cycle is the oxidative addition of the electron-rich $Pd^{(0)}$ into the electrophilic carbon-(pseudo)halide bond, which oxidises $Pd^{(0)}$ (the active catalyst in the Suzuki-Miyaura reaction) to $Pd^{(II)}$ (Scheme 3).

$$Pd^{(0)}L_n + R-X \xrightarrow{\textit{Oxidative addition}} \underset{X}{\overset{R}{\diagdown}} Pd^{(II)}L_n$$
$$\textbf{4} \qquad \textbf{7} \qquad\qquad\qquad\qquad \textbf{5}$$
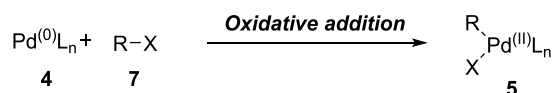
Scheme 3. Oxidative addition in transition metal-catalysed cross-coupling.

Oxidative addition is often the rate-determining step in the reaction[83] and is known to be accelerated by the use of electron-rich ligands on the Pd centre, making the metal more nucleophilic and, thus, more able to oxidatively add to the electron deficient carbon-(pseudo)halide bond.[84] As can be deduced from this, another factor which increases this rate is the electrophilicity of the carbon-(pseudo)halide bond its self. The strength of the formed Pd-R bond is also a determining factor in the oxidative addition event, with a stronger bond being more favourable.

The next step in the mechanism is the transmetallation event in which the organic fragment of the organometallic reagent (boron being the metalloid in Suzuki-Miyaura chemistry) is transferred from the metal to palladium. There is no change in the oxidation state of Pd in this process (Scheme 4).

$$X-Pd^{(II)}L_n + R-M \xrightarrow{\textit{Transmetallation}} R-Pd^{(II)}L_n + M-X$$
$$\textbf{5} \qquad \textbf{8} \qquad\qquad\qquad\qquad \textbf{6} \qquad \textbf{9}$$
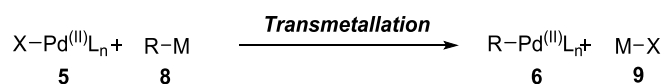
Scheme 4. Transmetallation in the palladium-catalysed cross-coupling.

The rate of transmetallation is enhanced by using more electropositive metals, i.e., R-ZnX > R-SnX > R-B(OH)$_2$. The rate also increases with decreasing p-character (increasing s-character) of the organic fragment (alkynyl (sp) > alkenyl (sp^2) > alkyl (sp^3)). This is because as the s-character of the organic fragment increases, its electropositivity also increases since the s-orbitals are closer in proximity to the electropositive atomic nucleus. This leads to an increased rate of nucleophilic attack by the carbon-metal bond on the metal centre.

The final step of the cross-coupling is the reductive elimination process, which is simply the reverse of oxidative addition. In this step, the product is eliminated and the active Pd[(0)] catalyst is regenerated and repeats the catalytic cycle (Scheme 5).
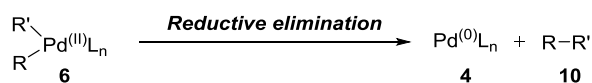
Scheme 5. Reductive elimination in palladium-catalysed cross-coupling.

Reductive elimination is aided by bulky ligands on the Pd centre,[85] forcing the organic fragments away from the Pd centre, lengthening and, thus, weakening the bonds. Weak Pd-R bonds are beneficial in reductive elimination in that it becomes easier to break the bonds, eliminating the product. By having lower electron density on Pd (which is controlled by the ligands directly attached to Pd), the Pd-R bonds become weaker.[85] These factors directly contrast what is required for efficient oxidative addition as it is the reverse process.

As would be expected, each different transition metal-catalysed cross-coupling reaction has its own unique mechanistic aspects,[86–88] and the Suzuki-Miyaura reaction is no exception. As such, there are two proposed mechanisms by which the reaction is generally accepted to proceed: i) the 'boronate pathway' and; ii) the 'oxopalladium pathway' which are shown in Scheme 6. [89, 90, 91, 92]
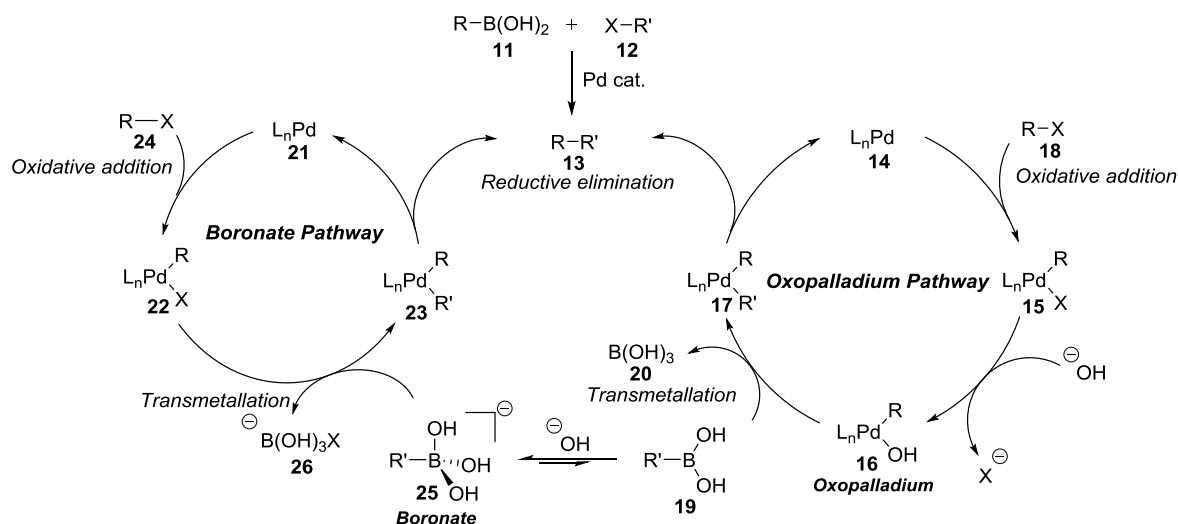
Scheme 6. The two elucidated mechanisms of the Suzuki-Miyaura reaction.

As can be seen from Scheme 6, the reaction can proceed *via* two mechanisms i) the boronate pathway, and/or ii) the oxopalladium pathway. For both these pathways, the oxidative

addition and reductive elimination steps keep with the accepted mechanisms discussed for general transition metal cross-coupling reactions. However, in Suzuki-Miyaura cross-couplings, the transmetallation step is more complex and can proceed *via* the two different processes shown in Scheme 7.

Much debate has been focussed on the nature of the active transmetallating species in the Suzuki-Miyaura reaction, with the outcome of investigations being that both the boronate and the oxopalladium can be the two active species in transmetallation.[93]
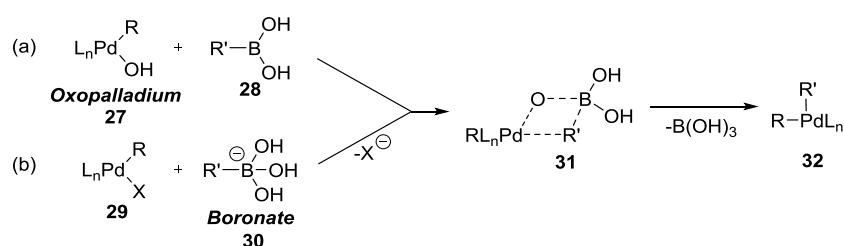
Scheme 7. Transmetallation in the Suzuki-Miyaura reaction.

Scheme 7 shows that the transmetallation event can proceed *via* one of two pathways: (a) the boronate pathway in which the neutral, Lewis-acidic boronic acid is activated *via* its negatively charged boronate. Formation of this boronate species is achieved when a hydroxide ion (generated by the aqueous base in the reaction mixture) forms a bond to the boronic acid boron (*via* its vacant p-orbital), generating the boronate. One of the oxygen atoms on the boronate species then coordinates to Pd and undergoes transmetallation *via* the four-membered palladacycle shown in Scheme 7. The formation of the boronate from the free boronic acid has been found to be essentially energetically barrierless[94, 95] which re-enforces the plausibility of this mechanism; (b) the oxopalladium pathway in which the hydroxide ion is coordinated to Pd to form an oxopalladium species which can then transmetallate *via* the same four-membered transition state.

Further debate has been focussed on which pathway is actually correct in the Suzuki-Miyaura reaction but since there is substantial evidence in favour of both the boronate pathway[95, 94] and the oxopalladium pathway,[89, 90] both have been generally accepted.

1.1.2. Boronic Acids as Suzuki-Miyaura Cross-coupling Partners

Boronic acids are the most widely used reagents in Suzuki-Miyaura cross-couplings. However, the range of organoboron compounds which can be employed in the Suzuki-Miyaura reaction is large and continues to grow with ongoing research in the field.[93] Figure 1 contains a selection of these reagents.

Borane **Boronic acid** **Organotrifluoroborate** **Pinacol boronic ester** **Catechol boronic ester**

MIDA boronate **BDAN**
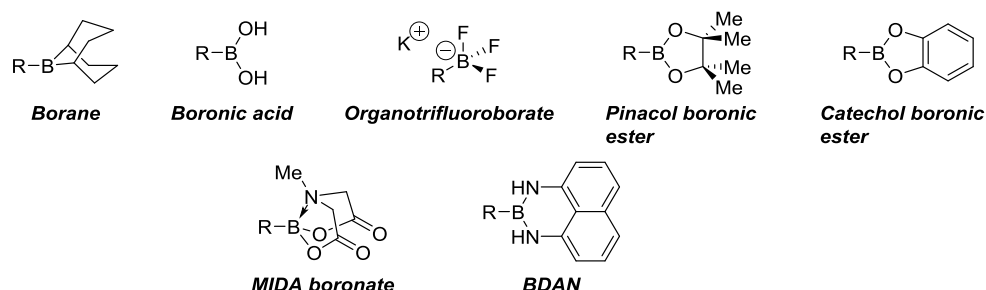
Figure 1. Boron reagents for use in the Suzuki-Miyaura cross-coupling.

Initially, the first boron reagents to be employed in the Suzuki-Miyaura cross-coupling were alkenylboranes and catechol boronic esters.[93] However, boronic acids had quickly become the preferred reagent due to their high reactivity and atom-economy.[93] Pinacol boronic esters also became widely used due to their increased stability over boronic acids.[93]

As work in the area of Suzuki-Miyaura cross-coupling progressed, a wide range of new boron reagents for Suzuki-Miyaura cross-coupling was developed (Figure 1), with varying reactivities and stabilities which have vastly increased scope in the area. Significant attention has been focussed on the development and utility of organotrifluoroborate salts[96,97] and MIDA boronates, initially reported by Mancilla[98,99] and developed by Burke,[100, 101] but many alternatives have also been well advanced such as BDAN reagents, pioneered by Suginome.[102]

In order to understand the properties and reactivities of boronic acids, and the many other boron reagents which are used in Suzuki-Miyaura cross-couplings, it is first necessary to understand the nature of the boron atom itself, with particular regards to its electron configuration and hybridisation states. Neutral boron's valence electrons ($2s^2$, $2p^1$) can be reconfigured to $2s^1$, $2p^2$ upon excitation of a 2s electron to the 2p energy level. Boron can then form three sp^2 hybridised bonds, resulting in a trigonal planar geometry with the remaining vacant 2p orbital orthogonal to the bonding plane (Figure 2).
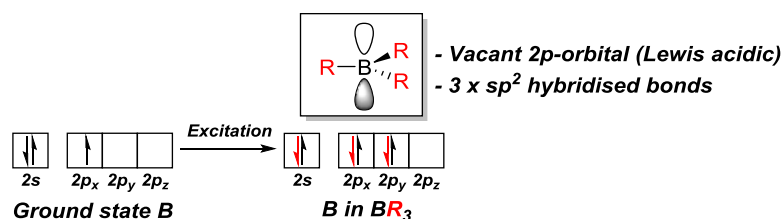
Figure 2. Bonding and hybridisation in neutral, trigonal boron species.

Neutral boronic acids in anhydrous media can act as Brønsted acids by deprotonation of the hydroxyl functionality.[103] However, under aqueous conditions, through either autoprotolysis of water (generating equivalent quantities of hydroxide and hydronium) or coordination of water into the vacant Lewis acidic 2p orbital of the boron atom, the anionic boronate complex, which is the active transmetallating species in the boronate pathway of the Suzuki-Miyaura reaction, is generated (Scheme 8).[103]
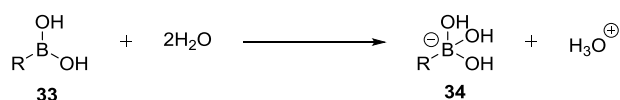
Scheme 8. Water-mediated boronate formation.

Boronate complexes have different properties to their neutral boronic acid precursors and, for that reason, generation of boronate complexes *in situ* can be desirable and is often achieved by the addition of water or aqueous base to the reaction mixture in Suzuki-Miyaura cross-coupling reactions.[103]

Boronic acids can also self-trimerise - an equilibrium-driven process favoured entropically by the liberation of three equivalents of water - to form boroxines which gain some stabilisation through pseudoaromatic character, with the generation of triply zwitterionic resonance structures (Scheme 9).[93, 103]
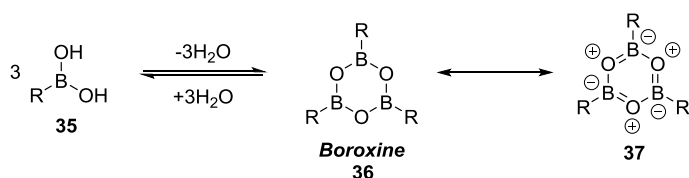
Scheme 9. Boroxine formation from neutral boronic acids.

Boroxines can be employed directly in the Suzuki-Miyaura reaction[104] but are not commonly sought as reaction products due to their equilibrium with the free boronic acid.

One major drawback of boronic acids is their inherent instability. The more labile C-B bonds in boronic acids than in other organoboron reagents increase their ability to 'protodeboronate' - a process in which the boronic acid functionality is replaced with a hydrogen atom (Scheme 10).[103,105–107]
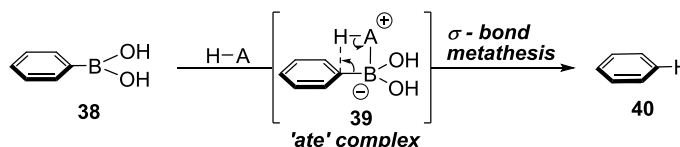
Scheme 10. Protodeboronation of boronic acids.

This is a common side reaction in Suzuki-Miyaura cross-couplings and other reactions which require the use of boronic acids, and is often overcome by using an excess of the boronic acid. Cheon and co-workers have studied the protodeboronation of boronic acids, highlighting under which conditions the boronic acid functionality is cleaved and which conditions leave the C-B bond intact.[105, 106] Generally, heating under non-anhydrous conditions leads to either partial or full protodeboronation of a selection of boronic acids in a matter of a few hours in some cases and days in others. This protodeboronation is believed to proceed *via* the coordination of a proton source (water, acid or aqueous base) into the vacant 2p orbital of the boronic acid, forming the boronate, followed by σ-bond metathesis to generate the corresponding arene compound (Scheme 10).

Lee developed a gold-catalysed protocol for the proto- and deuterodeboronation of aromatic boronic acids.[108] In this process, the ability the carbon-boron bond to be cleaved by the insertion of a transition metal has been utilised in a useful way. In doing so, the installation of deuterium and hydrogen atoms in aromatic systems which would otherwise be difficult to deuterate has been effectively achieved (Scheme 11).

$$Ar-B(OH)_2 \xrightarrow[\text{90 °C, μw, 2 h}]{\substack{PPh_3AuNTf_2 \text{ (cat.)} \\ \text{Solvent, } X_2O}} Ar-X$$

41 **42**

X = H, 24 examples   *X = D, 9 examples*
62-100% yield   *<10%-Quant. conversion*
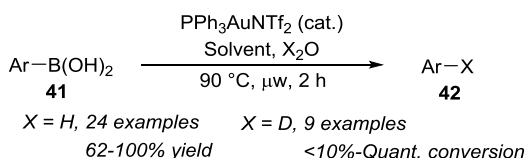
Scheme 11. Lee's proto- and deuterodeboronation reaction.

122

A particular advantage of this approach is the lack of strongly acidic or basic conditions which allows the tolerance of acid/base sensitive functionality such as esters, acetals, Boc-protected N-heterocycles and nitriles.

Protodeboronation of boronic acids is known to occur not only in aqueous solution but also in the solid state. To study this, Noonan and co-workers have carried out practical and computational studies of the possible mechanistic pathways for the protodeboronation of boronic acids when stored as neat reagents.[107] High energy barrier differences were calculated for protodeboronation of boronic acids by water versus protodeboronation as a neat reagent. Together with the practical observation that little protodeboronation occurred in the presence of excess water, this suggests that water alone is not the determining factor in protodeboronation of neat boronic acids.
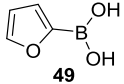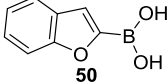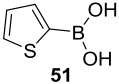
The authors proposed two solid-state pre-organization effects in which the boronic acid molecules arrange themselves such that the boronic acid functionalities coordinate each other through intermolecular hydrogen bonding networks (Figure 3 (a)) and/or Lewis acid-Lewis base pairs (Figure 3 (b)).
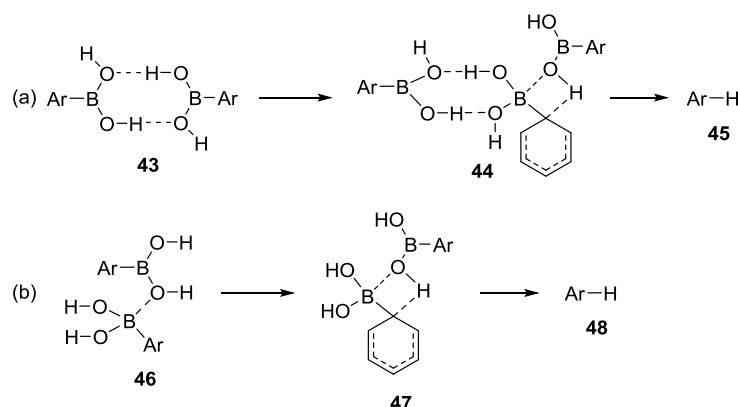
Figure 3. Proposed pre-organisation and self-protodeboronation of boronic acids in the solid state.

Based on the proposed solid-state protodeboronation mechanisms illustrated above, the authors hypothesised that boronic acids could be stored more stably in solution rather than as neat reagents. To test this hypothesis, three notoriously unstable boronic acids were monitored over the course of 15 days as neat reagents and over the course of >40 days as solutions in reagent grade, non-anhydrous, non-degassed THF (Figure 4).

	49	50	51
% remaining after 15 days as solid	*7*	*88*	*80*
% remaining after >40 days as THF solution	*100*	*84*	*100*

Figure 4. Stability of boronic acids in THF solution.

Upon investigation, it was observed that little or no protodeboronation was observed for unstable boronic acids when stored in solution for prolonged periods of time. As well as providing support for the proposed solid-state protodeboronation mechanism, this work provided a valuable method for the stable storage of such reagents.

1.2. Chemoselectivity in the Suzuki-Miyaura Reaction

Chemoselective cross-coupling is a synthetically attractive process which selectively cross-couples one coupling partner over another, typically less reactive, partner which is retained and may be employed in a subsequent chemical transformation (Scheme 12).
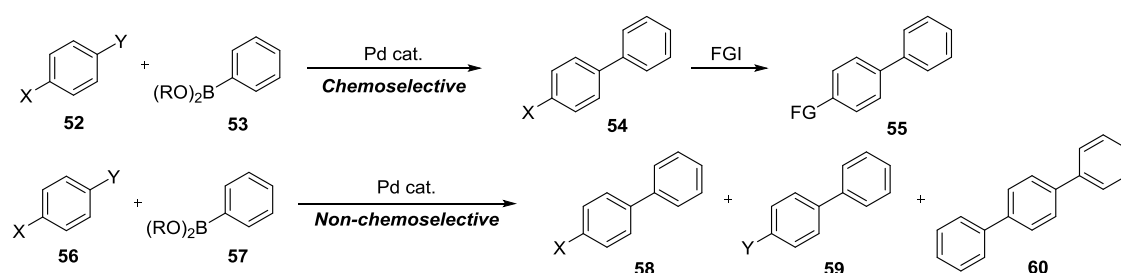
Scheme 12. Chemoselective and non-chemoselective cross-coupling in the Suzuki-Miyaura reaction. X = least reactive electrophile. Y = most reactive electrophile.

Chemoselective Suzuki-Miyaura cross-coupling may be achieved *via* either control of the rate of oxidative addition or transmetallation steps in the Suzuki-Miyaura mechanism.

1.2.1. Chemoselective Suzuki-Miyaura Cross-coupling *via* Selective Oxidative Addition

Chemoselective oxidative addition relies on the differences in rates of oxidative addition of (pseudo)halides in Pd-catalysed cross-coupling reactions, in which I > Br ≥ OTf > Cl.[109] Fu demonstrated this fundamental difference in oxidative addition rate in order to chemoselectively cross-couple boronic acids to dihaloarenes (Scheme 13).
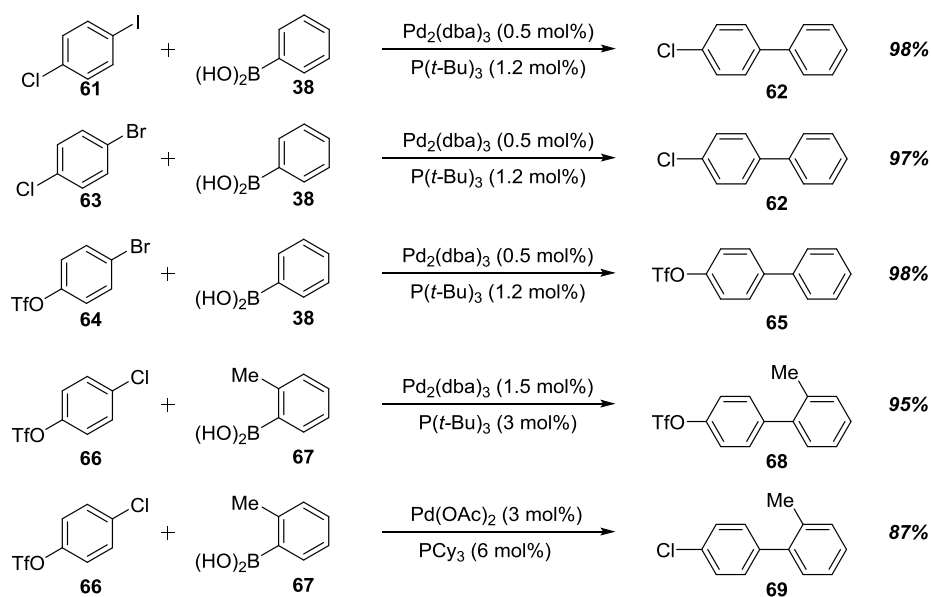
Scheme 13. Chemoselective oxidative addition in the Suzuki-Miyaura reaction.

This work demonstrates that chemoselective Suzuki-Miyaura cross-couplings can be achieved by control of the rate of the initial oxidative addition step by exploiting the inherent reactivity differential observed between (pseudo)haloarenes in the Suzuki-Miyaura reaction. An interesting result was observed when Ar-Cl was selectively cross-coupled in the presence of Ar-OTf (compound **68**). The more reactive OTf functionality remained intact after the cross-coupling by control of the catalyst system i.e. the reactivity of the (pseudo)haloarenes can be reversed.

Work within the Sherburn group has demonstrated that selective mono- and bis-coupling of dihaloarenes can be achieved through, again, exploiting the difference in reactivity of iodides *versus* bromides (Scheme 14).
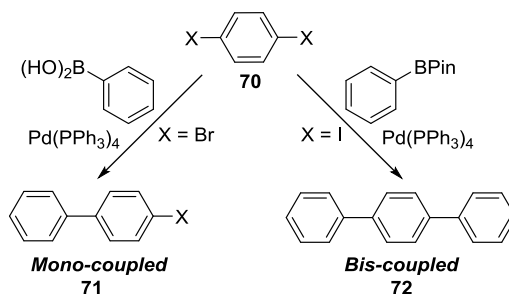
Scheme 14. Sherburn's selective mono- and bis-cross-couplings.

125

The outcome of the reaction is determined by both the nature of the boron species (i.e. mono-coupling is more pronounced in boronic acids than in BPins) and the nature of the dihaloarene (i.e., bis-coupling is favoured with diiodoarenes and mono-coupling with dibromoarenes). However, the identity of the halide is the major factor in determining selectivity, which suggests that the relative rates of oxidative addition *versus* transmetallation is faster for Ar-I than Ar-Br (Scheme 15).
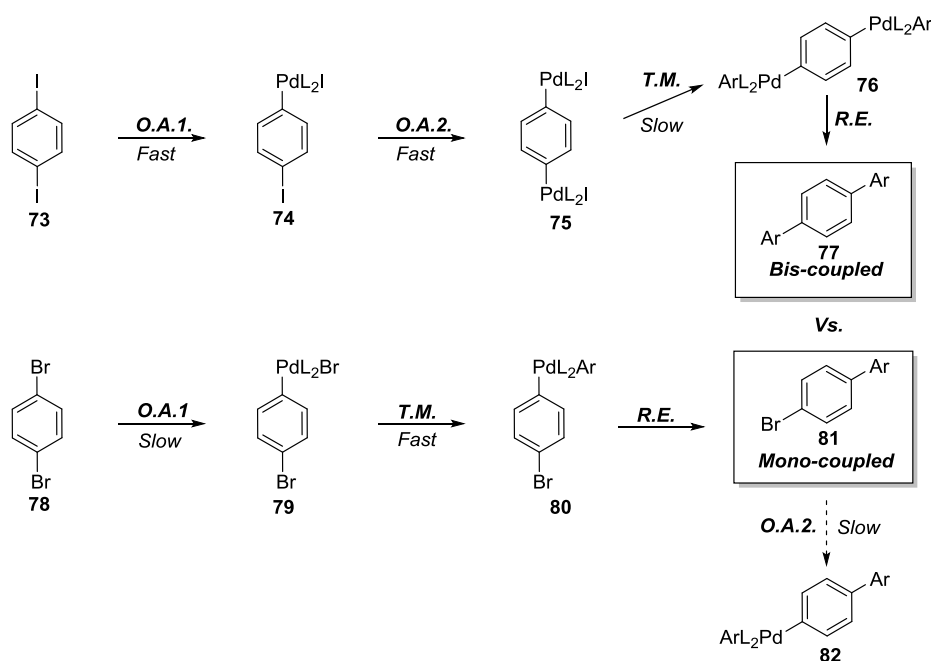
Scheme 15. Relative oxidative addition and transmetallation processes in Sherburn's selective mono- and bis- Suzuki-Miyaura cross-coupling. O.A. = oxidative addition. T.M. = transmetallation. R.E. = reductive elimination.

As can be seen from Scheme 15, the authors propose that the oxidative addition of Pd into the Ar-I bond is faster than insertion into the Ar-Br bond. This then means that both Ar-I bonds on the arene can be quickly palladated and subsequently transmetallated and reductively eliminated to form the bis-coupled product. However, with insertion of Pd into the Ar-Br bond being much slower, one Ar-Br bond can be palladated, transmetallated and reductively eliminated to form the product before the other has the chance to react. This would then lead to the mono-coupled product being formed.

1.2.2. Chemoselective Suzuki-Miyaura Cross-coupling *via* Selective Transmetallation

Transmetallation in the Suzuki-Miyaura cross-coupling relies, as well as on the nature of the pre-transmetallation palladium complex (after oxidative addition), largely on the nature of the boron species in the reaction. Two main methods for chemoselective transmetallation have currently been developed: i) the use of MIDA boronates and ii) the use of BDAN reagents . Both will be evaluated herein.

1.2.2.1. MIDA Boronates as Boronic Acid Protecting Groups and Their Role in Chemoselective Transmetallation

BMIDA reagents have been successfully employed in iterative synthesis due to their resistance towards a wide range of synthetic transformations such as oxidation, reduction, O/N-protection/deprotection, halogenation, olefination, alkylation, and aldol processes and many transition metal-catalysed cross-coupling reactions.[110,101] The reason for their robustness is due to the coordination of the nitrogen lone pair into the vacant 2p orbital on boron, forming an unreactive, tetrahedral boronate species which can be deprotected by basic hydrolysis to reveal the parent boronic acid for further manipulation as necessary (Figure 5).
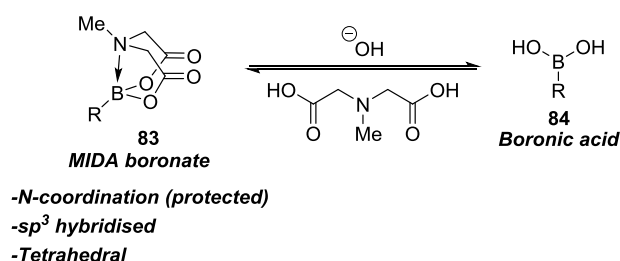
Figure 5. MIDA boronate stabilisation and deprotection.

Due to this stabilisation effect, BMIDA reagents are inert to transmetallation and, thus, can be subjected to Suzuki-Miyaura cross-coupling conditions, retaining the BMIDA functionality (provided that appropriate conditions are employed to avoid premature hydrolysis of the base-labile BMIDA). As well as being swiftly hydrolysed by NaOH, BMIDA reagents can be hydrolysed in a more controlled, slow-release fashion by using aqueous K_3PO_4.[111] Such controlled hydrolysis of BMIDA reagents provides a valuable method for the successful cross-coupling of notoriously unstable boronic acids such as heterocyclic and olefinic derivatives by releasing the parent boronic acid slowly to be cross-coupled.[112]

The slow-release strategy has valuable applications in polyene natural product synthesis since olefinic boronic acids can rapidly protodeboronate to prematurely afford the terminal alkene.[113] This strategy has made possible the iterative synthesis of a range of polyene natural products from simple halovinyl BMIDA building blocks (Scheme 16).[101]
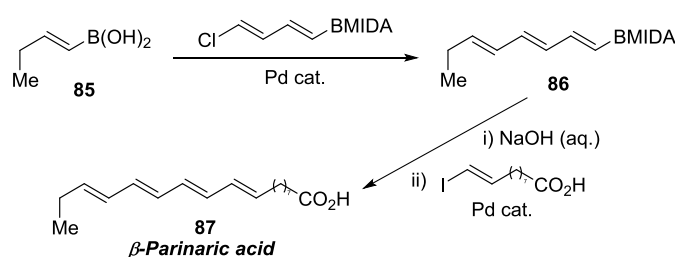
Scheme 16. Burke's iterative synthesis of β-parinaric acid.

Recently, the Watson group developed a method for the formal homologation of sp^2 hybridised BPin derivatives *via* controlling boron solution speciation in a chemoselective Suzuki-Miyaura cross-coupling (Scheme 17).[114]
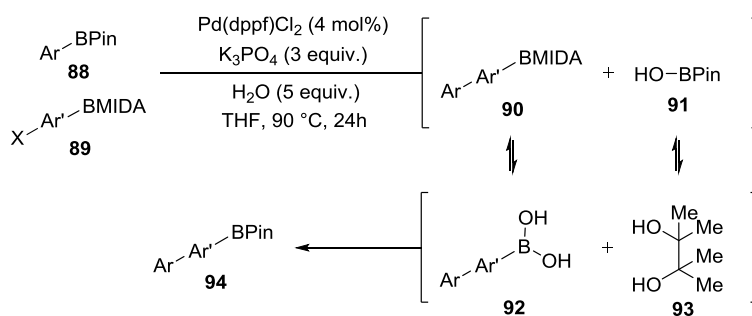
Scheme 17. Chemoselective BPin synthesis *via* control of boron solution speciation.

After the initial cross-coupling event, the intermediate BMIDA is then hydrolysed to the parent boronic acid *in situ* and combination of this with the free pinacol (generated by the hydrolysis of the HO-BPin by product of the cross-coupling) is driven towards the formation of the formally homologated BPin derivative.

This work is an important advance in the Suzuki-Miyaura cross-coupling in that, in addition to being a valuable method for chemoselective Suzuki-Miyaura cross-coupling of BPin and halo-BMIDA derivatives *via* chemoselective transmetallation, it also builds on Burke's previously reported stepwise iterative synthesis of polyene natural products. It does so by careful control of the boron solution speciation *via* the use of an aqueous, basic biphase to

generate the homologated, reactive, BPin derivative which can be reacted further in a one-pot fashion (in this case to afford triaryl derivatives), rather than having to isolate the BMIDA product, hydrolyse this to the reactive parent boronic acid, then subject this to the next transformation.

1.2.2.2. BDAN Reagents as Boronic Acid Protecting Groups and Their Role in Chemoselective Transmetallation

BDAN reagents, developed by Suginome[102], provide an additional protecting strategy for boronic acids, similar to BMIDA reagents in that one of the lone pairs on the DAN nitrogens can coordinate into boron, forming the boronate complex and, as with MIDA boronates, this renders the protected boronic acid inert to transmetallation. However, in the case of BDAN reagents, boron is not tetrahedral sp^3 but planar sp^2 and can be cleaved under acidic conditions (Figure 6).

-N-coordination (protected)
-sp^2 hybridised
-Trigonal planar
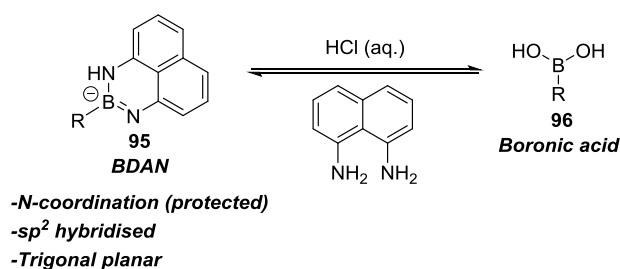
Figure 6. BDAN stabilisation and deprotection.

BDAN reagents have valuable utility in the field of chemoselective Suzuki-Miyaura cross-coupling reactions. As such, Suginome has demonstrated that bromo-BDAN reagents can be Miyaura-borylated to generate the BPin-R-BDAN compound which can be selectively cross-coupled *via* the BPin moiety to afford the retained BDAN derivative (Scheme 18).[115]
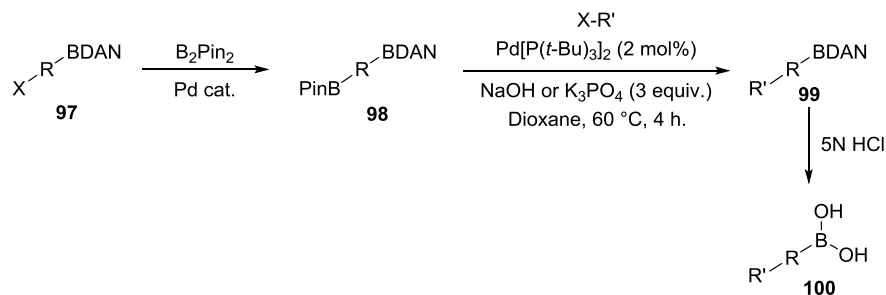
Scheme 18. Suginome's Miyaura-borylation and chemoselective Suzuki-Miyaura cross-coupling of BDAN derivatives.

Similarly to Burke's iterative polyene synthesis (Scheme 16), this methodology has been used in an iterative manner to prepare a range of oligoarene derivatives which can be further cross-coupled to form higher oligoarenes and deprotected to reveal their boronic acid derivatives for further manipulation.

Suginome has also demonstrated a unique faculty of the BDAN group, in which the formation of differentially protected BPin-BDAN olefinic derivatives can be achieved due to the greater steric bulk of BDAN over BPin (Scheme 19).[116] The generated borylated derivatives can then be chemoselectively cross-coupled.
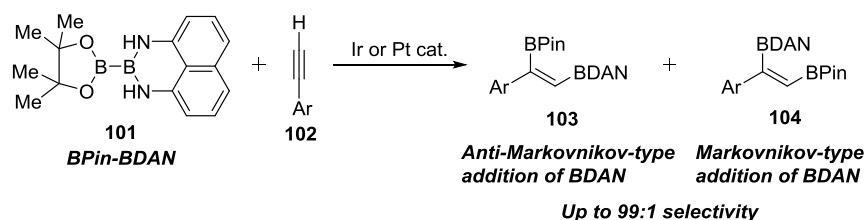
Scheme 19. Suginome's unsymmetrical selective bis-borylation of terminal alkynes.

Anti-Markovnikov-type addition of BDAN affords the unsymmetrically bis-borylated olefin which can be selectively manipulated whereas standard borylation with B_2Pin_2 affords the symmetrically borylated olefin which can then be selectively manipulated in the terminal position (Scheme 20).[116]
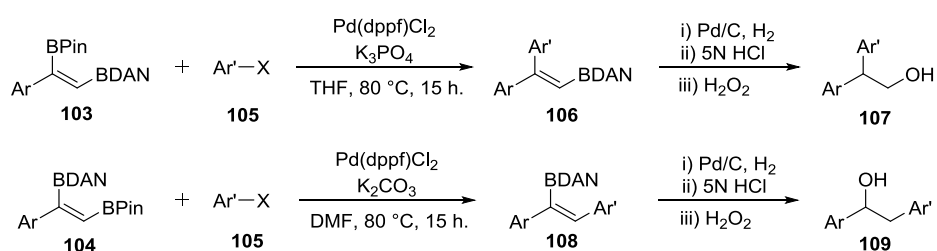
Scheme 20. Suginome's regiocomplementary synthesis of arylethanols.

This methodology represents a useful strategy for selective bis-functionalisation of alkyne derivatives and further demonstrates the ability of BDAN compounds to tolerate and undergo chemoselective transmetallation in Suzuki-Miyaura cross-coupling reactions.

The ability of olefinic BDAN compounds to undergo asymmetric hydroboration to afford chiral, geminal BPin-BDAN compounds which can then be chemoselectively Suzuki-Miyaura cross-coupled with both inversion[117] and retention[118] of stereochemistry, depending on the functionality surrounding the borylated carbon, has been demonstrated.
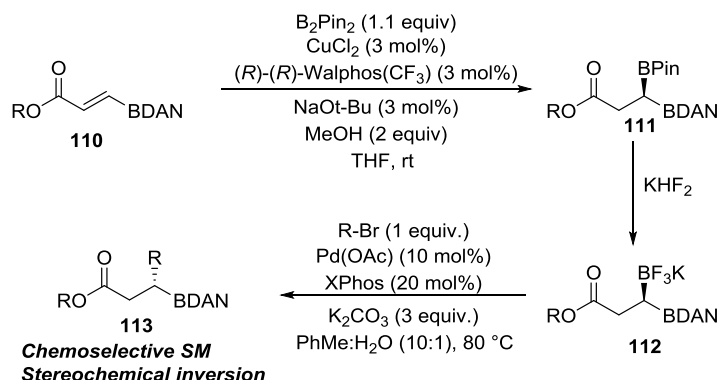
Scheme 21. Hall's asymmetric hydroboration of BDAN compounds and subsequent chemoselective Suzuki-Miyaura cross-coupling.

In this work,[118] Hall has demonstrated the ability of BDAN compounds to undergo asymmetric hydroboration, installing a geminal BPin moiety which is then converted to the potassium trifluoroborate salt and chemoselectively Suzuki-Miyaura cross-coupled, as discussed in previous examples, but with inversion of the stereochemistry on the bis-borylated carbon. This represents a valuable method for the asymmetric β-difunctionalisation of ester compounds *via* chemoselective Suzuki-Miyaura cross-coupling.
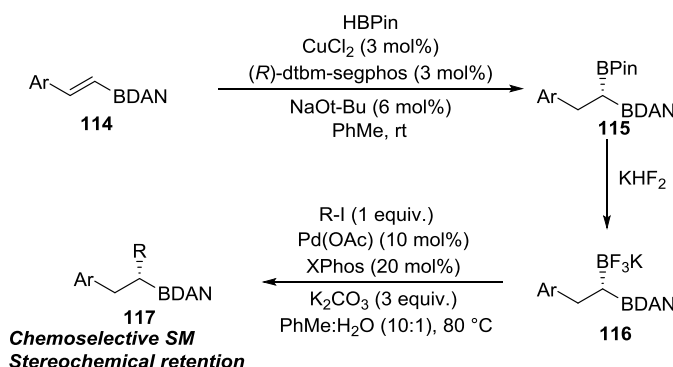
Scheme 22. Yun's asymmetric hydroboration of BDAN compounds and subsequent chemoselective Suzuki-Miyaura cross-coupling.

Here, as well as expanding on the scope of Hall's previous work in the area, Yun has demonstrated that geminal BPin-BDAN compounds containing an aromatic substituent, rather than an ester, in the β-position can be cross-coupled chemoselectively and stereoretentively.[118]

1.2.2.3. Neighbouring Group Activation of Vicinal and Geminal Diboron Species and Their Role in Chemoselective Transmetallation

The examples of chemoselective transmetallation discussed up to this point have been discriminatory for one boron species over another i.e. chemoselective Suzuki-Miyaura cross-coupling of a boronic acid over a BMIDA, of a BPin over a BDAN etc. However, identical boron species in a vicinal or geminal relationship can be chemoselectively Suzuki-Miyaura cross-coupled, operating on the premise of neighbouring group activation (Figure 7).[119,120,121]

-*Terminal B more Lewis acidic*
-*Proximal B less Lewis acidic*
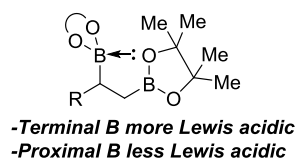
Figure 7. Neighbouring group activation in vicinal BPin species.

Figure 7 shows how vicinal boron species can activate and deactivate each other to transmetallation through coordination of the terminal BPin oxygen lone pair into the vacant 2p orbital of the proximal BPin. The terminal BPin, thus, becomes more Lewis acidic, making it the more capable transmetallating group.

Shibata demonstrated this effect in the chemo- and regioselective Suzuki-Miyaura coupling of multi-substituted sp³ hybridised geminal diboranes.[119] In this work, it was shown that geminal diboron species can be reacted selectively over mono-boronated species (Scheme 23).
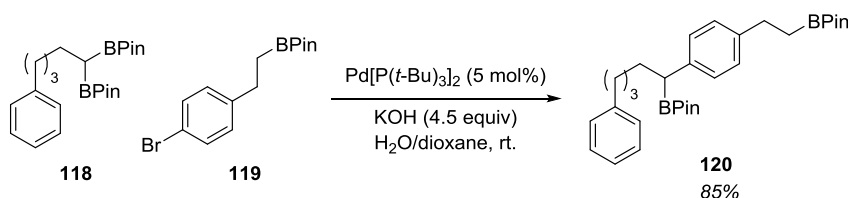
Scheme 23. Shibata's chemo – and regioselective Suzuki-Miyaura coupling.

Shibata's work here demonstrates the capacity of one BPin group to sufficiently activate another such that it becomes more reactive than any other BPin group in the reaction mixture. Here, it can be seen that the neighbouring group activation effect of the diboron moiety renders the geminal sp^3 BPin group more reactive than a singular sp^3 BPin group, enabling chemo- and regioselective Suzuki-Miyaura cross-coupling of the geminal BPin group to generate the corresponding product in 85% yield.

Morken has demonstrated this neighbouring group activation effect well in the chemoselective Suzuki-Miyaura cross-coupling of vicinal BPin derivatives towards the synthesis of a range of pharmaceutically relevant compounds (Scheme 24).[120]
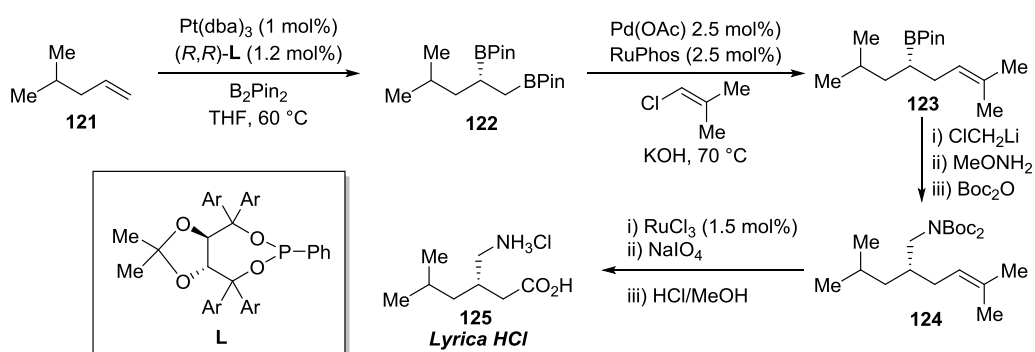
Scheme 24. Morken's chemoselective Suzuki-Miyaura cross-coupling of vicinal BPins towards the synthesis of anticonvulsant Lyrica HCl.

From this report, it can be seen that complex, enantioenriched aliphatic scaffolds can be prepared from simple olefinic starting materials *via* the asymmetric bis-borylation/chemoselective Suzuki-Miyaura cross-coupling strategy in relatively few steps.

Morken has also demonstrated the chemoselective Suzuki-Miyaura cross-coupling of geminal BPins in the synthesis of (*R*)-tolterodine (Scheme 25).[121]
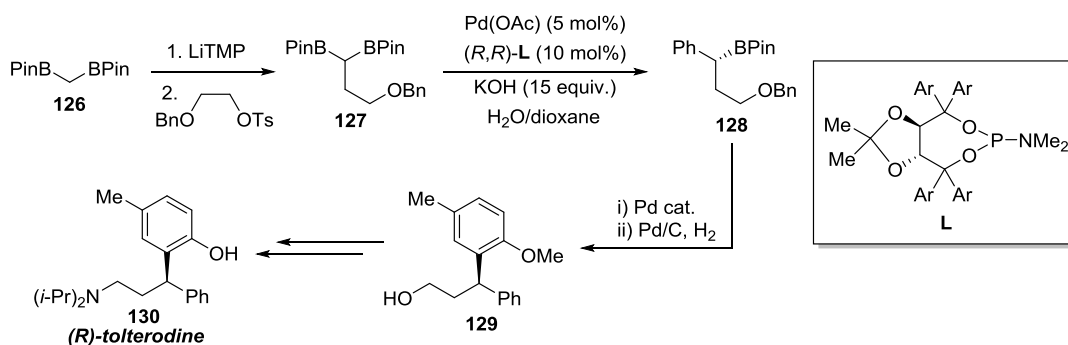
Scheme 25. Chemoselective Suzuki-Miyaura cross-coupling of geminal BPin derivatives.

This work demonstrates that geminal BPin derivatives can be chemoselectively and asymmetrically cross-coupled and has shown that the methodology can be applied to the synthesis of pharmaceutically relevant motifs.

One major advantage of Morken's strategies of chemoselective Suzuki-Miyaura cross-coupling over others which have been developed (BDAN and BMIDA reagents) is the lack of boronic acid protecting/deprotecting steps, which is enabled by the neighbouring group activation of one vicinal/geminal BPin over the other BPin. This is an important advance in the field of chemoselective Suzuki-Miyaura cross-coupling as it keeps with Baran's ethos of the 'ideal synthesis'[122] which argues that protecting group chemistry should be kept to a minimum in order to increase the step- and atom-efficiency of a synthesis.

1.3. The Diversity of the Boronic Acid Functional Group

Boronic acids are amongst the most versatile of functional groups.[103] There exists a wide range of reactions which boronic acids can undergo. Notably, there are different classes of reaction which can be performed on boronic acids:

i)   Boronic acid speciation processes: trifluoroborate formation,[93,96,97,123] Bpin formation,[93,96,124] BCat formation,[124] BMIDA formation,[93,100,101,111–113] and BDAN formation.[93,112,115,116,124]

ii) Ipso-substitution processes: protodeboronation,[105–107] halogenation,[125,126] acetylation,[127] and nitration.[128,129]

iii) Fragment migration processes: oxidation[130–132] and amination.[133,134]

134

iv)   Transition metal-mediated processes: azidation,[135] sp cross-coupling,[136] sp^2 cross-coupling,[93] sp^3 cross-coupling,[137,138] oxidative heck,[139] 1,4-addition,[140–142] 1,2-addition,[143–145] carbonylative cross-coupling,[146,147] and Chan-Evans-Lam coupling[148–152]

Figure 8 contains a representation of these reactions, organised into their respective reaction classes.
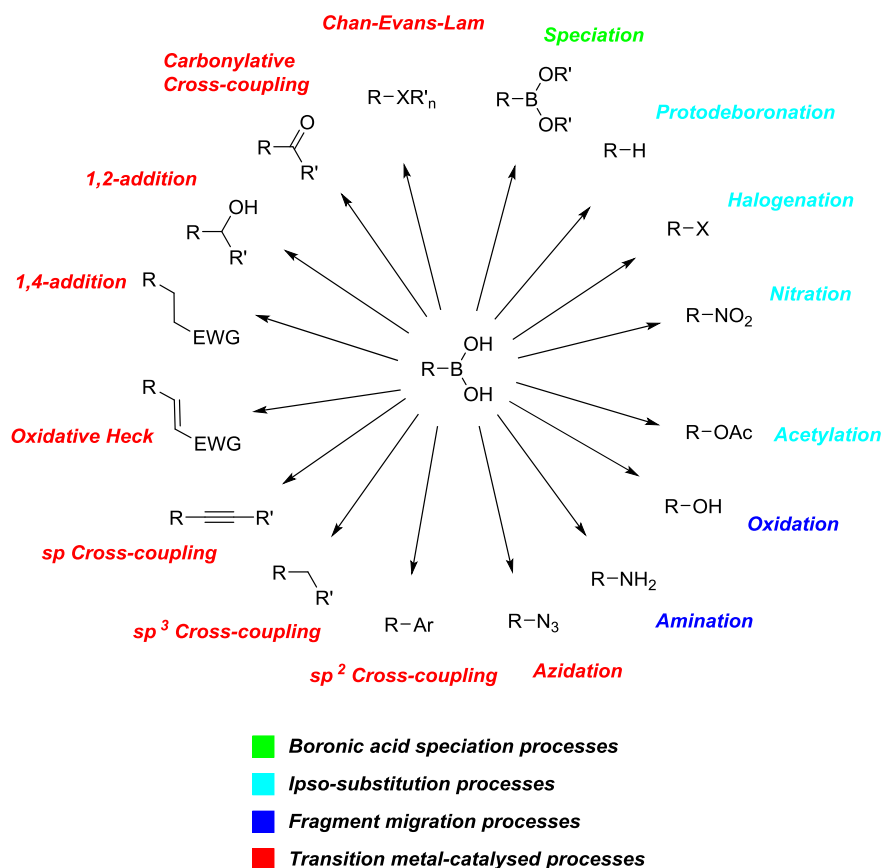
Figure 8. Reactions of boronic acids.

As can be seen from Figure 8, a remarkably wide range of bond formations such as C-C, C-H, C-Br, C-Cl, C-I, C-F, C-N, and C-O bonds can be performed on boronic acids, making them exceptionally useful groups for organic synthesis. It can thus be inferred that the generation of methodology which produces diversely functionalised boronic acids would be of high value to the chemical toolbox.

Not only are boronic acids amongst the most reactive of functional groups in general, they are also the most reactive of all the boron species, being susceptible to many reactions which

other boron species are inert to. As such, when compared to boronic acids, their corresponding BPins display limited reactivity in a number of reactions such as 1,4-addition (Scheme 26 (a)),[153] Cu-catalysed etherification (Scheme 26 (b)),[154,155] the Petasis reaction (Scheme 26 (c)),[156] and Cu-catalysed amination (Scheme 26 (d)).[155]
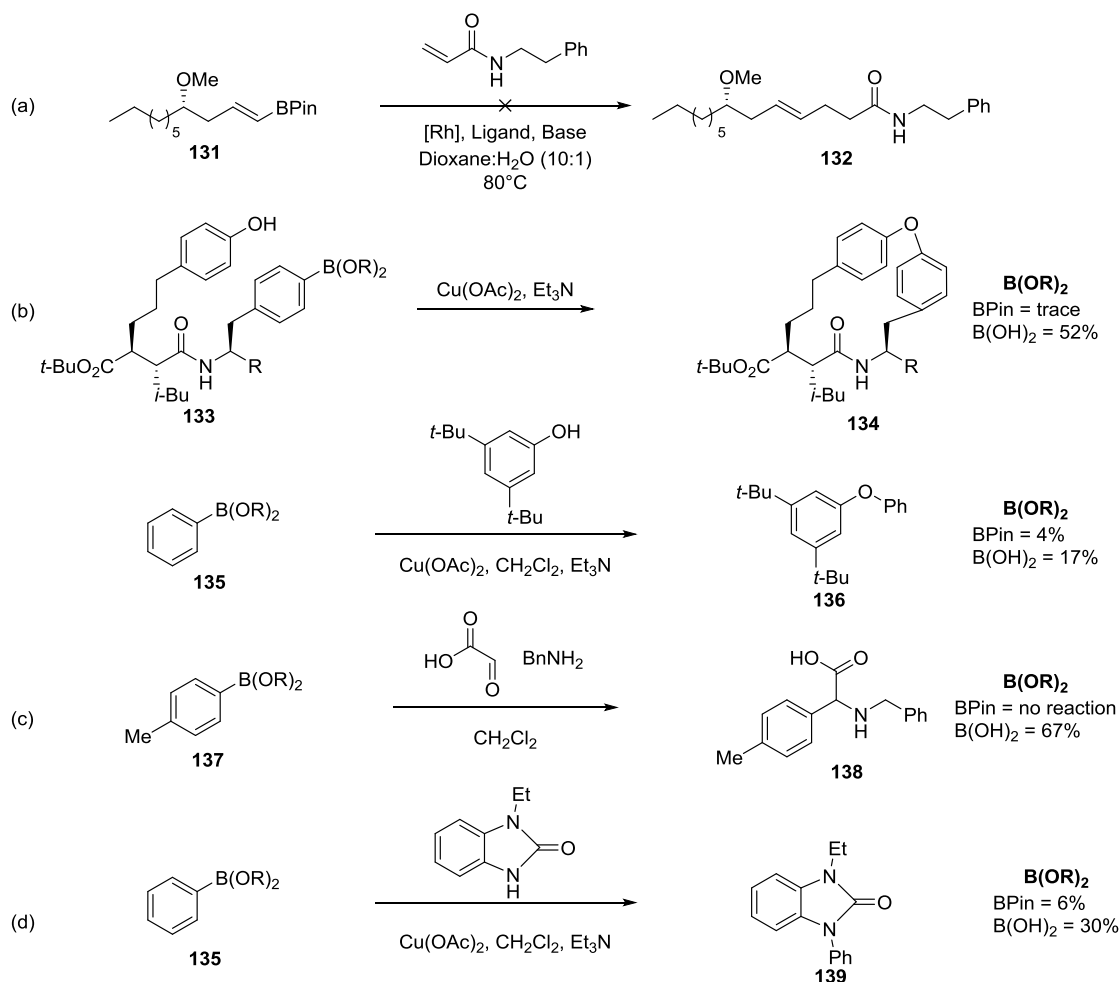
Scheme 26. Relative reactivities of boronic acids and BPins.

As can be seen from Scheme 26, boronic acids can be more reactive than BPins towards many transformations, making them generally more sought-after for organic transformations. It can also be seen that, even in cases where BPins do react, boronic acids generally outperform them. MIDA boronates and BDAN reagents (protected boronic acids) are also known to be inert to a wide range of transformations which boronic acids can undergo. These boron species and their reactivities are covered in sections 1.2.2.1. and 1.2.2.2., respectively.

A significant sector of boronic acids' exceptional reactivity as a functional group in general can be attributed to their ability to form their corresponding, reactive, boronate species (discussed in section 1.1.2.). This boronate species is fundamental to the vast majority of the reactions which boronic acids can undergo, and an analysis of the mechanisms of the different reaction classes of boronic acids (detailed in Figure 8) explains this (Scheme 27).[103]
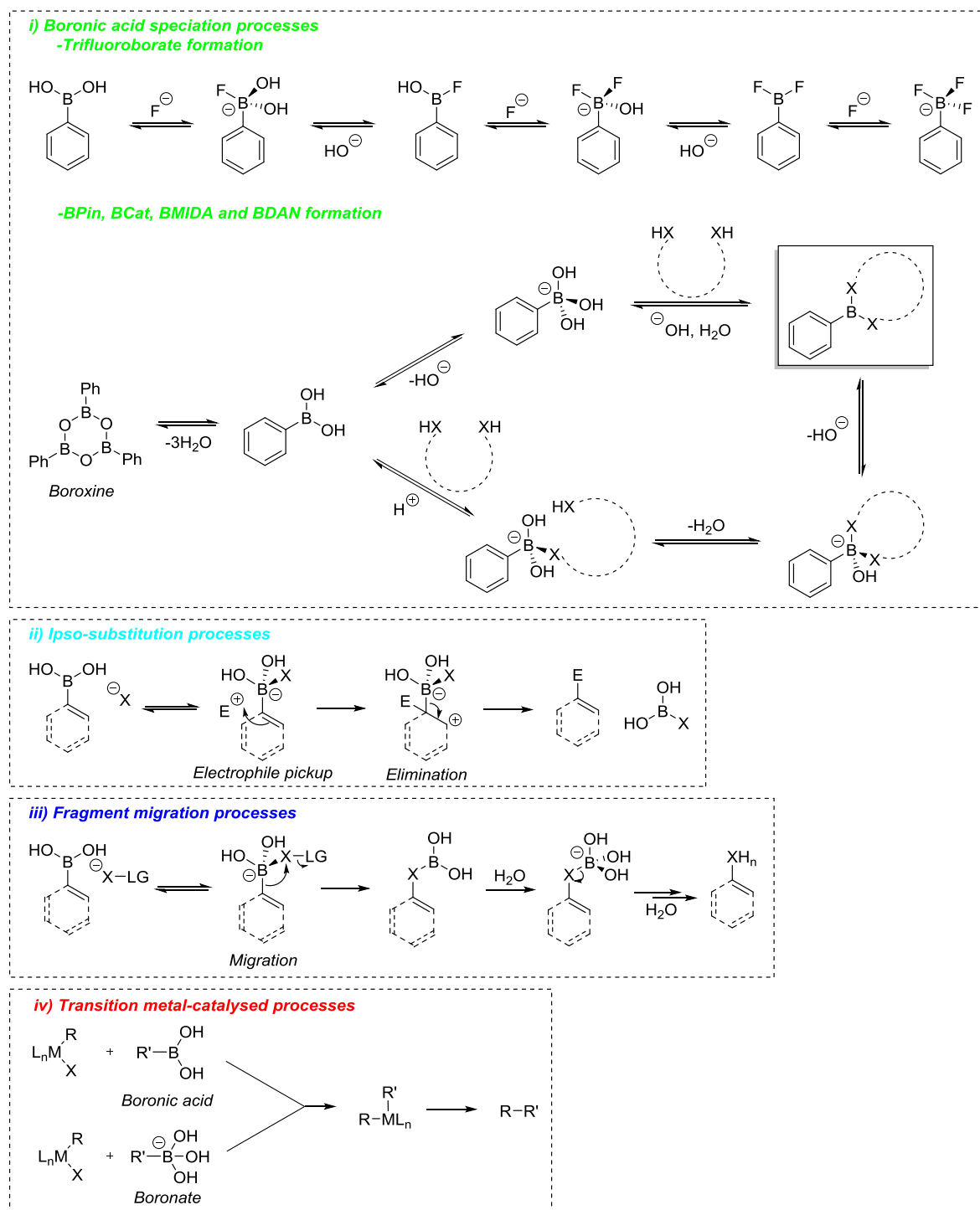
Scheme 27. Generic mechanisms of boronic acid processes.

From Scheme 27 it can be seen that each reaction class which the boronic acid can perform involves, in its mechanism, the formation of the reactive boronate species. Boron speciation events rely on the boronate species in order to facilitate the series of association/dissociation steps which lead to the formation of the new boron species.[93,96,97] *Ipso*-substitution processes

rely on formation of the boronate in order to facilitate the electrophile pickup by increasing the nucleophilicity of the organic fragment[157] (Figure 9), and subsequent elimination of the neutral boric acid species to quench the cationic charge also requires the boronate.[103] Fragment migration processes rely on formation of the boronate species in order to increase the nucleophilicity of the organic fragment which, in turn, promotes migration of the organic fragment to the electrophilie.[103] Lastly, transition metal-catalysed processes often require the boronate species to transmetallate due to a number of factors which are discussed in section 1.1.1.
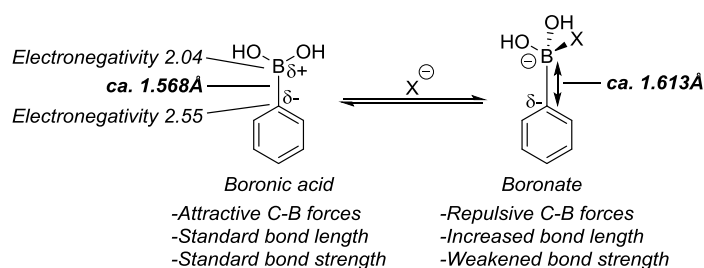
Figure 9. Nucleophilicity of boronic acid vs. boronate.

As can be seen in Figure 9, in phenylboronic acid the bonding carbon atom, with an electronegativity of *ca.* 2.55,[158] and boron atom, with an electronegativity of *ca.* 2.04,[158] forms a standard C-B bond of *ca.* 1.57Å in length.[159] When the boronic acid is converted to its corresponding boronate, the increase of electron density on the boron atom eliminates the formerly attractive forces between the relatively electronegative carbon atom and relatively electropositive boron atom. The result of this is that an electrostatically repulsive force is created between the carbon and boron atoms, inducing a weaker C-B bond of *ca.* 1.61 Å[160] in length. Understandably, it is this C-B bond lengthening and weakening which gives boronic acids the ability to react in such a large number of processes.

2. Proposed Work

The aims of this body of work were:

i) To validate the concept of the chemoselective formal homologation of boronic acids.

ii) To optimise the process to achieve high yields of homologated boronic acid product.

iii) To apply the developed methodology to a range of boronic acids and MIDA boronates to generate a diverse range of products.

iv) To apply the homologation methodology in the synthesis of pharmaceutically relevant motifs.

2.1. Concept Validation and Optimisation

To investigate the validity of the formal homologation reaction, it would be necessary to perform benchmark reactions to gain insight in to the reactivity of the system. Once validated, optimisation could then proceed to achieve a highly efficient system (Scheme 28)
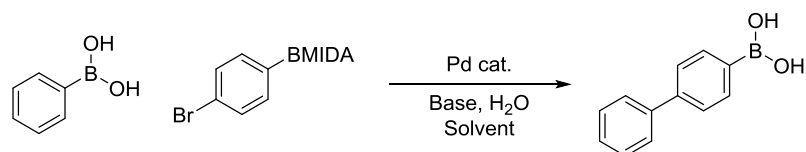
Scheme 28. Optimisation reaction for the formal homologation methodology.

2.2. Substrate Application

Once the concept had been validated and the process optimised, the next stage would be to apply the methodology to the synthesis of a range of structurally diverse boronic acids starting from substituted aryl boronic acids and aryl/olefinic MIDA boronates (Scheme 29).
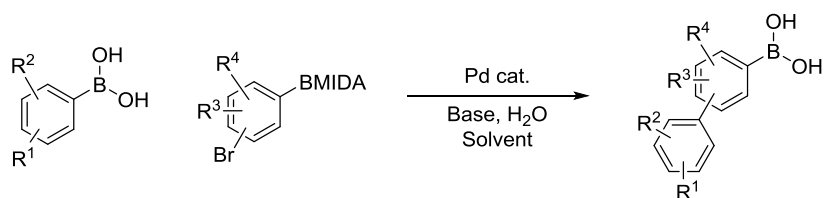
Scheme 29. Application of the boronic acid homologation methodology.

2.3. Application of the Methodology Towards the Synthesis of Pharmaceutically Relevant Motifs

To demonstrate the value of the methodology with regards to diversity-orientated synthesis for rapid SAR screening, the methodology would then to be applied to the synthesis of a range of pharmaceutically relevant compounds from one core homologated boronic acid intermediate (Scheme 30).
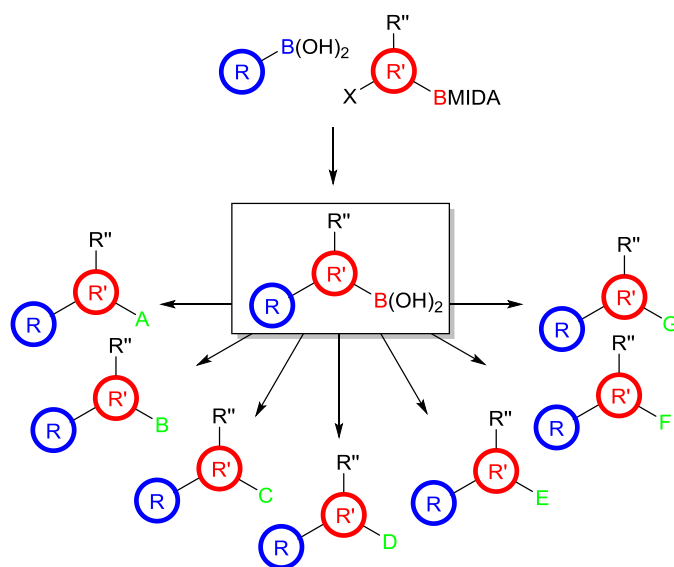
Scheme 30. Application of the methodology.

3. Results and Discussion

3.1. Benchmark Reaction

In order to gain an initial understanding into the homologation reaction, a benchmark system was set up with $PhB(OH)_2$ (**38**) and 4-bromophenylboronic acid MIDA ester (**140**), using a catalyst and medium composition based on our previous work (Scheme 31).[114]
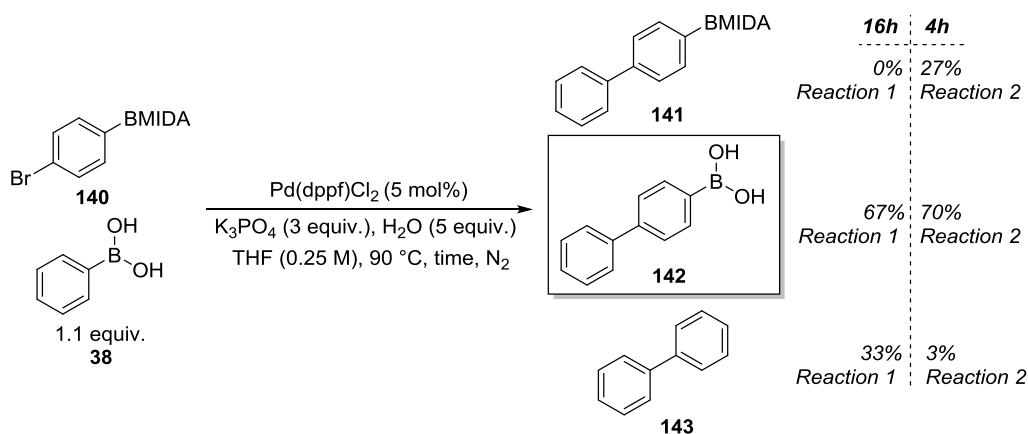
Scheme 31. Benchmark reaction outcome.

Upon initial investigation of the benchmark system, it was observed that the desired boronic acid product (**142**) was formed at promising conversion (67%) and hydrolysis of the cross-coupled BMIDA intermediate (**141**) had gone to completion. However, a significant quantity of biphenyl (**143**) was formed through protodeboronation of the boronic acid product and homocoupling of the boronic acid starting material. Shortening of the reaction time from 16 hours to four hours successfully tamed the protodeboronation, delivering the desired product in 70% yield. However, by shortening the reaction time, this also restricted the amount of time which the cross-coupled BMIDA intermediate had to hydrolyse to the parent boronic acid, leaving 27% of the reaction composition as the protected BMIDA intermediate. At this point, a thorough reaction optimisation was required.

3.2. Reaction Optimisation

3.2.1. Base and Water Studies

Optimisation of the boronic acid homologation began with a study of the reaction medium with specific regards to the basic biphase, i.e., the K_3PO_4 to H_2O ratio. Based on our

benchmark reaction results and also on our previous work,[114] it was believed that the reaction outcome would depend heavily upon the rate of hydrolysis of the BMIDA intermediate (**141**) (Scheme 32).
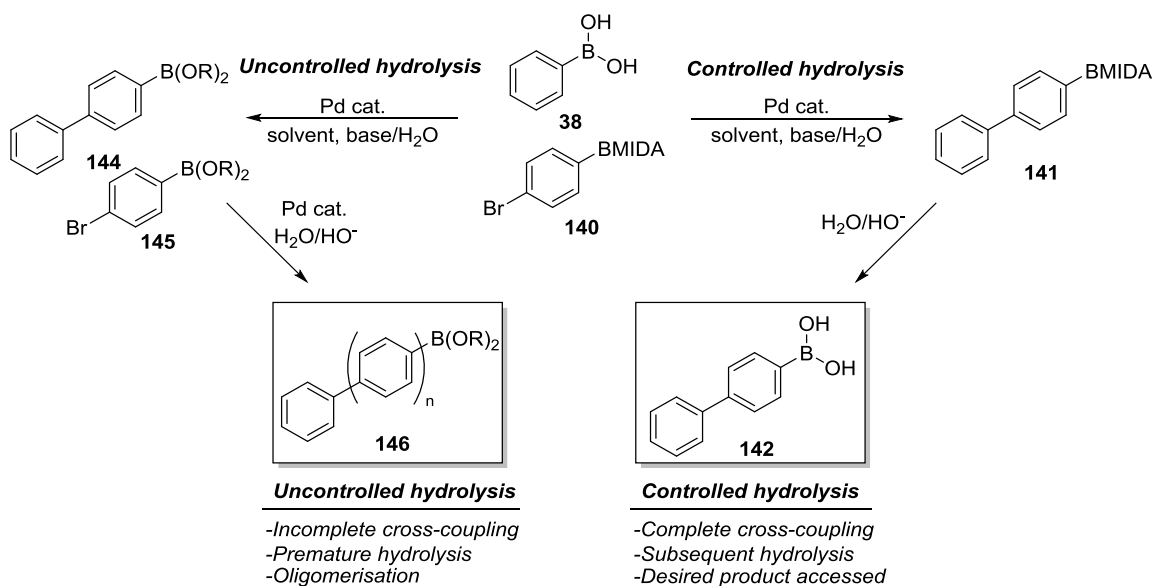
Scheme 32. Different reaction outcomes depending on the rate of BMIDA hydrolysis.

As can be seen from Scheme 32, complete cross-coupling conversion before BMIDA hydrolysis takes place would lead to high levels of singly homologated boronic acid product (**142**), whereas premature hydrolysis of the cross-coupled BMIDA intermediate (**141**) before completion of the cross-coupling would lead to oligomerisation of the aryl units (**146**).

Controlling the quantity of available H_2O/HO^- in the reaction mixture was fundamental to the rate of BMIDA hydrolysis and, consequently, the success of the homologation process. Typical Suzuki-Miyaura reactions are carried out using arbitrary quantities of base and water, for example, solvent/water mixtures of 10/1, 5/1, 4/1, or 1/1 are commonly used.[161–170] This, of course, would not be suitable for our process as the BMIDA hydrolysis is dependent on the quantity of available water and using water in co-solvent quantities would result in rapid and premature hydrolysis and subsequent, undesired, oligomerisation. Our solution to this was to use a suitably hygroscopic inorganic base (for example, K_3PO_4) with the addition of restricted quantities of water, generating a suitably tailored basic biphase (Figure 10) which would, through careful control of the quantity of available H_2O/HO^-, allow the initial cross-coupling to proceed to completion before the BMIDA hydrolysis could significantly take place.
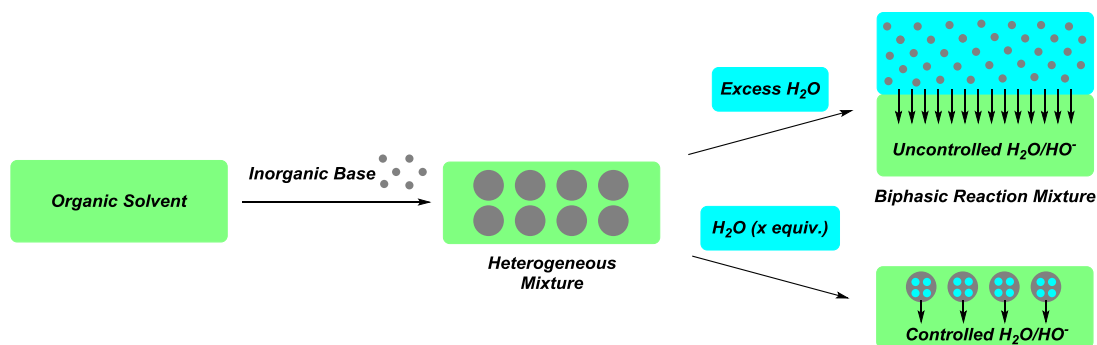
Figure 10. Generation of a suitable basic biphase.

Figure 10 depicts a scenario in which, after the addition of an inorganic base to an organic solvent, generating a heterogeneous mixture in which the base is suspended in the solvent, there are two possible reaction media compositions based on the quantity of added water:

i) Upon addition of excess water to the heterogeneous solvent/base mixture (for example, THF:H_2O = 10:1, 7:1, 4:1 etc.) generates a biphasic reaction mixture in which the inorganic base is fully soluble in the aqueous phase. This allows the H_2O/HO^- to be released into the organic phase in an uncontrolled fashion, which would lead to, in our system, uncontrolled hydrolysis of the BMIDA intermediate to the reactive boronic acid and subsequent oligomerisation of the aryl units.

ii) Upon addition of restricted quantities of water to the heterogeneous solvent/base mixture (for example, 3/4/5 equivalents etc.), the reaction mixture becomes one in which the hygroscopic base effectively sequesters the water such that a basic biphase is generated in which the extent of H_2O/HO^- release can be controlled. This, ultimately, would control the rate of hydrolysis of the BMIDA intermediate, leading to the success of the homologation reaction.

Based on the requirement for control of the quantity of available H_2O/HO^- in the reaction mixture, optimisation began with a study of the base and water (Table 1).
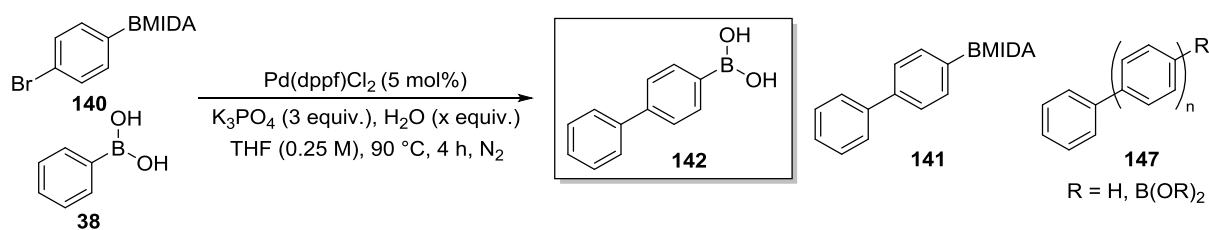
Equiv. H_2O	% 142[a]	% 141[a]	% 141+142[a]	% Ph_2[a]	Reaction no.
0	25	32	57[b]	14	3
5	70	27	97	7	4
10	40	24	64	10	5
15	78	0	78[c]	8	6
20	60	0	60[c]	8	7
25	62	0	62[c]	7	8

[a] Conversion Determined by HPLC analysis using an internal standard. [b] Remaining mass balance as unreacted starting material. [c] Remaining mass balance as oligomeric material (**147**). 1.1 equiv. phenylboronic acid used.

Table 1. Initial base and water study.

The results shown in Table 1 indicated that the optimum number of equivalents of water at three equiv. of base was five equiv.. Here, 97% cross-coupling conversion was observed, and 70% conversion to the boronic acid product was achieved. Given that Pd^{II} must first be reduced to Pd^0 before it is able to undergo oxidative addition to Pd^{II} in the Suzuki-Miyaura reaction (see section 1.1.1.), it can be assumed that, with 5 mol% of catalyst being used, approximately 5% of all Ph_2 being generated in each reaction can be attributed to oxidative homocoupling of the boronic acid starting material (two molecules of boronic acid per molecule of Pd). The results from Table 1 are graphically represented in Figure 11.
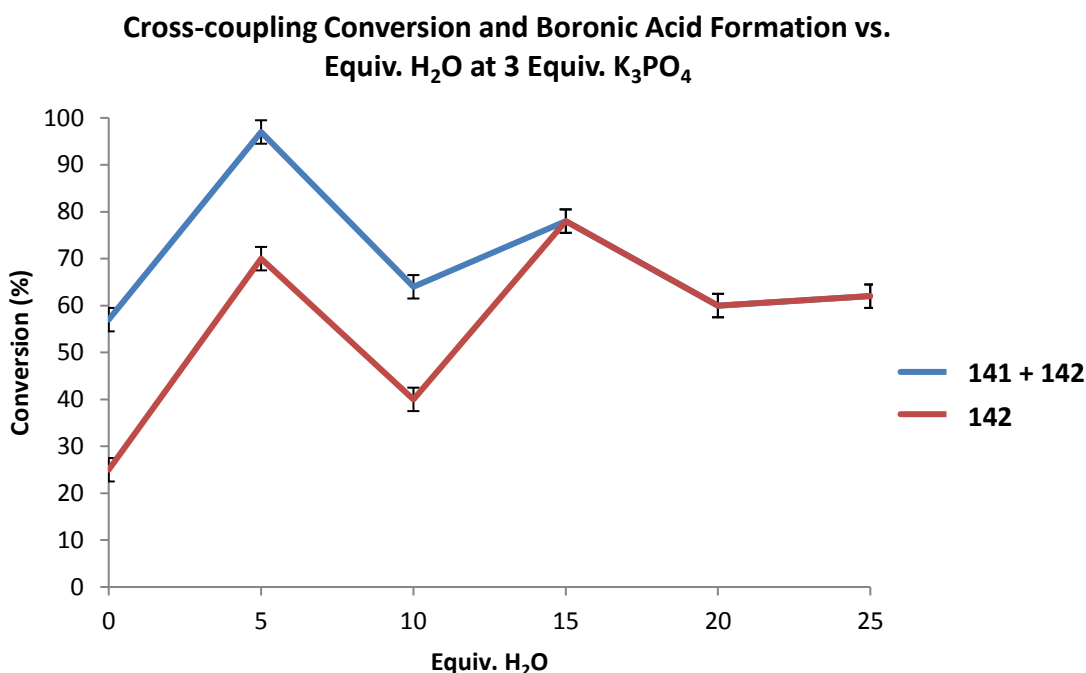
Figure 11. Cross-coupling conversion and boronic acid formation vs. equiv. H_2O at 3 equiv. K_3PO_4.

As can be seen from Figure 11, at 0 equiv. H_2O, the overall cross-coupling (**141**+**142**) did not proceed to completion. This, however, was to be expected as the Suzuki-Miyaura reaction requires the addition of water in conjunction with the base in order to achieve boronate and/or or oxopalladium formation (the active transmetallating species - see section 1.1.1.).

As the quantity of water was increased to five equiv., excellent cross-coupling conversion was observed. However, upon increasing water to 10 equiv., a decrease in cross-coupling conversion was observed. At 10 equiv. water, the H_2O/K_3PO_4 ratio (10/3) represents a critical point in the reaction medium composition in that, below 10 equiv water (i.e. H_2O/K_3PO_4 ratio <10/3), the hygroscopic K_3PO_4 is able to sequester the water such that the K_3PO_4 is essentially sub-saturated with water. This enables the control of the rate of hydrolysis of the BMIDA intermediate and, therefore, the overall success of the reaction. However, at ≥10 equiv. water (i.e. H_2O/K_3PO_4 ratio (>10/3), the K_3PO_4 becomes less able to fully sequester the increasing quantity of water. At this point, the reaction medium composition approaches a biphasic mixture which is more akin to what is seen in the literature i.e. with co-solvent levels of water being used (the water is sub-saturated with base) and the control over the rate of

146

hydrolysis of the BMIDA starting material and BMIDA intermediate decreases, leading to the formation of more oligomeric material and less desired product.

At quantities of water below 15 equiv. (i.e. 0 equiv., 5 equiv., and 10 equiv.), incomplete hydrolysis of the cross-coupled BMIDA intermediate was observed and large proportions of the product remained as the BMIDA intermediate. At 15 equiv. H_2O and above (i.e. 15 equiv., 20 equiv., and 25 equiv.), BMIDA intermediate hydrolysis was quantitative, as the base was less able to sequester the water, and the conversion to boronic acid product was exactly equal to the overall cross-coupling conversion.

By increasing the quantity of K_3PO_4 from 3 equiv. to 4 equiv. and varying quantities of water at this level, this increased the conversion to the boronic acid product (Table 2).
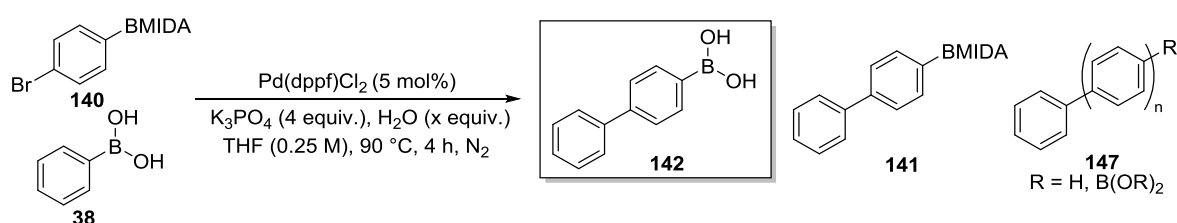
Equiv. H_2O	% 142[a]	% 141[a]	% 141+142[a]	% Ph_2[a]	Reaction no.
0	5	68	73[b]	6	9
5	72	0	72[b]	5	10
7	84	8	92	6	11
10	71	17	88[c]	6	12
15	74	0	74[c]	8	13
20	82	0	82[c]	6	14
25	81	0	81[c]	6	15

[a] Conversion Determined by HPLC analysis using an internal standard. [b] Remaining mass balance as unreacted starting material. [c] Remaining mass balance as oligomeric material (**147**). 1.1 equiv. phenylboronic acid used.

Table 2. Second base and water study.

The results shown in Table 2 indicated that 7 equiv. of water and 4 equiv. of base were optimal for conversion to boronic acid product. Here, 92% cross-coupling conversion was observed, and 84% conversion to the boronic acid product was achieved. The results from Table 2 are graphically represented in Figure 12.
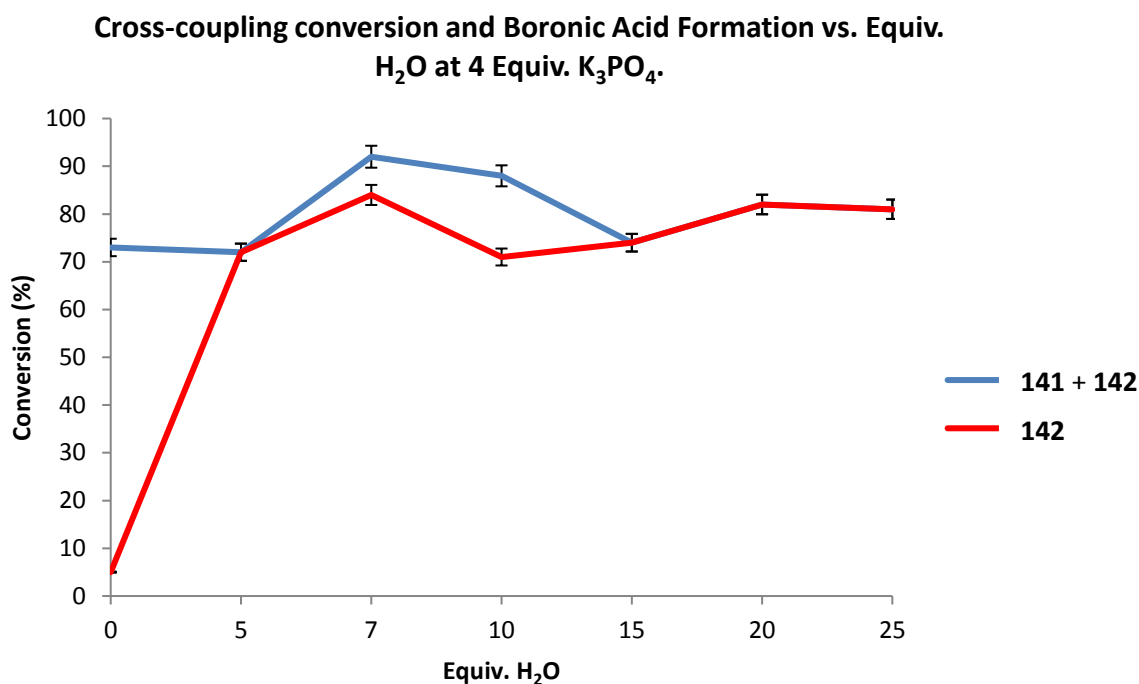
**Figure 12**. Cross-coupling conversion and boronic acid formation vs. equiv. H_2O at 4 equiv. K_3PO_4.

As can be seen form Figure 12, at 4 equiv. of K_3PO_4 both cross-coupling conversion and conversion to boronic acid product were both generally higher, but followed similar trends to the data at 3 equiv. water. The reasoning behind the observed trends remains the same as with 3 equiv. base, in that, with less water, less cross-coupling was observed and also less hydrolysis was observed and, with more water, more oligomerisation was observed due to the increased rate of hydrolysis of the BMIDA starting material and intermediate. Based on these results, 7 equiv. of water and 4 equiv. of base were taken as optimal and further optimisation proceeded at this base/water ratio.

3.2.2. Temperature Study

After the base and water studies, optimisation continued in the form of a temperature study, starting from room temperature and reaching 90 °C (Table 3).
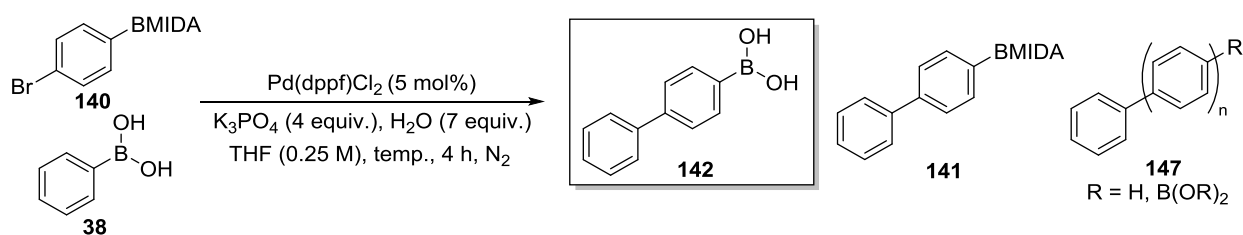
Temperature (°C)	% 142[a]	% 141[a]	% 141+142 [a]	% Ph$_2$[a]	*Reaction no.*
RT	1	28	29[b]	0	*16*
70	45	18	63[b]	7	*17*
80	63	1	64[b]	11	*18*
90	84	8	92	10	*19*

[a]Conversion determined by HPLC analysis using an internal standard. [b] Remaining mass balance as unreacted starting material. 1.1 equiv. phenylboronic acid used.

Table 3. Reaction temperature study.

The results shown in Table 3 confirmed that a reaction temperature of 90 °C was necessary for complete conversion of the cross-coupling in the reaction timeframe and a temperature of 80 °C and above was necessary for acceptable hydrolysis of the BMIDA intermediate to the boronic acid product. Lower reaction temperatures slowed down BMIDA hydrolysis. This data is represented graphically in Figure 13.
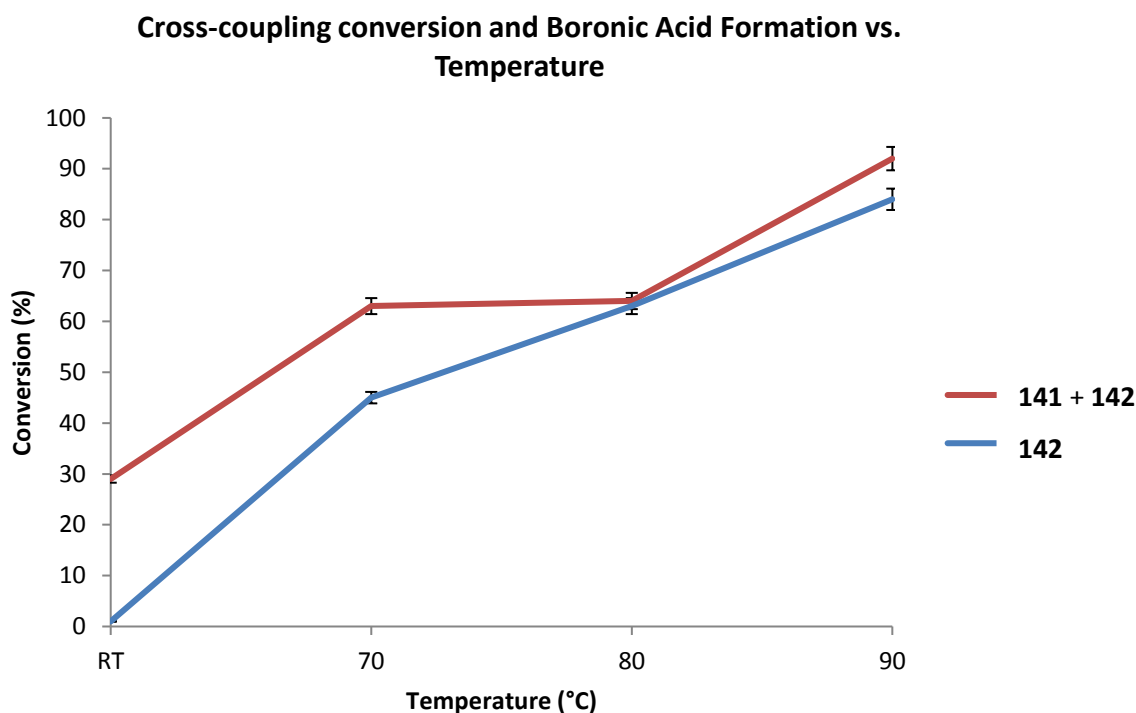
Figure 13. Cross-coupling conversion and boronic acid formation vs. temperature.

As can be seen from Figure 13, as the temperature increased, both cross-coupling conversion and BMIDA intermediate hydrolysis increased, with 90 °C being optimal. Based on these results, 90 °C was taken as the optimum reaction temperature.

3.2.3. Catalyst Screen

In an attempt to increase overall conversion in the homologation reaction, a catalyst screen was carried out. A range of Pd catalysts with varying oxidation states including Pd^{II} catalysts such as $PdCl_2$, $Pd(OAc)_2$, $Pd(OAc)_2$/SPhos, $Pd(dppf)Cl_2$, $Pd(PPh_3)_2Cl_2$, and Pd^0 catalysts such as $Pd(PPh_3)_4$ and $Pd(dba)_3$ were used (Table 4).
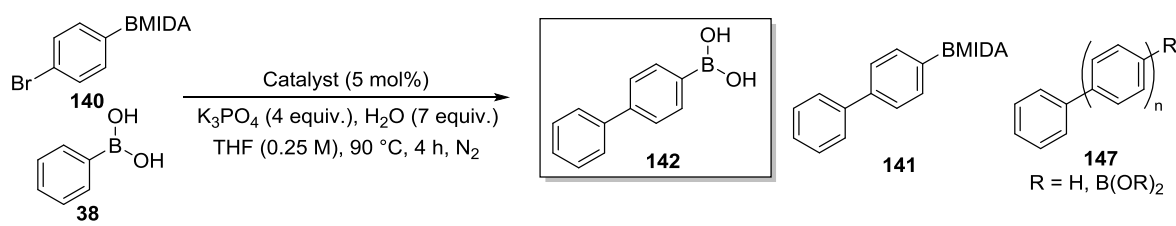
Catalyst	% 142[a]	% 141[a]	% 141+142[a]	% Ph$_2$[a]	*Reaction no.*
Pd$_2$(dba)$_3$	9	0	9[b]	11	*20*
Pd(PPh$_3$)$_4$	47	0	47[b]	13	*21*
PdCl$_2$	7	0	7[b]	10	*22*
Pd(PPh$_3$)$_2$Cl$_2$	77	0	77[b]	15	*23*
Pd(dppf)Cl$_2$	84	8	92	10	*24*
Pd(OAc)$_2$	37	0	37[b]	7	*25*
Pd(OAc)$_2$/SPhos[c]	32	2	34[b]	51	*26*

[a] Conversion determined by HPLC analysis using an internal standard. [b] Remaining mass balance as unreacted starting material. [c] 10 mol% SPhos was used. 1.1 equiv. phenylboronic acid used.

Table 4. Catalyst screen in the formal homologation reaction.

The results shown in Table 4 revealed that Pd(dppf)Cl$_2$ was the most efficient catalyst for the homologation reaction, leading to 92% cross-coupling conversion. Pd$_2$(dba)$_3$ and PdCl$_2$ each led to <10% cross-coupling conversion and both Pd(PPh$_3$)$_4$ and Pd(OAc)$_2$ led to <40% cross-coupling conversion. Pd(PPh$_3$)$_2$Cl$_2$, Pd(OAc)$_2$/SPhos and Pd(dppf)Cl$_2$ each led to >75% cross-coupling conversion with the Pd(OAc)$_2$/SPhos system generating 51% Ph$_2$. The increased quantity of Ph$_2$ being generated with the highly active Pd(OAc)$_2$/SPhos system[171] can be attributed to significant protodeboronation of the boronic acid product and/or significant oxidative homocoupling of the boronic acid starting material, since the Pd$^{(II)}$ being continually generated with the phosphine ligand is reduced to Pd$^{(0)}$ by transmetallation with boronic acid, and reductive elimination affords Ph$_2$. Based on these results, Pd(dppf)Cl$_2$ remained the catalyst of choice for the homologation reaction.

3.2.4. Concentration Study

In order to increase overall conversion, a concentration study was undertaken in which the reaction was diluted in increments (Table 5).
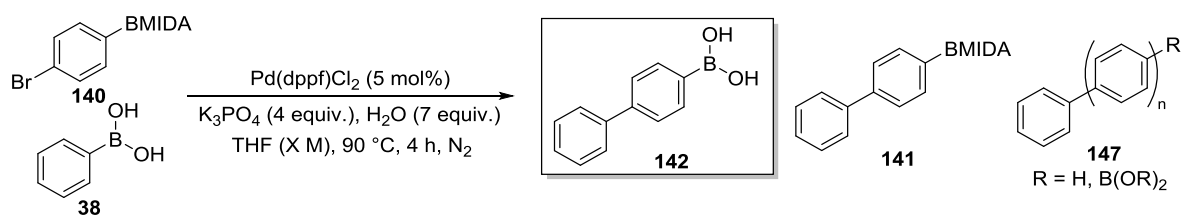
Concentration (M)	% 142[a]	% 141[a]	% 141+142 [a]	% Ph$_2$[a]	*Reaction no.*
0.1	90	6	96	6	*27*
0.15	88	2	90	7	*28*
0.185	86	0	86	8	*29*
0.25	84	8	92	6	*30*

[a]Conversion determined by HPLC analysis using an internal standard.

Table 5. Concentration screen in the formal homologation reaction.

Figure 14. Cross-coupling conversion and boronic acid formation vs. concentration.

The results shown in Table 5 indicated that the optimum concentration for the homologation reaction was 0.1 M.

3.4. Reaction Scope

With optimised conditions in hand, the next stage of the project was to investigate the scope of the homologation reaction. A range of boronic acid starting materials were tolerated, as were different bromoaryl MIDA boronates. The generated substrates are shown in Figure 15.
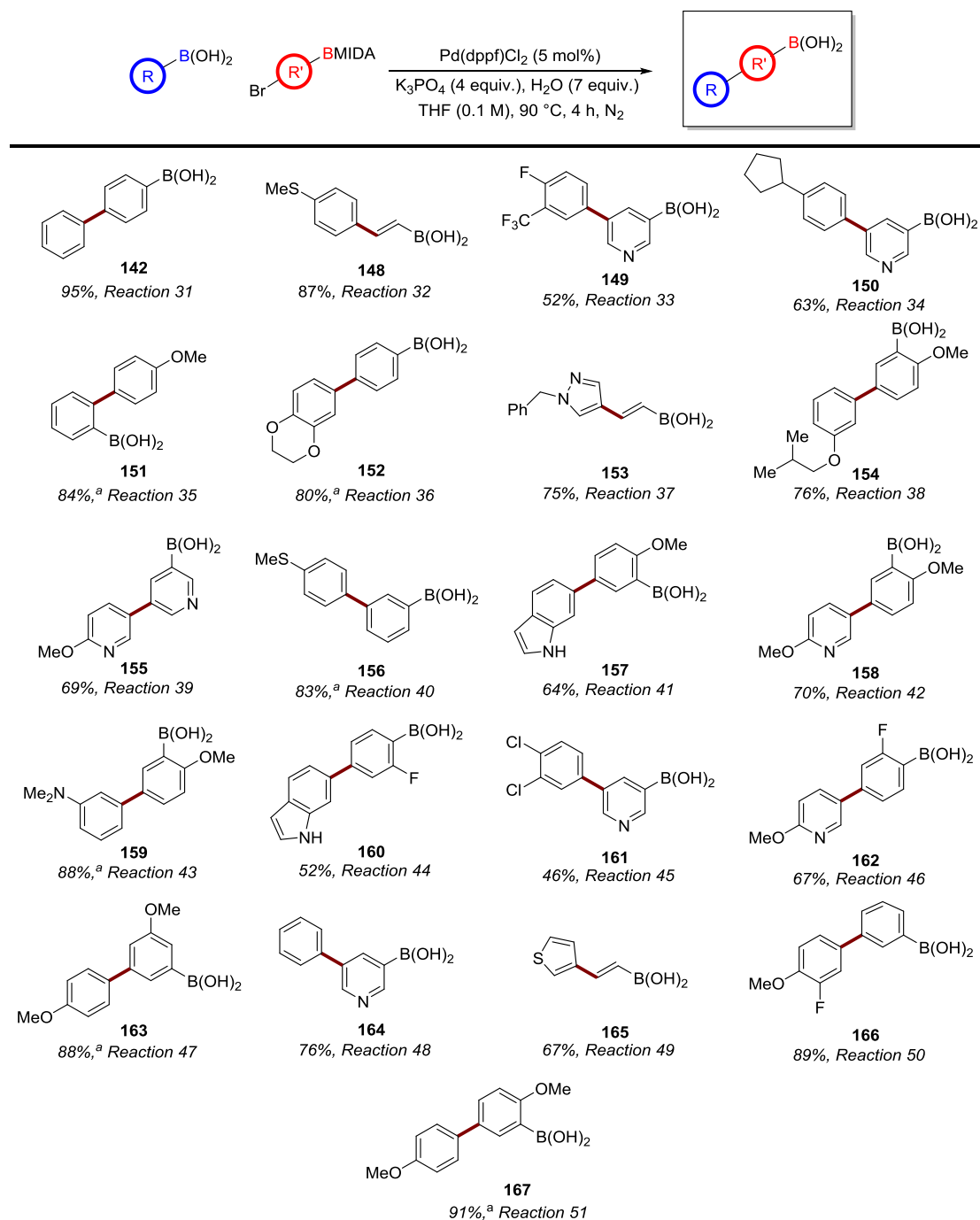
Figure 15. Formal homologation reaction substrate scope. Yields are isolated yields of pure compounds.[a] Compound isolated as the BF₃K derivative.

As shown in Figure 15, the homologation reaction tolerated a functionally diverse range of boronic acids and BMIDAs with functionality such as ethers (**151**, **152**, **154**, **155**, **157**, **158**, **159**, **162**, **163**, **166**, **167**), thioethers (**148**, **156**), fluoroarenes (**149**, **160**, **162**, **166**), trifluoromethyl groups (**149**), amines (**159**), indoles (**157**), pyridines (**149**, **150**, **155**, **158**, **161**, **162**, **164**), thiophenes (**165**), and pyrazoles (**153**). The developed reaction conditions also allowed for the chemoselective cross-coupling of aryl bromides over aryl chlorides (**x**). Not only was the homologation reaction applicable to bromoaryl BMIDAs but bromovinyl BMIDAs (**148**, **153**, **165**) also performed well in the homologation reaction, generating functionalised vinyl boronic acid derivatives in good yields. It is appropriate to note that both vinyl and heteroaryl boronic acids, which can be typically prone to protodeboronation,[112, 113] were generated efficiently in the developed process.

3.5. The Homologation Reaction as a Platform for Diversity-oriented Synthesis

Diversity-oriented synthesis (DOS) has emerged as a powerful method for the generation of privileged small molecule libraries which bear significant potential to explore novel chemical and biological space.[172,173] By investigating new areas of chemical space, new areas of biological space can in turn be discovered and targeted by utilising derivatives of privileged small molecule motifs (Scheme 33).[174] The development of DOS libraries can thus be of significant value for the exploration of druggable targets.
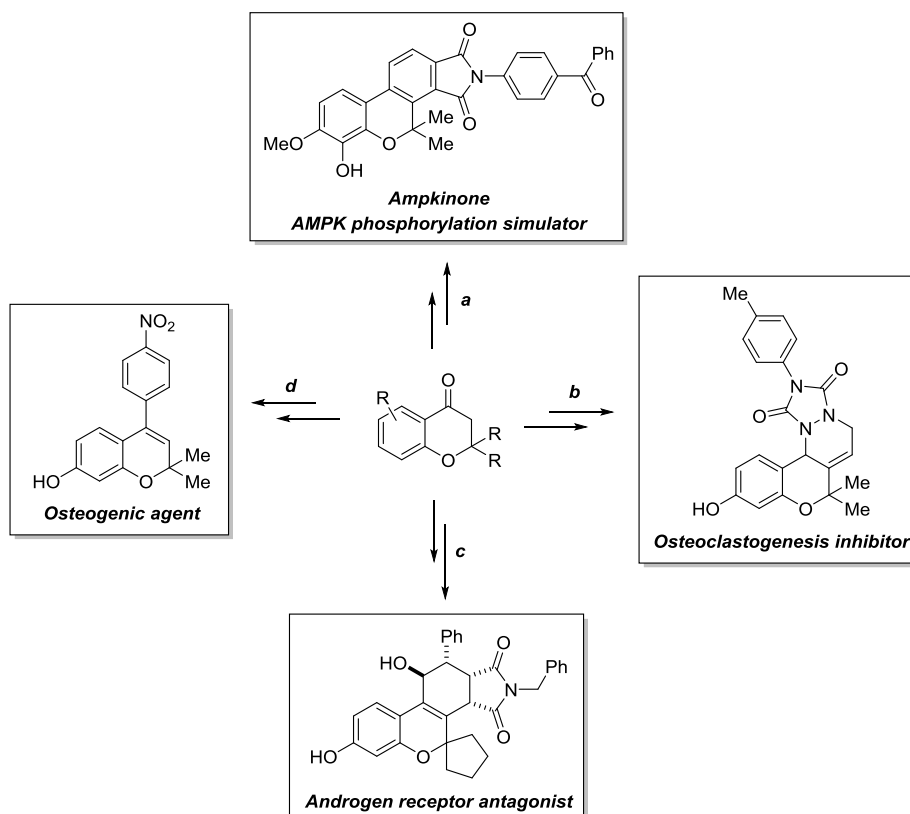
Scheme 33. Park's substructure-based design strategy for the discovery of specific small-molecule modulators.

Scheme 33 shows Park's work in utilizing a privileged chromone substructure as a starting material for the synthesis of a number of bioactive molecules *via* syntheses **a**,[175] **b**,[176] **c**,[177] and **d**.[178] This work is a representative example of DOS and shows the strong potential for using privileged motifs as small molecule modulator precursors.

In order to demonstrate the ability of the developed formal boronic acid homologation to provide rapid access to new chemical space, derivatives of a favored pharmacophore which is currently used within epigenetic drug discovery were to be prepared using the methodology. Bromodomain and extra terminal domain (BET) inhibitors are targets of particular interest within drug discovery programmes[179] and there are a number of compounds that have been developed which act as inhibitors of BET, a selection of which are shown in Figure 16.[180]
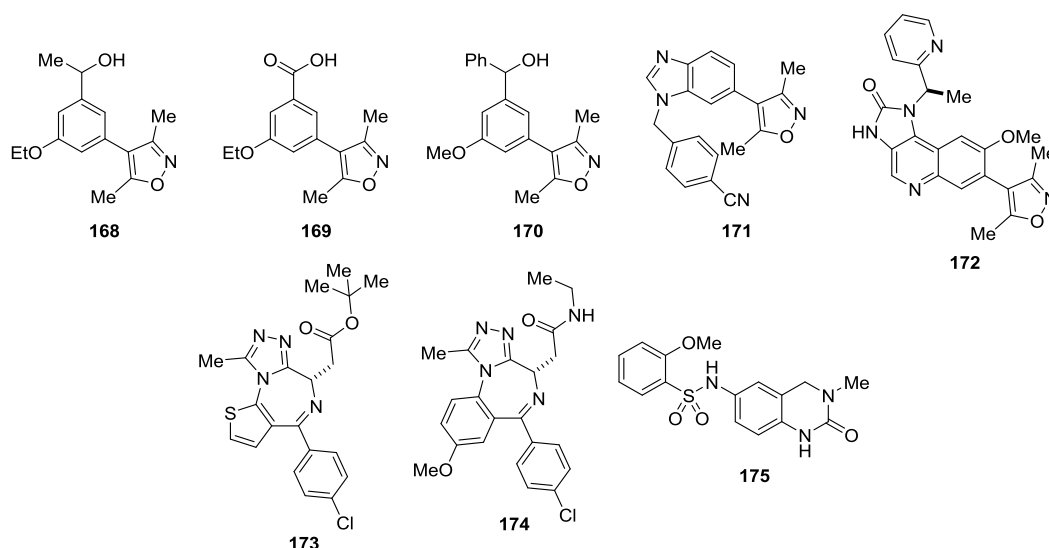
Figure 16. Known BET protein inhibitors.

As can be seen from Figure 16, a number of the compounds which are known potent BET protein binders are derivatives of 3,5-dimethylisoxazole motifs (**168**, **169**, **170**, **171, 172**). For example, compound **170** is an inhibitor of BRD4 and CREBBP BET proteins[180] which recognise and interact with acetylated lysine (AcK) residues on DNA histones, acting as selective readers of lysine acetylation.[181, 182] These BET protein-AcK interactions are known to have an adverse effect on transcriptional regulation and chromatin assembly which, in turn, can lead to a number of diseases.[183,184,185,186] The key feature of compound **170** is the dimethylisoxazole motif, which acts as an AcK mimic, inhibiting BET proteins from interacting with the AcK on the DNA histone, and the core trisubstituted arene and pendant phenylmethanol provides isoform selectivity and potency modulation vectors.[180]

Selecting compound **170** (Figure 16) as a suitable pharmacophore for the DOS-based application of the methodology, installation of dimethylisoxazole motif **177** onto the 1,3,5-trisubstituted aryl core, **176**, using the developed boronic acid homologation protocol provided the key intermediate **178** in 83% yield (Scheme 34).
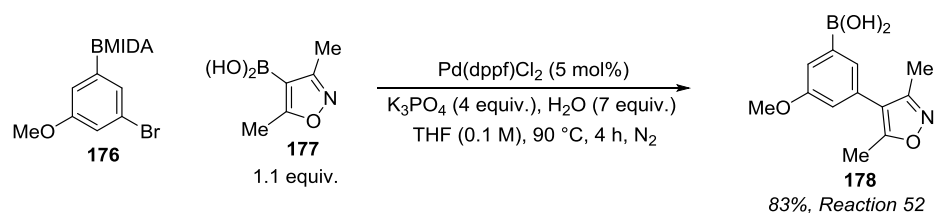
Scheme 34. Synthesis of intermediate **178** using the boronic acid homologation protocol.

From the key reactive boronic acid intermediate **178**, a range of derivatives of the BET inhibiting compounds shown in Figure 16 were expediently accessed, displaying the versatility of the boronic acid homologation towards privileged substructure-based DOS (Scheme 35).
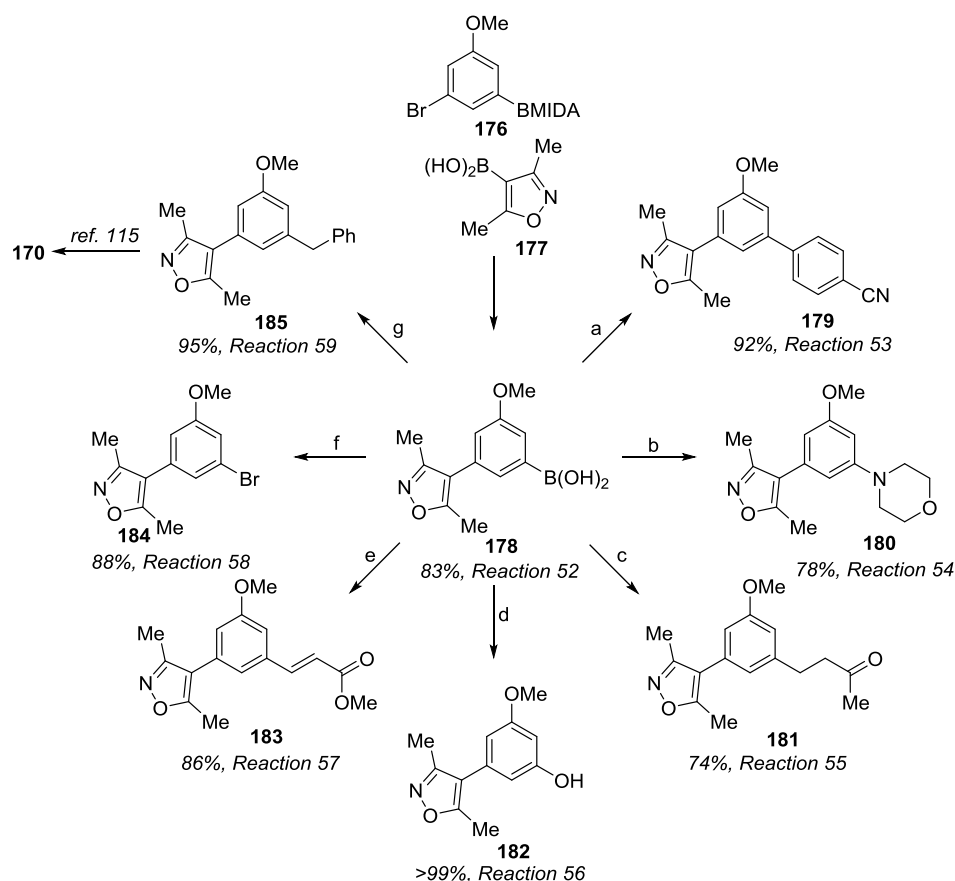
Scheme 35. DOS-based formal homologation and subsequent functionalisation of boronic acids. Reaction conditions: a) **178** (1.1 equiv.), 4-bromobenzonitrile (1 equiv.), PdCl₂dppf (5 mol%), K₃PO₄ (3 equiv.), H₂O (5 equiv.), THF, 70 °C, 1 h; b) **178** (1.5 equiv.), morpholine (1 equiv.), Cu(OAc)₂ (10 mol%), MS 4Å, O₂, CH₂Cl₂, 40 °C, 24 h; c) **178** (1 equiv.), methyl vinyl

ketone (2 equiv.), [Rh(COD)Cl]$_2$ (2 mol%), Na$_2$CO$_3$ (2 equiv.), H$_2$O, 80 °C, 16 h; d) **178** (1 equiv.), H$_2$O$_2$ (10 equiv.), THF, rt, 2 h; e) **178** (1 equiv.), methyl acrylate (1.5 equiv.), 1,4-benzoquinone (1 equiv.), Pd(OAc)$_2$ (2 mol%), phenanthroline (2.5 mol%), MeCN, 60 °C, 16 h; f) **178** (1 equiv.), N-bromosuccinimide (1.5 equiv.), THF, rt, 16 h; g) **178** (1 equiv.), benzyl bromide (1.5 equiv.), PdCl$_2$dppf (5 mol%), K$_3$PO$_4$ (4 equiv.), H$_2$O (20 equiv.), THF, 90 °C, 5 h.

Scheme 35 summarises the application of the developed methodology towards DOS-based privileged substructure generation and subsequent derivatisation. A number of derivatives of the biologically active BET protein binding compounds shown in Figure 16 were prepared in two synthetic steps (an improvement on the current 5-6 step routes towards these compounds)[180] *via* the reactive boronic acid intermediate, **178**. The versatility of the boronic acid motif made possible transformations such as Suzuki cross-couplings (a, g) to access compounds **179** and **185** in high yields. **178** could then be converted to **170** - another known BET binding compound - using conditions previously reported within the group.[187] Chan-Evans-Lam coupling (b) of **178** with morpholine enabled access to amine derivative **180** in high yield also. Using Hayashi chemistry (c), **178** was converted to the corresponding ketone derivative, **181**. Oxidation (d) of **178** to the phenol proceeded quantitatively and oxidative Heck chemistry (e) afforded the unsaturated ester derivative in high yield. Halogenation (f) of **178** provided the corresponding bromide product.

4. Conclusions

In conclusion, the chemoselective formal homologation of boronic acids was successfully validated and the process was optimised to achieve high yields of homologated boronic acid (Scheme 36).
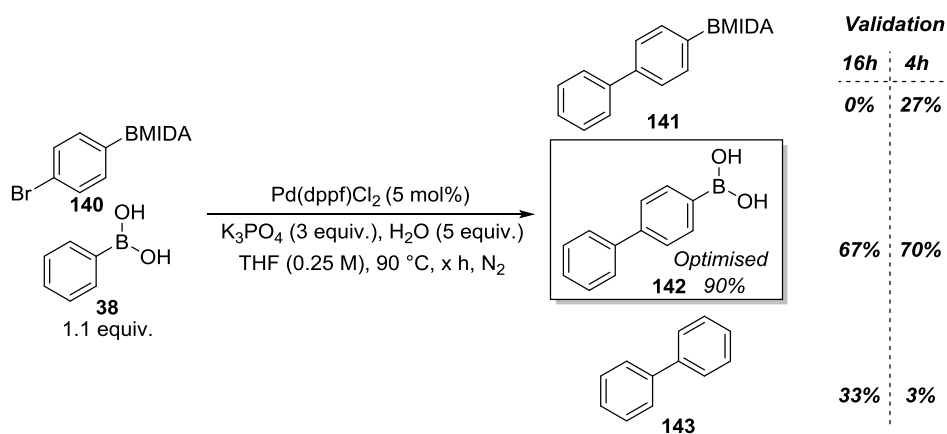
Scheme 36. Initial validation results of the homologation reaction and final optimised reaction conversion.

The methodology was then successfully applied to gain access to a wide range of 22 substrates, generating an attractive range of novel aryl, vinyl and heterocyclic boronic acids in moderate to excellent yields (Scheme 37).
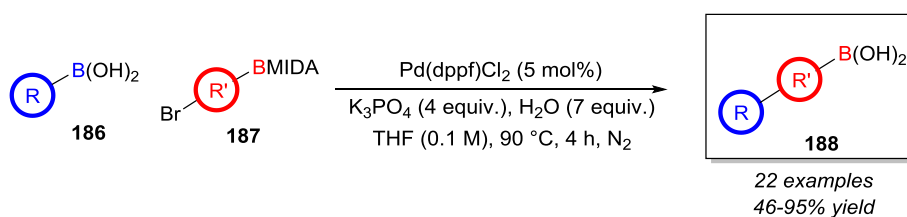
Scheme 37. Homologation reaction scope.

To demonstrate the utility of the methodology within diversity-oriented synthesis, the methodology was successfully applied to the expedient synthesis of a range of pharmaceutically relevant BET binding inhibitor compounds (Figure 17).
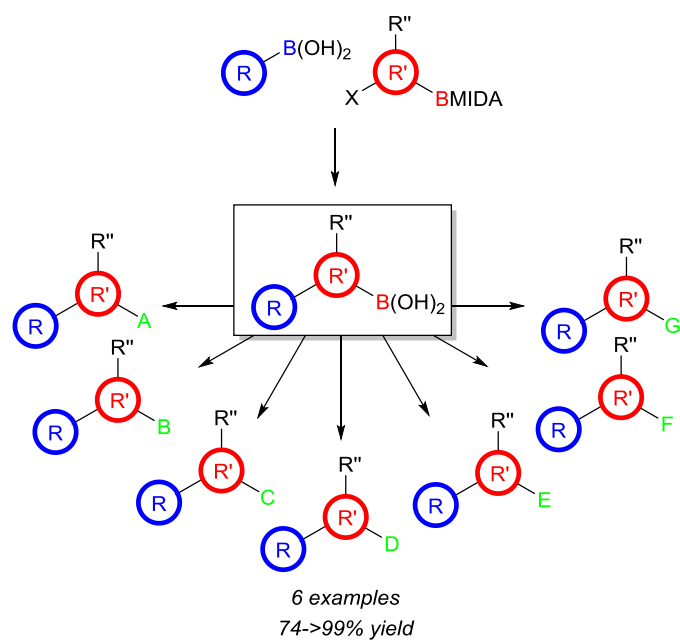
Figure 17. Application of the developed methodology in a diversity-oriented synthesis fashion.

5. Future work

The methodology which has been developed could be advanced in the following ways:

i) Work could be done to elucidate the mechanism of BMIDA hydrolysis. Isotopic labelling could be employed by using O^{18}-labelled water in the reaction and analysing the isotopic composition of the reaction products. Detecting O^{18}-labelled MIDA acid by-product would be a significant development in elucidating the mechanism, as the isotopic composition of this could correspond to a BAc^2 hydrolysis mechanism rather than the standard association/dissociation mechanism associated with Bpin hydrolysis.

ii) The development of one-pot protocols in which the generated boronic acid is further reacted *in situ* to generate more complex molecules in one synthetic step would be a valuable extension of the methodology (Scheme 38).
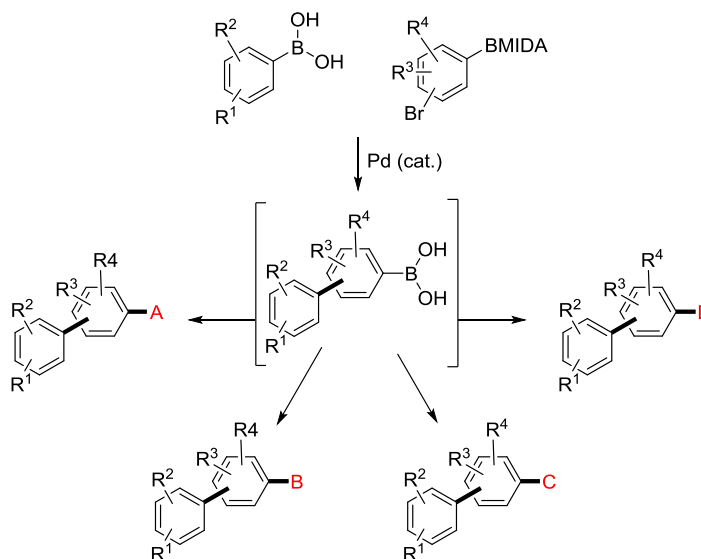
Scheme 38. One-pot boronic acid homologation/functionalisation protocol.

iii) Further optimising the homologation process to generate a system in which the reaction can be carried out in a vessel which does not have to be pressure-sealed or carried out at high temperature would also be beneficial to the methodology, as the scale could be increased and the reaction carried out more mildly. Thorough solvent and temperature screening could be a means of achieving these objectives.

6. Experimental

6.1. Reagents

All reagents and solvents were obtained from commercial suppliers and were used without further purification unless otherwise stated. Purification was carried out according to standard laboratory methods.[50]

6.2. Purification of Solvents

i) Tetrahydrofuran used for dry reactions was obtained from a PureSolv SPS-400-5 solvent purification system. These solvents were transferred to and stored in a septum-sealed oven-dried flask over previously activated 4 Å molecular sieves and purged with and stored under nitrogen.

ii) Acetonitrile, dichloromethane, diethyl ether, dimethylformamide, ethyl acetate, and petroleum ether 40-60 °C for reaction solvent or purification purposes were used as obtained from suppliers without further purification.

6.3. Experimental Details

i) Moisture-sensitive reactions were carried out using microwave vial glassware. The glassware was oven-dried and purged with N_2 before use.

ii) Purging refers to a vacuum/nitrogen-refilling procedure.

iii) Reactions were carried out at 0 °C using ice/water baths.

iv) Room temperature was generally *ca.* 18 °C.

v) Reactions carried out at elevated temperatures were done so using a temperature-regulated hotplate/stirrer.

6.4. Purification of Products

i) Thin layer chromatography was carried out using Merck silica plates coated with fluorescent indicator UV254. These were analysed under 254 nm UV light or developed using potassium permanganate solution.

ii) Normal phase flash chromatography was carried out using ZEOprep 60 HYD 40-63 µm silica gel. Reverse phase flash chromatography was carried out using Isolute SPE C18(EC) or ZEOprep 60 HYD 40-63 µm silica gel.

6.5. Analysis of Products

i) Fourier Transformed Infra-Red (FTIR) spectra were obtained on a Shimadzu IRAffinity-1 machine.

ii) ^{19}F NMR spectra were obtained on a Bruker AV 400 spectrometer at 376 MHz.

iii) ^{11}B NMR spectra were obtained on a Bruker AV 400 spectrometer at 128 MHz.

iv) ^{1}H and ^{13}C NMR spectra were obtained on either a Bruker AV 400 at 400 MHz and 125 MHz, respectively, or Bruker DRX 500 at 500 MHz and 126 MHz, respectively. Chemical shifts are reported in ppm and coupling constants are reported in Hz with $CDCl_3$ referenced at 7.27 ppm (^{1}H) and 77.36 ppm (^{13}C) and DMSO-d_6 referenced at 2.50 ppm (^{1}H) and 39.52 ppm (^{13}C).

v) High-resolution mass spectra were obtained through analysis at the EPSRC UK National Mass Spectrometry Facility at Swansea University or at the Strathclyde Institute of Pharmacy and Biomedical Sciences. Products in which the high-resolution mass spectra show the 'adduct + Et Gly' were generated by the addition of ethylene glycol to the sample to be analysed. This is a technique used by the EPSRC UK National Mass Spectrometry Facility to detect ethylene glycol ester derivatives of boronic acids which can be difficult to detect as the free boronic acid.

vi) Reverse phase HPLC data was obtained on an Agilent 1200 series HPLC using a Machery-Nagel Nucleodur C18 column. For **142**, analysis was performed using a gradient method, eluting with 5 - 80% MeCN/H_2O over 16 minutes at a flow rate of 2 mL/min. t_R = 6.7 min. Samples for HPLC analysis were prepared through the addition of 2 mL of caffeine standard solution to the completed reaction mixture, the resulting solution was then stirred before the removal of a 200 µL aliquot. The aliquot was diluted to 1 mL with MeCN and was then filtered through cotton wool/Celite. A 200 µL aliquot of the filtered solution was then further diluted with 800 µL MeCN and 500 µL H_2O for HPLC analysis against established conversion factors.

7. General Experimental Procedures and Reaction Data

General Experimental Procedure A: Preparation of BMIDA compounds.

For example, for 4-biphenylboronic acid MIDA ester, **141**

A round-bottomed flask with magnetic stirrer bar was charged with 4-biphenylboronic acid (1 equiv, 0.5 mmol, 99.0 mg), N-methyliminodiacetic acid (1.05 equiv, 0.525 mmol, 77.0 mg), and DMF (0.075 M, 227 mL). The reaction was heated to 100 °C for 16 hours. Upon completion the reaction was allowed to cool to room temperature and the solvent was removed under reduced pressure to afford a white slurry. Et_2O (50 mL) was added and the resulting white precipitate was removed by filtration and washed with Et_2O (2 x 50 mL). The solid was collected to afford **141** as a white amorphous solid (153.0 mg, 99%).

Reaction no.	Qty. Boronic Acid	Qty. MIDA Acid	Product, Mass, Yield
60	99.0 mg	77.0 mg	**141**, 153.0 mg, 99%
61	3.00 g	2.10 g	**189**, 4.31 g, 97%
62	875.0 mg	618.0 mg	**190**, 994.0 mg, 75%

General Experimental Procedure B: Formal homologation of boronic acids - isolation of the boronic acid.

For example, for 4-biphenylboronic acid, **142**.

An oven-dried microwave vial containing a magnetic stirrer bar was charged with 4-bromophenylboronic acid MIDA ester (**140**, 1 equiv, 0.25 mmol, 78.0 mg), phenylboronic acid (1.1 equiv, 0.275 mmol, 33.5 mg), $Pd(dppf)Cl_2 \cdot CH_2Cl_2$ (5 mol%, 0.0125 mmol, 10.2 mg), and anhydrous K_3PO_4 (4 equiv, 1 mmol, 212.3 mg). The vial was sealed and purged with N_2 before the addition of THF (0.1 M, 2.5 mL) and H_2O (7 equiv, 1.75 mmol, 31.5 μL). The reaction was heated to 90 °C for 4 hours then was allowed to cool to room temperature. The reaction mixture was loaded directly onto a reverse phase flash chromatography column with a short pad of celite on top and eluted with 25-40% MeCN (+0.1% TFA) in H_2O (+0.1% TFA). Fractions containing product were collected and evaporated to afford **142** as a white amorphous solid (47.0 mg, 95%).

Reaction no.	Qty. Br-R-BMIDA	Qty. Pd Cat.	Qty. Boronic Acid	Qty. K_3PO_4	Qty. H_2O	Product, Mass, Conversion[a]/Yield[b]
1	78.0 mg	10.2 mg	33.5 mg	159.2 mg	23 μL	**142**, 67%[a]
2	78.0 mg	10.2 mg	33.5 mg	159.2 mg	23 μL	**142**, 70%[a]
3	78.0 mg	10.2 mg	33.5 mg	159.2 mg	0 μL	**142**, 25%[a]
4	78.0 mg	10.2 mg	33.5 mg	159.2 mg	23 μL	**142**, 70%[a]
5	78.0 mg	10.2 mg	33.5 mg	159.2 mg	45 μL	**142**, 40%[a]
6	78.0 mg	10.2 mg	33.5 mg	159.2 mg	68 μL	**142**, 78%[a]
7	78.0 mg	10.2 mg	33.5 mg	159.2 mg	91 μL	**142**, 60%[a]
8	78.0 mg	10.2 mg	33.5 mg	159.2 mg	113 μL	**142**, 62%[a]
9	78.0 mg	10.2 mg	33.5 mg	212.3 mg	0 μL	**142**, 5%[a]
10	78.0 mg	10.2 mg	33.5 mg	212.3 mg	23 μL	**142**, 72%[a]
11	78.0 mg	10.2 mg	33.5 mg	212.3 mg	32 μL	**142**, 84%[a]
12	78.0 mg	10.2 mg	33.5 mg	212.3 mg	45 μL	**142**, 71%[a]
13	78.0 mg	10.2 mg	33.5 mg	212.3 mg	68 μL	**142**, 74%[a]
14	78.0 mg	10.2 mg	33.5 mg	212.3 mg	91 μL	**142**, 82%[a]
15	78.0 mg	10.2 mg	33.5 mg	212.3 mg	113 μL	**142**, 81%[a]
16	78.0 mg	10.2 mg	33.5 mg	212.3 mg	32 μL	**142**, 1%[a]
17	78.0 mg	10.2 mg	33.5 mg	212.3 mg	32 μL	**142**, 45%[a]
18	78.0 mg	10.2 mg	33.5 mg	212.3 mg	32 μL	**142**, 63%[a]
19	78.0 mg	10.2 mg	33.5 mg	212.3 mg	32 μL	**142**, 84%[a]
20	78.0 mg	10.2 mg	33.5 mg	212.3 mg	32 μL	**142**, 9%[a]
21	78.0 mg	10.2 mg	33.5 mg	212.3 mg	32 μL	**142**, 47%[a]
22	78.0 mg	10.2 mg	33.5 mg	212.3 mg	32 μL	**142**, 7%[a]
23	78.0 mg	10.2 mg	33.5 mg	212.3 mg	32 μL	**142**, 77%[a]
24	78.0 mg	10.2 mg	33.5 mg	212.3 mg	32 μL	**142**, 84%[a]
25	78.0 mg	10.2 mg	33.5 mg	212.3 mg	32 μL	**142**, 37%[a]
26	78.0 mg	10.2 mg	33.5 mg	212.3 mg	32 μL	**142**, 32%[a]
27	78.0 mg	10.2 mg	33.5 mg	212.3 mg	32 μL	**142**, 90%[a]
28	78.0 mg	10.2 mg	33.5 mg	212.3 mg	32 μL	**142**, 88%[a]
29	78.0 mg	10.2 mg	33.5 mg	212.3 mg	32 μL	**142**, 86%[a]
30	78.0 mg	10.2 mg	33.5 mg	212.3 mg	32 μL	**142**, 84%[a]

31	78.0 mg	10.2 mg	33.5 mg	212.3 mg	32 µL	**142**, 47.0 mg, 95%[b]
32	65.5 mg	10.2 mg	46.2 mg	212.3 mg	32 µL	**148**, 42.2 mg, 87%[b]
33	78.2 mg	10.2 mg	57.2 mg	212.3 mg	32 µL	**149**, 37.1 mg, 52%[b]
34	78.2 mg	10.2 mg	52.3 mg	212.3 mg	32 µL	**150**, 42.0 mg, 63%[b]
37	65.5 mg	10.2 mg	55.6 mg	212.3 mg	32 µL	**153**, 42.8 mg, 75%[b]
38	85.5 mg	10.2 mg	53.4 mg	212.3 mg	32 µL	**154**, 57.0 mg, 76%[b]
39	78.2 mg	10.2 mg	42.0 mg	212.3 mg	32 µL	**155**, 39.7 mg, 69%[b]
41	85.5 mg	10.2 mg	44.3 mg	212.3 mg	32 µL	**157**, 42.7 mg, 64%[b]
42	85.5 mg	10.2 mg	42.0 mg	212.3 mg	32 µL	**158**, 45.3 mg, 70%[b]
44	82.5 mg	10.2 mg	44.3 mg	212.3 mg	32 µL	**160**, 33.2 mg, 52%[b]
45	78.2 mg	10.2 mg	52.5 mg	212.3 mg	32 µL	**161**, 30.8 mg, 46%[b]
46	82.5 mg	10.2 mg	42.0 mg	212.3 mg	32 µL	**162**, 41.4 mg, 67%[b]
48	78.2 mg	10.2 mg	33.5 mg	212.3 mg	32 µL	**164**, 37.8 mg, 76%[b]
49	65.5 mg	10.2 mg	35.2 mg	212.3 mg	32 µL	**165**, 25.8 mg, 67%[b]
50	78.0 mg	10.2 mg	46.8 mg	212.3 mg	32 µL	**166**, 54.7 mg, 89%[b]
52	85.5 mg	10.2 mg	38.7 mg	212.3 mg	32 µL	**178**, 51.3 mg, 83%[b]

General Experimental Procedure C: Formal homologation of boronic acids - isolation as the potassium trifluoroborate.

For example, for (4-(2,3-dihydrobenzo[b][1,4]dioxin-6-yl)phenyl)boronic acid, potassium trifluoroborate derivative, **152**.

An oven-dried microwave vial containing a magnetic stirrer bar was charged with 4-bromophenylboronic acid MIDA ester (**140**, 1 equiv, 0.25 mmol, 78.0 mg), (2,3-dihydrobenzo[b][1,4]dioxin-6-yl)boronic acid (1.1 equiv, 0.275 mmol, 49.5 mg), Pd(dppf)Cl$_2$·CH$_2$Cl$_2$ (5 mol%, 0.0125 mmol, 10.2 mg), and anhydrous K$_3$PO$_4$ (4 equiv, 1 mmol, 212.3 mg). The vial was sealed and purged with N$_2$ before addition of THF (0.1 M, 2.5 mL) and H$_2$O (7 equiv, 1.75 mmol, 31.5 µL). The reaction was heated to 90 °C for 4 hours then was allowed to cool to room temperature. The reaction mixture was treated with KHF$_2$ (6 equiv, 1.5 mmol, 117.2 mg) and heated to 90 °C for a further 2 hours. The reaction mixture was allowed to cool to room temperature before addition of Et$_2$O (3 mL). The resulting precipitate

was filtered and washed with Et$_2$O (3 x 5 mL). The solid was collected to afford **152** as a white amorphous solid (63.6 mg, 80%).

Reaction no.	Qty. BMIDA	Qty. Pd Cat.	Qty. Boronic Acid	Qty. K$_3$PO$_4$	Qty. H$_2$O	Qty. KHF$_2$	Product, Mass, Yield
35	78.0 mg	10.2 mg	41.8 mg	212.3 mg	32 µL	117.2 mg	**151**, 60.9 mg, 84%
36	78.0 mg	10.2 mg	49.5 mg	212.3 mg	32 µL	117.2 mg	**152**, 63.6 mg, 80%
40	78.0 mg	10.2 mg	46.2 mg	212.3 mg	32 µL	117.2 mg	**156**, 63.5 mg, 83%
43	85.5 mg	10.2 mg	45.4 mg	212.3 mg	32 µL	117.2 mg	**159**, 73.3 mg, 88%
47	85.5 mg	10.2 mg	41.8 mg	212.3 mg	32 µL	117.2 mg	**163**, 70.4 mg, 88%
51	85.5 mg	10.2 mg	41.8 mg	212.3 mg	32 µL	117.2 mg	**167**, 72.8 mg, 91%

8. Compound Characterisation Data

2-([1,1'-Biphenyl]-4-yl)-6-methyl-1,3,6,2-dioxazaborocane-4,8-dione, **141**.
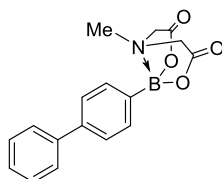
Prepared according to General Experimental Procedure A using 4-biphenylboronic acid (1 equiv, 0.5 mmol, 99.0 mg) and *N*-methyliminodiacetic acid (1.05 equiv, 0.525 mmol, 77.0 mg) to afford **141** as a white amorphous solid (153.0 mg, 99%).

υ_{max} (solid): 3006, 2958, 1742, 1461, 1448, 1210, 985 cm^{-1}.

^{1}H NMR (400 MHz, DMSO-d$_6$): δ 7.70-7.65 (m, 4H), 7.53 (d, 2H, *J* = 8.1 Hz), 7.47 (t, 2H, *J* = 7.9 Hz), 7.39-7.35 (m, 1H), 4.36 (d, 2H, *J* = 17.6 Hz), 4.14 (d, 2H, *J* = 17.8 Hz), 2.55 (s, 3H).

^{13}C NMR (400 MHz, DMSO-d$_6$): δ 169.4, 140.5, 140.1, 133.1, 128.9, 127.5, 126.6, 125.9, 61.8, 47.6. 1 carbon signal not observed/coincident.

^{11}B NMR (400 MHz, DMSO-d$_6$): δ 12.3.

HRMS: exact mass calculated for [M + NH$_4$]$^+$ (C$_{17}$H$_{20}$BN$_2$O$_4$) requires *m/z* 327.1511, found [M + NH$_4$]$^+$ *m/z* 327.1514.

[1,1'-Biphenyl]-4-ylboronic acid, **142**.
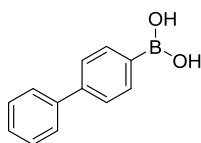
Prepared according to General Experimental Procedure B using phenylboronic acid (1.1 equiv, 0.275 mmol, 33.5 mg) and 4-bromophenylboronic acid MIDA ester (1 equiv, 0.25 mmol, 78.0 mg) to afford **142** as a white amorphous solid (47.0 mg, 95%).

υ_{max} (solid): 3330, 3054, 3032, 1606, 1552, 1331 cm^{-1}.

^{1}H NMR (400 MHz, DMSO-d$_6$): δ 8.07-8.00 (m, 2H), 7.88 (d, 2H, J = 8.0 Hz), 7.69 (d, 2H, J = 7.8 Hz), 7.64 (d, 2H, J = 8.1 Hz), 7.47 (t, 2H, J = 7.9 Hz), 7.37 (t, 1H, J = 7.9 Hz).

^{13}C NMR (400 MHz, DMSO-d$_6$): δ 141.6, 140.1, 134.8, 128.9, 127.5, 126.7, 125.6. 1 carbon signal not observed/coincident.

^{11}B NMR (400 MHz, DMSO-d$_6$): δ 28.4.

HRMS: exact mass calculated for [M + H]$^+$ (C$_{12}$H$_{12}$BO$_2$) requires m/z 199.0847, found [M + H]$^+$ m/z 199.0844.

HPLC assay: t$_R$ = 6.7 min.

(*E*)-(4-(Methylthio)styryl)boronic acid, **148**.
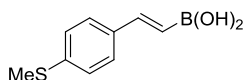
Prepared according to General Experimental Procedure B using (4-(methylthio)phenyl)boronic acid (1.1 equiv, 0.275 mmol, 46.2 mg) and (E)-(2-bromovinyl)boronic acid MIDA ester (1 equiv, 0.25 mmol, 65.5 mg) to afford **148** as a white amorphous solid (42.2 mg, 87%).

υ_{max} (solid): 3341, 2954, 2919, 2854, 1621, 1593, 1348, 987, 805 cm^{-1}.

^{1}H NMR (400 MHz, DMSO-d$_6$): δ 7.73 (s, 2H), 7.41 (m, 2H), 7.24 (m, 2H), 7.20 (d, 1H, J = 18.3 Hz), 6.06 (d, 1H, J = 18.3 Hz), 3.28 (s, 3H).

^{13}C NMR (400 MHz, DMSO-d$_6$): δ 145.2, 138.6, 134.3, 127.1, 125.9, 14.5. 1 carbon signal not observed/coincident.

^{11}B NMR (400 MHz, DMSO-d$_6$): δ 31.1.

HRMS: exact mass calculated for [M +Et Gly + H]$^+$ (C$_{11}$H$_{14}$BO$_2$S) requires m/z 221.0802, found [M + Et Gly + H]$^+$ m/z 221.0797.

M + Et Gly =
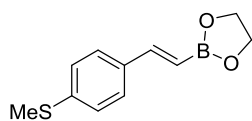
(5-(4-Fluoro-3-(trifluoromethyl)phenyl)pyridin-3-yl)boronic acid, **149**.
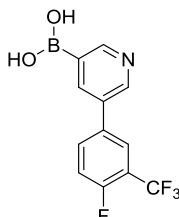
Prepared according to General Experimental Procedure B using (4-fluoro-3-(trifluoromethyl)phenyl)boronic acid (1.1 equiv, 0.275 mmol, 57.2 mg) and (5-bromopyridin-3-yl)boronic acid MIDA ester (1 equiv, 0.25 mmol, 78.2 mg) to afford **149** as a white amorphous solid (37.1 mg, 52%).

υ_{max} (solid): 1614, 1438, 1359, 1332, 1303, 1256, 1127, 1069, 732 cm^{-1}.

^{1}H NMR (500 MHz, DMSO-d$_6$): δ 8.68 (d, 1H, J = 2.0 Hz), 8.64 (d, 1H, J = 2.0 Hz), 8.33 (t, 1H, J = 2.1 Hz), 8.20-8.09 (m, 2H), 7.51-7.39 (m, 1H). 2 proton signals not observed.

^{13}C NMR (126 MHz, DMSO-d$_6$): δ 160.1 (d, $^1J_{C-F}$ = 254.5 Hz), 148.8, 147.0, 140.2 (td, J_{C-F} = 107.1 Hz, J_{C-F} = 8.2 Hz), 138.3, 132.69 (q, J_{C-F} = 3.8 Hz), 131.7, 131.7, 131.4 (d, $^4J_{C-F}$ = 3.8 Hz), 130.7 (d, J = 3.6 Hz), 126.2, 124.1, 121.3, 120.3, 116.3 (d, $^2J_{C-F}$ = 19.3 Hz), 119.8, 116.4, 116.3, 116.1 (d, $^4J_{C-F}$ = 3.7 Hz), 116.0 (d, $^3J_{C-F}$ = 6.9 Hz), 115.8 (d, $^3J_{C-F}$ = 11.3 Hz).

^{11}B NMR (128 MHz, DMSO-d$_6$): δ 26.1.

^{19}F NMR (376 MHz, DMSO-d$_6$): δ -59.9 (d, 3F, J = 11.3 Hz), -114.8 (m, 1F).

HRMS: exact mass calculated for [M+H]$^+$ (C$_{12}$H$_9$BF$_4$NO$_2$) requires m/z 286.0659, found [M+H]$^+$ m/z 286.0659.

(5-(4-Cyclopentylphenyl)pyridin-3-yl)boronic acid, **150**.
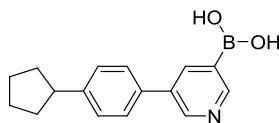
Prepared according to General Experimental Procedure B using (4-cyclopentylphenyl)boronic acid (1.1 equiv, 0.275 mmol, 52.3 mg) and (5-bromopyridin-3-yl)boronic acid MIDA ester (1 equiv, 0.25 mmol, 78.2 mg) to afford **150** as a white amorphous solid (42.0 mg, 63%).

υ_{max} (solid): 3265, 2963, 1612, 1409, 1350, 1185, 1089, 1020, 748 cm^{-1}.

^{1}H NMR (500 MHz, DMSO-d$_6$): δ 8.73 (d, 2H, *J* = 2.1 Hz), 8.46 (t, 1H, *J* = 2.2 Hz), 7.69 (d, 2H, *J* = 8.0 Hz), 7.19 (d, 2H, *J* = 7.9 Hz), 3.56 (br.s, 2H), 2.98-2.92 (m, 1H), 2.02-1.96 (m, 2H), 1.76-1.74 (m, 2H), 1.68-1.59 (m, 2H), 1.56-1.48 (m, 2H).

^{13}C NMR (126 MHz, DMSO-d$_6$): δ 149.1, 147.9, 140.9, 134.2, 126.0, 120.6, 45.3, 34.1, 25.1. 3 carbon signals not observed/coincident.

^{11}B NMR (128 MHz, DMSO-d$_6$): δ 29.9.

HRMS: exact mass calculated for [M+H]$^{+}$ (C$_{16}$H$_{19}$BNO$_2$) *m/z* requires 268.1432, found [M+H]$^{+}$ *m/z* 268.1431.

Trifluoro(4'-methoxy-[1,1'-biphenyl]-2-yl)-l4-borane, potassium salt, **151**.
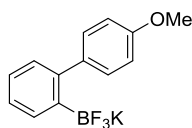
Prepared according to General Experimental Procedure C using (4-methoxyphenyl)boronic acid boronic acid (1.1 equiv, 0.275 mmol, 41.8 mg) and 2-bromophenylboronic acid MIDA ester (1 equiv, 0.25 mmol, 78.0 mg) to afford **151** as an off-white amorphous solid (60.9 mg, 84%).

υ_{max} (solid): 3006, 2835, 1608, 1515, 1435, 1247, 1190, 751 cm^{-1}.

¹H NMR (400 MHz, DMSO-d$_6$): δ 7.54 (dd, 1H, J = 7.8, 1.8 Hz), 7.39 (dt, 2H, J = 7.7, 2.0 Hz), 7.09-7.02 (m, 2H), 6.97 (dd, 1H, J = 7.1, 1.6 Hz), 6.82 (dd, 2H, J = 7.8, 1.9 Hz), 3.76 (s, 3H).

¹³C NMR (400 MHz, DMSO-d$_6$): δ 157.2, 144.9, 138.5, 133.0, 133.0, 130.1, 128.6, 125.1, 124.5, 112.2, 54.8.

¹¹B NMR (400 MHz, DMSO-d$_6$): δ 2.80.

¹⁹F NMR (400 MHz, DMSO-d$_6$): δ -139.2.

HRMS: exact mass calculated for [M - K]⁻ (C$_{13}$H$_{11}$BF$_3$O) requires m/z 251.0861, found [M - K]⁻ m/z 251.0863.

(4-(2,3-Dihydrobenzo[b][1,4]dioxin-6-yl)phenyl)trifluoro-l4-borane, potassium salt, **152**.
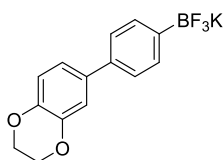
Prepared according to General Experimental Procedure C using (2,3-dihydrobenzo[b][1,4]dioxin-6-yl)boronic acid (1.1 equiv, 0.275 mmol, 49.5 mg) and 4-bromophenylboronic acid MIDA ester (1 equiv, 0.25 mmol, 78.0 mg) to afford **152** as an off-white amorphous solid (63.6 mg, 80%).

υ$_{max}$ (solid): 2961, 2881, 1587, 1493, 1312, 1230, 803 cm⁻¹.

¹H NMR (400 MHz, DMSO-d$_6$): δ 7.35 (d, 2H, J = 8.2 Hz), 7.29 (d, 2H, J = 8.1 Hz), 7.06-7.04 (m, 2H), 6.87 (d, 1H, J = 8.0 Hz), 4.25 (s, 4H).

¹³C NMR (400 MHz, DMSO-d$_6$): δ 143.5, 142.4, 136.2, 134.9, 131.8, 124.2, 119.1, 117.2, 114.6, 64.1. 2 carbon signals not observed/coincident.

¹¹B NMR (400 MHz, DMSO-d$_6$): δ 3.4.

¹⁹F NMR (400 MHz, DMSO-d$_6$): δ -139.0.

HRMS: exact mass calculated for [M - K]$^-$ (C$_{14}$H$_{11}$BF$_3$O$_2$) requires *m/z* 279.0810, found [M - K]$^-$ *m/z* 279.0812.

(*E*)-(2-(1-Benzyl-1*H*-pyrazol-4-yl)vinyl)boronic acid, **153**.
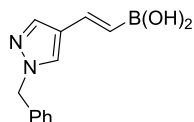
Prepared according to General Experimental Procedure B using (1-benzyl-1*H*-pyrazol-4-yl)boronic acid (1.1 equiv, 0.275 mmol, 55.6 mg) and (E)-(2-bromovinyl)boronic acid MIDA ester (1 equiv, 0.25 mmol, 65.5 mg) to afford **153** as a white amorphous solid (42.8 mg, 75%).

υ_{max} (solid): 3456, 3276, 2922, 1632, 1429, 1372, 1346, 987, 702 cm^{-1}.

^{1}H NMR (400 MHz, DMSO-d$_6$): δ 7.96 (s, 1H), 7.63 (s, 1H), 7.56 (brs, 1.5H), 7.34 (t, 2H, *J* = 7.4 Hz), 7.28 (t, 1H, *J* = 7.3 Hz), 7.23 (d, 2H, *J* = 7.3 Hz), 7.09 (d, 1H, *J* = 18.4 Hz), 5.73 (d, 1H, *J* = 18.5 Hz), 5.29 (s, 2H).

^{13}C NMR (400 MHz, DMSO-d$_6$): δ 137.4, 137.4, 136.9, 136.7, 128.9, 128.5, 127.6, 127.5, 121.8, 54.8.

^{11}B NMR (400 MHz, DMSO-d$_6$): δ 27.8.

HRMS: exact mass calculated for [M + Et Gly + H]$^+$ (C$_{14}$H$_{16}$BN$_2$O$_2$) requires *m/z* 255.1299, found [M + Et Gly + H]$^+$ *m/z* 255.1296.

M + Et Gly =
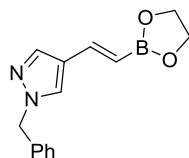
(3'-Isobutoxy-4-methoxy-[1,1'-biphenyl]-3-yl)boronic acid, **154**.
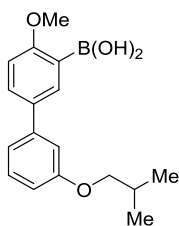
Prepared according to General Experimental Procedure B using (3-isobutoxyphenyl)boronic acid (1.1 equiv, 0.275 mmol, 53.4 mg) and (5-bromo-2-methoxyphenyl)boronic acid MIDA ester (1 equiv, 0.25 mmol, 85.5 mg) to afford **154** as a white amorphous solid (57.0 mg, 76%).

υ_{max} (solid): 3406, 2980, 2913, 1598, 1485, 1468, 1390, 1178, 1214, 1030 cm^{-1}.

^{1}H NMR (400 MHz, DMSO-d$_6$): δ 7.82 (d, 1H, *J* = 1.9 Hz), 7.79 (br.s., 2H,), 7.68 (dd, 1H, *J* = 7.9, 2.0 Hz), 7.32 (t, 1H, *J* = 8.1 Hz), 7.15 (d, 1H, *J* = 8.0 Hz), 7.11 (s, 1H), 7.05 (d, 1H, *J* = 8.1 Hz), 6.87 (dd, 1H, *J* = 8.1, 2.1 Hz), 3.84 (s, 3H), 3.81 (d, 2H, *J* = 3.9 Hz), 2.03 (app. sept, 1H, *J* = 7.7 Hz, 3.9 Hz), 1.00 (d, 6H, *J* = 8.2 Hz).

^{13}C NMR (400 MHz, DMSO-d$_6$): δ 163.1, 159.3, 141.5, 133.5, 132.0, 129.9, 129.8, 118.4, 112.7, 112.3, 110.8, 73.7, 55.5, 27.8, 19.1. 1 carbon signal not observed/coincident.

^{11}B NMR (400 MHz, DMSO-d$_6$): δ 27.8.

HRMS: exact mass calculated for [M + H]$^{+}$ (C$_{17}$H$_{22}$BO$_4$) requires *m/z* 301.1606, found [M + H]$^{+}$ *m/z* 301.1607.

(6'-Methoxy-[3,3'-bipyridin]-5-yl)boronic acid, **155**.
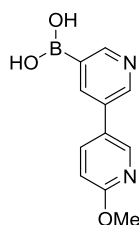
Prepared according to General Experimental Procedure B using (6-methoxypyridin-3-yl)boronic acid (1.1 equiv, 0.275 mmol, 42.0 mg) and (5-bromopyridin-3-yl)boronic acid MIDA ester (1 equiv, 0.25 mmol, 78.2 mg) to afford **155** as a white amorphous solid (39.7 mg, 69%).

υ_{max} (solid): 3323, 2955, 1655, 1603, 1562, 1598, 1329, 1245, 1057, 1014, 794 cm^{-1}.

^{1}H NMR (500 MHz, DMSO-d$_6$): δ 8.69 (d, 1H, J = 1.9 Hz), 8.65 (d, 1H, J = 2.0 Hz), 8.52 (dd, 1H, J = 2.0, 0.7 Hz), 8.33 (t, 1H, J = 2.0 Hz), 8.07 (br.s, 2H), 8.00 (dd, 1H, J = 8.3, 2.0 Hz), 6.75 (dd, 1H, J = 8.3, 0.7 Hz), 3.85 (s, 3H).

^{13}C NMR (126 MHz, DMSO-d$_6$): δ 164.8, 153.2, 148.8, 146.9, 144.4, 138.3, 131.7, 120.3, 109.5, 52.9. 1 carbon signal not observed/coincident.

^{11}B NMR (128 MHz, DMSO-d$_6$): δ 28.4.

HRMS: exact mass calculated for [M+H]$^+$ (C$_{11}$H$_{12}$BN$_2$O$_3$) requires *m/z* 231.0942, found [M+H]$^+$ *m/z* 231.0943.

Trifluoro(4'-(methylthio)-[1,1'-biphenyl]-3-yl)-Λ^4-borane, potassium salt, **156**.
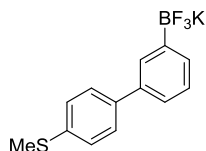
Prepared according to General Experimental Procedure C using (4-(methylthio)phenyl)boronic acid (1.1 equiv, 0.275 mmol, 46.2 mg) and 3-bromophenylboronic acid MIDA ester (1 equiv, 0.25 mmol, 78.0 mg) to afford **156** as a white amorphous solid (63.5 mg, 83%).

υ_{max} (solid): 3633, 3515, 1591, 1416, 1290, 1191, 948 cm^{-1}.

^{1}H NMR (400 MHz, DMSO-d$_6$): δ 7.57-7.52 (m, 3H), 7.33-7.29 (m, 4H), 7.19-7.17 (m, 1H). CH$_3$ signal not observed.

^{13}C NMR (400 MHz, DMSO-d$_6$): δ 138.7, 137.2, 136.1, 130.6, 129.4, 126.9, 126.8, 126.5, 123.2, 14.9. 1 carbon signal not observed/coincident.

<superscript>11</superscript>B NMR (400 MHz, DMSO-d$_6$): δ 2.9.

^{19}F NMR (400 MHz, DMSO-d$_6$): δ -139.2.

HRMS: exact mass calculated for [M - K]$^-$ (C$_{13}$H$_{11}$BF$_3$S) requires *m/z* 267.0632, found [M - K]$^-$ *m/z* 267.0632.

(5-(1*H*-Indol-6-yl)-2-methoxyphenyl)boronic acid, **157**.
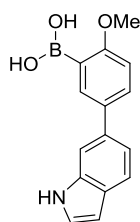
Prepared according to General Experimental Procedure B using (1*H*-indol-6-yl)boronic acid (1.1 equiv, 0.275 mmol, 44.3 mg) and (5-bromo-2-methoxyphenyl)boronic acid MIDA ester (1 equiv, 0.25 mmol, 85.5 mg) to afford **157** as a white amorphous solid (42.7 mg, 64%).

υ$_{max}$ (solid): 3378, 1616, 1510, 1451, 1402, 1356, 1334, 1077, 1010, 681 cm^{-1}.

^{1}H NMR (400 MHz, DMSO-d$_6$): δ 11.08 (s, 1H), 7.89 (d, 1H, *J* = 0.6 Hz), 7.75 (br.s, 1H), 7.58 (d, 1H, *J* = 8.4 Hz), 7.49-7.44 (m, 2H), 7.35 (t, 1H, *J* = 0.7 Hz), 7.20 (d, 1H, *J* = 2.3 Hz), 6.96 (dd, 1H, *J* = 8.4, 2.3 Hz), 6.44-6.40 (m, 1H), 3.87 (s, 3H). 1 proton signal not observed.

^{13}C NMR (126 MHz, DMSO-d$_6$): δ 164.8, 153.2, 148.8, 146.9, 144.4, 139.8, 138.3, 131.7, 120.3, 119.1, 109.5, 52.9. 3 carbon signals not observed/coincident.

^{11}B NMR (128 MHz, DMSO-d$_6$): δ 28.8.

HRMS: exact mass calculated for [M+H]$^+$ (C$_{15}$H$_{15}$BNO$_3$) requires *m/z* 268.1141, found [M+H]$^+$ *m/z* 268.1142.

(2-Methoxy-5-(6-methoxypyridin-3-yl)phenyl)boronic acid, **158**.
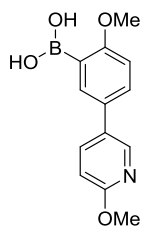
Prepared according to General Experimental Procedure B using (6-methoxypyridin-3-yl)boronic acid (1.1 equiv, 0.275 mmol, 42.0 mg) and (5-bromo-2-methoxyphenyl)boronic acid MIDA ester (1 equiv, 0.25 mmol, 85.5 mg) to afford **158** as a white amorphous solid (45.3 mg, 70%).

υ_{max} (solid): 3091, 2972, 1579, 1474, 1391, 1259, 1124, 1091, 1035, 1018, 797 cm^{-1}.

^{1}H NMR (400 MHz, DMSO-d$_6$): δ 8.53 (dd, 1H, J = 2.0, 0.7 Hz), 8.06 (br.s, 2H), 8.00 (dd, 1H, J = 8.3, 2.0 Hz), 7.57 (d, 1H, J = 8.5 Hz), 7.19 (d, 1H, J = 2.3 Hz), 6.96 (dd, 1H, J = 8.5, 2.3 Hz), 6.75 (dd, 1H, J = 8.3, 0.7 Hz), 3.87-3.85 (m, 6H).

^{13}C NMR (126 MHz, DMSO-d$_6$): δ 164.8, 156.2, 153.2, 144.4, 133.7, 133.2, 121.6, 113.1, 109.5, 109.2, 56.6, 52.9. 1 carbon signal not observed/coincident.

^{11}B NMR (128 MHz, DMSO-d$_6$): δ 30.5.

HRMS: exact mass calculated for [M+H]$^+$ (C$_{13}$H$_{15}$BNO$_4$) requires m/z 260.1091, found [M+H]$^+$ m/z 260.1099.

4'-Methoxy-N,N-dimethyl-3'-(trifluoro-ʎ^4-boranyl)-[1,1'-biphenyl]-3-amine, potassium salt, **159**.
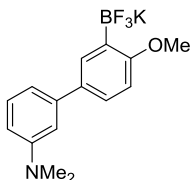
Prepared according to General Experimental Procedure C using (3-(dimethylamino)phenyl)boronic acid (1.1 equiv, 0.275 mmol, 45.4 mg) and (5-bromo-2-

methoxyphenyl)boronic acid MIDA ester (1 equiv, 0.25 mmol, 85.5 mg) to afford **159** as a white amorphous solid (73.3 mg, 88%).

υ_{max} (solid): 2937, 2841, 1766, 1602, 1485, 1294, 1175, 957 cm^{-1}.

^{1}H NMR (400 MHz, DMSO-d$_6$): δ 7.56 (d, 1H, J = 4.1 Hz), 7.28 (dd, 1H, J = 8.1, 4.0 Hz), 7.18 (t, 1H, J = 7.9 Hz), 6.81-6.80 (m, 2H), 7.64 (d, 1H, J = 8.2 Hz), 6.63 (dd, 1H, J = 8.0, 4.0 Hz), 3.65 (s, 3H), 2.93 (s, 6H).

^{13}C NMR (400 MHz, DMSO-d$_6$): δ 162.4, 150.7, 142.6, 131.9, 131.9, 131.8, 129.0, 125.0, 114.6, 110.3, 110.2, 109.9, 54.9. 1 carbon signal not observed/coincident.

^{11}B NMR (400 MHz, DMSO-d$_6$): δ 3.2.

^{19}F NMR (400 MHz, DMSO-d$_6$): δ -136.8.

HRMS: exact mass calculated for [M - K]$^-$ (C$_{15}$H$_{16}$BF$_3$NO) requires m/z 294.1283, found [M - K]$^-$ m/z 294.1277.

(2-Fluoro-4-(1*H*-indol-6-yl)phenyl)boronic acid, **160**.
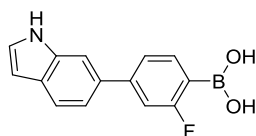
Prepared according to General Experimental Procedure B using (1*H*-indol-6-yl)boronic acid (1.1 equiv, 0.275 mmol, 44.3 mg) and (4-bromo-2-fluorophenyl)boronic acid MIDA ester (1 equiv, 0.25 mmol, 82.5 mg) to afford **160** as a beige amorphous solid (33.2 mg, 52%).

υ_{max} (solid): 3479, 3368, 1601, 1519, 1415, 1340, 1227, 1140, 1019, 872 cm^{-1}.

^{1}H NMR (500 MHz, DMSO-d$_6$): δ 11.10 (s, 1H), 7.89 (d, 1H, J = 0.7 Hz), 7.80 (dd, 2H, J = 8.4, 1.8 Hz), 7.53-7.44 (m, 5H), 7.36 (t, 1H, 0.7 Hz), 6.40-6.39 (m, 1H).

^{13}C NMR (126 MHz DMSO-d$_6$): δ 158.1 (d, $^1J_{C-F}$ = 250.1), 135.7, 135.1 (d, $^4J_{C-F}$ = J = 3.7 Hz), 135.0, 129.2, 126.0, 125.5 (d, $^2J_{C-F}$ = 24.1 Hz), 124.5, 118.8, 117.8, 108.2 (d, $^2J_{C-F}$ = 20.6 Hz), 100.8, 93.7 (d, $^3J_{C-F}$ = 7.0 Hz). 1 carbon signal not observed/coincident.

^{11}B NMR (128 MHz, DMSO-d$_6$): δ 28.4.

^{19}F NMR (376 MHz, DMSO-d$_6$): δ -105.8.

HRMS: exact mass calculated for [M+H]$^+$ (C$_{14}$H$_{12}$BFNO$_2$) requires *m/z* 256.0942, found [M+H]$^+$ *m/z* 256.0943.

(5-(3,4-Dichlorophenyl)pyridin-3-yl)boronic acid, **161**.
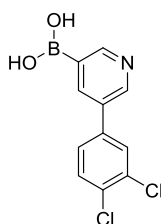
Prepared according to General Experimental Procedure B using (3,4-dichlorophenyl)boronic acid (1.1 equiv, 0.275 mmol, 52.5 mg) and (5-bromopyridin-3-yl)boronic acid MIDA ester (1 equiv, 0.25 mmol, 78.2 mg) to afford **161** as a yellow amorphous solid (30.8 mg, 46%).

υ$_{max}$ (solid): 3558, 3367, 3069, 1586, 1467, 1372, 1325, 1036, 1001, 819, 720 cm^{-1}.

^{1}H NMR (500 MHz, DMSO-d$_6$): δ 8.72 (d, 2H, *J* = 2.0 Hz), 8.45 (t, 1H, *J* = 2.0 Hz), 7.95-7.94 (m, 1H), 7.81-7.71 (m, 1H), 7.64-7.59 (m, 1H). 2 OH proton signals not observed, br.s. at 8.32.

^{13}C NMR (126 MHz, DMSO-d$_6$): δ 148.8, 146.9, 138.3, 135.8, 134.9, 134.1, 133.4, 131.6, 130.6, 130.0, 120.3.

^{11}B NMR (128 MHz, DMSO-d$_6$): δ 26.7.

HRMS: exact mass calculated for [M+H]$^+$ (C$_{11}$H$_9$BCl$_2$NO$_2$) requires *m/z* 268.0026 (Cl^{35}), found [M+H]$^+$ *m/z* 268.0025 (Cl^{35}).

(2-Fluoro-4-(6-methoxypyridin-3-yl)phenyl)boronic acid, **162**.
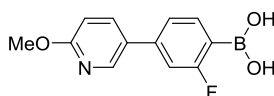
Prepared according to General Experimental Procedure B using (6-methoxypyridin-3-yl)boronic acid (1.1 equiv, 0.275 mmol, 42.0 mg) and (4-bromo-2-fluorophenyl)boronic acid MIDA ester (1 equiv, 0.25 mmol, 82.5 mg) to afford **162** as a white amorphous solid (41.4 mg, 67%).

υ_{max} (solid): 3479, 3366, 1601, 1519, 1444, 1415, 1340, 1226, 1227, 1140, 1019, 764 cm^{-1}.

^{1}H NMR (500 MHz, DMSO-d$_6$): δ 8.52 (dd, 1H, J = 2.0, 0.7 Hz), 8.06 (m, 2H), 8.00 (dd, 1H, J = 8.3, 2.0 Hz), 7.79 (dd, 1H, J = 8.4, 1.8 Hz), 7.53-7.45 (m, 2H), 6.75 (dd, 1H, J = 8.3, 0.7 Hz), 3.85 (s, 3H).

^{13}C NMR (126 MHz, DMSO-d$_6$): δ 164.8, 158.1 (d, $^1J_{C-F}$ = 250.1 Hz), 153.2, 144.4, 135.0 (d, $^4J_{C-F}$ = 3.7 Hz), 135.0, 125.4 (d, $^2J_{C-F}$ = 24.1 Hz), 109.5, 108.2 (d, $^2J_{C-F}$ = 20.6 Hz), 93.6 (d, $^3J_{C-F}$ = 6.9 Hz), 52.9. 1 carbon signal not observed/coincident.

^{11}B NMR (128 MHz, DMSO-d$_6$): δ 28.7.

^{19}F NMR (376 MHz, DMSO-d$_6$): δ -105.9.

HRMS: exact mass calculated for [M+H]$^+$ (C$_{12}$H$_{12}$BFNO$_3$) requires m/z 248.0891, found [M+H]$^+$ m/z 248.0899.

(4',5-Dimethoxy-[1,1'-biphenyl]-3-yl)trifluoro-ᴧ^4-borane, potassium salt, **163**.
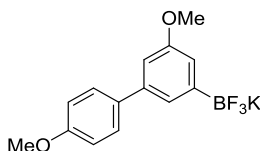
Prepared according to General Experimental Procedure C using (4-methoxyphenyl)boronic acid (1.1 equiv, 0.275 mmol, 41.8 mg) and (3-bromo-5-methoxyphenyl)boronic acid MIDA ester (1 equiv, 0.25 mmol, 85.5 mg) to afford **163** as a grey amorphous solid (70.4 mg, 88%).

υ_{max} (solid): 2941, 2835, 1587, 1587, 1517, 1331, 1216 cm^{-1}.

^{1}H NMR (400 MHz, DMSO-d$_6$): δ 7.51-7.49 (m, 2H), 7.13 (s, 1H), 6.99-6.97 (m, 2H), 6.83 (d, 1H, J = 2.3 Hz), 6.78 (t, 1H, J = 1.9 Hz), 3.78 (s, 3H), 3.74 (s, 3H).

^{13}C NMR (400 MHz, DMSO-d$_6$): δ 158.6, 158.3, 139.0, 134.3, 127.5, 122.0, 114.9, 114.1, 108.9, 55.1, 54.5. 1 carbon signal not observed/coincident.

^{11}B NMR (400 MHz, DMSO-d$_6$): δ 2.88.

^{19}F NMR (400 MHz, DMSO-d$_6$): δ -140.1.

HRMS: exact mass calculated for [M - K]$^-$ (C$_{14}$H$_{13}$BF$_3$O$_2$) requires m/z 281.0966, found [M - K]$^-$ m/z 281.0962.

(5-Phenylpyridin-3-yl)boronic acid, **164**.
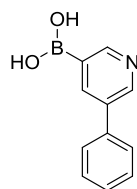
Prepared according to General Experimental Procedure B using phenylboronic acid (1.1 equiv, 0.275 mmol, 33.5 mg) and (5-bromopyridin-3-yl)boronic acid MIDA ester (1 equiv, 0.25 mmol, 78.2 mg) to afford **164** as a beige amorphous solid (37.8 mg, 76%).

υ$_{max}$ (solid): 3385, 1638, 1432, 1358, 1263, 1178, 1127, 1065, 757 cm^{-1}.

^{1}H NMR (500 MHz, DMSO-d$_6$): δ 8.69 (d, 1H, J = 2.4 Hz), 8.65 (d, 1H, J = 2.5 Hz), 8.33 (t, 1H, J = 2.5 Hz), 7.97 (br.s, 2H), 7.80-7.77 (m, 2H), 7.41-7.36 (m, 1H), 7.34-7.30 (m, 2H).

^{13}C NMR (126 MHz, DMSO-d$_6$): δ 148.8, 146.9, 138.3, 134.0, 133.4, 131.7, 129.9, 127.3, 120.3.

^{11}B NMR (128 MHz, DMSO-d$_6$): δ 28.8.

HRMS: exact mass calculated for [M+H]$^+$ (C$_{11}$H$_{11}$BNO$_2$) requires m/z 200.0879, found [M+H]$^+$ m/z 200.0882.

(*E*)-(2-(Thiophen-3-yl)vinyl)boronic acid, **165**.
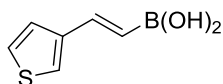
Prepared according to General Experimental Procedure B using thiophen-3-ylboronic acid (1.1 equiv, 0.275 mmol, 35.2 mg) and (*E*)-(2-bromovinyl)boronic acid MIDA ester (1 equiv, 0.25 mmol, 65.5 mg) to afford **165** as an off-white amorphous solid (25.8 mg, 67%).

υ_{max} (solid): 2976, 2926, 1615, 1517, 1323, 1138 cm^{-1}.

^{1}H NMR (400 MHz, DMSO-d$_6$): δ 7.71 (d, 1H, *J* = 2.1 Hz), 7.54 (dd, 2H, *J* = 4.3 Hz, 2.1 Hz), 7.43 (d, 1H, *J* = 2.0 Hz), 7.30 (d, 1H, *J* = 18.4 Hz), 5.92 (d, 1H, *J* = 18.4 Hz). 2 OH signals not observed.

^{13}C NMR (400 MHz, DMSO-d$_6$): δ 143.3, 140.9, 127.1, 126.1, 125.4, 82.9.

^{11}B NMR (400 MHz, DMSO-d$_6$): δ 28.4.

HRMS: exact mass calculated for [M - H]$^-$ (C$_6$H$_6$BO$_2$S) requires *m/z* 153.0176, found [M - H]$^-$ *m/z* 153.0173.

(3'-Fluoro-4'-methoxy-[1,1'-biphenyl]-3-yl)boronic acid, **166**.
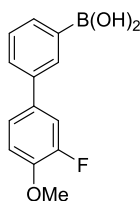
Prepared according to General Experimental Procedure B using (3-fluoro-4-methoxyphenyl)boronic acid (1.1 equiv, 0.275 mmol, 46.8 mg) and 3-bromophenylboronic acid MIDA ester (1 equiv, 0.25 mmol, 78.0 mg) to afford **166** as a white amorphous solid (54.7 mg, 89%).

υ_{max} (solid): 3224, 2984, 1604, 1524, 1448, 1346, 1169, 1019 cm^{-1}.

^{1}H NMR (400 MHz, DMSO-d$_6$): δ 8.11 (s, 2H), 8.08 (m, 1H), 7.73 (dt, 1H, J = 8.2, 1.1 Hz), 7.68 (ddd, 1H, J = 7.9, 1.9, 1.2 Hz), 7.55 (dd, 1H, J = 13.0, 2.1 Hz), 7.48 (ddd, 1H, J = 8.5, 2.1, 1.0 Hz), 7.40 (t, 1H, J = 7.8 Hz), 7.26 (t, 1H, J = 8.9 Hz), 3.88 (s, 3H).

^{13}C NMR (400 MHz, DMSO-d$_6$): δ 151.8 (d, $^1J_{C-F}$ = 243.5 Hz), 146.5, 146.4, 137.5, 133.5 (d, $^3J_{C-F}$ = 6.1 Hz), 133.0, 132.0, 127.9 (d, $^4J_{C-F}$ =, 1.4 Hz), 122.6 (d, $^3J_{C-F}$ = 2.5 Hz), 114.2, 113.9 (d, $^2J_{C-F}$ = 18.9 Hz). 1 carbon signal not observed/coincident.

^{11}B NMR (400 MHz, DMSO-d$_6$): δ 28.8.

^{19}F NMR (400 MHz DMSO-d$_6$): δ -135.1.

HRMS: exact mass calculated for [M + Et Gly + H]$^+$ (C$_{15}$H$_{14}$BFO$_3$) requires *m/z* 272.1015, found [M + Et Gly + H]$^+$ *m/z* 272.1011.

M + Et Gly =
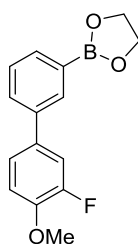
(4,4'-Dimethoxy-[1,1'-biphenyl]-3-yl)trifluoro-Λ^4-borane, potassium salt, **167**.
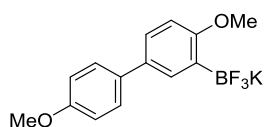
Prepared according to General Experimental Procedure C using (4-methoxyphenyl)boronic acid (1.1 equiv, 0.275 mmol, 41.8 mg) and (5-bromo-2-methoxyphenyl)boronic acid MIDA ester (1 equiv, 0.25 mmol, 85.5 mg) to afford **167** as a grey amorphous solid (72.8 mg, 91%).

υ$_{max}$ (solid): 3030, 2846, 1602, 1481, 1470, 1255, 1203, 1156, 972 cm^{-1}.

^{1}H NMR (400 MHz, DMSO-d$_6$): δ 7.65-7.62 (m, 2H), 7.59 (d, 1H, J = 2.6 Hz), 7.37-7.33 (m, 3H), 6.78 (d, 1H, J = 8.4 Hz), 3.66 (s, 3H). 1 CH$_3$ signal not observed.

^{13}C NMR (400 MHz, DMSO-d$_6$): δ 162.9, 146.7, 141.1, 131.8, 131.8, 129.3, 127.5, 125.1, 121.2, 110.0, 54.8. 1 carbon signal not observed/coincident.

^{11}B NMR (400 MHz, DMSO-d$_6$): δ 2.83.

^{19}F NMR (400 MHz, DMSO-d$_6$): δ -138.3.

HRMS: exact mass calculated for [M - K]$^-$ (C$_{14}$H$_{13}$BF$_3$O$_2$) requires *m/z* 281.0966, found [M - K]$^-$ *m/z* 281.0965.

(3-(3,5-Dimethylisoxazol-4-yl)-5-methoxyphenyl)boronic acid, **178**.
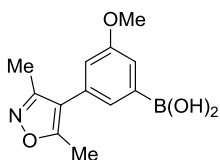
Prepared according to General Experimental Procedure B using (3,5-dimethylisoxazol-4-yl)boronic acid (1.1 equiv, 0.275 mmol, 38.7 mg) and (3-bromo-5-methoxyphenyl)boronic acid MIDA ester (1 equiv, 0.25 mmol, 85.5 mg) to afford **178** as a white amorphous solid (51.3 mg, 83%).

$υ_{max}$ (solid): 3318, 2943, 2848, 1600, 1586, 1418, 1348, 1212, 1049 cm^{-1}.

^{1}H NMR (400 MHz, DMSO-d$_6$): δ 8.13 (s, 2H), 7.36 (dd, 1H, *J* = 2.4, 1.6 Hz), 7.33 (m, 1H), 6.94 (dd, 1H, *J* = 2.5, 1.6 Hz), 3.79 (s, 3H), 2.39 (s, 3H), 2.22 (s, 3H).

^{13}C NMR (400 MHz, DMSO-d$_6$): δ 165.0, 158.9, 158.1, 130.3, 126.8, 118.1, 116.3, 116.1, 55.0, 11.3, 10.4. 1 carbon signal not observed/coincident.

^{11}B NMR (400 MHz, DMSO-d$_6$): δ 29.0.

HRMS: exact mass calculated for [M + H]$^+$ (C$_{12}$H$_{15}$BNO$_4$) requires *m/z* 248.1089, found [M + H]$^+$ *m/z* 248.1090.

3'-(3,5-Dimethylisoxazol-4-yl)-5'-methoxy-[1,1'-biphenyl]-4-carbonitrile, **179**.
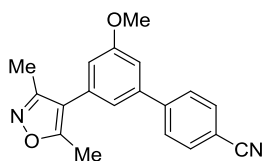
Reaction 53. A round-bottomed flask containing a magnetic stirrer bar was charged with THF (0.8 mL, 0.25 M), **178** (1.1 equiv, 0.222 mmol, 55.0 mg), 4-bromobenzonitrile (1 equiv, 0.202 mmol, 36.8 mg), K_3PO_4 (3 equiv, 0.606 mmol, 128.6 mg), H_2O (5 equiv, 1.01 mmol, 18.2 µL), and $Pd(dppf)Cl_2 \cdot CH_2Cl_2$ (5 mol %, 0.01 mmol, 8.2 mg). The reaction was heated at 70 °C for 1 hour. The reaction mixture was then allowed to cool to room temperature, passed through a pad of Celite, and the filtrate was concentrated under reduced pressure. The crude residue was purified by Si column chromatography (15% EtOAc in petroleum ether 40 °C - 60 °C) to afford **179** as an off-white amorphous solid (56.6 mg, 92%).

υ_{max} (solid): 2854, 2922, 2221, 1729, 1539, 1418, 1212, 836 cm^{-1}.

^{1}H NMR (500 MHz, CDCl$_3$): δ 7.76 (d, 2H, J = 8.4 Hz), 7.69 (d, 2H, J = 8.4 Hz), 7.10 (t, 1H, J = 1.7 Hz), 7.04 (t, 1H, J = 1.3 Hz), 6.85 (dd, 1H, J = 2.1, 1.4 Hz), 3.91 (s, 3H), 2.46 (s, 3H), 2.32 (s, 3H).

^{13}C NMR (500 MHz, CDCl$_3$): δ165.9, 160.8, 158.9, 145.5, 141.6, 133.1, 133.0, 128.2, 120.8, 119.1, 116.6, 115.4, 112.3, 111.8, 55.9, 12.0, 11.2.

HRMS: exact mass calculated for [M+H]$^+$ (C$_{19}$H$_{17}$N$_2$O$_2$) requires m/z 305.1285, found [M+H]$^+$ m/z 305.1287.

4-(3-(3,5-Dimethylisoxazol-4-yl)-5-methoxyphenyl)morpholine, **180**.
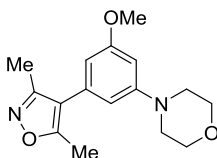
Reaction 54. A microwave vial containing a magnetic stirrer bar was charged with CH_2Cl_2 (0.6 mL, 0.33 M), **178** (1.5 equiv, 0.303 mmol, 75.0 mg), morpholine (1 equiv, 0.202 mmol, 17.6 µL), $Cu(OAc)_2$ (10 mol%, 0.020 mmol, 2.6 mg), and molecular sieves (3Å powdered, 76.0 mg).

The vial was sealed before purging and fitting with a balloon of oxygen connected *via* needle. The reaction was heated at 40 °C for 24 hours. The reaction mixture was then allowed to cool to room temperature, passed through a pad of Celite, and the filtrate was concentrated under reduced pressure. The crude residue was purified by Si column chromatography (40% EtOAc in petroleum ether 40 °C - 60 °C) to afford **180** as a white amorphous solid (45.4 mg, 78%).

υ_{max} (solid): 2952, 2921, 2852, 1738, 1634, 1587, 1418, 1255 cm^{-1}.

^{1}H NMR (500 MHz, CDCl$_3$): δ 6.45 (t, 1H, J = 2.2 Hz), 6.38-6.37 (m, 1H), 6.31 (dd, 1H, J = 2.0, 1.3 Hz), 3.88-3.86 (m, 4H), 3.83 (s, 3H), 3.20-3.18 (m, 4H), 2.42 (s, 3H), 2.28 (s, 3H).

^{13}C NMR (500 MHz, CDCl$_3$): δ 165.5, 161.2, 159.0, 153.2, 132.6, 109.7, 106.5, 101.3, 67.2, 55.7, 49.5, 25.2, 12.0, 11.2.

HRMS: exact mass calculated for [M+H]$^+$ (C$_{16}$H$_{21}$N$_2$O$_3$) requires *m/z* 289.1547, found [M+H]$^+$ *m/z* 289.1547.

4-(3-(3,5-Dimethylisoxazol-4-yl)-5-methoxyphenyl)butan-2-one, **181**.
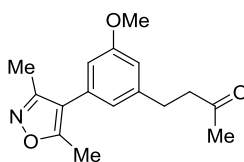
Reaction 55. A round-bottomed flask containing a magnetic stirrer bar was charged with H$_2$O (0.4 mL, 0.5 M), **178** (1 equiv, 0.202 mmol, 50.0 mg), methyl vinyl ketone (2 equiv, 0.404 mmol, 32.7 µL), [Rh(COD)Cl]$_2$ (2 mol%, 0.004 mmol, 2.0 mg), and Na$_2$CO$_3$ (2 equiv, 0.404 mmol, 42.8 mg). The reaction mixture was heated at 80 °C for 16 hours. The reaction mixture was then allowed to cool to room temperature, passed through a pad of Celite, and the filtrate was concentrated under reduced pressure. The crude residue was purified by Si column chromatography (15% EtOAc in petroleum ether 40 °C - 60 °C) to afford **181** as a clear oil (40.9 mg, 74%).

υ_{max} (solid): 2956, 2926, 2850, 1714, 1632, 1591, 1415, 1329, 1154 cm^{-1}.

^{1}H NMR (500 MHz, CDCl$_3$): δ 6.73 (t, 1H, *J* = 1.8 Hz), 6.67 (m, 1H), 6.62 (dd, 1H, *J* = 2.1, 1.5 Hz), 3.83 (s, 3H), 2.92 (t, 2H, *J* = 7.5 Hz), 2.80 (t, 2H, *J* = 7.5 Hz), 2.41 (s, 3H), 2.28 (s, 3H), 2.17 (s, 3H).

^{13}C NMR (500 MHz, CDCl$_3$): δ 207.9, 165.6, 160.3, 159.0, 143.5, 132.2, 121.9, 116.9, 113.3, 113.0, 55.6, 45.3, 30.4, 30.0, 12.0, 11.2.

HRMS: exact mass calculated for [M+H]$^+$ (C$_{16}$H$_{20}$NO$_3$) requires *m/z* 274.1438, found [M+H]$^+$ *m/z* 274.1437.

3-(3,5-Dimethylisoxazol-4-yl)-5-methoxyphenol, **182**.
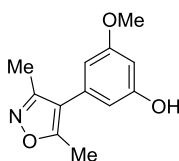
Reaction 56. A round-bottomed flask containing a magnetic stirrer bar was charged with THF (0.3M, 0.7 mL). **178** (1 equiv, 0.202 mmol, 50.0 mg), K$_3$PO$_4$ (3 equiv, 0.606 mmol, 128.6 mg), and water (20 equiv, 4.04 mmol, 72 μL). The mixture was cooled to 0 °C before addition of hydrogen peroxide (30% w/v, 10 equiv, 2.02 mmol, 228.9 μL). The reaction mixture was then allowed to warm to room temperature and stirred for 2 hours. The mixture was cooled to 0 °C and quenched with sodium metabisulphite (4 equiv). The solvent was then removed under reduced pressure and ethyl acetate (10 mL) was added. The organic layer was separated and then washed with saturated NH$_4$Cl (2 x 10 mL) and brine (2 x 10 mL). The organics were separated and passed through a hydrophobic frit containing a layer of Celite. The filtrate was concentrated under reduced pressure to afford **182** as a white amorphous solid (43.8 mg, >99%).

υ$_{max}$ (solid): 3153, 2960, 2924, 2842, 1641, 1593, 1342, 1162, 836 cm^{-1}.

^{1}H NMR (400 MHz, DMSO-d$_6$): δ 9.59 (s, 1H), 6.35-6.32 (m, 3H), 3.72 (s, 3H), 2.38 (S, 3H), 2.20 (s, 3H).

^{13}C NMR (400 MHz, DMSO-d$_6$): δ 164.9, 160.7, 158.8, 158.0, 131.6, 116.0, 108.4, 105.5, 100.3, 55.0, 11.4, 10.5.

HRMS: exact mass calculated for [M + H]$^+$ (C$_{12}$H$_{14}$NO$_3$) requires m/z 220.0968, found [M + H]$^+$ m/z 220.0966.

Methyl (E)-3-(3-(3,5-dimethylisoxazol-4-yl)-5-methoxyphenyl)acrylate, **183**.
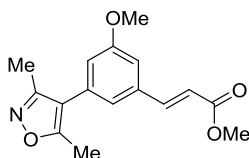
Reaction 57. A microwave vial containing a magnetic stirrer bar was charged with MeCN (0.2 mL, 0.1 M), **178** (1 equiv, 0.202 mmol, 50.0 mg), methyl acrylate (1.5 equiv, 0.303 mmol, 27.3 µL), p-benzoquinone (1 equiv, 0.202 mmol, 21.8 mg), Pd(OAc)$_2$ (2 mol%, 0.004 mmol, 0.9 mg), and 1,10-phenanthroline (2.5 mol%, 0.0051 mmol, 0.9 mg). The vial was capped and the reaction mixture was heated at 60 °C for 16 hours. The reaction mixture was then allowed to cool to room temperature, passed through a pad of Celite, and the filtrate was concentrated under reduced pressure. The crude residue was purified by Si column chromatography (20% EtOAc in petroleum ether 40 °C - 60 °C) to afford **183** as a white amorphous solid (49.9 mg, 86%).

υ_{max} (solid): 2948, 2924, 2852, 1729, 1716, 1641, 1589, 1407, 1292, 979 cm^{-1}.

^{1}H NMR (400 MHz, CDCl$_3$): δ 7.69 (d, 1H, J = 16.0 Hz), 7.05 (t, 1H, J = 1.8 Hz), 6.99 (m, 1H), 6.82 (dd, 1H, J = 2.2, 1.5 Hz), 6.46 (d, 1H, J = 16.0 Hz), 3.87 (s, 3H), 3.83 (s, 3H), 2.43 (s, 3H), 2.29 (s, 3H).

^{13}C NMR (400 MHz, CDCl$_3$): δ 167.5, 165.9, 160.6, 158.9, 144.6, 136.6, 132.8, 122.0, 119.2, 117.5, 116.4, 111.8, 55.8, 52.2, 12.0, 11.2.

HRMS: exact mass calculated for [M+H]$^+$ (C$_{16}$H$_{18}$NO$_4$) requires m/z 288.1230, found [M+H]$^+$ m/z 288.1228.

4-(3-Bromo-5-methoxyphenyl)-3,5-dimethylisoxazole, **184**.
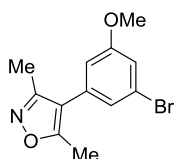
Reaction 58. A round-bottomed flask containing a magnetic stirrer bar was charged with THF (0.6 mL, 0.33 M), **178** (1 equiv, 0.202 mmol, 50.0 mg) and *N*-bromosuccinimide (1.5 equiv, 0.303 mmol, 53.9 mg). The reaction mixture was stirred at room temperature for 16 hours at room temperature before the addition of sodium thiosulphate (5 mL of a ½ sat. solution). EtOAc (5 mL) was then added and the layers separated. The organic extract was washed with ½ sat. sodium thiosulphate solution (2 x 5 mL) and then concentrated under reduced pressure to afford a crude residue which was purified by Si column chromatography (30% EtOAc in petroleum ether 40 °C - 60 °C) to afford **184** as a white amorphous solid (88%, 50.1 mg).

υ_{max} (solid): 2974, 2945, 2839, 1632, 1602, 1558, 1409, 1214, 1028 cm^{-1}.

^{1}H NMR (400 MHz, CDCl$_3$): δ 7.06 (dd, 1H, *J* = 2.3, 1.8 Hz), 6.98 (t, 1H, *J* = 1.5 Hz), 6.72 (dd, 1H, *J* = 2.3, 1.5 Hz), 3.83 (s, 3H), 2.41 (s, 3H), 2.27 (s, 3H).

^{13}C NMR (400 MHz, CDCl$_3$): δ 166.0, 160.8, 158.7, 133.6, 124.7, 123.5, 116.3, 115.8, 114.7, 55.9, 11.9, 11.1.

HRMS: exact mass calculated for [M + H]$^+$ (C$_{12}$H$_{13}$BBrO$_2$) requires *m/z* 282.0124 (Br^{79}) and 284.0104 (Br^{81}), found [M + H]$^+$ *m/z* 282.0127 (Br^{79}), and *m/z* 284.0101 (Br^{81}).

4-(3-Benzyl-5-methoxyphenyl)-3,5-dimethylisoxazole, **185**.
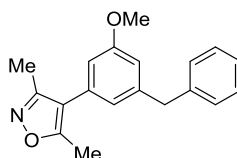
Reaction 59. A sealable microwave vial containing a magnetic stirrer bar was charged with THF (0.8 mL, 0.25 M), **178** (1 equiv, 0.202 mmol, 50.0 mg), benzyl bromide (1.5 equiv, 0.303 mmol, 36.0 µL), K$_3$PO$_4$ (4 equiv, 0.808 mmol, 171.5 mg), H$_2$O (20 equiv, 4.04 mmol, 72.8 µL),

and Pd(dppf)Cl$_2$·CH$_2$Cl$_2$ (5 mol%, 0.01 mmol, 8.2 mg). The vial was capped and the reaction mixture was heated at 90 °C for 5 hours. The reaction mixture was then allowed to cool to room temperature, passed through a pad of Celite, and the filtrate was concentrated under reduced pressure. The crude residue was purified by Si column chromatography (10% EtOAc in petroleum ether 40 °C - 60 °C) to afford **185** as a white amorphous solid (56.3 mg, 95%).

υ_{max} (solid): 2956, 2922, 2848, 1632, 1589, 1415, 1327, 1255, 1052, 704 cm^{-1}.

^{1}H NMR (500 MHz, CDCl$_3$): δ 7.33-7.30 (m, 2H), 7.24-7.21 (m, 3H), 6.74 (m, 1H), 6.65-6.63 (m, 2H), 4.00 (s, 2H), 3.81 (s, 3H), 2.38 (s, 3H), 2.24 (s, 3H).

^{13}C NMR (500 MHz, CDCl$_3$): δ 165.5, 160.3, 159.0, 143.6, 140.8, 132.1, 129.3, 128.9, 126.7, 122.5, 116.9, 113.8, 112.9, 55.6, 42.8, 11.9, 11.2.

HRMS: exact mass calculated for [M+H]$^+$ (C$_{19}$H$_{20}$NO$_2$) requires *m/z* 294.1489, found [M+H]$^+$ *m/z* 294.1486.

2-(3-Bromo-5-methoxyphenyl)-6-methyl-1,3,6,2-dioxazaborocane-4,8-dione, **189**.
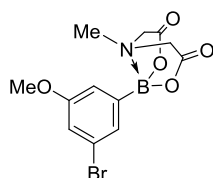
Prepared according to General Experimental Procedure A using (3-bromo-5-methoxyphenyl)boronic acid (1 equiv, 13 mmol, 3.00 g) and *N*-methyliminodiacetic acid (1.05 equiv, 14.3 mmol, 2.10 g) to afford **189** as a white amorphous solid (4.31 g, 97%).

υ_{max} (solid): 3400, 3069, 3015, 1747, 1591, 1268, 1032 cm^{-1}.

^{1}H NMR (400 MHz, DMSO-d$_6$): δ 7.15 (m, 2H), 6.96 (t, 1H, *J* = 1.0 Hz), 4.34 (d, 2H, *J* = 17.2 Hz), 4.15 (d, 2H, *J* = 17.2 Hz), 3.79 (s, 3H), 2.57 (s, 3H).

^{13}C NMR (400 MHz, DMSO-d$_6$): δ 169.2, 159.8, 127.0, 122.1, 117.3, 117.0, 62.0, 55.4, 47.8. 1 carbon signal not observed/coincident.

^{11}B NMR (500 MHz, DMSO-d$_6$): δ 10.8.

HRMS: exact mass calculated for [M + NH$_4$]$^+$ (C$_{12}$H$_{17}$BBrN$_2$O$_5$) requires *m/z* 359.0409 (Br^{79}) and *m/z* 361.0388 (Br^{81}), found [M + NH$_4$]$^+$ *m/z* 359.0413 (Br^{79}) and *m/z* 361.0391 (Br^{81}).

2-(4-Bromo-2-fluorophenyl)-6-methyl-1,3,6,2-dioxazaborocane-4,8-dione, **190**.[114]
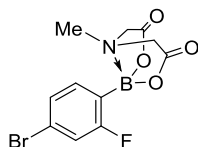
Prepared according to General Experimental Procedure A using (4-bromo-2-fluorophenyl)boronic acid (1 equiv, 4 mmol, 875.0 mg) and *N*-methyliminodiacetic acid (1.05 equiv, 4.2 mmol, 618.0 mg) to afford **190** as a white amorphous solid (994.0 mg, 75%).

υ_{max} (solid): 3351, 1771, 1602, 1557, 1403, 1025, 871, 734 cm^{-1}.

^{1}H NMR (500 MHz, DMSO-d$_6$): δ 7.47-7.40 (m, 3H), 4.41 (d, 2H, *J* = 17.3 Hz), 4.09 (d, 2H, *J* = 17.3 Hz), 2.62 (s, 3H).

^{13}C NMR (500 MHz, DMSO-d$_6$): δ 168.9, 165.3 (d, $^1J_{C-F}$ = 246.3 Hz), 136.4 (d, $^3J_{C-F}$ = 10.1 Hz), 127.4 (d, $^4J_{C-F}$ = 3.0 Hz), 123.4 (d, $^3J_{C-F}$ = 10.4 Hz), 118.4 (d, $^2J_{C-F}$ = 28.7 Hz), 62.4, 47.5. 1 carbon signal not observed/coincident

^{11}B NMR (500 MHz, DMSO-d$_6$): δ 11.3.

^{19}F NMR (500 MHz, DMSO-d$_6$): δ -102.9.

HRMS: exact mass calculated for [M + H]$^+$ (C$_{11}$H$_{11}$BBrFNO$_4$) requires *m/z* 329.9943 (Br^{79}) and *m/z* 331.9923 (Br^{81}), found [M + H]$^+$ *m/z* 329.9954 (Br^{79}) and *m/z* 331.9928 (Br^{81}).

9. References

(1) Muir, C. W.; Vantourout, J. C.; Isidro-Llobet, A.; Macdonald, S. J. F.; Watson, A. J. B. *Org. Lett.* **2015**, *17* (24), 6030.

(2) Duhamel, L.; Duhamel, P.; Plaquevent, J.-C. *Tetrahedron: Asymmetry,* **2004**, *15*, 3653.

(3) Mohr, J. T.; Hong, A. Y.; Stoltz, B. M. *Nat. Chem.* **2009**, *1*, 359.

(4) Oudeyer, S.; Brière, J.-F.; Levacher, V. *Eur. J. Org. Chem.* **2014**, 6103.

(5) Edon Vitaku, Elizabeth A. Ilardi, J. T. N. Top 200 Pharmacetical Products by US Retail Sales in 2012 http://cbc.arizona.edu/njardarson/group/sites/default/files/Top200 Pharmacetical Products by US Retail Sales in 2012_0.pdf.

(6) Nagasaka, M.; Kondoh, H.; Amemiya, K.; Ohta, T.; Iwasawa, Y. *Phys. Rev. Lett.* **2008**, *100*, 8.

(7) Sakai, T.; Matsuda, A.; Tanaka, Y.; Korenaga, T.; Ema, T. *Tetrahedron: Asymmetry* **2004**, *15*, 1929.

(8) Uraguchi, D.; Kinoshita, N.; Ooi, T. *J. Am. Chem. Soc.* **2010**, *132*, 12240.

(9) Guin, J.; Varseev, G.; List, B. *J. Am. Chem. Soc.* **2013**, *135*, 2100.

(10) Poisson, T.; Yamashita, Y.; Kobayashi, S. *J. Am. Chem. Soc.* **2010**, *132*, 7890.

(11) Vedejs, E.; Kruger, A. W.; Suna, E. *J. Org. Chem.,* **1999**, 7863.

(12) Cheon, C. H.; Yamamoto, H. *J. Am. Chem. Soc.* **2008**, *130*, 9246.

(13) Hoffmann, S.; Seayad, A. M.; List, B. *Angew. Chemie Int. Ed.* **2005**, *44* (45), 7424.

(14) Yang, C.; Xue, X. S.; Jin, J. L.; Li, X.; Cheng, J. P. *J. Org. Chem.* **2013**, *78*, 7076.

(15) Matoishi, K.; Ueda, M.; Miyamoto, K.; Ohta, H. *J. Mol. Catal. B Enzym.* **2004**, *27*, 161.

(16) Navarre, L.; Darses, S.; Genet, J. P. *Angew. Chemie - Int. Ed.* **2004**, *43*, 719.

(17) Hodous, B. L.; Ruble, J. C.; Fu, G. C. *J. Am. Chem. Soc.,* **1999**, *121*, 2637.

(18) Nishimura, T.; Hirabayashi, S.; Yasuhara, Y.; Hayashi, T. *J. Am. Chem. Soc.* **2006**, *128*, 2556.

(19) Akiyama, T. *Chem. Rev.* **2007**, *107* (12), 5744.

(20) Wang, Y.; Liu, X.; Deng, L. *J. Am. Chem. Soc.* **2006**, *128*, 3928.

(21) Perlmutter, P. *Conjugate Addition Reactions in Organic Synthesis*; Pergamon: Oxford, 1992.

(22) Nising, C. F.; Bräse, S. *Chem. Soc. Rev.* **2008**, *37*, 1218.

(23) Jiang, H.; Nielsen, J. B.; Nielsen, M.; Jørgensen, K. A. *Chem. - A Eur. Journal,* **2007**, *13*, 9068.

(24) Emori, E.; Arai, T.; Sasai, H.; Uni, T. **1998**, *7863*, 4043.

(25) Enders, D.; Saint-Dizier, A.; Lannou, M.-I.; Lenzen, A. *European J. Org. Chem.* **2006**, *2006* (1), 29.

(26) Johnson, J. S.; Evans, D. A. *Acc. Chem. Res.,* **2000**, *33*, 325.

(27) Alexakis, A.; Benhaim, C. *Eur. J. Org. Chem.* **2002**, *2002*, 3221.

(28) Villacorta, G. M.; Rao, C. P.; Lippard, S. J. *J. Am. Chem. Soc.* **1988**, *110*, 3175.

(29) Desimoni, G., Quadrelli, P., Righetti, P. *Tetrahedron,* **1990**, *46*, 2927.

(30) Reich, H. E.; Levine, R. *J. Am. Chem. Soc.,* **1955**, *77*, 4913.

(31) Schaaf, G. M.; Mukherjee, S.; Waterson, A. G. *Tetrahedron Lett.* **2009**, *50*, 1928.

(32) Burns, A. R.; Kerr, J. H.; Kerr, W. J.; Passmore, J.; Paterson, L. C.; Watson, A. J. B. *Org. Biomol. Chem.* **2010**, *8*, 2777.

(33) Rupnicki, L.; Saxena, A.; Lam, H. W. *J. Am. Chem. Soc.* **2009**, *131*, 10386.

(34) Luo, R.; Li, K.; Hu, Y.; Tang, W. *Adv. Synth. Catal.* **2013**, *355*, 1297.

(35) Klumpp, D. *Synlett,* **2012**, *23*, 1590.

(36)   Watanabe, M.; Suga, S.; Yoshida, J.-I. *Bull. Chem. Soc. Jpn.,* **2000**, 243.

(37)   Dalby, K. N.; Jencks, W. P. *J. Chem. Soc. Perkin Trans. 2* **1997**, No. 8, 1555.

(38)   http://evans.harvard.edu/pdf/evans_pka_table.pdf
         http://www.chem.wisc.edu/areas/reich/pkatable/

(39)   Baschieri, A.; Bernardi, L.; Ricci, A.; Suresh, S.; Adamo, M. F. a. *Angew. Chemie Int.
         Ed.* **2009**, *48*, 9342.

(40)   Roy, I. D.; Burns, A. R.; Pattison, G.; Michel, B.; Parker, A. J.; Lam, H. W. *Chem.
         Commun. (Camb).* **2014**, *50*, 2865.

(41)   Wright, R. O.; Baccarelli, A. *J. Nutr.* **2007**, *137* (12), 2809.

(42)   Carter, D. E.; Fernando, Q. *J. Chem. Educ.* **1979**, *56* (8), 490.

(43)   *Transition Metal Toxicity: Transition Metal Toxicity*; Elsevier, 2013.

(44)   Wang, Y.-Y.; Kanomata, K.; Korenaga, T.; Terada, M. *Angew. Chem. Int. Ed. Engl.*
         2015.

(45)   Houk, K. N.; Strozier, R. W. *J. Am. Chem. Soc.* **1973**, *95*, 4094.

(46)   Fehr, C. *Angew. Chem. Int. Ed. Engl.* **1996**.

(47)   Christ, P.; Lindsay, A. G.; Vormittag, S. S.; Neudörfl, J.-M.; Berkessel, A.; O'Donoghue,
         A. C. *Chemistry* **2011**, *17*, 8524.

(48)   Yang, C.; Xue, X.-S.; Jin, J.-L.; Li, X.; Cheng, J.-P. *J. Org. Chem.* **2013**, *78*, 7076.

(49)   *M. J. Frisch, G. W. Trucks, H. B. Schlegel, G. E. Scuseria, M. A. Robb, J. R. Cheeseman,
         G. Scalamani, V. Barone, B. Mennucci, G. A. Petersson, H. Nakatsuji, M. Caricato, X.
         Li, H. P. Hratchian, A. F. Izmaylov, J. Bloino, G. Zheng, J. L. Sonnenberg, M. Ha*.

(50)   Perrin, D. D.; Armarego, W. L. F. *Purification of Laboratory Chemicals*, 4th ed.;
         Butterworth- Heinemann Ltd. Oxford, 1996.

(51)   Nuñez, A.; Abarca, B.; Cuadro, A. M.; Alvarez-Builla, J.; Vaquero, J. J. *J. Org. Chem.*
         2009, *74*, 4166.

(52)   Yang, J.; Dudley, G. B. *J. Org. Chem.* **2009**, *74*, 7998.

(53)   Buchdahl, Myron R.; Soine, T. O. *J. Am. Pharm. Assoc. Sci. Ed.* **1952**, *41*, 225.

(54)   Correia, C. A.; Yang, L.; Li, C.-J. *Org. Lett.* **2011**, *13*, 4581.

(55)   Campbell, K. N.; Helbing, C. H.; Kerwin, J. F. *J. Am. Chem. Soc.* **1946**, *68*, 1840.

(56)   Chan, B. K.; Ciufolini, M. A. *J. Org. Chem.* **2007**, *72*, 8489.

(57)   Li, Y.; Guo, F.; Zha, Z.; Wang, Z. *Chem. Asian J.* **2013**, *8*, 534.

(58)   Kazuo Ito, K. Y. *Heterocycles* **2012**, 1603.

(59)   Walters, L. R.; Iyer, N. T.; McEwen, W. E. *J. Am. Chem. Soc.* **1958**, *80*, 1177.

(60)   Hatano, M.; Ikeno, T.; Matsumura, T.; Torii, S.; Ishihara, K. *Adv. Synth. Catal.* **2008**,
         350, 1776.

(61)   Klussmann, M.; Ratjen, L.; Hoffmann, S.; Wakchaure, V.; Goddard, R.; List, B. *Synlett*
         2010, *2010*, 2189.

(62)   Dagousset, G.; Drouet, F.; Masson, G.; Zhu, J. *Org. Lett.* **2009**, *11*, 5546.

(63)   Chen, X.-H.; Xu, X.-Y.; Liu, H.; Cun, L.-F.; Gong, L.-Z. *J. Am. Chem. Soc.* **2006**, *128*,
         14802.

(64)   Liang, T.; Zhang, Z.; Antilla, J. C. *Angew. Chem. Int. Ed. Engl.* **2010**, *49*, 9734.

(65)   Xie, W.; Jiang, G.; Liu, H.; Hu, J.; Pan, X.; Zhang, H.; Wan, X.; Lai, Y.; Ma, D. *Angew.
         Chem. Int. Ed. Engl.* **2013**, *52*, 12924.

(66)   Zhang, Y.; Lim, C.-S.; Sim, D. S. B.; Pan, H.-J.; Zhao, Y. *Angew. Chem. Int. Ed. Engl.*
         2014, *53*, 1399.

(67)   Takasaki, M.; Motoyama, Y.; Yoon, S.-H.; Mochida, I.; Nagashima, H. *J. Org. Chem.*
         2007, *72*, 10291.

(68)   Brenet, S.; Baptiste, B.; Philouze, C.; Berthiol, F.; Einhorn, J. *Eur. J. Org. Chem.* **2013**,

2013, 1041.

(69) Wu, T. R.; Shen, L.; Chong, J. M. *Org. Lett.* **2004**, *6*, 2701.

(70) Xiao, B.; Fu, Y.; Xu, J.; Gong, T.-J.; Dai, J.-J.; Yi, J.; Liu, L. *J. Am. Chem. Soc.* **2010**, *132*, 468.

(71) Egami, H.; Katsuki, T. *J. Am. Chem. Soc.* **2009**, *131*, 6082.

(72) Heumann, L. V; Keck, G. E. *J. Org. Chem.* **2008**, *73*, 4725.

(73) Pousse, G.; Devineau, A.; Dalla, V.; Humphreys, L.; Lasne, M.-C.; Rouden, J.; Blanchet, J. *Tetrahedron* **2009**, *65*, 10617.

(74) McDougal, N. T.; Trevellini, W. L.; Rodgen, S. A.; Kliman, L. T.; Schaus, S. E. *Adv. Synth. Catal.* **2004**, *346*, 1231.

(75) McDougal, N. T.; Schaus, S. E. *J. Am. Chem. Soc.* **2003**, *125*, 12094.

(76) Bartoszek, M.; Beller, M.; Deutsch, J.; Klawonn, M.; Köckritz, A.; Nemati, N.; Pews-Davtyan, A. *Tetrahedron* **2008**, *64*, 1316.

(77) Castelló, L. M.; Hornillos, V.; Vila, C.; Giannerini, M.; Fañanás-Mastral, M.; Feringa, B. L. *Org. Lett.* **2015**, *17*, 62.

(78) Gribkov, D. V; Hultzsch, K. C.; Hampel, F. *Chemistry* **2003**, *9*, 4796.

(79) Miyaura, Norio, A. S. *J. Chem. Soc., Chem. Commun.* **1979**, 866.

(80) Cooper, T. W. J.; Campbell, I. B.; Macdonald, S. J. F. *Angew. Chem. Int. Ed. Engl.* **2010**, *49*, 8082.

(81) Torborg, C.; Beller, M. *Adv. Synth. Catal.* **2009**, *351*, 3027.

(82) The Nobel Prize in Chemistry 2010 http://www.nobelprize.org/nobel_prizes/chemistry/laureates/2010/ (accessed Oct 19, 2015).

(83) Barrios-Landeros, F.; Hartwig, J. F. *J. Am. Chem. Soc.* **2005**, *127*, 6944.

(84) Tolman, C. A. *Chem. Rev.* **1977**, *77*, 313.

(85) Zhang, H.; Luo, X.; Wongkhan, K.; Duan, H.; Li, Q.; Zhu, L.; Wang, J.; Batsanov, A. S.; Howard, J. A. K.; Marder, T. B.; Lei, A. *Chemistry* **2009**, *15*, 3823.

(86) Mc Cartney, D.; Guiry, P. J. *Chem. Soc. Rev.* **2011**, *40*, 5122.

(87) Heravi, M. M.; Hajiabbasi, P. *Monatshefte für Chemie - Chem. Mon.* **2012**, *143*, 1575.

(88) Schilz, M.; Plenio, H. *J. Org. Chem.* **2012**, *77*, 2798.

(89) Amatore, C.; Jutand, A.; Le Duc, G. *Chem. Eur. J.* **2011**, *17*, 2492.

(90) Carrow, B. P.; Hartwig, J. F. **2011**, 2116.

(91) Amatore, C.; Jutand, A.; Le Duc, G. *Chem. Eur. J.* **2012**, *18*, 6616.

(92) Amatore, C.; Jutand, A.; Le Duc, G. *Angew. Chem. Int. Ed. Engl.* **2012**, *51*, 1379.

(93) Lennox, A. J. J.; Lloyd-Jones, G. C. *Chem. Soc. Rev.* **2014**, *43*, 412.

(94) Braga, A. a C.; Ujaque, G.; Maseras, F. *Organometallics* **2006**, *25*, 3647.

(95) Braga, A. a C.; Morgon, N. H.; Ujaque, G.; Maseras, F. *J. Am. Chem. Soc.* **2005**, *127*, 9298.

(96) Darses, S.; Genet, J. P. *Chem. Rev.* **2008**, *108*, 288.

(97) Molander, G. a.; Ellis, N. *Acc. Chem. Res.* **2007**, *40*, 275.

(98) Contreras, R.; García, C.; Mancilla, T.; Wrackmeyer, B. *J. Organomet. Chem.* **1983**, *246*, 213.

(99) Mancilla, T.; Contreras, R.; Wrackmeyer, B. *J. Organomet. Chem.* **1986**, *307*, 1.

(100) Gillis, E. P.; Gillis, E. P.; Burke, M. D.; Burke, M. D. *Synthesis (Stuttg).* **2005**, 5161.

(101) Suk, J. L.; Gray, K. C.; Paek, J. S.; Burke, M. D. *J. Am. Chem. Soc.* **2008**, *130*, 466.

(102) Noguchi, H.; Hojo, K.; Suginome, M. *J. Am. Chem. Soc.* **2007**, *129*, 758.

(103) Hall, D. G. *Structure, Properties, and Preparation of Boronic Acid Derivatives. Overview of Their Reactions and Applications*; Wiley-VCH Verlag GmbH & Co. KGaA:

Weinheim, FRG, 2006.

(104) Pan, F.; Wang, H.; Shen, P.-X.; Zhao, J.; Shi, Z.-J. *Chem. Sci.* **2013**, *4*, 1573.

(105) Lee, C. Y.; Ahn, S. J.; Cheon, C. H. *J. Org. Chem.* **2013**, *78*, 12154.

(106) Ahn, S. J.; Lee, C. Y.; Kim, N. K.; Cheon, C. H. *J. Org. Chem.* **2014**, *79*, 7277.

(107) Noonan, G.; Leach, A. G. *Org. Biomol. Chem.* **2015**, *13*, 2555.

(108) Barker, G.; Webster, S.; Johnson, D. G.; Curley, R.; Andrews, M.; Young, P. C.; Macgregor, S. A.; Lee, A.-L. *J. Org. Chem.* **2015**, *80* (20), 9807.

(109) Miyaura, Norio, A. S. *Chem. Rev.* **1995**, 2457.

(110) Gillis, E. P.; Burke, M. D. *J. Am. Chem. Soc.,* **2008**, 14084.

(111) Knapp, D. M.; Gillis, E. P.; Burke, M. D. *J. Am. Chem. Soc.* **2009**, *131*, 6961.

(112) Dick, G. R.; Woerly, E. M.; Burke, M. D. *Angew. Chemie - Int. Ed.* **2012**, *51*, 2667.

(113) Woerly, E. M.; Roy, J.; Burke, M. D. *Nat. Chem.* **2014**, *6*, 484.

(114) Fyfe, J. W. B.; Seath, C. P.; Watson, A. J. B. *Angew. Chemie Int. Ed.* **2014**, *53*, 12077.

(115) Noguchi, H.; Shioda, T.; Chou, C. M.; Suginome, M. *Org. Lett.* **2008**, *10*, 377.

(116) Iwadate, N.; Suginome, M. *J. Am. Chem. Soc.,* **2010**, *2*, 2548.

(117) Lee, J. C. H.; McDonald, R.; Hall, D. G. *Nat. Chem.* **2011**, *3*, 894.

(118) Feng, X.; Jeon, H.; Yun, J. *Angew. Chemie - Int. Ed.* **2013**, *52*, 3989.

(119) Endo, K.; Ohkubo, T.; Hirokami, M.; Shibata, T. *J. Am. Chem. Soc.* **2010**, *132*, 11033.

(120) Mlynarski, S. N.; Schuster, C. H.; Morken, J. P. *Nature* **2013**, 1.

(121) Sun, C.; Potter, B.; Morken, J. P. *J. Am. Chem. Soc.* **2014**, *136*, 6534.

(122) Gaich, T.; Baran, P. S. *J. Org. Chem.* **2010**, *75*, 4657.

(123) Molander, G. A.; Cavalcanti, L. N.; García-García, C. *J. Org. Chem.* **2013**, *78*, 6427.

(124) Kaupp, G.; Naimi-Jamal, M. R.; Stepanenko, V. *Chemistry* **2003**, *9*, 4156.

(125) Thiebes, C.; Prakash, G. K. S.; Petasis, N. A.; Olah, G. A. *Synlett* **1998**, *1998*, 141.

(126) Niu, L.; Zhang, H.; Yang, H.; Fu, H. *Synlett* **2014**, *25*, 995.

(127) Murata, M.; Satoh, K.; Watanabe, S.; Yuzuru, M. *J. Chem. Soc., Perkin Trans. 1* **1998**, 1465.

(128) Yadav, R. R.; Vishwakarma, R. A.; Bharate, S. B. *Tetrahedron Lett.* **2012**, *53*, 5958.

(129) Wu, X.-F.; Schranck, J.; Neumann, H.; Beller, M. *Chem. Commun. (Camb).* **2011**, *47*, 12462.

(130) Guo, S.; Lu, L.; Cai, H. *Synlett* **2013**, *24*, 1712.

(131) Chen, D.-S.; Huang, J.-M. *Synlett* **2013**, *24*, 499.

(132) Cheng, G.; Zeng, X.; Cui, X. *Synthesis (Stuttg).* **2013**, *46*, 295.

(133) Voth, S.; Hollett, J. W.; McCubbin, J. A. *J. Org. Chem.* **2015**, *80*, 2545.

(134) Zhu, C.; Li, G.; Ess, D. H.; Falck, J. R.; Kürti, L. *J. Am. Chem. Soc.* **2012**, *134*, 18253.

(135) Grimes, K. D.; Gupte, A.; Aldrich, C. C. *Synthesis (Stuttg).* **2010**, *2010*, 1441.

(136) Yasukawa, T.; Miyamura, H.; Kobayashi, S. *Org. Biomol. Chem.* **2011**, *9*, 6208.

(137) Kondolff, I.; Doucet, H.; Santelli, M. *Tetrahedron* **2004**, *60*, 3813.

(138) Kirchhoff, J. H.; Netherton, M. R.; Hills, I. D.; Fu, G. C. *J. Am. Chem. Soc.* **2002**, *124*, 13662.

(139) Ruan, J.; Li, X.; Saidi, O.; Xiao, J. *J. Am. Chem. Soc.* **2008**, *130*, 2424.

(140) Zhang, L.; Xie, X.; Fu, L.; Zhang, Z. *J. Org. Chem.* **2013**, *78*, 3434.

(141) Vautravers, N.; Breit, B. *Synlett* **2011**, *2011*, 2517.

(142) Lu, X.; Lin, S. *J. Org. Chem.* **2005**, *70*, 9651.

(143) Kuriyama, M.; Shimazawa, R.; Shirai, R. *J. Org. Chem.* **2008**, *73*, 1597.

(144) Qin, C.; Wu, H.; Cheng, J.; Chen, X.; Liu, M.; Zhang, W.; Su, W.; Ding, J. *J. Org. Chem.* **2007**, *72*, 4102.

(145) Yamamoto, T.; Ohta, T.; Ito, Y. *Org. Lett.* **2005**, *7*, 4153.

(146) Ma, W.; Xue, D.; Yu, T.; Wang, C.; Xiao, J. *Chem. Commun. (Camb).* **2015**, *51*, 8797.

(147) Wu, X.-F.; Neumann, H.; Beller, M. *Tetrahedron Lett.* **2010**, *51*, 6146.

(148) Xu, H.-J.; Zhao, Y.-Q.; Feng, T.; Feng, Y.-S. *J. Org. Chem.* **2012**, *77*, 2878.

(149) Zhuang, R.; Xu, J.; Cai, Z.; Tang, G.; Fang, M.; Zhao, Y. *Org. Lett.* **2011**, *13*, 2110.

(150) Zhang, L.; Zhang, G.; Zhang, M.; Cheng, J. *J. Org. Chem.* **2010**, *75*, 7472.

(151) Evans, D. A.; Katz, J. L.; West, T. R. *Tetrahedron Lett.* **1998**, *39*, 2937.

(152) Chan, D. M. .; Monaco, K. L.; Wang, R.-P.; Winters, M. P. *Tetrahedron Lett.* **1998**, *39*, 2933.

(153) Frost, C. G.; Penrose, S. D.; Gleave, R. *Org. Biomol. Chem.* **2008**, *6*, 4340.

(154) Decicco, C. P.; Song, Y.; Evans, D. A. *Org. Lett.* **2001**, *3*, 1029.

(155) Chan, D. M. T.; Monaco, K. L.; Li, R.; Bonne, D.; Clark, C. G.; Lam, P. Y. S. *Tetrahedron Lett.* **2003**, *44*, 3863.

(156) Koolmeister, T.; Södergren, M.; Scobie, M. *Tetrahedron Lett.* **2002**, *43*, 5965.

(157) Negishi, E. *J. Organomet. Chem.* **1976**, *108*, 281.

(158) Pauling, L. *J. Am. Chem. Soc.* **1932**, *54*, 3570.

(159) Rettig, S. J.; Trotter, J. *Can. J. Chem.* **1977**, *55*, 3071.

(160) Rettig, S. J.; Trotter, J. *Can. J. Chem.* **1975**, *53*, 1393.

(161) Dreher, S. D.; Lim, S.-E.; Sandrock, D. L.; Molander, G. A. *J. Org. Chem.* **2009**, *74*, 3626.

(162) Guram, A. S.; Wang, X.; Bunel, E. E.; Faul, M. M.; Larsen, R. D.; Martinelli, M. J. *J. Org. Chem.* **2007**, *72*, 5104.

(163) Lu, G.-P.; Voigtritter, K. R.; Cai, C.; Lipshutz, B. H. *J. Org. Chem.* **2012**, *77*, 3700.

(164) Molander, G. A.; Petrillo, D. E. *Org. Lett.* **2008**, *10*, 1795.

(165) Peh, G.-R.; Kantchev, E. A. B.; Er, J.-C.; Ying, J. Y. *Chem. Eur. J.* **2010**, *16*, 4010.

(166) Alacid, E.; Nájera, C. *J. Org. Chem.* **2009**, *74*, 2321.

(167) Li, S.; Lin, Y.; Cao, J.; Zhang, S. *J. Org. Chem.* **2007**, *72*, 4067.

(168) Molander, G. A.; Bernardi, C. R. *J. Org. Chem.* **2002**, *67*, 8424.

(169) Cui, X.; Qin, T.; Wang, J.-R.; Liu, L.; Guo, Q.-X. *Synthesis (Stuttg).* **2007**, *2007*, 393.

(170) Samarasimhareddy, M.; Prabhu, G.; Vishwanatha, T.; Sureshbabu, V. *Synthesis (Stuttg).* **2013**, *45*, 1201.

(171) Martin, R.; Buchwald, S. L. *Acc. Chem. Res.* **2008**, *41*, 1461.

(172) O' Connor, C. J.; Beckmann, H. S. G.; Spring, D. R. *Chem. Soc. Rev.* **2012**, *41*, 4444.

(173) Tan, D. S. *Nat. Chem. Biol.* **2005**, *1*, 74.

(174) Oh, S.; Park, S. B. *Chem. Commun. (Camb).* **2011**, *47*, 12754.

(175) Oh, S.; Kim, S. J.; Hwang, J. H.; Lee, H. Y.; Ryu, M. J.; Park, J.; Kim, S. J.; Jo, Y. S.; Kim, Y. K.; Lee, C.-H.; Kweon, K. R.; Shong, M.; Park, S. B. *J. Med. Chem.* **2010**, *53*, 7405.

(176) Zhu, M.; Kim, M. H.; Lee, S.; Bae, S. J.; Kim, S. H.; Park, S. B. *J. Med. Chem.* **2010**, *53*, 8760.

(177) Oh, S.; Nam, H. J.; Park, J.; Beak, S. H.; Park, S. B. *ChemMedChem* **2010**, *5*, 529.

(178) Oh, S.; Cho, S. W.; Yang, J.-Y.; Sun, H. J.; Chung, Y. S.; Shin, C. S.; Park, S. B. *Med. Chem. Commun.* **2011**, *2*, 76.

(179) Filippakopoulos, P.; Knapp, S. *Nat. Rev. Drug Discov.* **2014**, *13*, 337.

(180) Hewings, D. S.; Fedorov, O.; Filippakopoulos, P.; Martin, S.; Picaud, S.; Tumber, A.; Wells, C.; Olcina, M. M.; Freeman, K.; Gill, A.; Others; Ritchie, A. J.; Sheppard, D. W.; Russell, A. J.; Hammond, E. M.; Knapp, S.; Brennan, P. E.; Conway, S. J. *J. Med. Chem.* **2013**, *56*, 3217.

(181) Zeng, L.; Zhou, M.-M. *FEBS Lett.* **2002**, *513*, 124.

(182) Filippakopoulos, P.; Knapp, S. *FEBS Lett.* **2012**, *586*, 2692.

(183) Strahl, B. D.; Allis, C. D. *Nature* **2000**, *403*, 41.

(184) Dawson, M. A.; Prinjha, R. K.; Dittmann, A.; Giotopoulos, G.; Bantscheff, M.; Chan, W.-I.; Robson, S. C.; Chung, C.; Hopf, C.; Savitski, M. M.; Huthmacher, C.; Gudgin, E.; Lugo, D.; Beinke, S.; Chapman, T. D.; Roberts, E. J.; Soden, P. E.; Auger, K. R.; Mirguet, O.; Doehner, K.; Delwel, R.; Burnett, A. K.; Jeffrey, P.; Drewes, G.; Lee, K.; Huntly, B. J. P.; Kouzarides, T. *Nature* **2011**, *478*, 529.

(185) Delmore, J. E.; Issa, G. C.; Lemieux, M. E.; Rahl, P. B.; Shi, J.; Jacobs, H. M.; Kastritis, E.; Gilpatrick, T.; Paranal, R. M.; Qi, J.; Chesi, M.; Schinzel, A. C.; McKeown, M. R.; Heffernan, T. P.; Vakoc, C. R.; Bergsagel, P. L.; Ghobrial, I. M.; Richardson, P. G.; Young, R. A.; Hahn, W. C.; Anderson, K. C.; Kung, A. L.; Bradner, J. E.; Mitsiades, C. S. *Cell* **2011**, *146*, 904.

(186) Zuber, J.; Shi, J.; Wang, E.; Rappaport, A. R.; Herrmann, H.; Sison, E. A.; Magoon, D.; Qi, J.; Blatt, K.; Wunderlich, M.; Taylor, M. J.; Johns, C.; Chicas, A.; Mulloy, J. C.; Kogan, S. C.; Brown, P.; Valent, P.; Bradner, J. E.; Lowe, S. W.; Vakoc, C. R. *Nature* **2011**, *478*, 524.

(187) Seath, C. P.; Fyfe, J. W. B.; Molloy, J. J.; Watson, A. J. B. *Angew. Chemie Int. Ed.* **2015**, 9976.